

**Electronic Supplementary Information**

**Reactivities of allenic and olefinic Michael acceptors towards phosphines**

Feng An,<sup>a</sup> Harish Jangra,<sup>a</sup> Yin Wei,<sup>b</sup> Min Shi,\*<sup>bc</sup> Hendrik Zipse,\*<sup>a</sup> and Armin R. Ofial\*<sup>a</sup>

<sup>a</sup> Department Chemie, Ludwig-Maximilians-Universität München, Butenandtstr. 5-13, 81377 München (Germany), E-Mail: zipse@cup.uni-muenchen.de (H.Z.), ofial@lmu.de (A.R.O.)

<sup>b</sup> State Key Laboratory of Organometallic Chemistry,  
Shanghai Institute of Organic Chemistry, Chinese Academy of  
Sciences, 354 Fenglin Road, Shanghai 200032 (P. R. China)

E-mail: mshi@mail.sioc.ac.cn

<sup>a</sup> Key Laboratory for Advanced Materials and Institute of Fine  
Chemicals, East China University of Science and Technology,  
130 MeiLong Road, Shanghai 200237 (P. R. China)

## Table of Contents

1	Additional Figures and Tables.....	S3
2	Synthesis and Analytics .....	S8
2.1	General.....	S8
2.2	Synthesis and purification of alkyl allenotes .....	S9
2.3	Purification of phosphines .....	S13
2.4	Synthesis and purification of phosphonium and 2,4,6-collidinium triflates .....	S13
3	Studies on the Interactions between Electrophiles, Nucleophiles and Proton Sources in CD <sub>2</sub> Cl <sub>2</sub> .....	S15
3.1	Ph <sub>3</sub> P with collidinium triflate (CT) .....	S15
3.2	Ethyl allenote <b>1f</b> with CT .....	S16
3.3	Ethyl allenote <b>1f</b> with TBPT .....	S17
3.4	Stability of the R <sub>3</sub> P adducts of alkyl allenote <b>1f</b> .....	S18
3.4.1	Analysis of mixtures of Bu <sub>3</sub> P with <b>1f</b> .....	S18
3.4.2	Analysis of mixtures of Ph <sub>3</sub> P with <b>1f</b> .....	S19
3.4.3	Analysis of mixtures of Bu <sub>3</sub> P with <i>N</i> -methylmaleimide ( <b>4s</b> ) .....	S20
3.4.4	Analysis of mixtures of Ph <sub>3</sub> P with <i>N</i> -methylmaleimide ( <b>4s</b> ) .....	S21
3.4.5	Analysis of mixtures of Bu <sub>3</sub> P with phenyl <i>N</i> -tosyl imine ( <b>4t</b> ) .....	S22
3.4.6	Analysis of mixtures of Bu <sub>3</sub> P with benzylidenemalononitrile ( <b>4v</b> ) .....	S23
3.4.7	Analysis of mixtures of Ph <sub>3</sub> P with benzylidenemalononitrile ( <b>4v</b> ).....	S24
4	Product Studies .....	S25
4.1	Reaction of triphenylphosphonium triflate with phenyl buta-2,3-dienoate ( <b>1a</b> ) .....	S25
4.2	Reaction of triphenylphosphonium triflate with 3-vinylidenedihydrofuran-2(3H)-one ( <b>1d</b> ).....	S25
4.3	Reaction of triphenylphosphonium triflate with ethyl buta-2,3-dienoate ( <b>1f</b> ).....	S26
4.4	Reaction of triphenylphosphonium triflate with diethyl 2-vinylidenesuccinate ( <b>1i</b> ) .....	S26
5	Kinetics .....	S28
5.1	General.....	S28
5.2	Kinetics of the reactions of R <sub>3</sub> P with alkyl allenotes 1 .....	S29
5.2.1	Kinetics of the reactions of 1 with Bu <sub>3</sub> P in dichloromethane .....	S29
5.2.2	Kinetics of the reactions of 1 with Ph <sub>3</sub> P in dichloromethane .....	S34
5.3	Kinetics of the reactions of tributylphosphine with Michael acceptors <b>4</b> .....	S46
6	Methyl Anion Affinities (MAA) and Phosphine Affinities (PA).....	S64
7	Copies of NMR Spectra.....	S77
7.1	NMR spectra of alkyl allenotes <b>1</b> .....	S77
7.2	NMR spectra of phosphines .....	S91
7.3	NMR spectra of phosphonium triflates and 2,4,6-collidinium triflate .....	S94
7.4	NMR and IR spectra of the product studies .....	S98
8	References .....	S114

## 1 Additional Figures and Tables

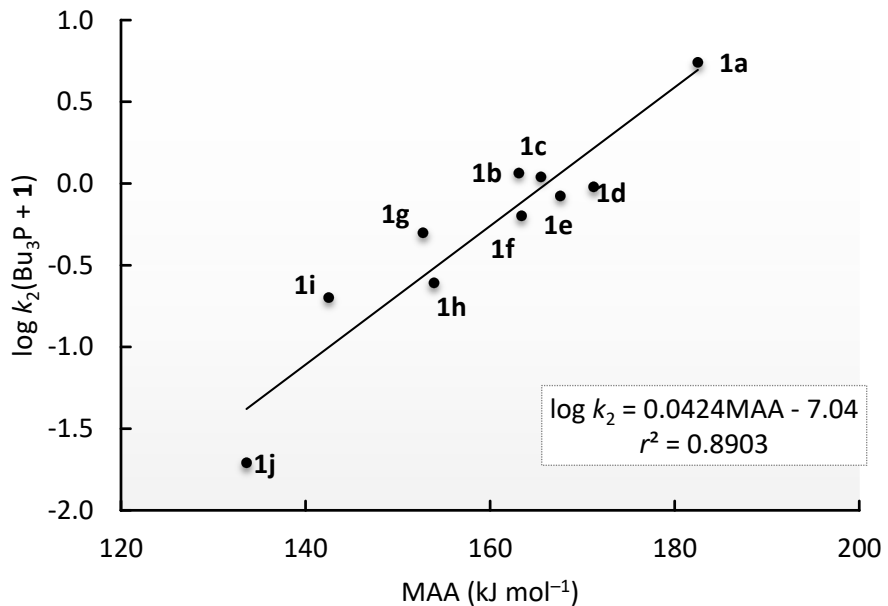


**Figure S1.** Linear relationship between  $\log k_2(\text{Bu}_3\text{P})$  for reactions of  $\text{Bu}_3\text{P}$  with alkyl allenoates **1** and calculated methyl anion affinities (MAA) of **1** (correlation drawn with data from Table 1, main text).

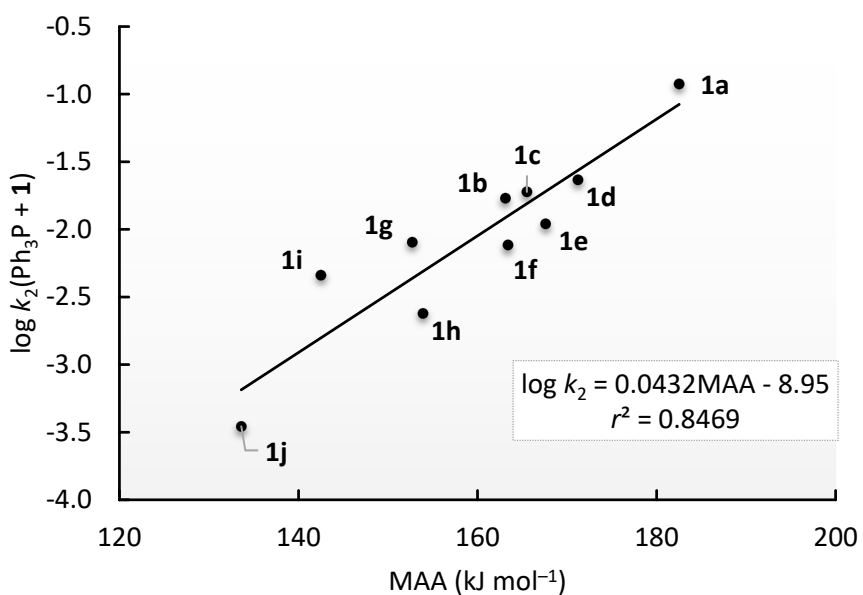


**Figure S2.** Linear relationship between  $\log k_2(\text{Ph}_3\text{P})$  for reactions of  $\text{Ph}_3\text{P}$  with alkyl allenoates **1** and calculated methyl anion affinities MAA of **1** (correlation drawn with data from Table 1, main text).

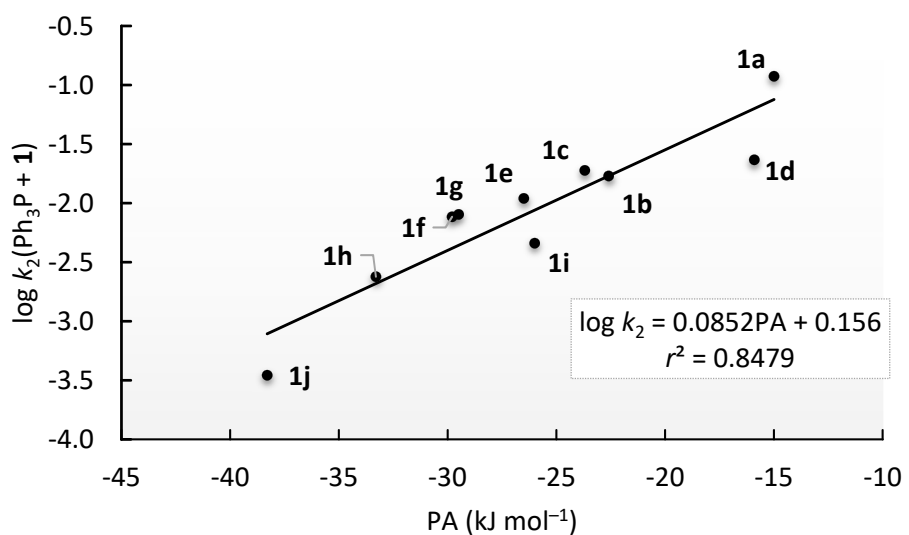
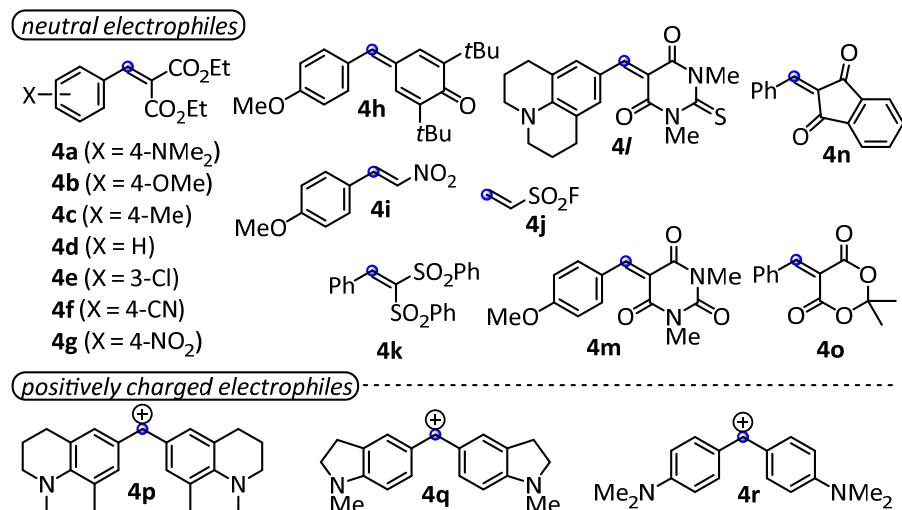


**Figure S3.** Linear relationship between  $\log k_2(\text{Ph}_3\text{P})$  for reactions of  $\text{Ph}_3\text{P}$  with alkyl allenoates **1** and calculated **phosphine affinities (PA)** of **1** (correlation drawn with data from Table S42).

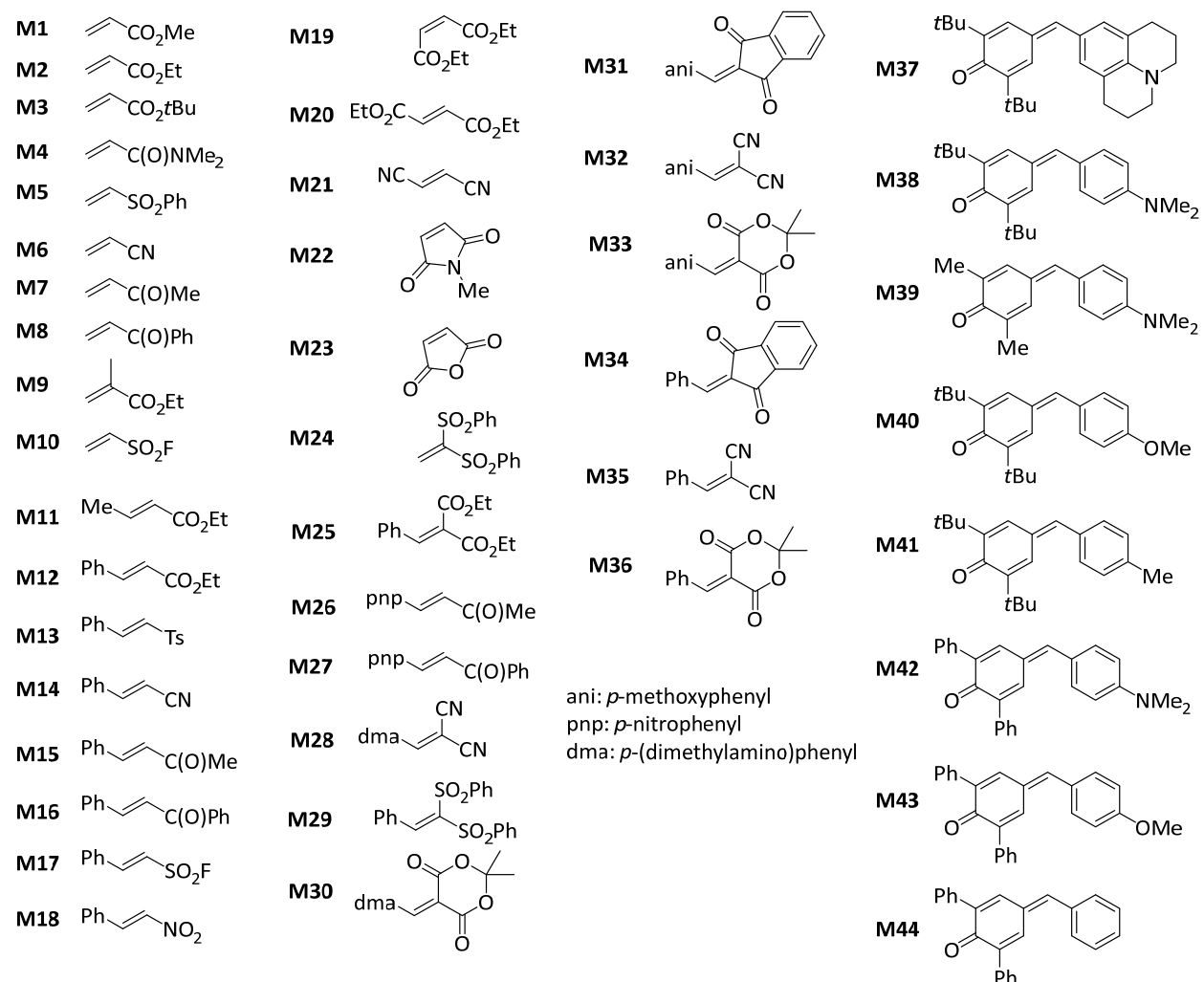
**Table S1** (data for Figure 6). Mayr electrophilicity parameters  $E$  for **4a-4r** and the second-order rate constants of their reactions of  $\text{Bu}_3\text{P}$  ( $\text{CH}_2\text{Cl}_2$ , 20 °C).



Michael acceptor	Electrophilicity $E^a$	$k_2(\text{Bu}_3\text{P})^b (\text{M}^{-1} \text{s}^{-1})$	$\log k_2(\text{Bu}_3\text{P})$
<b>4a</b>	-23.10	$3.03 \times 10^{-2}$	-1.519
<b>4b</b>	-21.47	0.137	-0.863
<b>4c</b>	-21.11	0.208	-0.682
<b>4d</b>	-20.55	0.369	-0.433
<b>4e</b>	-18.98	0.979	-0.009
<b>4f</b>	-18.06	2.61	0.417
<b>4g</b>	-17.67	3.21	0.507
<b>4h</b>	-16.11	1.86	0.270
<b>4i</b>	-14.70	19.9	1.299
<b>4j</b>	-12.09	799	2.903
<b>4k</b>	-12.93	$3.09 \times 10^3$	3.490
<b>4l</b>	-11.89	$6.98 \times 10^3$	3.844
<b>4m</b>	-10.37	$3.25 \times 10^4$	4.512
<b>4n</b>	-10.11	$1.65 \times 10^4$	4.217
<b>4o</b>	-9.15	$2.71 \times 10^5$	5.433
<b>4p</b>	-10.04	$1.13 \times 10^4$	4.053
<b>4q</b>	-8.76	$8.91 \times 10^4$	4.950
<b>4r</b>	-7.02	$1.39 \times 10^6$	6.145

<sup>a</sup> From ref S1. <sup>b</sup> This work.

**Table S2** (data for Figure 7). Methyl anion affinities (MAAs) of Michael acceptors (with data from ref S2) and estimated Mayr *E* parameters for alkyl allenoates.



Michael acceptors	Mayr <i>E</i> <sup>a</sup>	MAA <sup>b</sup> (kJ mol <sup>-1</sup> )
<b>M1</b>	-18.84	80.7
<b>M2</b>	-19.07	75.1
<b>M3</b>	-20.22	71.6
<b>M4</b>	-23.54	59.6
<b>M5</b>	-18.36	96.8
<b>M6</b>	-19.05	109.4
<b>M7</b>	-16.76	104.2
<b>M8</b>	-15.25	116.7
<b>M9</b>	-22.77	51.9
<b>M10 (= 4j)</b>	-12.09	160.5
<b>M11</b>	-23.59	49.8
<b>M12</b>	-24.52	36.1
<b>M13</b>	-24.69	51.8
<b>M14</b>	-24.60	66.1
<b>M15</b>	-23.01	60.4
<b>M16</b>	-19.39	74.8

<b>M17</b>	-16.63	113.3
<b>M18</b>	-13.85	123.8
<b>M19</b>	-19.49	93.1
<b>M20</b>	-17.79	74.2
<b>M21</b>	-15.71	132.4
<b>M22 (= 4s)</b>	-14.07	113.9
<b>M23</b>	-11.31	149.8
<b>M24</b>	-7.50	174.8
<b>M25</b>	-20.55	104.8
<b>M26</b>	-19.36	75.2
<b>M27</b>	-17.33	86.8
<b>M28</b>	-13.30	141.3
<b>M29 (= 4k)</b>	-12.93	155.9
<b>M30</b>	-12.76	135.3
<b>M31</b>	-11.32	147.1
<b>M32</b>	-10.80	161.9
<b>M33</b>	-10.28	154.4
<b>M34 (= 4n)</b>	-10.11	160.7
<b>M35 (= 4v)</b>	-9.42	177.4
<b>M36 (= 4o)</b>	-9.15	169.6
<b>M37</b>	-17.90	120.4
<b>M38</b>	-17.29	123.2
<b>M39</b>	-16.36	130.7
<b>M40 (= 4h)</b>	-16.11	137.4
<b>M41</b>	-15.83	141.3
<b>M42</b>	-13.39	147.3
<b>M43</b>	-12.18	163.6
<b>M44</b>	-11.87	174.6
Alkyl allenoates	Estimated Mayr $E^c$	MAA <sup>d</sup> (kJ mol <sup>-1</sup> )
<b>1a</b>	(-17.57) <sup>c</sup>	182.5
<b>1b</b>	(-18.97) <sup>c</sup>	163.1
<b>1c</b>	(-19.02) <sup>c</sup>	165.5
<b>1d</b>	(-19.15) <sup>c</sup>	171.2
<b>1e</b>	(-19.26) <sup>c</sup>	167.6
<b>1f</b>	(-19.51) <sup>c</sup>	163.4
<b>1g</b>	(-19.73) <sup>c</sup>	152.7
<b>1h</b>	(-20.37) <sup>c</sup>	153.9
<b>1i</b>	(-20.55) <sup>c</sup>	142.5
<b>1j</b>	(-22.65) <sup>c</sup>	133.6

<sup>a</sup> Empirical Mayr electrophilicity parameter  $E$  (data taken from ref. S1). <sup>b</sup> Methyl anion affinities MAA =  $-\Delta G_{\text{sol-sp}}$  (data taken from ref S2). <sup>c</sup> To construct Figure 7, electrophilicities  $E$  for the allenoates **1a-1j** were estimated by using the rearranged correlation equation from Figure 6, that is,  $E = \{\log k_2(\text{Bu}_3\text{P}) - 9.208\}/0.482$ . **Caveat:** These  $E$  parameters refer to single-point calibrations of the reactivities of **1a-1j** towards  $\text{Bu}_3\text{P}$ , which is not a member of the standard group of reference nucleophiles for the construction of Mayr reactivity scales. Furthermore, it remains to be shown that electrophilic reactivities of the allenoates **1a-1j** follow eqn (1) when calibrated with a wider range of reference nucleophiles. <sup>d</sup> Methyl anion affinities MAA from Table 1, main text.

## 2 Synthesis and Analytics

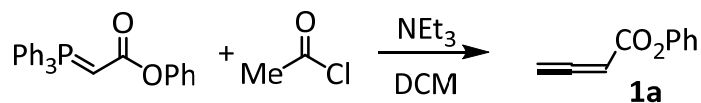
### 2.1 General

**Analytics:**  $^1\text{H}$ ,  $^{13}\text{C}$ ,  $^{19}\text{F}$  and  $^{31}\text{P}$  NMR spectra were measured on 400 MHz, 600 MHz, or 800 MHz NMR spectrometers. Chemical shifts ( $\delta$ ) are given in ppm.  $^1\text{H}$  and  $^{13}\text{C}$  NMR spectra were calibrated to residual solvent peaks.<sup>53</sup> Coupling constants are given in Hz. Multiplicities are abbreviated as follows: s = singlet, d = doublet, t = triplet, q = quartet, hept = heptet, m = multiplet, and br = broad.  $^{13}\text{C}\{^1\text{H}\}$  NMR spectra were acquired with broad band proton decoupling. Numbers of C-attached hydrogen atoms were obtained from gHSQC experiments and reported as C, CH, CH<sub>2</sub>, or CH<sub>3</sub>. The assignments of individual NMR signals were based on additional 2D-NMR experiments (gHSQC, gHMBC, and COSY). HRMS spectra were determined on a Finnigan MAT 95 mass spectrometer. IR spectra were recorded on a FTIR Spectrometer SPECTRUM BX II (Perkin Elmer). Melting points were obtained on a BÜCHI M-560 melting point apparatus and are uncorrected.

**Synthesis:** Flash column chromatography was performed on Merck silica gel 60 (0.040–0.063 mm) using compressed air. Thin layer chromatography (TLC) was performed using Merck silica gel 60 F254 aluminum plates. Compounds on eluted plates were visualized using a 254 nm UV lamp and/or by treatment with a suitable stain followed by heating. Concentration under reduced pressure was performed on rotary evaporators with a water bath temperature of 40 °C. Starting materials and reagents were purchased from Sigma-Aldrich or ABCR and were used as supplied or, in the case of some liquids, distilled. Solvents were distilled or dried prior to use over appropriate drying agents: Dichloromethane (calcium hydride), diethyl ether (sodium/benzophenone), and acetonitrile (phosphorus pentoxide). Solvents for filtration, chromatography, and recrystallization were purchased from Fisher and used as received.

## 2.2 Synthesis and purification of alkyl allenoates

### 2.2.1 Phenyl buta-2,3-dienoate (**1a**)<sup>S4</sup>

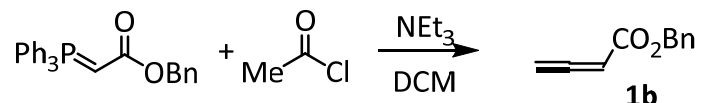


The ylide phenyl 2-(triphenyl-λ<sup>5</sup>-phosphoranylidene)acetate<sup>S5</sup> (5.09 g, 12.8 mmol) and triethylamine (1.37 g, 13.5 mmol) were dissolved in dichloromethane (50 mL). Under ice bath cooling, acetyl chloride (1.04 g, 13.2 mmol) was added dropwise via a syringe. The reaction mixture was kept stirring at ambient temperature for 60 min. Then triethylamine (0.960 mL, 6.89 mmol) and acetyl chloride (0.200 mL, 2.80 mmol) were added dropwise into the reaction mixture by using a syringe. The mixture was kept stirring for 16 h. Then sat aq NaHCO<sub>3</sub> solution (50 mL) was added. After separating the phases, the volatiles of the organic phase were removed under reduced pressure. The residue was purified by column chromatography on silica gel (pentane/ethyl acetate 50:1 to 30:1 to provide **1a** (0.835 g, 41%) as a colorless oil, which was stored at -30 °C under Ar atmosphere. NMR spectroscopic data in CDCl<sub>3</sub> agree with those described in ref.<sup>S4</sup>

<sup>1</sup>H NMR (600 MHz, CDCl<sub>3</sub>) δ 7.40–7.36 (m, 2 H), 7.25–7.21 (m, 1 H), 7.14–7.11 (m, 2 H), 5.83 (t, *J* = 6.5 Hz, 1 H), 5.34 (d, *J* = 6.5 Hz, 2 H). <sup>13</sup>C{<sup>1</sup>H} NMR (151 MHz, CDCl<sub>3</sub>) δ 216.8, 164.3, 150.9, 129.6, 126.0, 121.7, 87.9, 80.0.

<sup>1</sup>H NMR (400 MHz, CD<sub>2</sub>Cl<sub>2</sub>) δ 7.43–7.36 (m, 2 H), 7.28–7.23 (m, 1 H), 7.13–7.09 (m, 2 H), 5.83 (t, *J* = 6.5 Hz, 1 H), 5.35 (d, *J* = 6.5 Hz, 1 H). <sup>13</sup>C{<sup>1</sup>H} NMR (101 MHz, CD<sub>2</sub>Cl<sub>2</sub>) δ 217.0, 164.5, 151.3, 129.8, 126.3, 122.0, 87.8, 79.9.

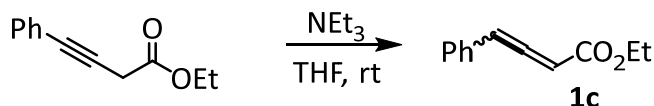
### 2.2.2 Benzyl buta-2,3-dienoate (**1b**)<sup>S4</sup>



Benzyl 2-(triphenyl-λ<sup>5</sup>-phosphoranylidene)acetate (6.56 g, 16.0 mmol) and triethylamine (2.70 mL, 19.4 mmol) were dissolved in dichloromethane (45 mL). Under ice bath cooling, acetyl chloride (1.25 mL, 17.6 mmol) was added dropwise via a syringe. The reaction mixture was kept stirring at ambient temperature for 60 min. The volatiles were removed under reduced pressure. The residue was purified by column chromatography on silica gel (pentane/ethyl acetate 30:1 to 20:1) followed by a quick distillation (9 × 10<sup>-3</sup> mbar, 90 °C, distillate condensed under liquid nitrogen cooling bath) to furnish **1b** (1.66 g, 60%) as a colorless oil, which was stored at -30 °C under Ar atmosphere. NMR spectroscopic data in CDCl<sub>3</sub> agree with those described in ref.<sup>S6</sup>

<sup>1</sup>H NMR (600 MHz, CDCl<sub>3</sub>) δ 7.39–7.31 (m, 5 H), 5.69 (t, *J* = 6.6 Hz, 1 H), 5.24 (d, *J* = 6.5 Hz, 2 H), 5.20 (s, 3 H). <sup>13</sup>C{<sup>1</sup>H} NMR (151 MHz, CDCl<sub>3</sub>) δ 216.2, 165.7, 136.0, 128.7, 128.4, 128.3, 88.0, 79.6, 66.8. <sup>1</sup>H NMR (400 MHz, CD<sub>2</sub>Cl<sub>2</sub>) δ 7.42–7.27 (m, 5 H), 5.71–5.67 (m, 1 H), 5.24 (d, *J* = 6.5 Hz, 2 H), 5.17 (s, 2 H). <sup>13</sup>C{<sup>1</sup>H} NMR (101 MHz, CD<sub>2</sub>Cl<sub>2</sub>) δ 216.3, 165.7, 136.5, 128.9, 128.6, 128.5, 88.0, 79.5, 66.9.

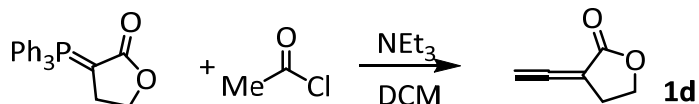
### 2.2.3 Ethyl 4-phenylbuta-2,3-dienoate (1c)



Ethyl 4-phenylbut-3-ynoate<sup>57</sup> (5.39 g, 26.6 mmol) and triethylamine (2.93 g, 29.0 mmol) were dissolved in dry THF (65 mL). The reaction mixture was kept stirring at ambient temperature under nitrogen atmosphere for 15 h. The solvent was removed under reduced pressure and the residue was purified by column chromatography on silica gel (pentane/ethyl acetate 100:1 to 50:1) to provide **1c** (0.871 g, 16%) as a slightly yellow oil, which was kept at –30 °C under Ar atmosphere. Starting materials were converted to a degree of around 85% after 15 h, and higher yields of **1c** can be achieved by repeated column chromatographic separations. NMR spectroscopic data agree with those reported in CDCl<sub>3</sub> solution.<sup>58</sup>

<sup>1</sup>H NMR (400 MHz, CD<sub>2</sub>Cl<sub>2</sub>) δ 7.41–7.22 (m, 5 H), 6.64 (d, *J* = 6.4 Hz, 1 H), 6.02 (dq, *J* = 6.4, 0.5 Hz, 1 H), 4.20 (qd, *J* = 7.1, 2.2 Hz, 2 H), 1.27 (t, *J* = 7.1 Hz, 3 H). <sup>13</sup>C{<sup>1</sup>H} NMR (201 MHz, CD<sub>2</sub>Cl<sub>2</sub>) δ 214.8, 165.2, 131.7, 129.3, 128.5, 127.8, 98.8, 92.3, 61.5, 14.4.

### 2.2.4 3-Vinylidenedihydrofuran-2(3H)-one (1d)

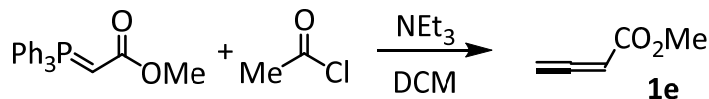


3-(Triphenyl-λ<sup>5</sup>-phosphoranylidene)dihydrofuran-2(3H)-one<sup>59</sup> (3.29 g, 9.50 mmol) and triethylamine (1.01 g, 9.98 mmol) were dissolved in dichloromethane (30 mL). Under ice bath cooling, acetyl chloride (0.798 g, 10.2 mmol) was added dropwise via a syringe. The reaction mixture was kept stirring at ambient temperature for 45 min. The volatiles were removed under reduced pressure. The residue was purified by column chromatography on silica gel (pentane/ethyl acetate 3:1 to 2:1) followed by a quick distillation (4 × 10<sup>−3</sup> mbar, 80 °C, distillate condensed under liquid nitrogen cooling bath) to give **1d** (0.374 g, 36%) as a colorless oil, which was stored at –30 °C under Ar atmosphere. NMR spectroscopic data agree with those described in ref.<sup>59</sup>

<sup>1</sup>H NMR (600 MHz, CD<sub>2</sub>Cl<sub>2</sub>) δ 5.28–5.27 (m, 2 H), 4.32 (t, *J* = 7.5 Hz, 2 H), 3.01 (tt, *J* = 7.5, 5.1 Hz, 2 H).

<sup>13</sup>C{<sup>1</sup>H} NMR (151 MHz, CD<sub>2</sub>Cl<sub>2</sub>) δ 209.5, 170.4, 93.7, 82.1, 66.5, 26.8.

### 2.2.5 Methyl buta-2,3-dienoate (1e)<sup>S10</sup>



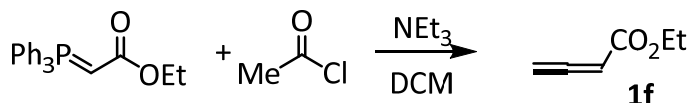
From methyl 2-(triphenyl-λ<sup>5</sup>-phosphaneylidene)acetate (16.00 g, 47.85 mmol), trimethylamine (5.33 g, 52.64 mmol), and acetyl chloride (3.76 g, 47.85 mmol): **1e** (4.25 g, 91%). NMR spectroscopic data agree with those described in ref.<sup>S11</sup>

<sup>1</sup>H NMR (400 MHz, CD<sub>2</sub>Cl<sub>2</sub>) δ 5.63 (t, *J* = 6.6 Hz, 1 H), 5.22 (d, *J* = 6.6 Hz, 2 H), 3.71 (s, 3 H). <sup>13</sup>C{<sup>1</sup>H} NMR (101 MHz, CD<sub>2</sub>Cl<sub>2</sub>) δ 216.2, 166.3, 87.9, 79.3, 52.3.

### 2.2.6 Ethyl buta-2,3-dienoate (1f)

Method 1: Commercially available **1f** (Aldrich) was purified by column chromatography on silica gel (pentane/diethyl ether 25:1 to 15:1).

Method 2: Ethyl 2,3-butadienoate **1f** was synthesized by a modified literature procedure reported by Hansen.<sup>S10</sup>

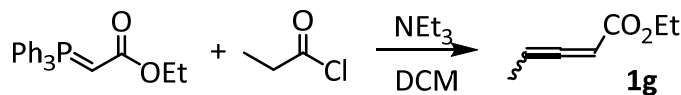


Ethyl 2-(triphenyl-λ<sup>5</sup>-phosphaneylidene)acetate (7.71 g, 22.1 mmol) and triethylamine (2.24 g, 22.1 mmol) were dissolved in dichloromethane (50 mL). Under ice bath cooling, acetyl chloride (1.74 g, 22.2 mmol) was added dropwise via a syringe. The mixture was kept stirring at ambient temperature for 60 min. Then sat aq NaHCO<sub>3</sub> solution (50 mL) was added. The organic phase was separated, and the aqueous phase was extracted by the dichloromethane (2 × 50 mL). After drying the unified organic phases (MgSO<sub>4</sub>), the volatiles were removed under only slightly reduced pressure (500 mbar). After purification by column chromatography on silica gel (pentane/diethyl ether 25:1 to 15:1), the residue was kept in vacuum (5 mbar) at 0 °C for 30 min. A quick distillation (3 × 10<sup>-3</sup> mbar, ambient temperature, distillate condensed under liquid nitrogen cooling bath) delivered **1f** (1.65 g, 67%) as a colorless oil. NMR spectroscopic data in CDCl<sub>3</sub> agree with those described in ref.<sup>S12</sup>

<sup>1</sup>H NMR (600 MHz, CDCl<sub>3</sub>) δ 5.64 (t, *J* = 6.5 Hz, 1 H), 5.22 (d, *J* = 6.5 Hz, 2 H), 4.21 (q, *J* = 7.1 Hz, 2 H), 1.29 (t, *J* = 7.1 Hz, 3 H). <sup>13</sup>C{<sup>1</sup>H} NMR (151 MHz, CDCl<sub>3</sub>) δ 215.9, 165.9, 88.2, 79.4, 61.2, 14.4.

<sup>1</sup>H NMR (400 MHz, CD<sub>2</sub>Cl<sub>2</sub>) δ 5.62 (t, *J* = 6.6 Hz, 1 H), 5.21 (d, *J* = 6.6 Hz, 2 H), 4.16 (q, *J* = 7.1 Hz, 2 H), 1.26 (t, *J* = 7.1 Hz, 3 H). <sup>13</sup>C{<sup>1</sup>H} NMR (101 MHz, CD<sub>2</sub>Cl<sub>2</sub>) δ 216.0, 165.8, 88.2, 79.3, 61.3, 14.4.

### 2.2.7 Ethyl penta-2,3-dienoate (1g)<sup>S13</sup>

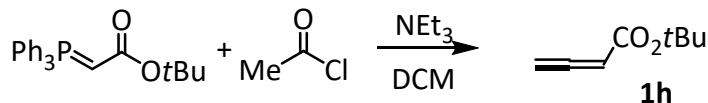


Ethyl 2-(triphenyl- $\lambda^5$ -phosphaneylidene)acetate<sup>S10</sup> (4.50 g, 12.9 mmol) and triethylamine (2.00 mL, 14.4 mmol) was dissolved in dichloromethane (45 mL). Under ice bath cooling, acetyl chloride (1.25 mL, 17.6 mmol) added dropwise via a syringe. The reaction mixture was kept stirring at ambient temperature for 30 min. Then sat aq NaHCO<sub>3</sub> solution (50 mL) was added. The organic phase was separated, and the aqueous phase was extracted by the dichloromethane (3 × 50 mL). After drying (MgSO<sub>4</sub>), the volatiles were removed under reduced pressure. The residue was purified by column chromatography on silica gel (pentane/ethyl acetate 20:1) and provided **1g** (700 mg, 54%) as a colorless oil, which was stored at -30 °C under Ar atmosphere. NMR spectroscopic data in CDCl<sub>3</sub> agree with those described in ref.<sup>S13</sup>

<sup>1</sup>H NMR (400 MHz, CDCl<sub>3</sub>) δ 5.62–5.52 (m, 2 H), 4.18 (q, *J* = 7.1 Hz, 2 H), 1.77 (dd, *J* = 7.2, 3.3 Hz, 3 H), 1.27 (t, *J* = 7.1 Hz, 3 H). <sup>13</sup>C{<sup>1</sup>H} NMR (101 MHz, CDCl<sub>3</sub>) δ 213.0, 166.4, 90.4, 87.8, 60.9, 14.4, 13.0.

<sup>1</sup>H NMR (400 MHz, CD<sub>2</sub>Cl<sub>2</sub>) δ 5.64–5.51 (m, 2 H), 4.15 (qd, *J* = 7.1, 0.9 Hz, 2 H), 1.77 (dd, *J* = 7.3, 3.3 Hz, 3 H), 1.25 (t, *J* = 7.1 Hz, 3 H). <sup>13</sup>C{<sup>1</sup>H} NMR (101 MHz, CD<sub>2</sub>Cl<sub>2</sub>) δ 213.1, 166.3, 90.5, 87.9, 61.1, 14.4, 13.0.

### 2.2.8 tert-Butyl buta-2,3-dienoate (1h)

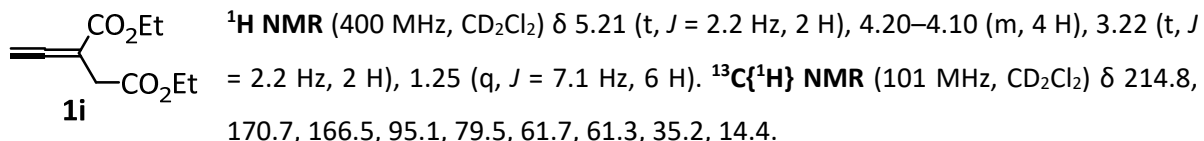


**1h** was prepared in a yield of 33% following the procedure reported by Hansen.<sup>S10</sup> NMR spectroscopic data agree with those reported in CDCl<sub>3</sub> solution.<sup>S9</sup>

<sup>1</sup>H NMR (600 MHz, CD<sub>2</sub>Cl<sub>2</sub>) δ 5.53 (t, *J* = 6.6 Hz, 1 H), 5.16 (d, *J* = 6.6 Hz, 2 H), 1.45 (s, 9 H). <sup>13</sup>C{<sup>1</sup>H} NMR (151 MHz, CD<sub>2</sub>Cl<sub>2</sub>) δ 215.6, 165.1, 89.7, 81.2, 78.9, 28.2.

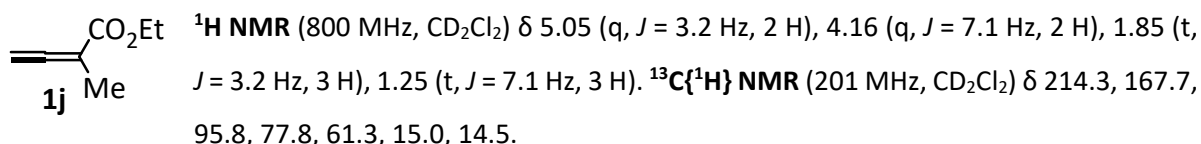
### 2.2.9 Diethyl 2-vinylidenesuccinate (1i)

Commercially available **1i** (Aldrich) was purified by column chromatography on silica gel (pentane/diethyl ether 8:1 to 5:1). NMR spectroscopic data agree with those reported in CDCl<sub>3</sub> solution.<sup>S14</sup>



### 2.2.10 Ethyl 2-methylbuta-2,3-dienoate (1j)

Commercially available **1j** (Aldrich) was purified by column chromatography on silica gel (pentane/diethyl ether 25:1 to 15:1). NMR spectroscopic data agree with those reported in  $\text{CDCl}_3$  solution.<sup>S13</sup>



## 2.3 Purification of phosphines

### 2.3.1 Tributylphosphine

$\text{Bu}_3\text{P}$  was purified by vacuum distillation ( $83.5^\circ\text{C}$ , 0.75 mbar).

**1H NMR** (400 MHz,  $\text{CD}_2\text{Cl}_2$ )  $\delta$  1.41–1.33 (m, 18 H), 0.93–0.87 (m, 9 H). **13C{1H} NMR** (101 MHz,  $\text{CD}_2\text{Cl}_2$ )  $\delta$  28.6 (d,  $J_{\text{C,P}} = 12.8$  Hz), 27.4 (d,  $J_{\text{C,P}} = 12.6$  Hz), 25.0 (d,  $J_{\text{C,P}} = 10.9$  Hz), 14.1. **31P NMR** (162 MHz,  $\text{CD}_2\text{Cl}_2$ )  $\delta$  –31.3.

### 2.3.2 Triphenylphosphine

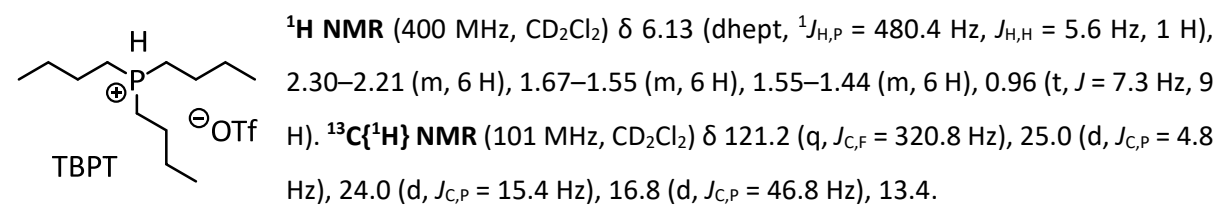
$\text{Ph}_3\text{P}$  was purified by a quick distillation ( $3 \times 10^{-3}$  mbar,  $140$ – $165^\circ\text{C}$ , distillate condensed under liquid nitrogen cooling bath).

**1H NMR** (400 MHz,  $\text{CD}_2\text{Cl}_2$ )  $\delta$  7.39–7.32 (m, 15 H). **13C{1H} NMR** (101 MHz,  $\text{CD}_2\text{Cl}_2$ )  $\delta$  137.8 (d,  $J_{\text{C,P}} = 11.4$  Hz), 134.1 (d,  $J_{\text{C,P}} = 19.6$  Hz), 129.1, 128.91 (d,  $J_{\text{C,P}} = 6.9$  Hz). **31P NMR** (162 MHz,  $\text{CD}_2\text{Cl}_2$ )  $\delta$  –5.5.

## 2.4 Synthesis and Purification of Phosphonium and 2,4,6-Collidinium Triflates

### 2.4.1 Tributylphosphonium Triflate (TBPT)

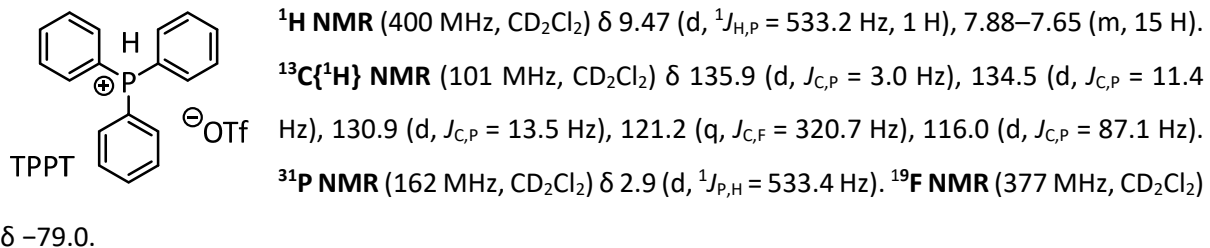
Under ice bath cooling and nitrogen atmosphere protection  $\text{Bu}_3\text{P}$  (1.30 g, 6.43 mmol) was added dropwise into a solution of triflic acid (964 mg, 6.42 mmol) in anhydrous diethyl ether (10 mL). The suspension was filtered, and the collected solid was washed with anhydrous diethyl ether under an inert gas atmosphere. Drying the solid under high vacuum provided  $\text{Bu}_3\text{PH}^+ \text{TfO}^-$  (TBPT, 2.13 g, 94%) as a colorless solid. NMR spectroscopic data agree with those reported in  $\text{CDCl}_3$  solution.<sup>S15</sup>



**31P NMR** (162 MHz,  $\text{CD}_2\text{Cl}_2$ )  $\delta$  13.2 (dtt,  ${}^1J_{\text{P,H}} = 480.9$  Hz,  ${}^2J_{\text{P,H}} = 25.2$  Hz,  ${}^3J_{\text{P,H}} = 12.0$  Hz).

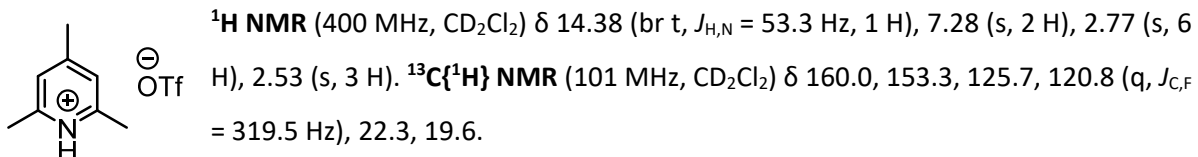
### 2.4.2 Triphenylphosphonium Triflate (TPPT)

Under ice bath cooling and nitrogen atmosphere protection a solution of Ph<sub>3</sub>P (3.49 g, 13.3 mmol) in anhydrous diethyl ether (15 mL) was added dropwise into a solution of triflic acid (2.03 g, 13.5 mmol) in anhydrous diethyl ether (5 mL). The suspension was filtered, and the collected solid was washed with anhydrous diethyl ether under inert gas atmosphere. Drying the solid under high vacuum furnished Ph<sub>3</sub>PH<sup>+</sup> TfO<sup>-</sup> (TPPT, 4.55 g, 83%) as a colorless solid. NMR spectroscopic data agree with those reported in CDCl<sub>3</sub> solution.<sup>S16</sup>



### 2.4.3 2,4,6-Collidinium Triflate (CT)

Under ice bath cooling and nitrogen atmosphere protection 2,4,6-trimethylpyridine (= 2,4,6-collidine, 1.12 g, 9.24 mmol) was added dropwise into an ethereal solution of triflic acid (1.38 g, 9.20 mmol in 15 mL). The suspension was filtered, and the collected solid was washed with anhydrous diethyl ether under inert gas atmosphere. Drying the solid under high vacuum furnished 2,4,6-collidinium triflate CT (2.32 g, 93%) as a colorless solid. NMR spectroscopic data agree with those reported in CDCl<sub>3</sub> solution.<sup>S17</sup>



### 3 Studies on the Interactions between Electrophiles, Nucleophiles and Proton Sources in CD<sub>2</sub>Cl<sub>2</sub>

#### 3.1 Ph<sub>3</sub>P with collidinium triflate (CT)

Figures S4 and S5 show that 2,4,6-collidine is a stronger Brønsted base than Ph<sub>3</sub>P (in CD<sub>2</sub>Cl<sub>2</sub>).

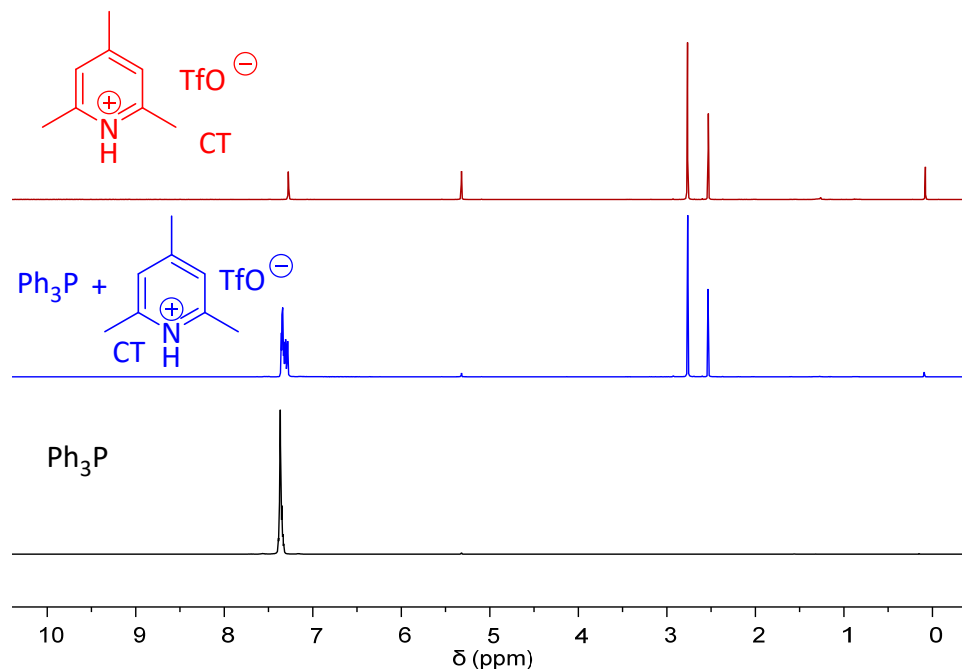


**Figure S4.** Comparison of the <sup>1</sup>H NMR spectra of CT (59.5 mM, top) and Ph<sub>3</sub>P (58.3 mM, bottom) with that of the mixture of Ph<sub>3</sub>P and CT in CD<sub>2</sub>Cl<sub>2</sub> (central).

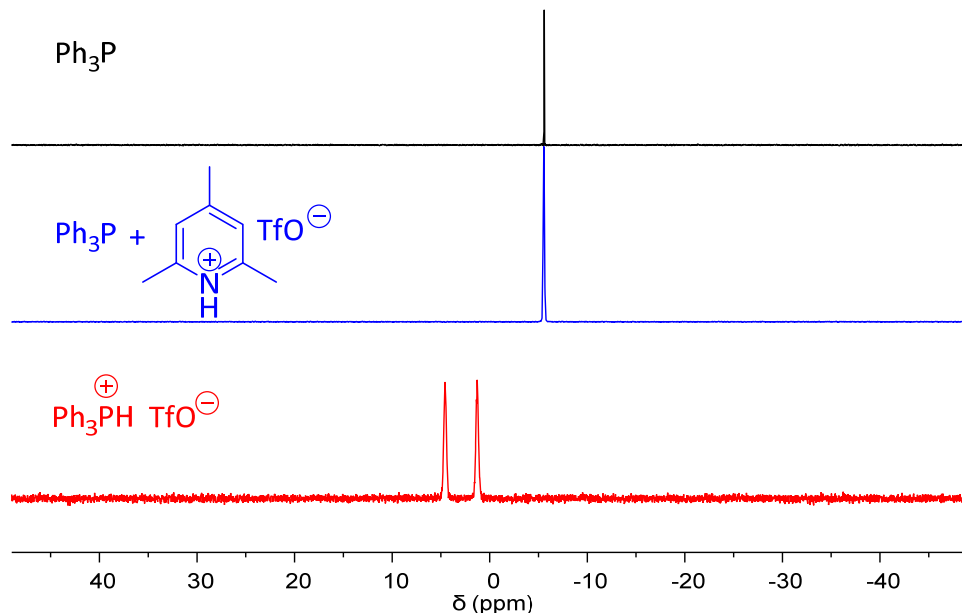


**Figure S5.** Comparison of the <sup>31</sup>P NMR spectra of Ph<sub>3</sub>P (top), Ph<sub>3</sub>PH<sup>+</sup> TfO<sup>-</sup> (bottom) with that of the mixture of Ph<sub>3</sub>P (58.3 mM) and CT (59.5 mM) in CD<sub>2</sub>Cl<sub>2</sub> (central).

### 3.2 Ethyl allenolate **1f** with CT

Figure S6 indicates that CT does not change the  $^1\text{H}$  NMR spectrum of alkyl allenolate **1f** (in  $\text{CD}_2\text{Cl}_2$ ).

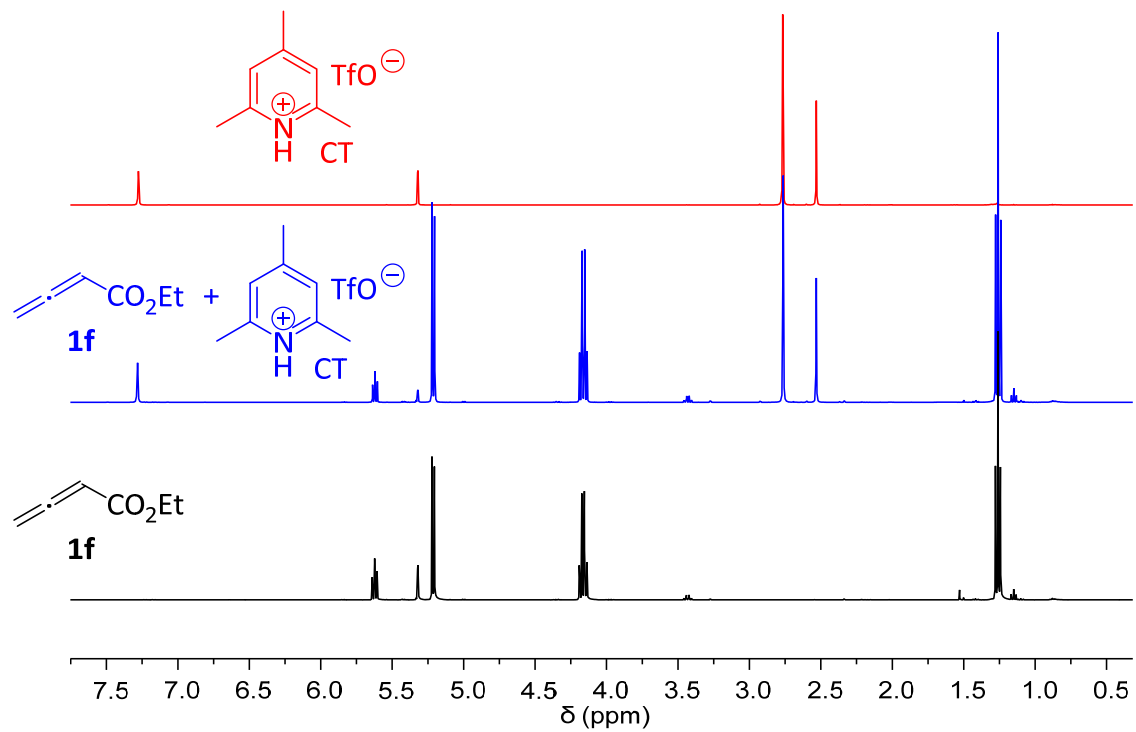


**Figure S6.** Comparison of the  $^1\text{H}$  NMR spectra of CT (top) and **1f** (bottom) with that of the mixture of CT (60 mM) and **1f** (180 mM) in  $\text{CD}_2\text{Cl}_2$  (central).

### 3.3 Ethyl allenolate **1f** with TBPT

Figure S7 shows that TBPT does not change the  $^1\text{H}$  NMR spectrum of alkyl allenolate **1f** (in  $\text{CD}_2\text{Cl}_2$ ).

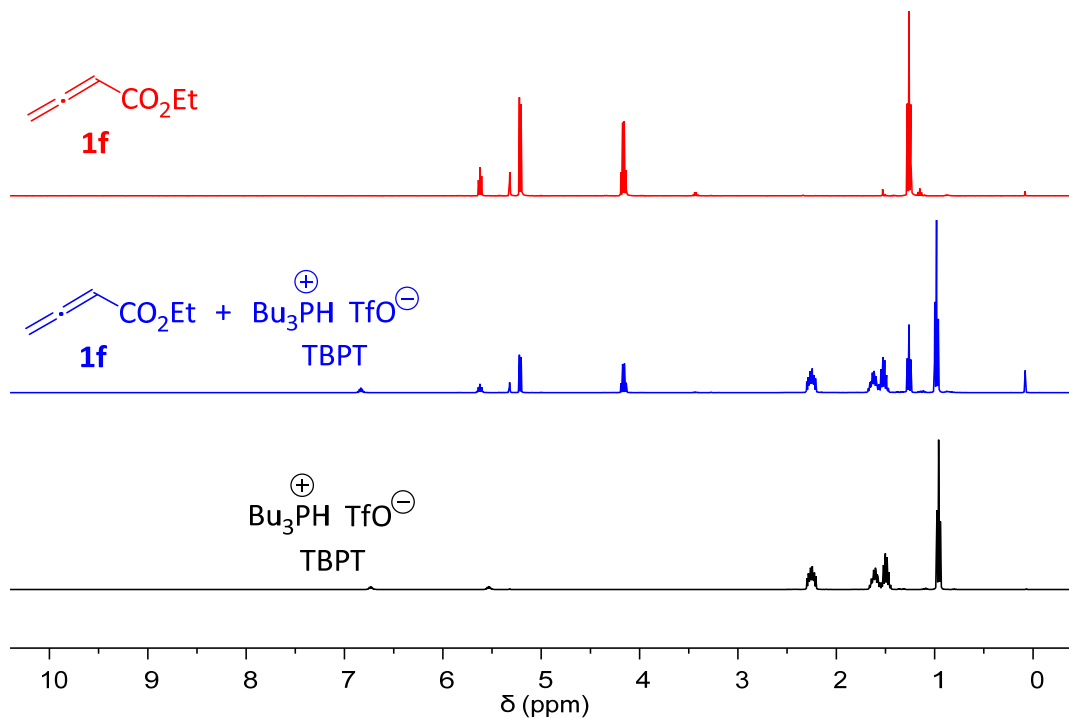
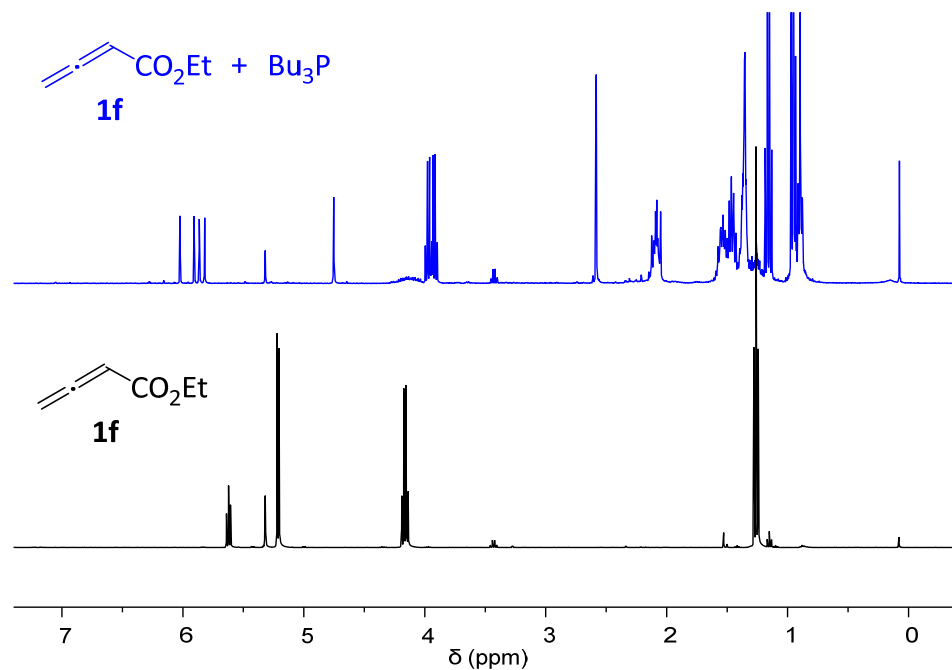


**Figure S7.** Comparison of the  $^1\text{H}$  NMR spectra of **1f** (top) and TBPT (bottom) with that of the mixture of **1f** (28.5 mM) and TBPT (28.9 mM, central) in  $\text{CD}_2\text{Cl}_2$  (central).

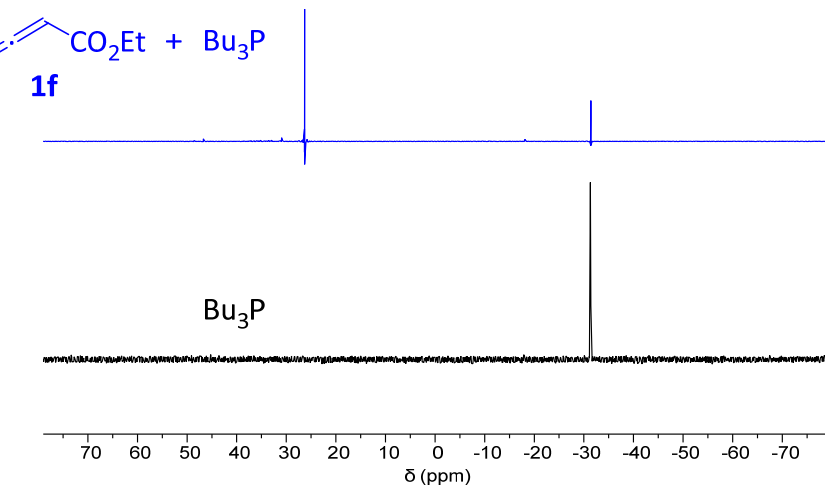
### 3.4 Stability of the R<sub>3</sub>P adducts of alkyl allenolate **1f**

#### 3.4.1 Analysis of mixtures of Bu<sub>3</sub>P with **1f**

Figures S8 and S9 shows that Bu<sub>3</sub>P reacts with alkyl allenolate **1f** (in CD<sub>2</sub>Cl<sub>2</sub>).



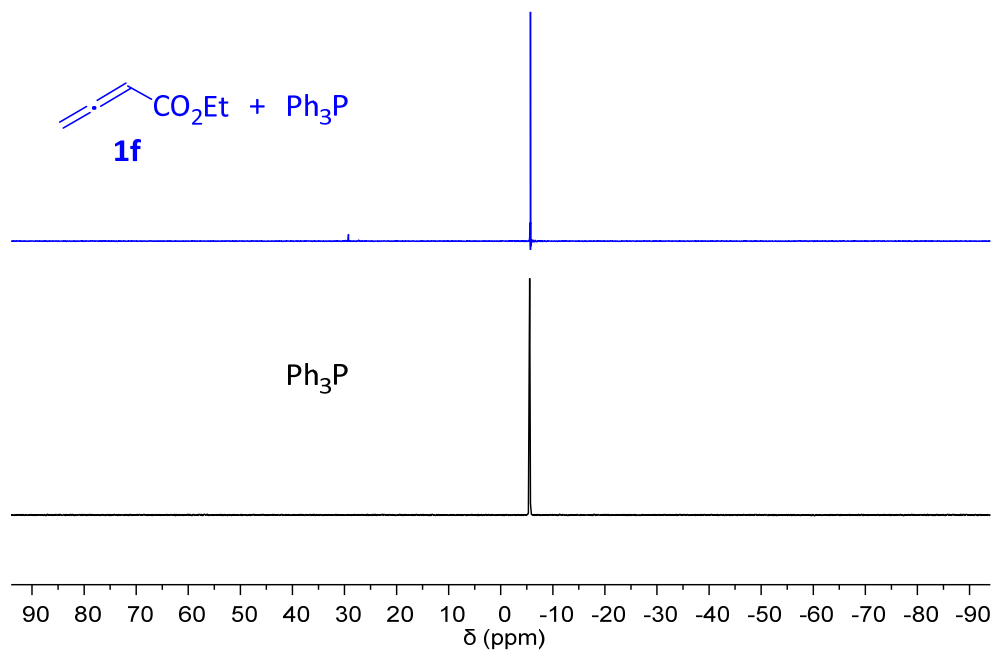
**Figure S8.** Comparison of the <sup>1</sup>H NMR spectra of **1f** (bottom) with that of a mixture of **1f** (69.0 mM) and Bu<sub>3</sub>P (59.3 mM) in CD<sub>2</sub>Cl<sub>2</sub> (top).



**Figure S9.** Comparison of the <sup>31</sup>P NMR spectra of Bu<sub>3</sub>P (bottom) with that of a mixture of **1f** (69.0 mM) and Bu<sub>3</sub>P (59.3 mM) in CD<sub>2</sub>Cl<sub>2</sub> (top).

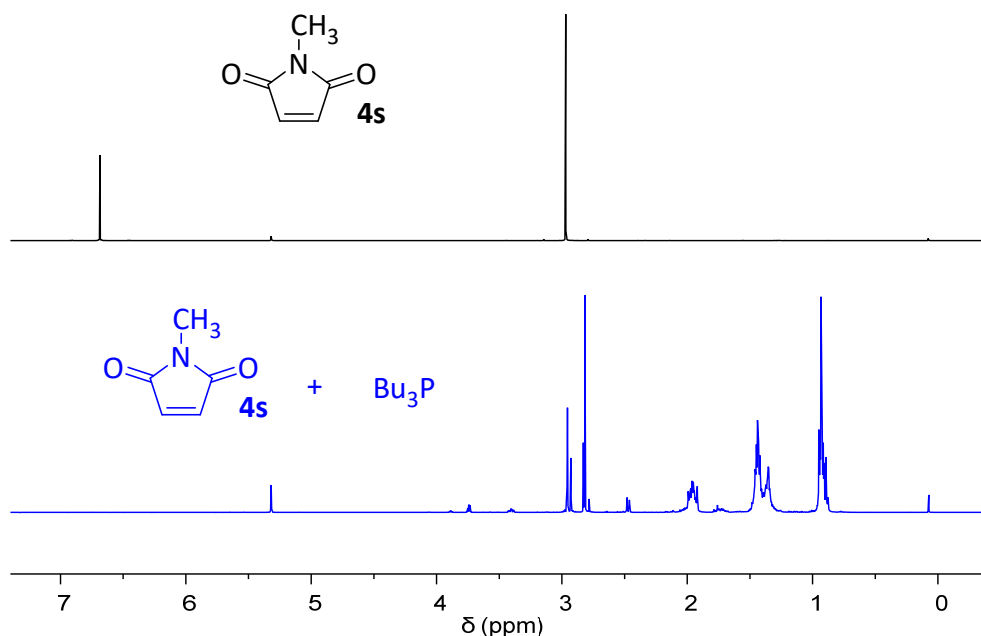
### 3.4.2 Analysis of mixtures of Ph<sub>3</sub>P with **1f**

Figure S10 shows that Ph<sub>3</sub>P, without a proton source, forms only a minor equilibrium concentration of adduct with alkyl allenoate **1f** (in CD<sub>2</sub>Cl<sub>2</sub>).



**Figure S10.** Comparison of the <sup>31</sup>P NMR spectra of Ph<sub>3</sub>P (bottom) with that of a mixture of **1f** (74.9 mM) and Ph<sub>3</sub>P (88.8 mM) in CD<sub>2</sub>Cl<sub>2</sub> at 20 °C (top).

### 3.4.3 Analysis of mixtures of $\text{Bu}_3\text{P}$ with *N*-methylmaleimide (**4s**)



**Figure S11.** Comparison of the  $^1\text{H}$  NMR spectra of **4s** (top) with that of the mixture of **4s** (54.3 mM) and  $\text{Bu}_3\text{P}$  (48.9 mM) in  $\text{CD}_2\text{Cl}_2$  (bottom).

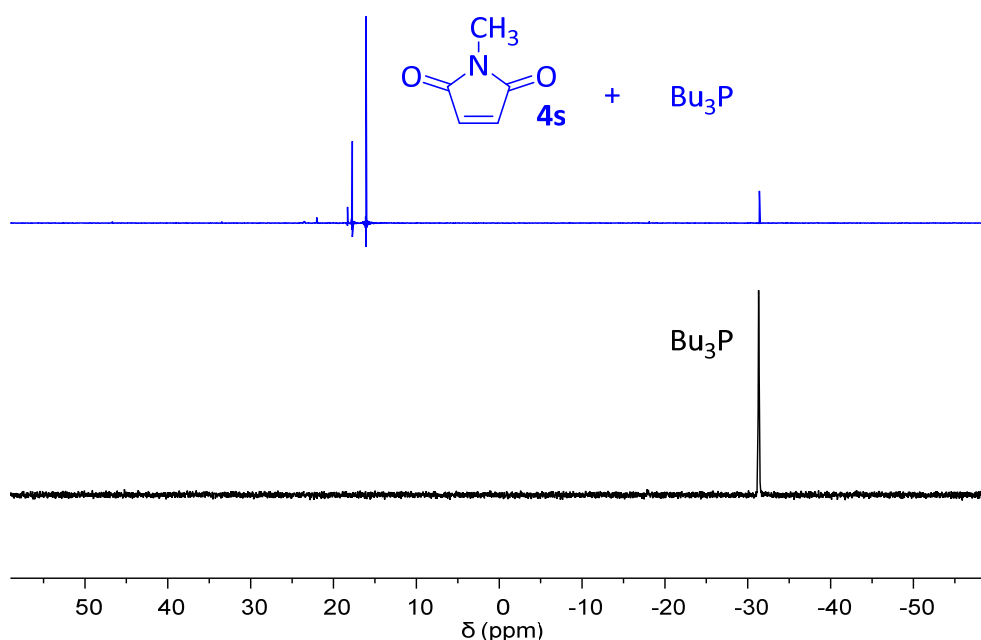


**Figure S12.** Comparison of the  $^{31}\text{P}$  NMR spectra of  $\text{Bu}_3\text{P}$  (bottom) with that of a mixture of  $\text{Bu}_3\text{P}$  (48.9 mM) and **4s** (54.3 mM) in  $\text{CD}_2\text{Cl}_2$  (top).

### 3.4.4 Analysis of mixtures of Ph<sub>3</sub>P with N-methylmaleimide (**4s**)

Figures S13 and S14 indicate that Ph<sub>3</sub>P does not form a detectable amount of adduct with **4s** (in CD<sub>2</sub>Cl<sub>2</sub>).

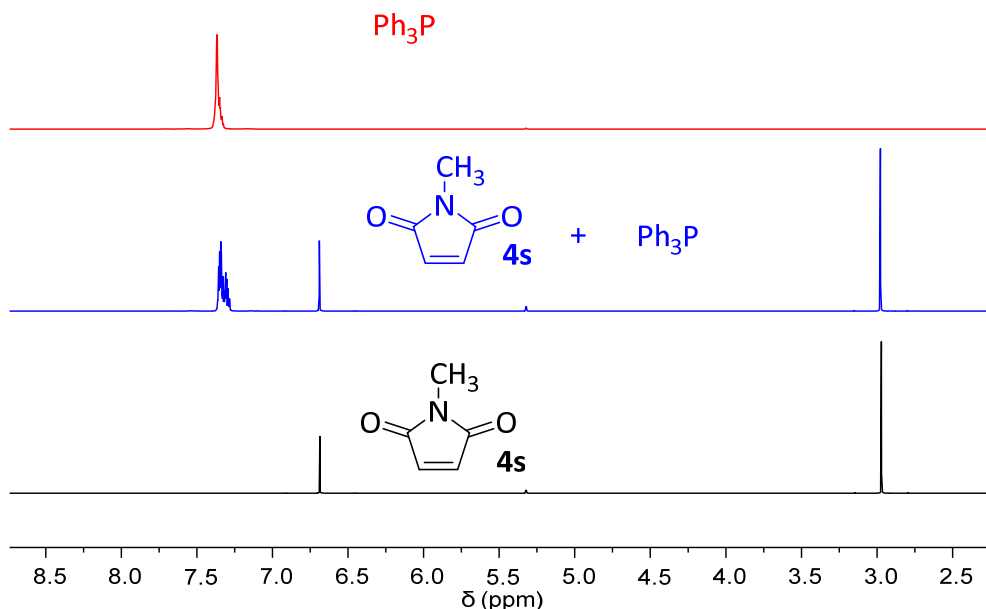


**Figure S13.** Comparison of the <sup>1</sup>H NMR spectra of Ph<sub>3</sub>P (top) and **4s** (bottom) with that of a mixture of **4s** (79.9 mM) and Ph<sub>3</sub>P (85.0 mM) in CD<sub>2</sub>Cl<sub>2</sub> at 20 °C (central).

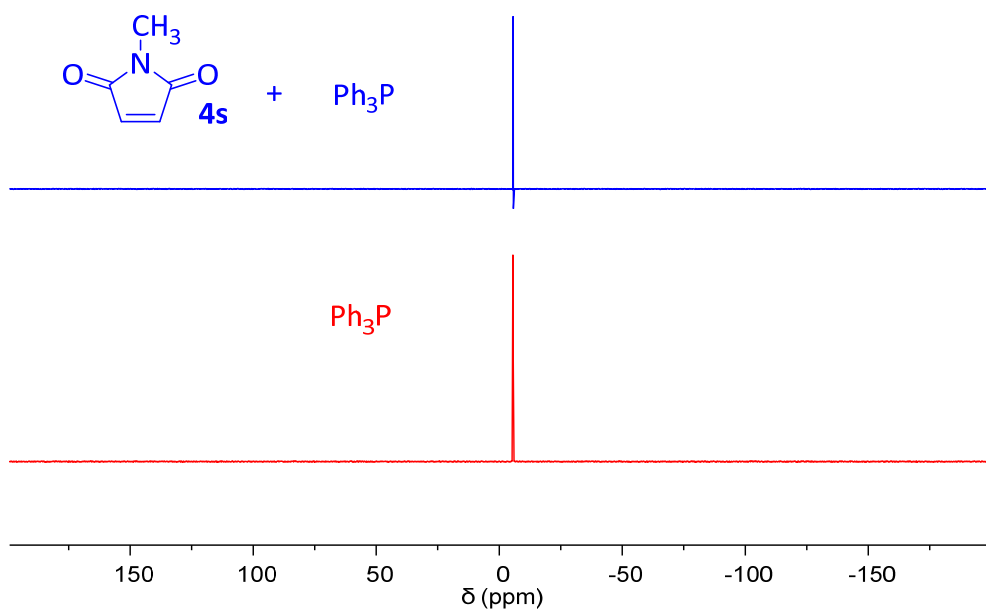


**Figure S14.** Comparison of the <sup>31</sup>P NMR spectra of Ph<sub>3</sub>P (bottom) with that of a mixture of **4s** (79.9 mM) and Ph<sub>3</sub>P (85.0 mM) in CD<sub>2</sub>Cl<sub>2</sub> at 20 °C (top).

### 3.4.5 Analysis of mixtures of $\text{Bu}_3\text{P}$ with phenyl N-tosyl imine (**4t**)

Figure S15 shows that  $\text{Bu}_3\text{P}$  slowly reacts with **4t** (in  $\text{CD}_2\text{Cl}_2$ ). However, a major part of free  $\text{Bu}_3\text{P}$  remains in a 1:1 mixture of  $\text{Bu}_3\text{P}$  with **4t**.

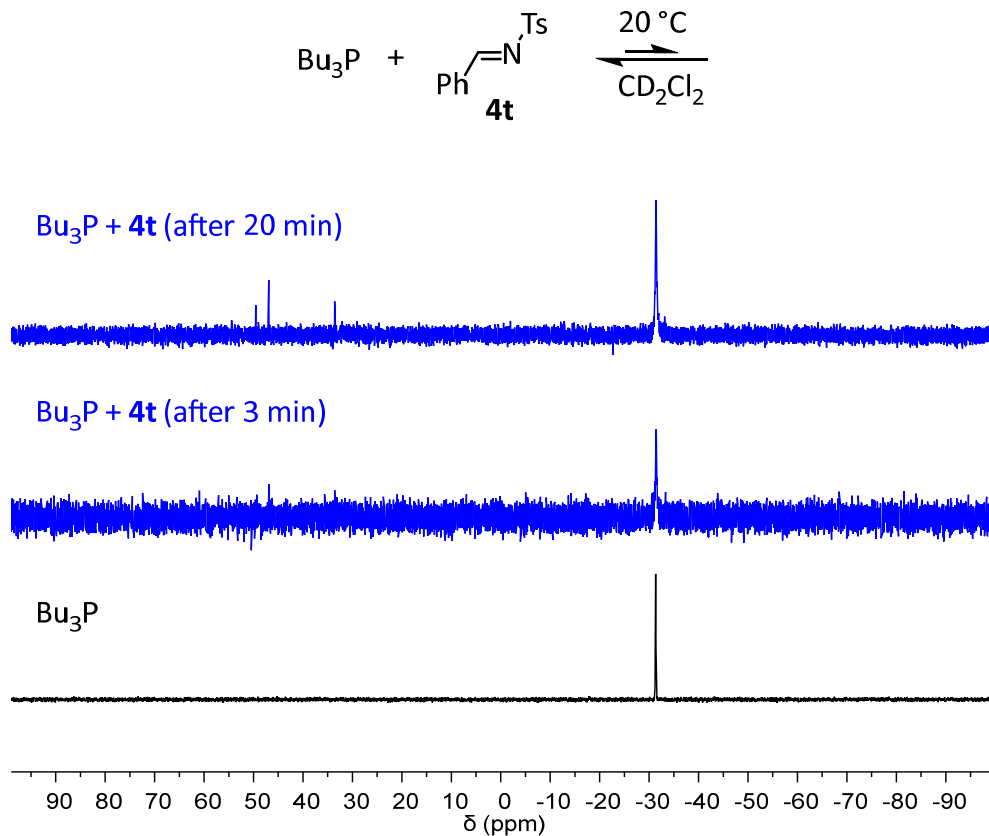


**Figure S15.** Comparison of the  ${}^{31}\text{P}$  NMR spectra of  $\text{Bu}_3\text{P}$  (bottom) with those of the mixture of **4t** (21.2 mM) and  $\text{Bu}_3\text{P}$  (16.8 mM) in  $\text{CD}_2\text{Cl}_2$  at different times (central: after 3 min, top: after 20 min).

### 3.4.6 Analysis of mixtures of $\text{Bu}_3\text{P}$ with benzylidene malononitrile (**4v**)

Figure S16 shows that  $\text{Bu}_3\text{P}$  reacts with **4v** (in  $\text{CD}_2\text{Cl}_2$ ). However, a part of free  $\text{Bu}_3\text{P}$  remains in an equilibrated 1:1 mixture of  $\text{Bu}_3\text{P}$  with **4v**.

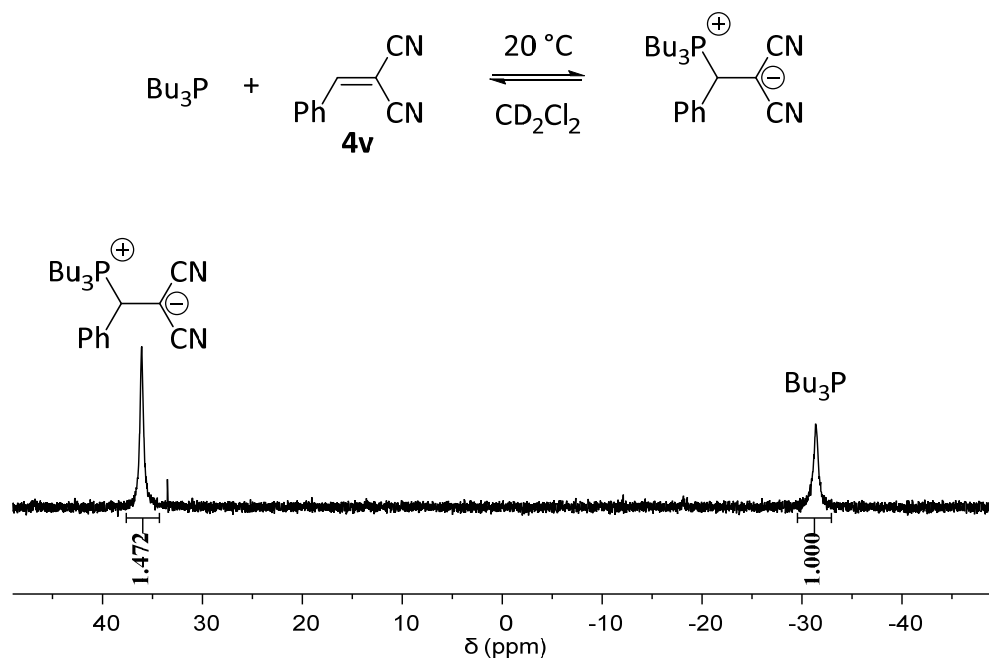


**Figure S16.**  $^{31}\text{P}$  NMR spectrum of the mixture of **4v** ( $c_0 = 40.8 \text{ mM}$ ) and  $\text{Bu}_3\text{P}$  ( $c_0 = 37.6 \text{ mM}$ ) in  $\text{CD}_2\text{Cl}_2$ , which shows an equilibrium with the adduct zwitterion.

### 3.4.7 Analysis of mixtures of Ph<sub>3</sub>P with benzylidenemalononitrile (**4v**)

Figures S17 and S18 indicate that Ph<sub>3</sub>P does not form a detectable amount of adduct with **4v** (in CD<sub>2</sub>Cl<sub>2</sub>).

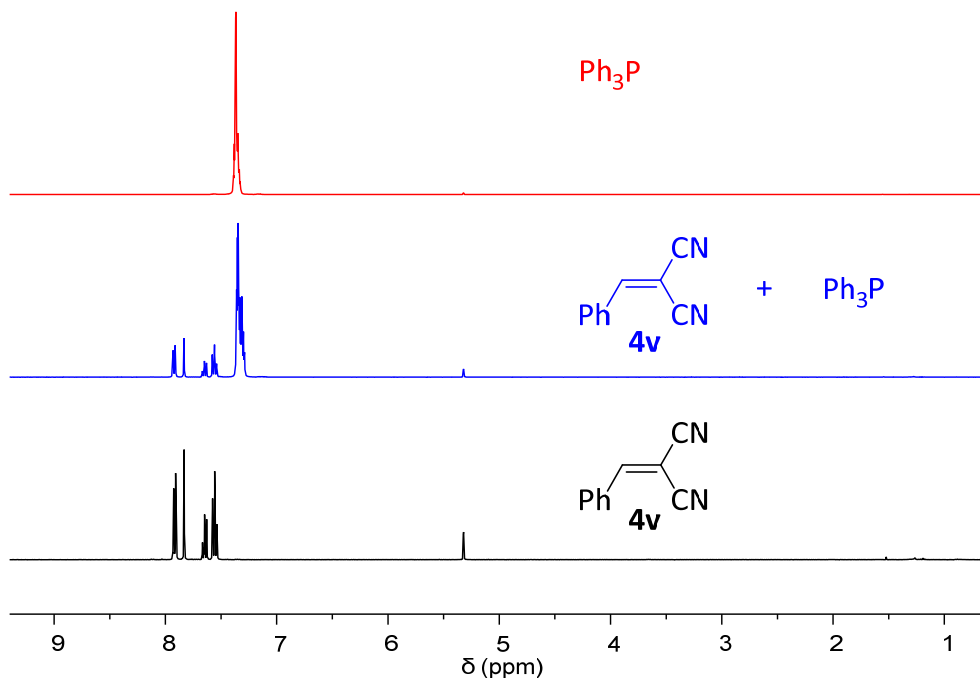


**Figure S17.** Comparison of the <sup>1</sup>H NMR spectra of Ph<sub>3</sub>P (top) and **4v** (bottom) with that of the mixture of **4v** (69.4 mM) and Ph<sub>3</sub>P (88.5 mM) in CD<sub>2</sub>Cl<sub>2</sub> at 20 °C (central).

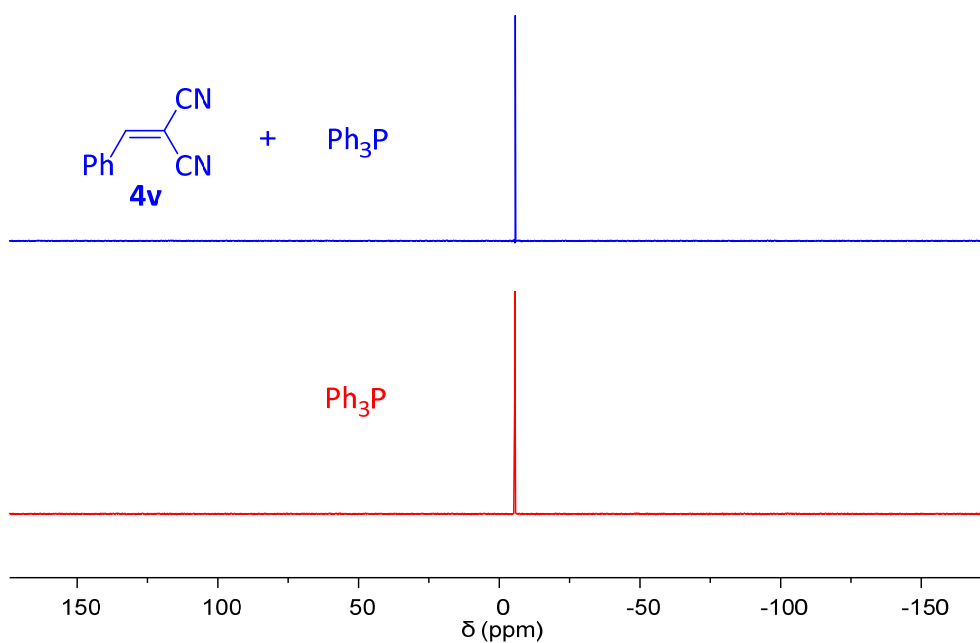
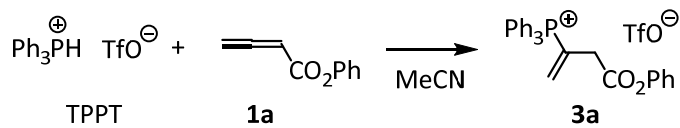


**Figure S18.** Comparison of the <sup>31</sup>P NMR spectra of Ph<sub>3</sub>P (bottom) with that of the mixture of **4v** (69.4 mM) and Ph<sub>3</sub>P (88.5 mM) in CD<sub>2</sub>Cl<sub>2</sub> at 20 °C (top).

## 4 Product Studies

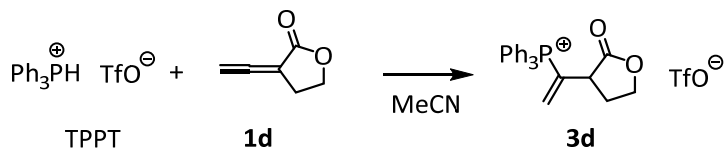
### 4.1 Reaction of triphenylphosphonium triflate with phenyl buta-2,3-dienoate (1a)



TPPT (48.9 mg, 119 mmol) and **1a** (30.7 mg, 192 mmol) were mixed in acetonitrile (1 mL). The mixture was kept under inert gas atmosphere at ambient temperature for 18 h. The volatiles were removed under reduced pressure. The residue was washed with diethyl ether and dried under high vacuum to provide **3a** (57.3 mg, 84%) as a white solid; mp 184.3–186.9 °C.

**$^1\text{H NMR}$**  (400 MHz,  $\text{CD}_2\text{Cl}_2$ )  $\delta$  7.99–7.86 (m, 3 H), 7.80–7.69 (m, 12 H), 7.35–7.32 (m, 2 H), 7.25–7.21 (m, 1 H), 7.09 (d,  $J_{\text{H},\text{P}} = 45.4$  Hz, 1 H), 6.74 (d,  $J_{\text{H},\text{P}} = 7.9$  Hz, 2 H), 6.37 (d,  $J_{\text{H},\text{P}} = 20.9$  Hz, 1 H), 3.91 (d,  $J_{\text{H},\text{P}} = 15.3$  Hz, 2 H).  **$^{13}\text{C}\{^1\text{H}\} \text{NMR}$**  (101 MHz,  $\text{CD}_2\text{Cl}_2$ )  $\delta$  168.6 (d,  $^3J_{\text{C},\text{P}} = 2.9$  Hz,  $\text{C}_\text{q}$ ), 150.4 ( $\text{C}_\text{q}$ ), 146.5 (d,  $^2J_{\text{C},\text{P}} = 7.5$  Hz,  $=\text{CH}_2$ ), 136.2 (d,  $J_{\text{C},\text{P}} = 3.0$  Hz, CH), 135.0 (d,  $J_{\text{C},\text{P}} = 10.4$  Hz, CH), 131.0 (d,  $J_{\text{C},\text{P}} = 12.9$  Hz, CH), 129.9 (CH), 126.8 (CH), 124.8 (d,  $^1J_{\text{C},\text{P}} = 78.7$  Hz,  $\text{C}_\text{q}$ ), 121.4 (CH), 117.1 (d,  $^1J_{\text{C},\text{P}} = 88.7$  Hz,  $\text{C}_\text{q}$ ), 39.2 (d,  $^2J_{\text{C},\text{P}} = 11.4$  Hz,  $\text{CH}_2$ ); resonances of the  $\text{CF}_3$  group superimpose with other signals and could not be assigned unequivocally.  **$^{31}\text{P NMR}$**  (162 MHz,  $\text{CD}_2\text{Cl}_2$ )  $\delta$  25.1.  **$^{19}\text{F NMR}$**  (377 MHz,  $\text{CD}_2\text{Cl}_2$ )  $\delta$  –78.9. **IR** (neat, ATR):  $\tilde{\nu} = 3065, 2925, 1752, 1589, 1485, 1439, 1340, 1261, 1224, 1192, 1147, 1108, 1030, 998, 754, 726, 712, 690 \text{ cm}^{-1}$ . **HRMS (ESI)**:  $m/z$  calcd for  $\text{C}_{28}\text{H}_{24}\text{O}_2\text{P}^+$  ( $\text{M} - \text{TfO}^-$ ): 423.15084, found: 423.15067.

### 4.2 Reaction of triphenylphosphonium triflate with 3-vinylidenedihydrofuran-2(3H)-one (1d)

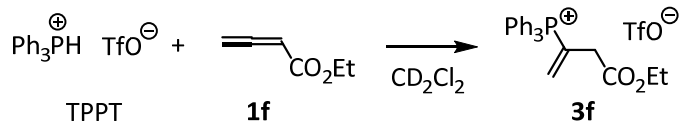


TPPT (50.8 mg, 123 mmol) and **1d** (22.8 mg, 207 mmol) were mixed in acetonitrile (1 mL). The mixture was kept under inert gas atmosphere at ambient temperature for 22 h. The volatiles were removed under reduced pressure. The residue was washed with diethyl ether and dried under high vacuum to provide **3d** (62.5 mg, 97%) as a white solid.

**$^1\text{H NMR}$**  (400 MHz,  $\text{CD}_2\text{Cl}_2$ )  $\delta$  7.92–7.77 (m, 15 H), 6.90 (d,  $J_{\text{H},\text{P}} = 46.1$  Hz, 1 H), 6.35 (d,  $J_{\text{H},\text{P}} = 21.9$  Hz, 1 H), 4.43–4.38 (m, 1 H), 4.21 (q,  $J = 8.7$  Hz, 1 H), 3.63 (q,  $J = 10.7$  Hz, 1 H), 2.44–2.38 (m, 2 H).  **$^{13}\text{C}\{^1\text{H}\} \text{NMR}$**  (101 MHz,  $\text{CD}_2\text{Cl}_2$ )  $\delta$  175.2 (d,  $^3J_{\text{C},\text{P}} = 6.9$  Hz,  $\text{C}_\text{q}$ ), 144.1 (d,  $^2J_{\text{C},\text{P}} = 7.8$  Hz,  $=\text{CH}_2$ ), 136.1 (d,  $J_{\text{C},\text{P}} = 3.1$  Hz, CH), 135.0 (d,  $J_{\text{C},\text{P}} = 10.3$  Hz, CH), 131.0 (d,  $J_{\text{C},\text{P}} = 12.9$  Hz, CH), 129.3 (d,  $^1J_{\text{C},\text{P}} = 79.4$  Hz,  $\text{C}_\text{q}$ ), 121.4 (q,  $^1J_{\text{C},\text{F}} = 320.9$  Hz,  $\text{CF}_3$ ), 116.9 (d,  $^1J_{\text{C},\text{P}} = 88.8$  Hz,  $\text{C}_\text{q}$ ), 67.4 (CH<sub>2</sub>), 43.7 (d,  $^2J_{\text{C},\text{P}} = 11.9$  Hz, CH), 31.3 (d,  $J_{\text{C},\text{P}} = 3.8$  Hz, CH<sub>2</sub>).  **$^{31}\text{P NMR}$**  (162 MHz,  $\text{CD}_2\text{Cl}_2$ )  $\delta$  26.1.  **$^{19}\text{F NMR}$**  (377 MHz,  $\text{CD}_2\text{Cl}_2$ )  $\delta$  –78.9. **IR** (neat, ATR):  $\tilde{\nu} =$

$\nu$  = 3065, 1762, 1588, 1485, 1439, 1379, 1263, 1224, 1153, 1108, 1030, 998, 754, 726, 692  $\text{cm}^{-1}$ . **HRMS** (ESI):  $m/z$  calcd for  $\text{C}_{24}\text{H}_{22}\text{O}_2\text{P}^+$  ( $\text{M} - \text{TfO}^-$ ): 373.13519, found: 373.13511.

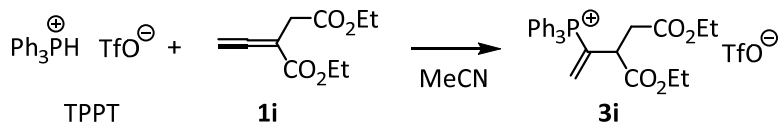
#### 4.3 Reaction of triphenylphosphonium triflate with ethyl buta-2,3-dienoate (1f)



TPPT (186 mg, 451 mmol) and **1f** (54.5 mg, 486 mmol) were mixed in  $\text{CD}_2\text{Cl}_2$  (1.5 mL). The mixture was kept under inert gas atmosphere at ambient temperature for 40 h. The volatiles were removed under reduced pressure. The residue was washed with pentane and dried under high vacuum to provide **3f** (230 mg, 97%) as a white solid; mp 97.3–98.3 °C.

**$^1\text{H NMR}$**  (600 MHz,  $\text{CD}_2\text{Cl}_2$ )  $\delta$  7.92–7.89 (m, 3 H), 7.76–7.68 (m, 12 H), 6.94 (dd,  $J_{\text{H,P}} = 45.6$  Hz,  $J_{\text{H,H}} = 1.2$  Hz, 1 H), 6.29 (dd,  $J_{\text{H,P}} = 21.0$  Hz,  $J_{\text{H,H}} = 1.2$  Hz, 1 H), 3.86 (q,  $J_{\text{H,H}} = 7.1$  Hz, 2 H), 3.56 (dd,  $J_{\text{H,P}} = 15.4$  Hz,  $J_{\text{H,H}} = 1.1$  Hz, 2 H), 1.06 (t,  $J_{\text{H,H}} = 7.1$  Hz, 3 H).  **$^{13}\text{C}\{^1\text{H}\} \text{NMR}$**  (151 MHz,  $\text{CD}_2\text{Cl}_2$ )  $\delta$  169.2 (d,  $^3J_{\text{C,P}} = 3.1$  Hz,  $\text{C}_\text{q}$ ), 145.6–145.5 (m, = $\text{CH}_2$ ), 136.1 (d,  $J_{\text{C,P}} = 3.1$  Hz, CH), 134.9 (d,  $J_{\text{C,P}} = 10.3$  Hz, CH), 130.9 (d,  $J_{\text{C,P}} = 12.9$  Hz, CH), 125.3 (d,  $^1J_{\text{C,P}} = 78.1$  Hz,  $\text{C}_\text{q}$ ), 121.4 (q,  $^1J_{\text{C,F}} = 321.5$  Hz,  $\text{CF}_3$ ), 117.1 (d,  $^1J_{\text{C,P}} = 88.6$  Hz,  $\text{C}_\text{q}$ ), 62.3 ( $\text{CH}_2$ ), 39.2 (d,  $^2J_{\text{C,P}} = 11.6$  Hz,  $\text{CH}_2$ ), 14.1 ( $\text{CH}_3$ ).  **$^{31}\text{P NMR}$**  (162 MHz,  $\text{CD}_2\text{Cl}_2$ )  $\delta$  25.3.  **$S^{18} \text{F NMR}$**  (377 MHz,  $\text{CD}_2\text{Cl}_2$ )  $\delta$  –78.9. **IR** (neat, ATR):  $\tilde{\nu}$  = 2983, 1732, 1586, 1484, 1441, 1334, 1258, 1223, 1204, 1154, 1107, 1027, 996, 970, 948, 861, 755, 724, 712, 690, 658  $\text{cm}^{-1}$ . **HRMS** (ESI):  $m/z$  calcd for  $\text{C}_{24}\text{H}_{24}\text{O}_2\text{P}^+$  ( $\text{M} - \text{TfO}^-$ ): 375.15084, found: 375.15072.

#### 4.4 Reaction of triphenylphosphonium triflate with diethyl 2-vinylidenesuccinate (1i)



TPPT (50.0 mg, 121 mmol) and **1i** (30.5 mg, 154 mmol) were mixed in acetonitrile (1.0 mL). The mixture was kept under inert gas atmosphere at ambient temperature for one week. The volatiles were removed under reduced pressure. The residue was washed with pentane and dried under high vacuum to provide **3i** (55.5 mg, 75%) as a colorless liquid.

**$^1\text{H NMR}$**  (400 MHz,  $\text{CD}_2\text{Cl}_2$ )  $\delta$  7.93–7.89 (m, 3 H), 7.77–7.68 (m, 12 H), 6.90 (ddd,  $J_{\text{H,P}} = 46.3$  Hz,  $J_{\text{H,H}} = 2.4, 0.8$  Hz, 1 H), 6.34 (dd,  $J_{\text{H,P}} = 21.6$  Hz,  $J_{\text{H,H}} = 2.3$  Hz, 1 H), 4.12–3.99 (m, 3 H), 3.89 (dq,  $J = 10.8, 7.1$  Hz, 1 H), 3.77 (ddd,  $J_{\text{H,P}} = 12.9$  Hz,  $^3J_{\text{H,H}} = 9.4$  Hz, 5.8 Hz, 1 H), 3.06 (ddd,  $^2J_{\text{H,H}} = 17.6$  Hz,  $^3J_{\text{H,H}} = 5.8$  Hz,  $^4J_{\text{H,P}} = 1.5$  Hz, 1 H), 2.90 (dd,  $^2J_{\text{H,H}} = 17.6$  Hz,  $^3J_{\text{H,H}} = 9.4$  Hz, 1 H), 1.21 (t,  $J_{\text{H,H}} = 7.1$  Hz, 3 H), 1.03 (t,  $J_{\text{H,H}} = 7.2$  Hz, 3 H).  **$^{13}\text{C}\{^1\text{H}\} \text{NMR}$**  (101 MHz,  $\text{CD}_2\text{Cl}_2$ )  $\delta$  170.7 ( $\text{C}_\text{q}$ ), 170.1 (d,  $^3J_{\text{C,P}} = 3.9$  Hz,  $\text{C}_\text{q}$ ), 142.0 (d,  $^2J_{\text{C,P}} = 7.4$

Hz, =CH<sub>2</sub>), 136.2 (d,  $J_{C,P}$  = 3.1 Hz, CH), 135.1 (d,  $J_{C,P}$  = 10.3 Hz, CH), 130.8 (d,  $J_{C,P}$  = 12.9 Hz, CH), 130.2 (d,  $^1J_{C,P}$  = 77.8 Hz, C<sub>q</sub>), 121.5 (q,  $^1J_{C,F}$  = 321.3 Hz, CF<sub>3</sub>), 117.2 (d,  $^1J_{C,P}$  = 88.8 Hz, C<sup>q</sup>), 62.9 (CH<sub>2</sub>), 62.0 (CH<sub>2</sub>), 42.9 (d,  $^2J_{C,P}$  = 11.3 Hz, CH), 36.3 (d,  $J_{C,P}$  = 5.4 Hz, CH<sub>2</sub>), 14.3 (CH<sub>3</sub>), 13.9 (CH<sub>3</sub>). **<sup>31</sup>P NMR** (162 MHz, CD<sub>2</sub>Cl<sub>2</sub>) δ 27.5. **<sup>19</sup>F NMR** (377 MHz, CD<sub>2</sub>Cl<sub>2</sub>) δ -78.9. **IR** (neat, ATR):  $\tilde{\nu}$  = 3066, 2985, 1730, 1587, 1485, 1440, 1263, 1224, 1150, 1107, 1030, 998, 857, 754, 725, 692 cm<sup>-1</sup>. **HRMS** (ESI): *m/z* calcd for C<sub>28</sub>H<sub>30</sub>O<sub>4</sub>P<sup>+</sup> (M - TfO<sup>-</sup>): 461.18762, found: 461.18744.

## 5 Kinetics

### 5.1 General

#### Kinetic Measurements with the stopped-flow UV-Vis spectrometer

The kinetics of the faster reactions ( $t_{1/2} < 20$  s) were followed by UV/vis spectroscopy by using a stopped-flow spectrophotometer system (Applied Photophysics SX20 Stopped Flow Spectrometers; 5 or 10 mm light path). The kinetic runs were initiated by mixing equal volumes of dichloromethane solutions of the nucleophiles and the electrophiles. The temperature of the solutions during the kinetic studies was maintained to  $20 \pm 0.2$  °C by using circulating bath cryostats. Stock solutions were prepared in anhydrous dichloromethane, which was freshly distilled from calcium hydride. The R<sub>3</sub>P solutions were freshly prepared under argon atmosphere before each measurement.

#### Kinetic measurements with conventional UV-Vis spectroscopy

The rates of slow reactions ( $t_{1/2} > 20$  s) were determined by using a J&M TIDAS diode array spectrophotometers controlled by Labcontrol Spectacle or TIDAS DAQ 3.8.1 software and connected to Hellma 661.502-QX quartz Suprasil immersion probe (5 mm light path) via fiber optic cables and standard SMA connectors. The temperature of the solutions during the kinetic studies was maintained to  $20 \pm 0.1$  °C by using circulating bath cryostats. Anhydrous dichloromethane was freshly distilled from calcium hydride under an atmosphere of dry nitrogen. The R<sub>3</sub>P solutions were freshly prepared under argon atmosphere before each measurement.

#### Kinetic measurements with NMR spectroscopy

The kinetics for reactions with  $k_2 < 2.0 \times 10^{-1}$  M<sup>-1</sup> s<sup>-1</sup> were followed by using a Bruker Avance III HD 400 MHz NMR spectrophotometer, which is equipped with a N<sub>2</sub> cooling temperature unit ( $20 \pm 0.1$  °C). <sup>1</sup>H NMR kinetics used mesitylene (internal integration standard) or CD<sub>2</sub>Cl<sub>2</sub> residual peak as internal reference standard. Stock solutions were prepared in CD<sub>2</sub>Cl<sub>2</sub>, which was stored under Ar atmosphere protection. The exact 1.0 mL solutions in NMR tube were prepared freshly under Ar atmosphere protection and monitored immediately after complete mixing of the reactants.

## 5.2 Kinetics of the reactions of R<sub>3</sub>P with alkyl allenoates 1

### 5.2.1 Kinetics of the reactions of 1 with Bu<sub>3</sub>P in dichloromethane

#### 5.2.1.1 Kinetics of the reaction of Bu<sub>3</sub>P with phenyl buta-2,3-dienoate (1a)

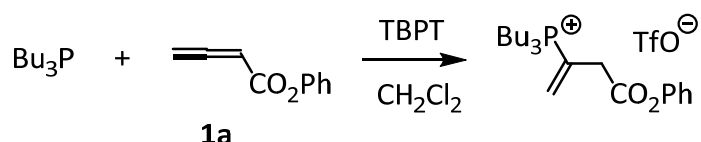
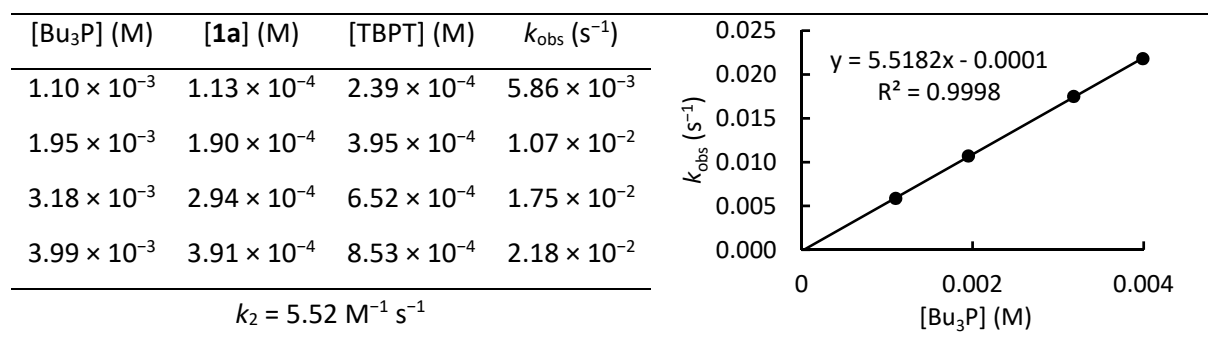


**Table S3.** Kinetics of the reactions of Bu<sub>3</sub>P and **1a** (proton source: TBPT, conventional UV-Vis method, detection at 242 nm, in CH<sub>2</sub>Cl<sub>2</sub>)



#### 5.2.1.2 Kinetics of the reaction of Bu<sub>3</sub>P with benzyl buta-2,3-dienoate (1b)

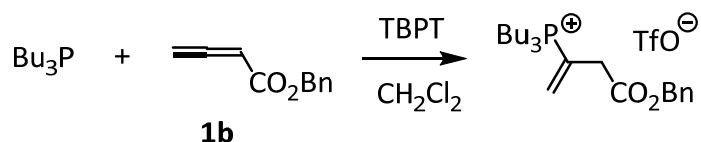
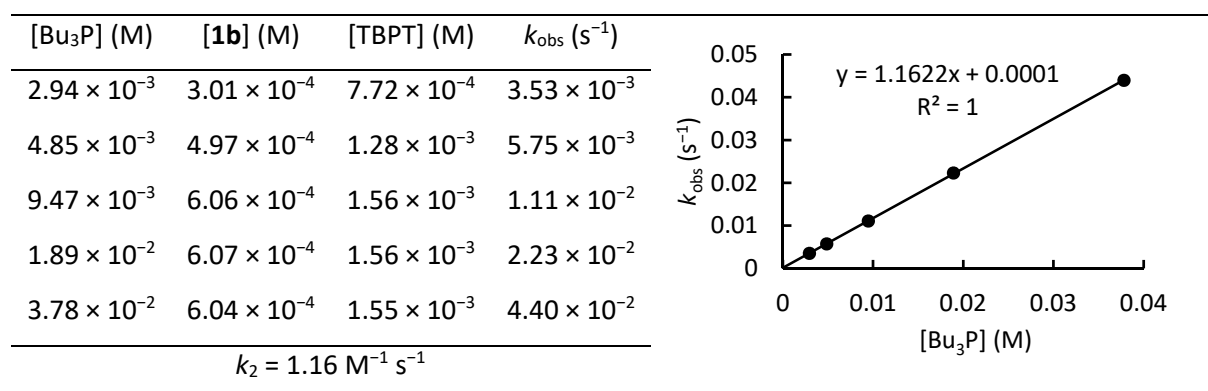


**Table S4.** Kinetics of the reactions of Bu<sub>3</sub>P and **1b** (proton source: TBPT, conventional UV-Vis method, detection at 250 nm, in CH<sub>2</sub>Cl<sub>2</sub>)



### 5.2.1.3 Kinetics of the reaction of $\text{Bu}_3\text{P}$ with ethyl 4-phenylbuta-2,3-dienoate (**1c**)

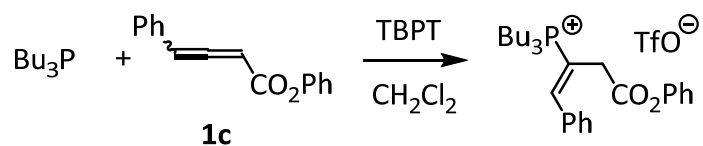
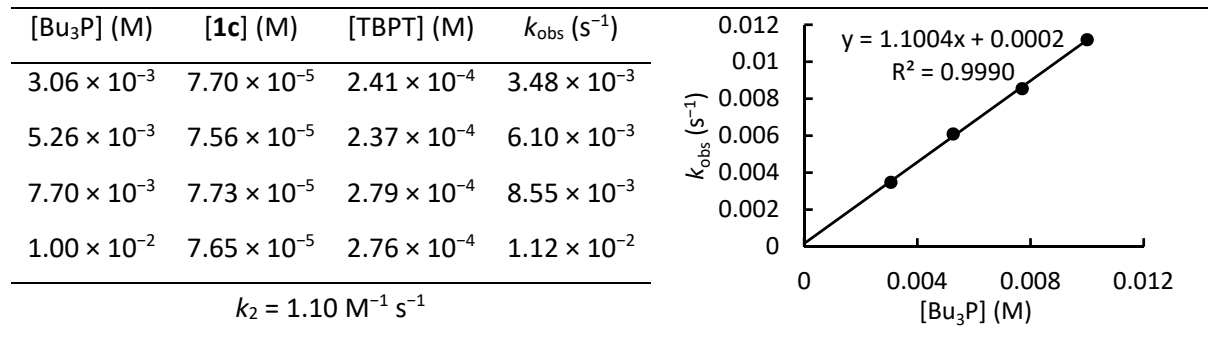


**Table S5.** Kinetics of the reactions of  $\text{Bu}_3\text{P}$  and **1c** (proton source: TBPT, conventional UV-Vis method, detection at 248 nm, in  $\text{CH}_2\text{Cl}_2$ )



### 5.2.1.4 Kinetics of the reaction of $\text{Bu}_3\text{P}$ with 3-vinylidenedihydrofuran-2(3H)-one (**1d**)

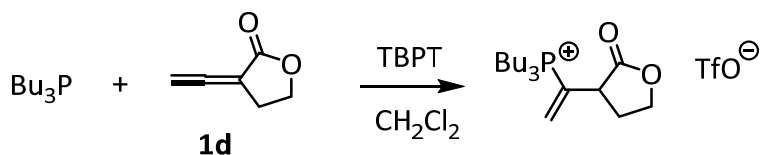
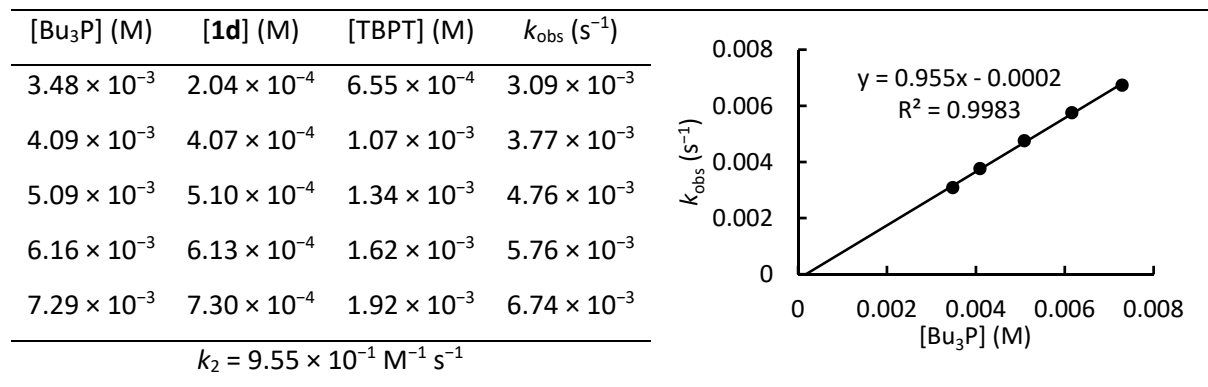


**Table S6** Kinetics of the reactions of  $\text{Bu}_3\text{P}$  and **1d** (proton source: TBPT, conventional UV-Vis method, detection at 259 nm, in  $\text{CH}_2\text{Cl}_2$ )



### 5.2.1.5 Kinetics of the reaction of $\text{Bu}_3\text{P}$ with methyl buta-2,3-dienoate (**1e**)

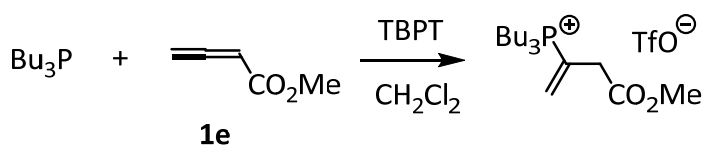
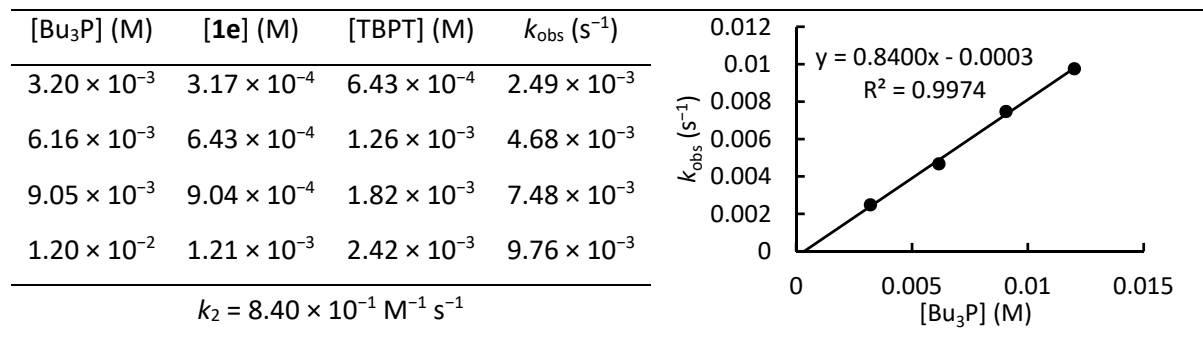


**Table S7.** Kinetics of the reactions of  $\text{Bu}_3\text{P}$  and **1e** (proton source: TBPT, conventional UV-Vis method, detection at 250 nm, in  $\text{CH}_2\text{Cl}_2$ )



### 5.2.1.6 Kinetics of the reaction of $\text{Bu}_3\text{P}$ with ethyl buta-2,3-dienoate (**1f**)

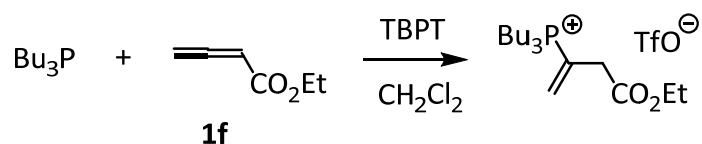
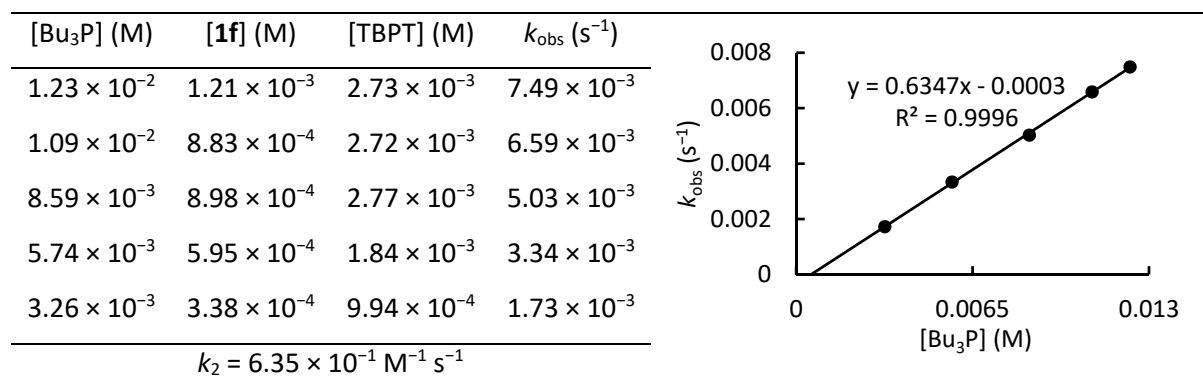


**Table S8.** Kinetics of the reactions of  $\text{Bu}_3\text{P}$  and **1f** (proton source: TBPT, conventional UV-Vis method, detection at 250 nm, in  $\text{CH}_2\text{Cl}_2$ )



### 5.2.1.7 Kinetics of the reaction of $\text{Bu}_3\text{P}$ with ethyl penta-2,3-dienoate (**1g**)

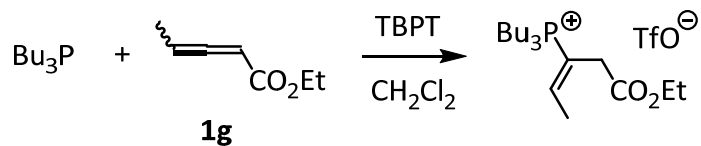
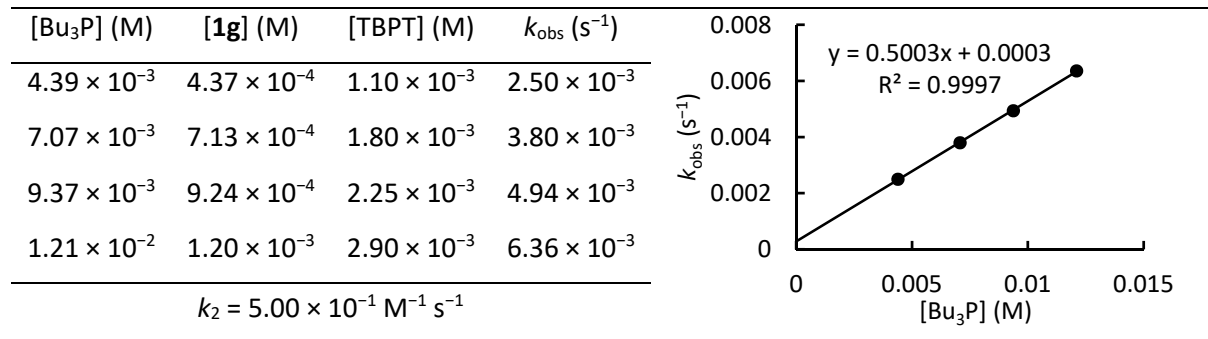


**Table S9.** Kinetics of the reactions of  $\text{Bu}_3\text{P}$  and **1g** (proton source: TBPT, conventional UV-Vis method, detection at 258 nm, in  $\text{CH}_2\text{Cl}_2$ )



### 5.2.1.8 Kinetics of the reaction of $\text{Bu}_3\text{P}$ with *tert*-butyl buta-2,3-dienoate (**1h**)

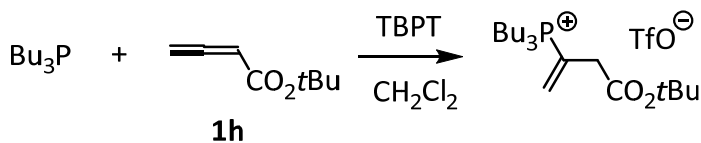
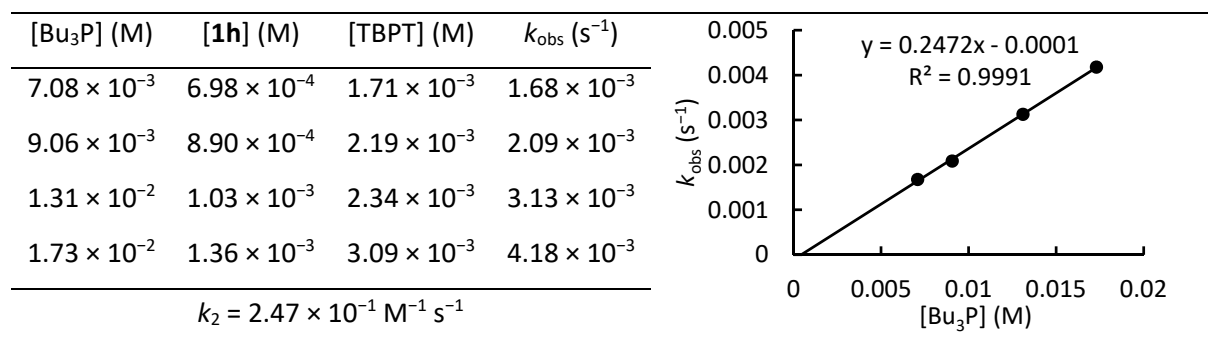


**Table S10.** Kinetics of the reactions of  $\text{Bu}_3\text{P}$  and **1h** (proton source: TBPT, conventional UV-Vis method, detection at 256 nm, in  $\text{CH}_2\text{Cl}_2$ )



### 5.2.1.9 Kinetics of the reaction of $\text{Bu}_3\text{P}$ with diethyl 2-vinylidenesuccinate (**1i**)

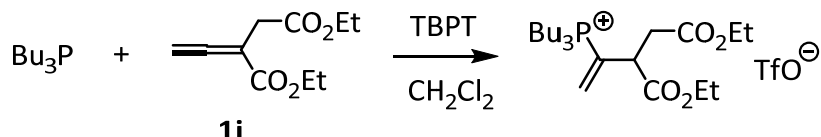
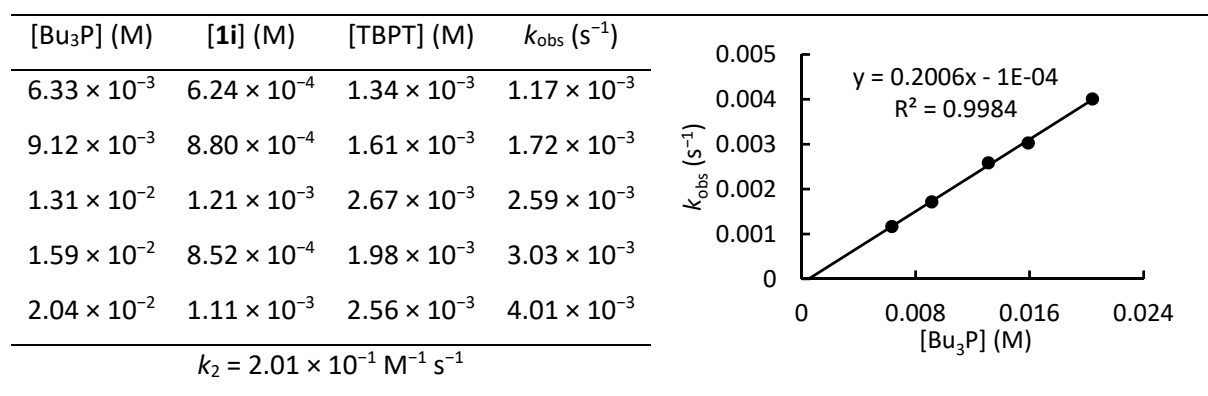


**Table S11.** Kinetics of the reactions of  $\text{Bu}_3\text{P}$  and **1i** (proton source: TBPT, conventional UV-Vis method, detection at 250 nm, in  $\text{CH}_2\text{Cl}_2$ )



### 5.2.1.10 Kinetics of the reaction of $\text{Bu}_3\text{P}$ with ethyl 2-methylbuta-2,3-dienoate (**1j**)

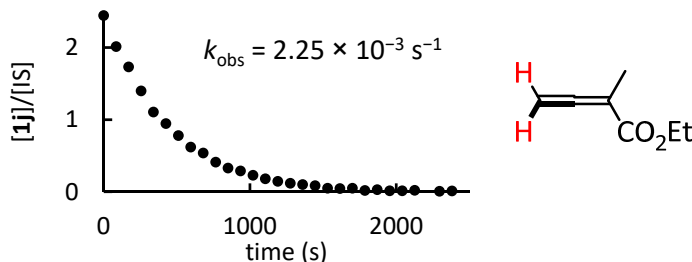
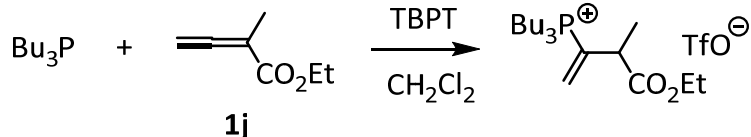
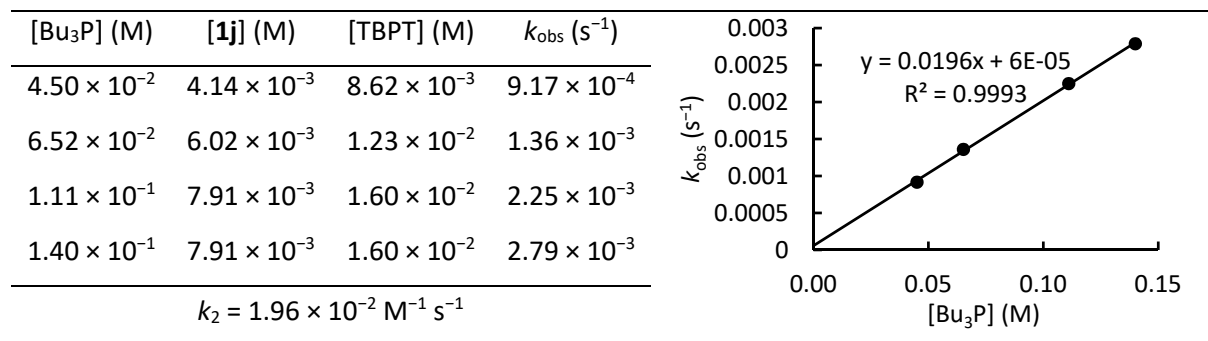


**Table S12.** Kinetics of the reactions of  $\text{Bu}_3\text{P}$  and **1j** (proton source: TBPT,  $^1\text{H}$  NMR method, monitoring of the decreasing signal for the  $=\text{CH}_2$  group in **1j** at 5.05 ppm, in  $\text{CD}_2\text{Cl}_2$ , residual solvent signal as internal integration standard IS)



## 5.2.2 Kinetics of the reactions of **1** with $\text{Ph}_3\text{P}$ in dichloromethane

### 5.2.2.1 Kinetics of the reaction of $\text{Ph}_3\text{P}$ with phenyl buta-2,3-dienoate (**1a**)

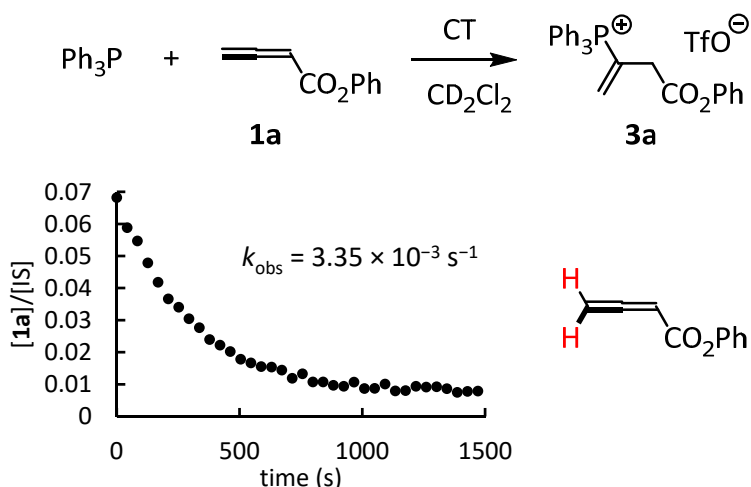
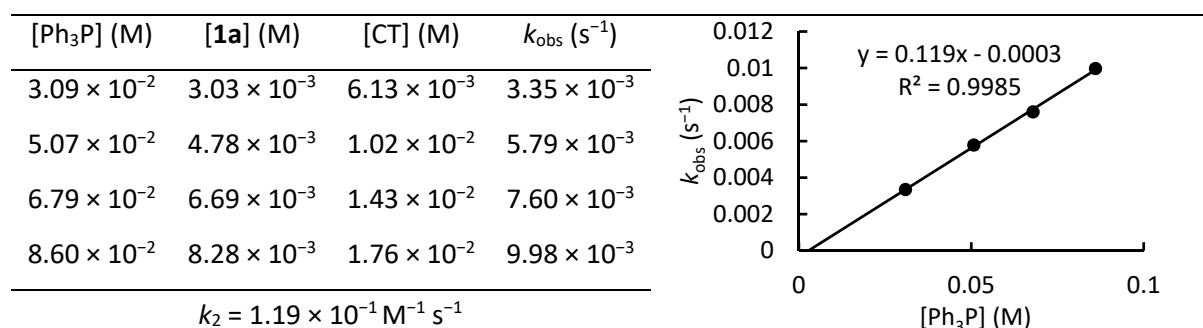


**Table S13.** Kinetics of the reactions of  $\text{Ph}_3\text{P}$  and **1a** (proton source: CT,  $^1\text{H}$  NMR method, monitoring of the decreasing signal for the  $=\text{CH}_2$  group in **1a** at 5.34 ppm, in  $\text{CD}_2\text{Cl}_2$ , mesitylene as internal integration standard IS)



$^{31}\text{P}$  NMR spectroscopic analysis of selected samples indicated selective conversion of **1a** to **3a** under the conditions of the kinetic experiments (Figure S19).

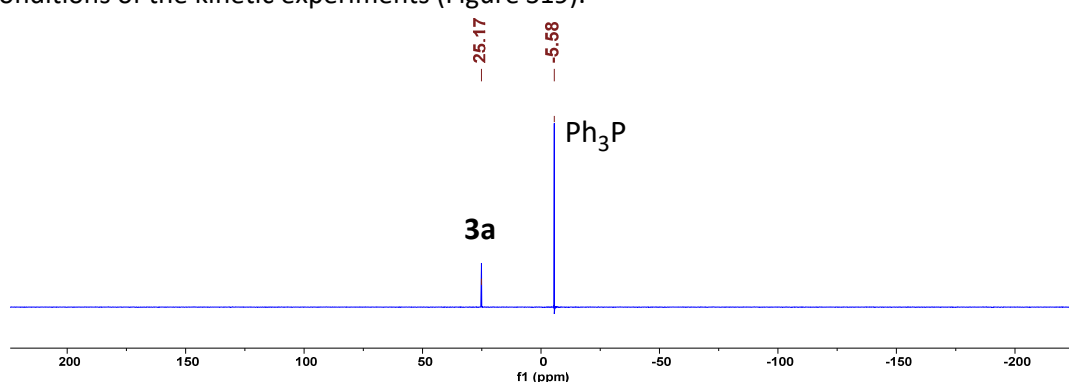


**Figure S19.**  $^{31}\text{P}$  NMR (162 MHz) spectrum of the sample with  $[\text{Ph}_3\text{P}]_0 = 76.6 \text{ mM}$ ,  $[\text{1a}]_0 = 7.59 \text{ mM}$  and  $[\text{CT}]_0 = 15.4 \text{ mM}$  in  $\text{CD}_2\text{Cl}_2$  after completion of their reaction.

### 5.2.2.2 Kinetics of the reaction of Ph<sub>3</sub>P with benzyl buta-2,3-dienoate (1b)

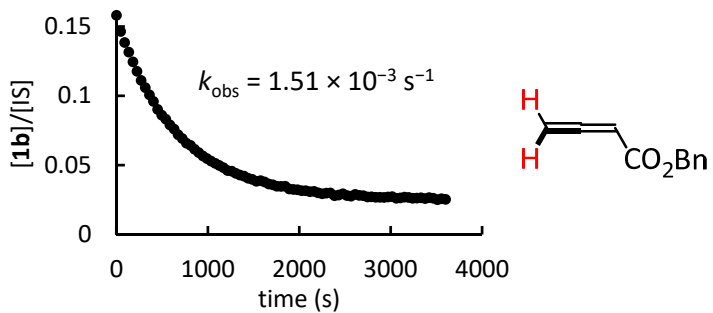
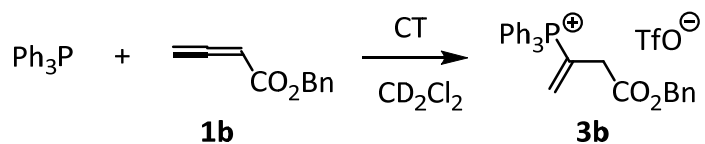
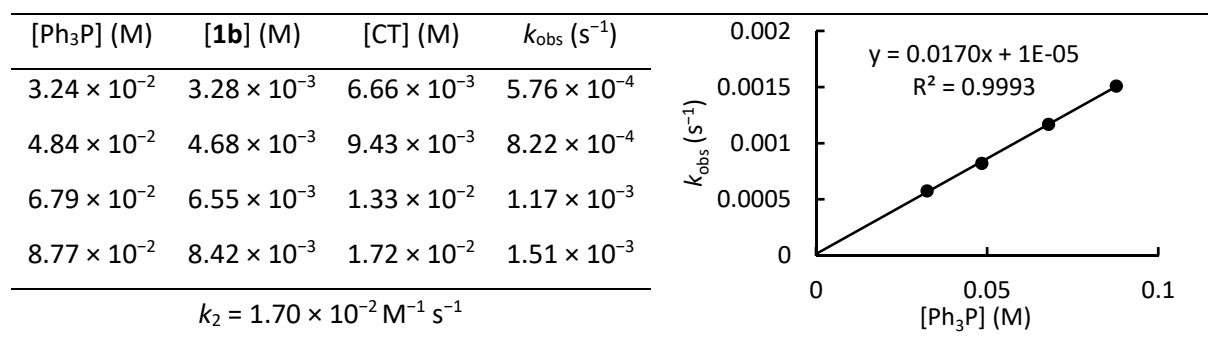
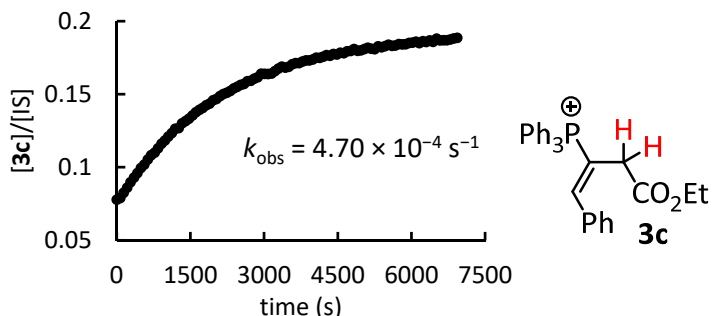
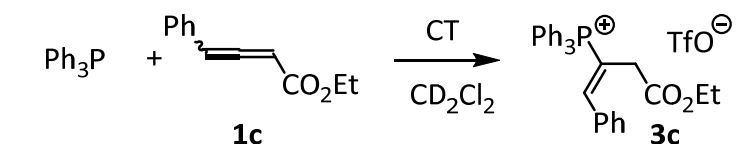


**Table S14.** Kinetics of the reactions of Ph<sub>3</sub>P and **1b** (proton source: CT, <sup>1</sup>H NMR method, monitoring of the decreasing signal for the =CH<sub>2</sub> group in **1b** at 5.24 ppm, in CD<sub>2</sub>Cl<sub>2</sub>, mesitylene as internal integration standard)



### 5.2.2.3 Kinetics of the reaction of Ph<sub>3</sub>P with ethyl 4-phenylbuta-2,3-dienoate (1c)



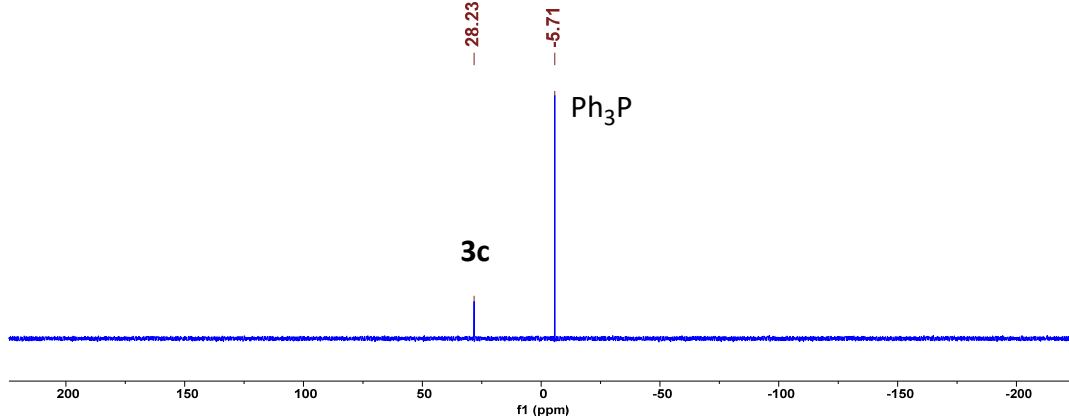
Time scale does not consider the time needed between the sample preparation and the first measured NMR spectrum (ca. 300 s).

**Table S15.** Kinetics of the reactions of Ph<sub>3</sub>P and **1c** (proton source: CT, <sup>1</sup>H NMR method, monitoring of the increasing signal for the CH<sub>2</sub> group in **3c** at 3.67 ppm, in CD<sub>2</sub>Cl<sub>2</sub>, mesitylene as internal integration standard)

[Ph <sub>3</sub> P] (M)	[1c] (M)	[CT] (M)	<i>k</i> <sub>obs</sub> (s <sup>-1</sup> )
2.29 × 10 <sup>-2</sup>	2.36 × 10 <sup>-3</sup>	1.13 × 10 <sup>-2</sup>	4.70 × 10 <sup>-4</sup>
3.81 × 10 <sup>-2</sup>	3.15 × 10 <sup>-3</sup>	6.45 × 10 <sup>-3</sup>	8.09 × 10 <sup>-4</sup>
5.64 × 10 <sup>-2</sup>	5.12 × 10 <sup>-3</sup>	1.05 × 10 <sup>-2</sup>	1.10 × 10 <sup>-3</sup>
6.90 × 10 <sup>-2</sup>	6.69 × 10 <sup>-3</sup>	1.37 × 10 <sup>-2</sup>	1.37 × 10 <sup>-3</sup>

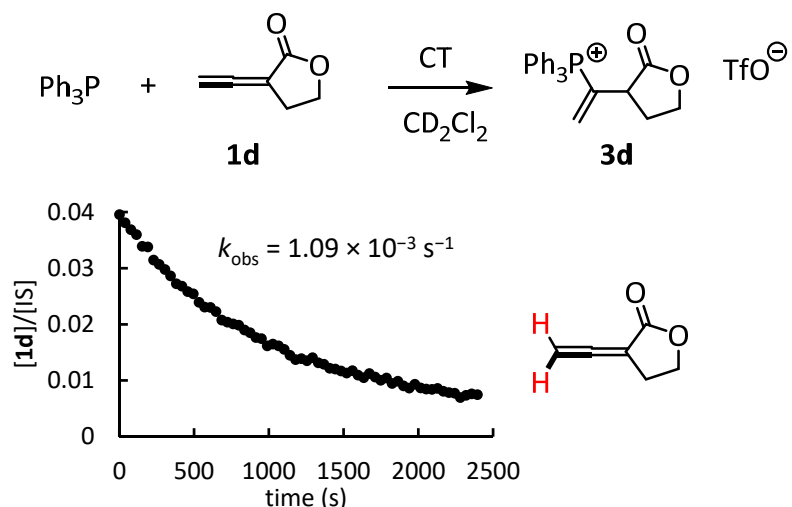
*k*<sub>2</sub> = 1.90 × 10<sup>-2</sup> M<sup>-1</sup> s<sup>-1</sup>

<sup>31</sup>P NMR spectroscopic analysis indicated selective conversion of **1c** to **3c** under the conditions of the kinetic experiments (Figure S20).

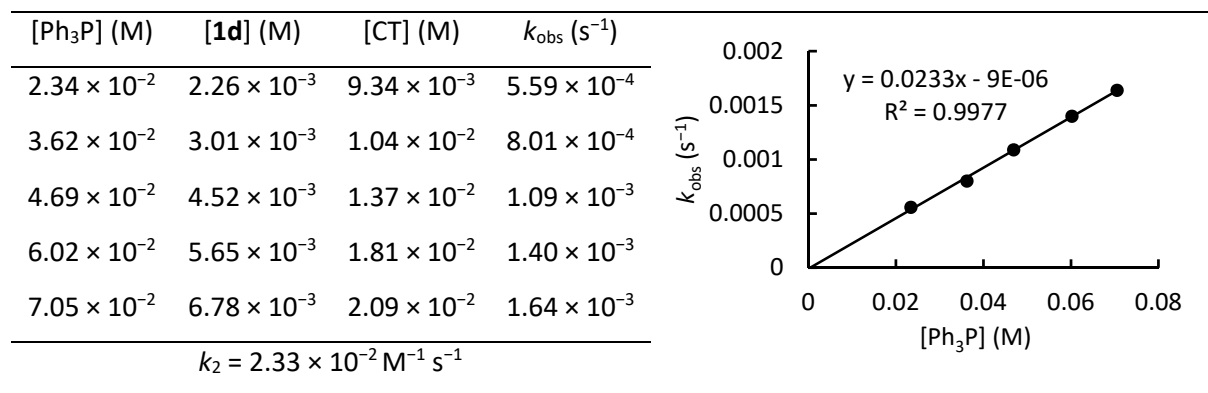


**Figure S20.**  $^{31}\text{P}$  NMR (162 MHz) spectrum of the sample with  $[\text{Ph}_3\text{P}]_0 = 38.1 \text{ mM}$ ,  $[\mathbf{1c}]_0 = 3.15 \text{ mM}$  and  $[\text{CT}]_0 = 6.45 \text{ mM}$  in  $\text{CD}_2\text{Cl}_2$  after completion of their reaction.

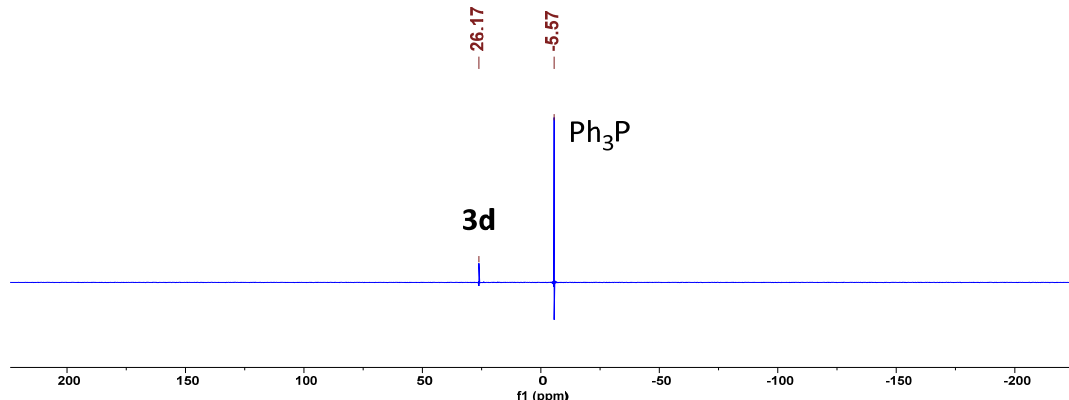
#### 5.2.2.4 Kinetics of the reaction of $\text{Ph}_3\text{P}$ with 3-vinyldenedihydrofuran-2(3H)-one (**1d**)



**Table S16.** Kinetics of the reactions of  $\text{Ph}_3\text{P}$  and **1d** (proton source: CT,  $^1\text{H}$  NMR method, monitoring of the decreasing signal for the  $=\text{CH}_2$  group in **1d** at 5.28–5.27 ppm, in  $\text{CD}_2\text{Cl}_2$ , mesitylene as internal integration standard)

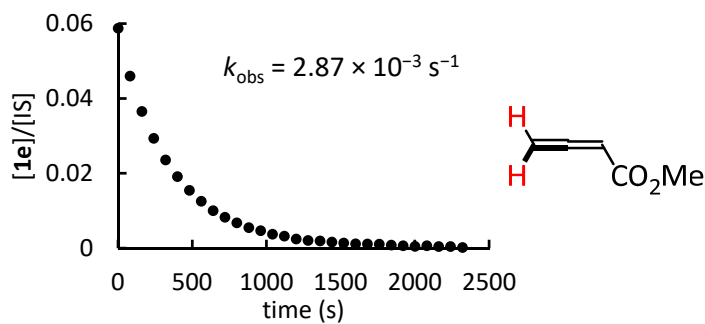
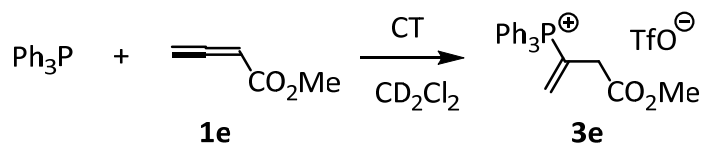


$^{31}\text{P}$  NMR spectroscopic analysis indicated selective conversion of **1d** to **3d** under the conditions of the kinetic experiments (Figure S21).

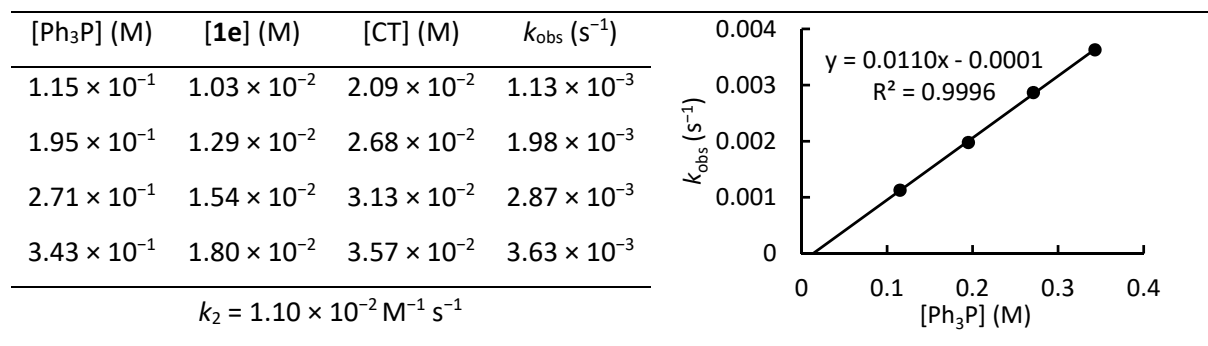


**Figure S21.**  $^{31}\text{P}$  NMR (162 MHz) spectrum of a sample with  $[\text{Ph}_3\text{P}]_0 = 141 \text{ mM}$ ,  $[\text{1d}]_0 = 12.7 \text{ mM}$  and  $[\text{CT}]_0 = 25.9 \text{ mM}$  in  $\text{CD}_2\text{Cl}_2$  after completion of their reaction.

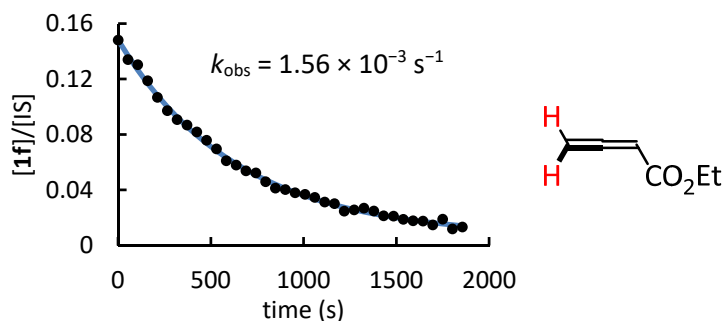
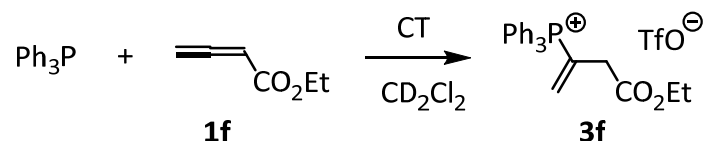
### 5.2.2.5 Kinetics of the reaction of Ph<sub>3</sub>P with methyl buta-2,3-dienoate (1e)



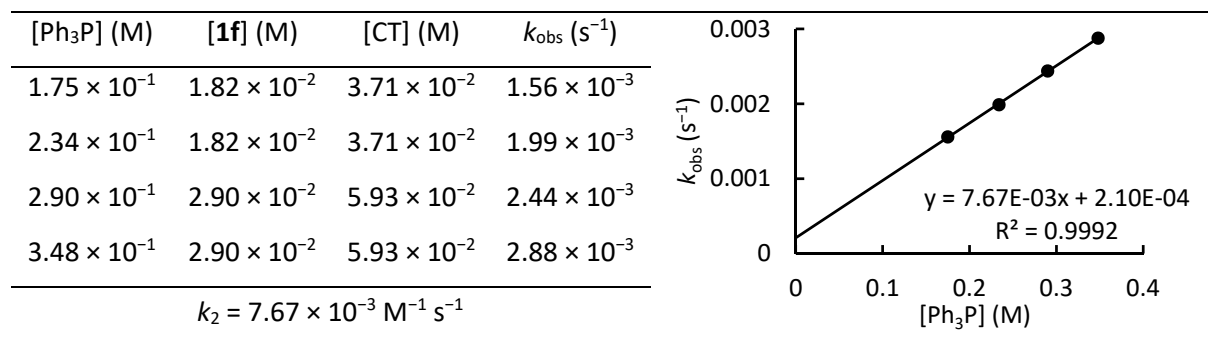
**Table S17.** Kinetics of the reactions of Ph<sub>3</sub>P and **1e** (proton source: CT, <sup>1</sup>H NMR method, monitoring of the decreasing signal for the =CH<sub>2</sub> group in **1e** at 5.22 ppm, in CD<sub>2</sub>Cl<sub>2</sub>, mesitylene as internal integration standard)



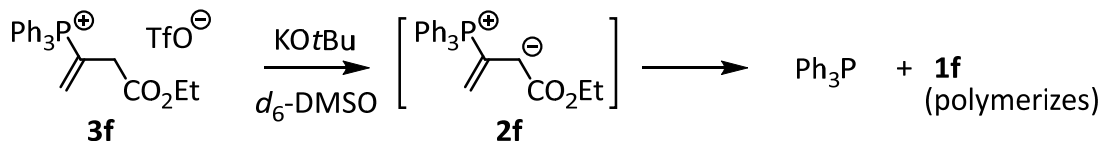
### 5.2.2.6 Kinetics of the reaction of Ph<sub>3</sub>P with ethyl buta-2,3-dienoate (1f)



**Table S18.** Kinetics of the reactions of Ph<sub>3</sub>P and **1f** (proton source: CT, <sup>1</sup>H NMR method, monitoring of the decreasing signal for the =CH<sub>2</sub> group in **1f** at 5.21 ppm, in CD<sub>2</sub>Cl<sub>2</sub>, mesitylene as internal integration standard)



Our attempts to generate zwitterion **2f** in order to determine the rate constant of the Ph<sub>3</sub>P-retroaddition did not allow us to measure the kinetics of the C-P bond cleavage reaction. Already the first <sup>1</sup>H NMR spectrum recorded after mixing the vinylphosphonium triflate **3f** with 4 equiv of potassium *tert*-butoxide in DMSO showed quantitative conversion to free Ph<sub>3</sub>P and polymerised **1f** (Figure S22). Subsequent <sup>13</sup>C and <sup>31</sup>P NMR spectroscopic analysis of this sample confirmed this interpretation (Figure S23 and S24).



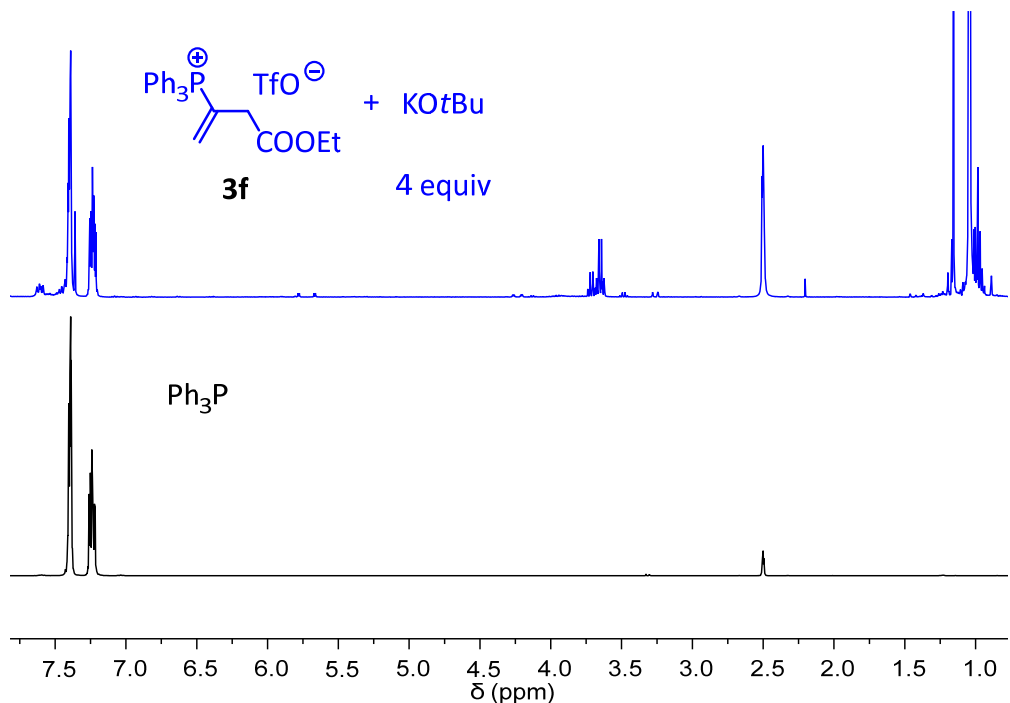


**Figure S22.** Comparison of the 400 MHz <sup>1</sup>H NMR spectrum of the **3f**/KOtBu mixture with that of Ph<sub>3</sub>P (*d*<sub>6</sub>-DMSO).

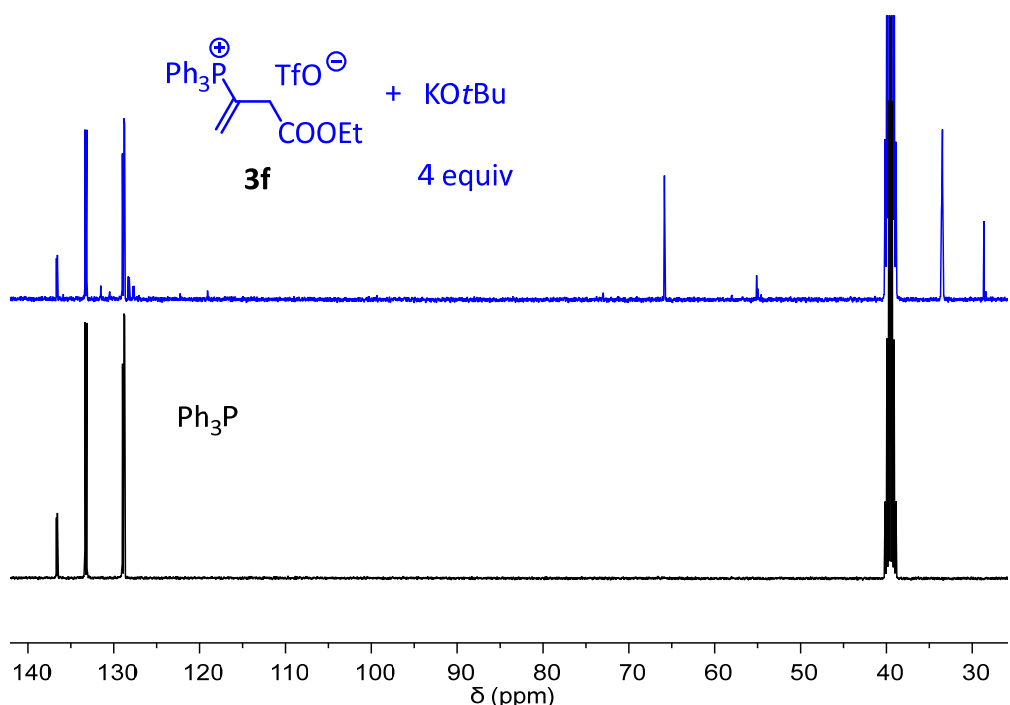


**Figure S23.** Comparison of the 101 MHz <sup>13</sup>C NMR spectrum of the **3f**/KOtBu mixture with that of Ph<sub>3</sub>P (*d*<sub>6</sub>-DMSO).

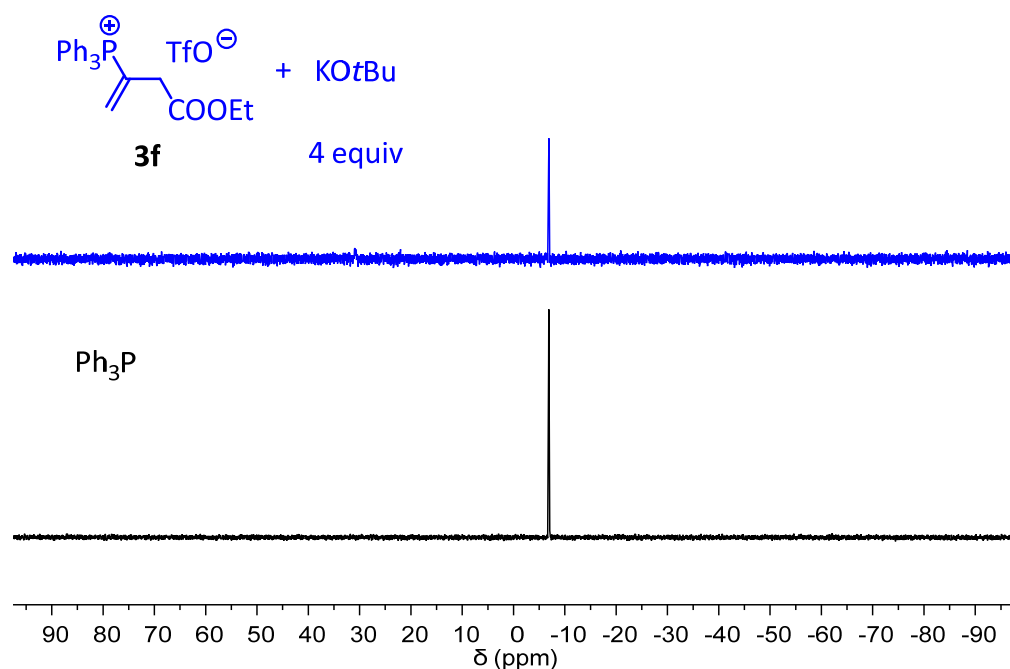


**Figure S24.** Comparison of the 162 MHz <sup>31</sup>P NMR spectrum of the **3f**/KO*t*Bu mixture with that of Ph<sub>3</sub>P (*d*<sub>6</sub>-DMSO).

**5.2.2.7 Kinetics of the reaction of  $\text{Ph}_3\text{P}$  with ethyl penta-2,3-dienoate (**1g**)**

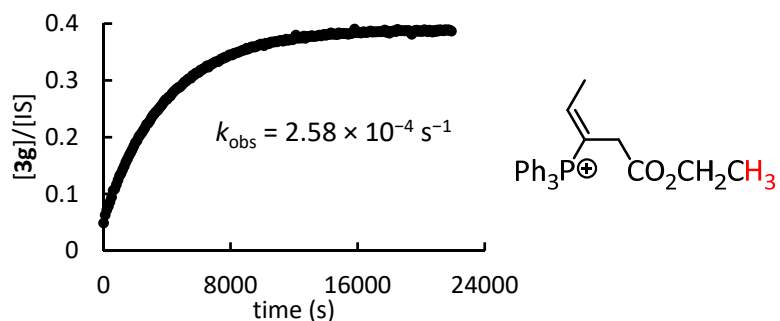
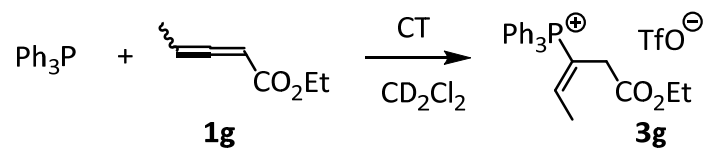


**Table S19.** Kinetics of the reactions of  $\text{Ph}_3\text{P}$  and **1g** (proton source: CT,  $^1\text{H}$  NMR method, monitoring of the increasing signal for the  $\text{OCH}_2\text{CH}_3$  group in **3g** at 1.07 ppm, in  $\text{CD}_2\text{Cl}_2$ , mesitylene as internal integration standard)

$[\text{Ph}_3\text{P}] (\text{M})$	$[\text{1g}] (\text{M})$	$[\text{CT}] (\text{M})$	$k_{\text{obs}} (\text{s}^{-1})$	$k_{\text{obs}} (\text{s}^{-1})$
$2.97 \times 10^{-2}$	$2.66 \times 10^{-3}$	$6.14 \times 10^{-3}$	$2.58 \times 10^{-4}$	
$4.00 \times 10^{-2}$	$3.96 \times 10^{-3}$	$8.32 \times 10^{-3}$	$3.48 \times 10^{-4}$	
$6.44 \times 10^{-2}$	$6.34 \times 10^{-3}$	$1.43 \times 10^{-2}$	$5.44 \times 10^{-4}$	
$8.96 \times 10^{-2}$	$8.72 \times 10^{-3}$	$1.78 \times 10^{-2}$	$7.49 \times 10^{-4}$	
$1.14 \times 10^{-1}$	$1.11 \times 10^{-2}$	$2.24 \times 10^{-2}$	$9.37 \times 10^{-4}$	
$k_2 = 8.05 \times 10^{-3} \text{ M}^{-1} \text{ s}^{-1}$				$y = 8.05E-03x + 2.36E-05$ $R^2 = 0.9998$

**5.2.2.8 Kinetics of the reaction of  $\text{Ph}_3\text{P}$  with *tert*-butyl buta-2,3-dienoate (**1h**)**

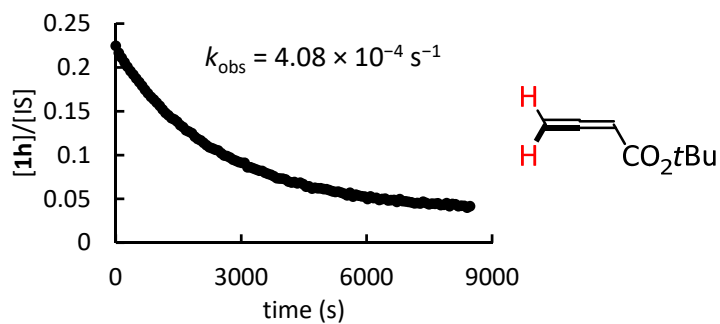
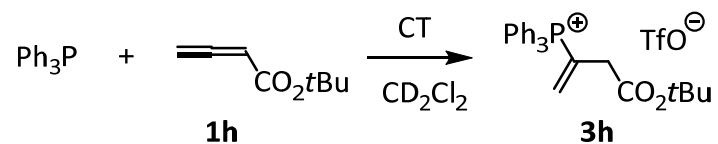
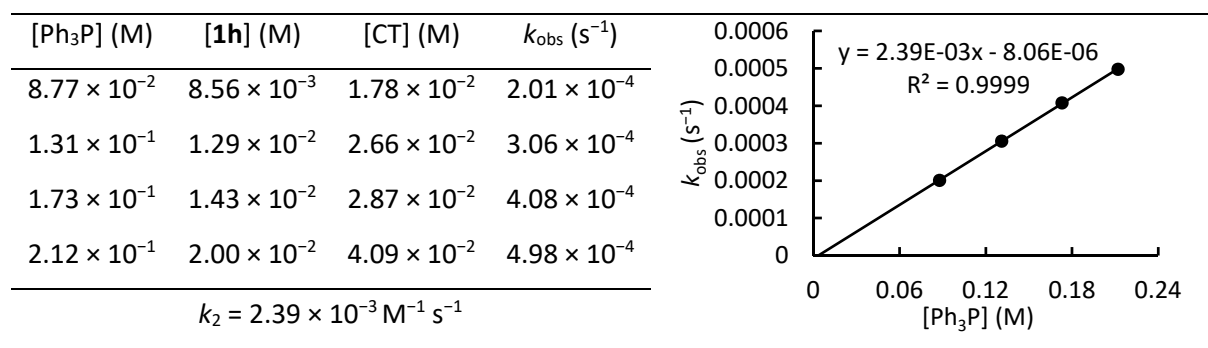


**Table S20.** Kinetics of the reactions of  $\text{Ph}_3\text{P}$  and **1h** (proton source: CT,  $^1\text{H}$  NMR method, monitoring of the decreasing signal for the  $=\text{CH}_2$  group in **1h** at 5.16 ppm, in  $\text{CD}_2\text{Cl}_2$ , mesitylene as internal integration standard)



### 5.2.2.9 Kinetics of the reaction of Ph<sub>3</sub>P with diethyl 2-vinylidenesuccinate (1i)

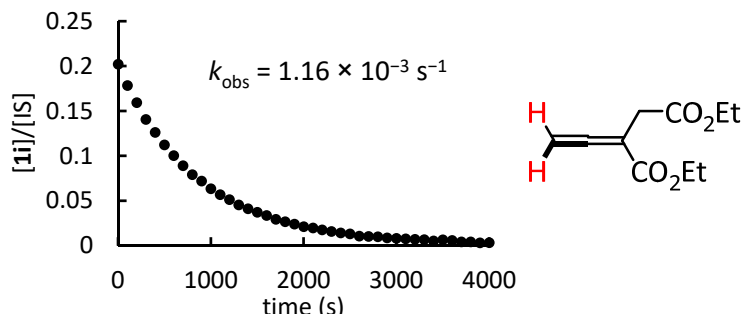
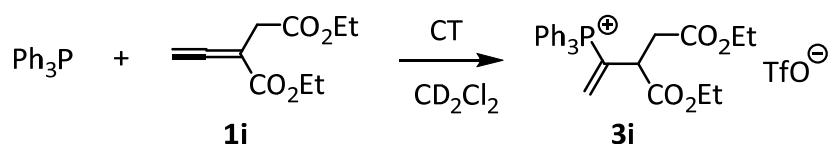
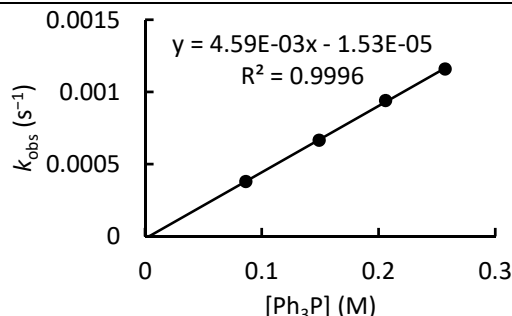


**Table S21.** Kinetics of the reactions of Ph<sub>3</sub>P and **1i** (proton source: CT, <sup>1</sup>H NMR method, monitoring of the decreasing signal for the =CH<sub>2</sub> group in **1i** at 5.21 ppm, in CD<sub>2</sub>Cl<sub>2</sub>, mesitylene as internal integration standard)

[Ph <sub>3</sub> P] (M)	[1i] (M)	[CT] (M)	<i>k</i> <sub>obs</sub> (s <sup>-1</sup> )
8.62 × 10 <sup>-2</sup>	8.40 × 10 <sup>-3</sup>	1.80 × 10 <sup>-2</sup>	3.80 × 10 <sup>-4</sup>
1.49 × 10 <sup>-1</sup>	1.42 × 10 <sup>-2</sup>	2.98 × 10 <sup>-2</sup>	6.66 × 10 <sup>-4</sup>
2.06 × 10 <sup>-1</sup>	1.57 × 10 <sup>-2</sup>	3.14 × 10 <sup>-2</sup>	9.41 × 10 <sup>-4</sup>
2.57 × 10 <sup>-1</sup>	1.57 × 10 <sup>-2</sup>	3.13 × 10 <sup>-2</sup>	1.16 × 10 <sup>-3</sup>
<i>k</i> <sub>2</sub> = 4.59 × 10 <sup>-3</sup> M <sup>-1</sup> s <sup>-1</sup>			



<sup>31</sup>P NMR spectroscopic analysis indicated selective conversion of **1i** to **3i** under the conditions of the kinetic experiments (Figure S25).

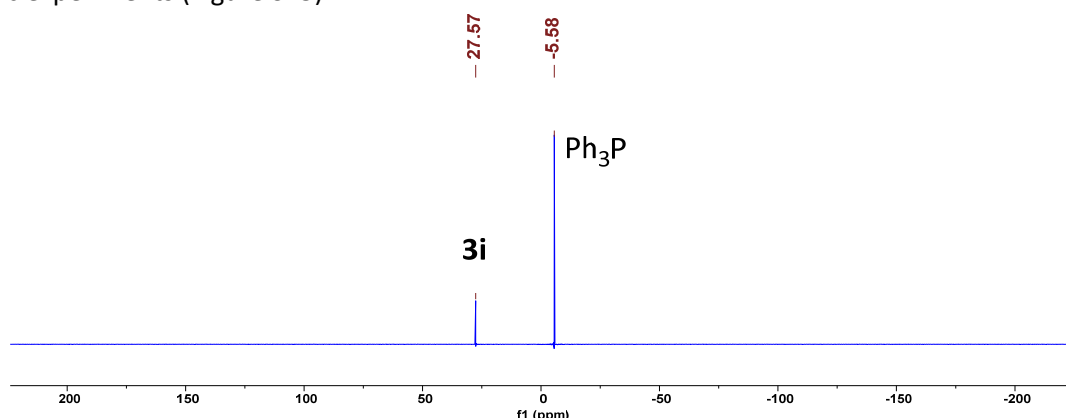


**Figure S25.**  $^{31}\text{P}$  NMR (162 MHz) spectrum of a sample with  $[\text{Ph}_3\text{P}]_0 = 118 \text{ mM}$ ,  $[\mathbf{1i}]_0 = 11.2 \text{ mM}$  and  $[\text{CT}]_0 = 22.8 \text{ mM}$  in  $\text{CD}_2\text{Cl}_2$ , after completion of their reaction.

#### 5.2.2.10 Kinetics of the reaction of Ph<sub>3</sub>P with ethyl 2-methylbuta-2,3-dienoate (1j)

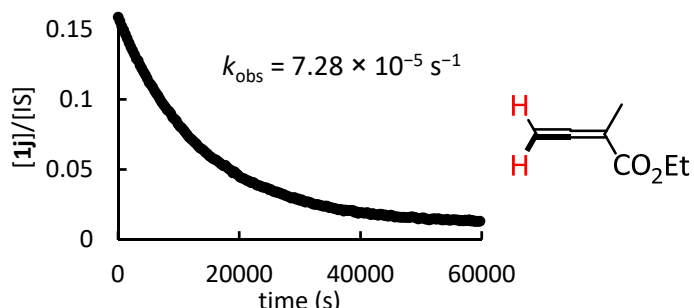
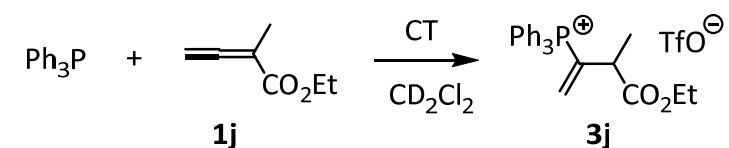
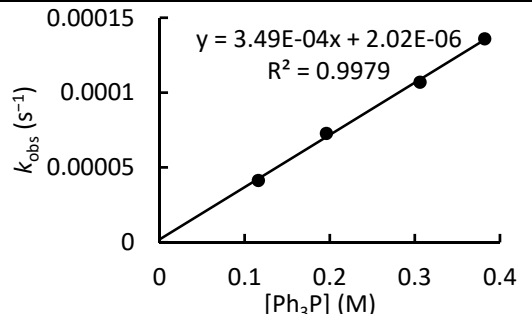


**Table S22.** Kinetics of the reactions of Ph<sub>3</sub>P and **1j** (proton source: CT, <sup>1</sup>H NMR method, monitoring of the decreasing signal for the =CH<sub>2</sub> group in **1j** at 5.05 ppm, in CD<sub>2</sub>Cl<sub>2</sub>, mesitylene as internal integration standard)

[Ph <sub>3</sub> P] (M)	[1j] (M)	[CT] (M)	<i>k</i> <sub>obs</sub> (s <sup>-1</sup> )
1.16 × 10 <sup>-1</sup>	1.13 × 10 <sup>-2</sup>	2.38 × 10 <sup>-2</sup>	4.14 × 10 <sup>-5</sup>
1.96 × 10 <sup>-1</sup>	1.51 × 10 <sup>-2</sup>	3.13 × 10 <sup>-2</sup>	7.28 × 10 <sup>-5</sup>
3.06 × 10 <sup>-1</sup>	1.51 × 10 <sup>-2</sup>	3.13 × 10 <sup>-2</sup>	1.07 × 10 <sup>-4</sup>
3.82 × 10 <sup>-1</sup>	1.78 × 10 <sup>-2</sup>	3.75 × 10 <sup>-2</sup>	1.36 × 10 <sup>-4</sup>



<sup>31</sup>P NMR spectroscopic analysis indicated selective conversion of **1j** to **3j** under the conditions of the kinetic experiments (Figure S26).

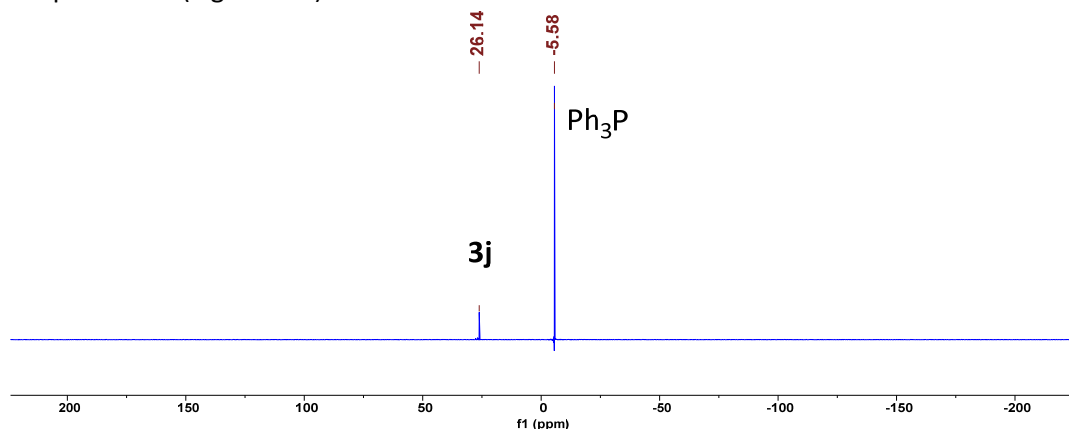


**Figure S26.**  $^{31}\text{P}$  NMR (162 MHz) spectrum of a sample with  $[\text{Ph}_3\text{P}]_0 = 118 \text{ mM}$ ,  $[\mathbf{1j}]_0 = 10.8 \text{ mM}$  and  $[\text{CT}]_0 = 19.8 \text{ mM}$  in  $\text{CD}_2\text{Cl}_2$  after completion of their reaction.

### 5.3 Kinetics of the reactions of tributylphosphine with Michael acceptors 4

#### 5.3.1 Kinetics of the reaction of $\text{Bu}_3\text{P}$ with 4a

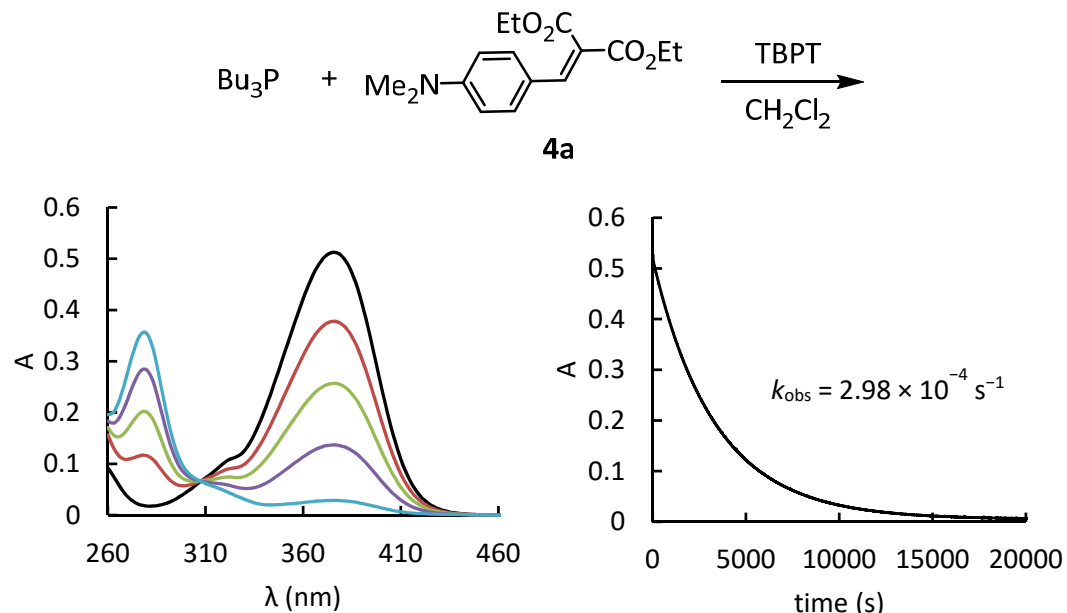
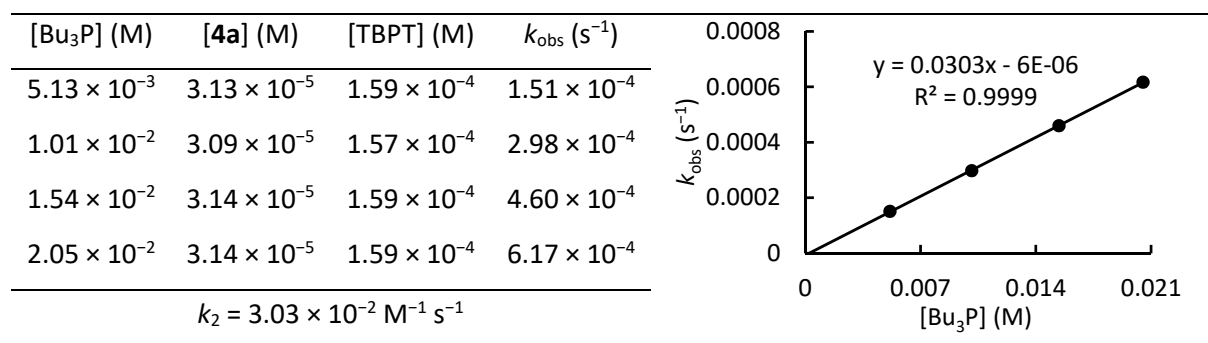


**Table S23.** Kinetics of the reactions of  $\text{Bu}_3\text{P}$  and **4a** (proton source: TBPT, conventional UV-Vis method, detection at 376 nm, in  $\text{CH}_2\text{Cl}_2$ )



### 5.3.2 Kinetics of the reaction of $\text{Bu}_3\text{P}$ with **4b**

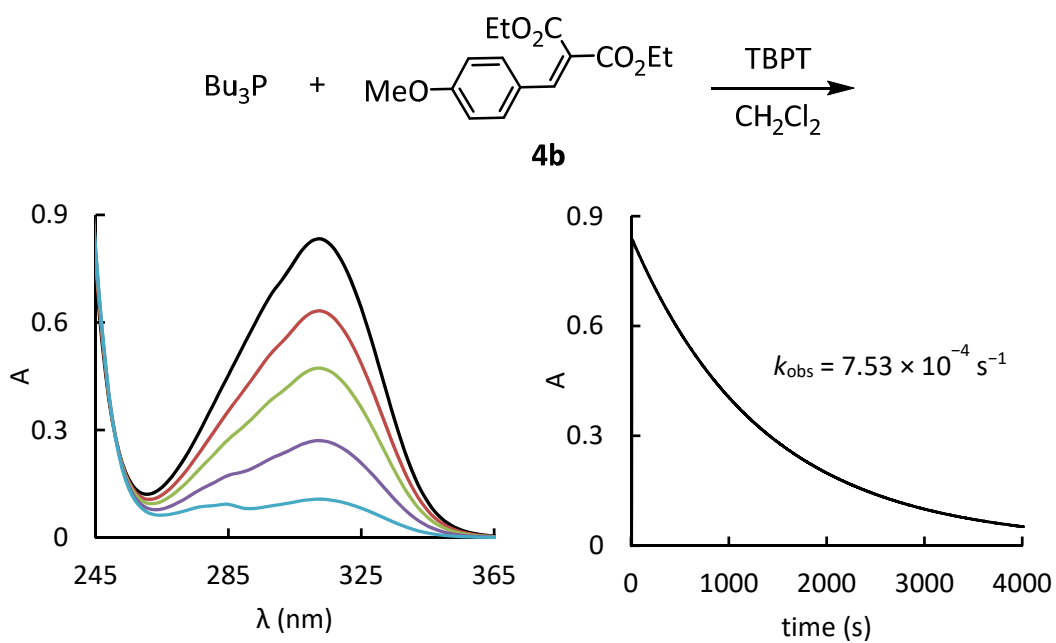


**Table S24.** Kinetics of the reactions of  $\text{Bu}_3\text{P}$  and **4b** (proton source: TBPT, conventional UV-Vis method, detection at 312 nm, in  $\text{CH}_2\text{Cl}_2$ )

$[\text{Bu}_3\text{P}] (\text{M})$	$[\text{4b}] (\text{M})$	$[\text{TBPT}] (\text{M})$	$k_{\text{obs}} (\text{s}^{-1})$
$1.69 \times 10^{-3}$	$6.34 \times 10^{-5}$	0	$2.78 \times 10^{-4}$
$1.85 \times 10^{-3}$	$6.27 \times 10^{-5}$	$3.10 \times 10^{-4}$	$3.05 \times 10^{-4}$
$3.50 \times 10^{-3}$	$6.22 \times 10^{-5}$	0	$5.71 \times 10^{-4}$
$5.07 \times 10^{-3}$	$6.02 \times 10^{-5}$	$2.98 \times 10^{-4}$	$7.53 \times 10^{-4}$
$6.76 \times 10^{-3}$	$6.01 \times 10^{-5}$	$2.98 \times 10^{-4}$	$9.77 \times 10^{-4}$

$k_2 = 1.37 \times 10^{-1} \text{ M}^{-1} \text{ s}^{-1}$

A linear plot of  $k_{\text{obs}}$  (s<sup>-1</sup>) versus  $[\text{Bu}_3\text{P}] (\text{M})$ . The y-axis is logarithmic, ranging from 0 to 0.001. The x-axis ranges from 0 to 0.007. Four data points are plotted, showing a positive linear correlation. The equation for the line is  $y = 0.1373x + 6\text{E}-05$  and the coefficient of determination is  $R^2 = 0.9962$ .

### 5.3.3 Kinetics of the reaction of Bu<sub>3</sub>P with **4c**

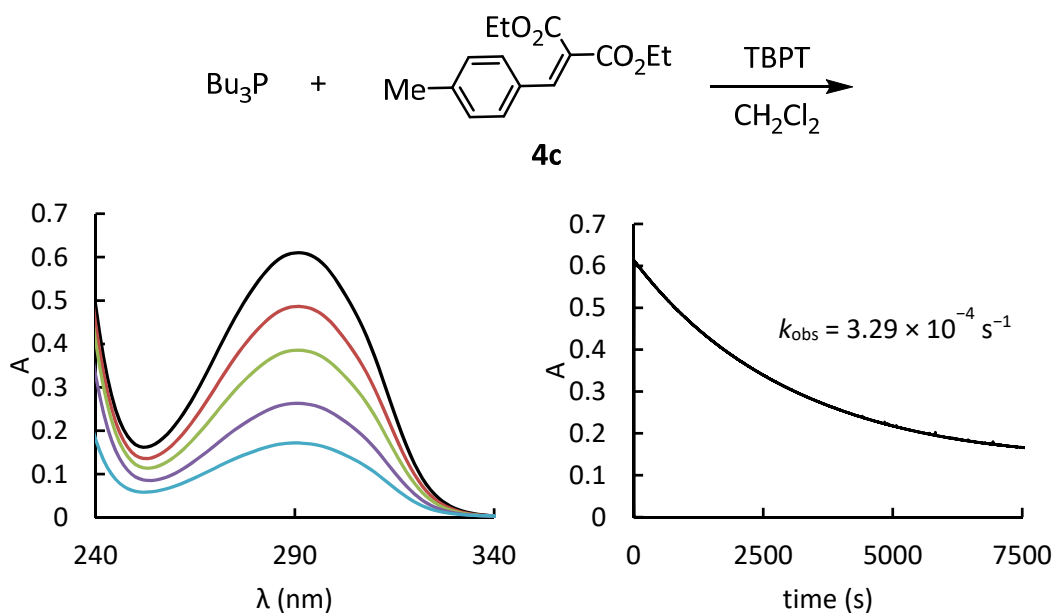


**Table S25.** Kinetics of the reactions of Bu<sub>3</sub>P and **4c** (proton source: TBPT, conventional UV-Vis method, detection at 291 nm, in CH<sub>2</sub>Cl<sub>2</sub>)

[Bu <sub>3</sub> P] (M)	[ <b>4c</b> ] (M)	[TBPT] (M)	$k_{\text{obs}} (\text{s}^{-1})$	
$1.25 \times 10^{-3}$	$4.61 \times 10^{-5}$	$2.30 \times 10^{-4}$	$3.29 \times 10^{-4}$	
$1.78 \times 10^{-3}$	$4.20 \times 10^{-5}$	0	$4.13 \times 10^{-4}$	
$2.48 \times 10^{-3}$	$4.57 \times 10^{-5}$	$2.29 \times 10^{-4}$	$5.69 \times 10^{-4}$	
$3.67 \times 10^{-3}$	$4.50 \times 10^{-5}$	$2.25 \times 10^{-4}$	$8.11 \times 10^{-4}$	
$4.51 \times 10^{-3}$	$4.43 \times 10^{-5}$	$2.22 \times 10^{-4}$	$1.00 \times 10^{-3}$	
				$y = 0.2076x + 6E-05$ $R^2 = 0.9986$
				$k_2 = 2.08 \times 10^{-1} \text{ M}^{-1} \text{ s}^{-1}$

### 5.3.4 Kinetics of the reaction of $\text{Bu}_3\text{P}$ with **4d**

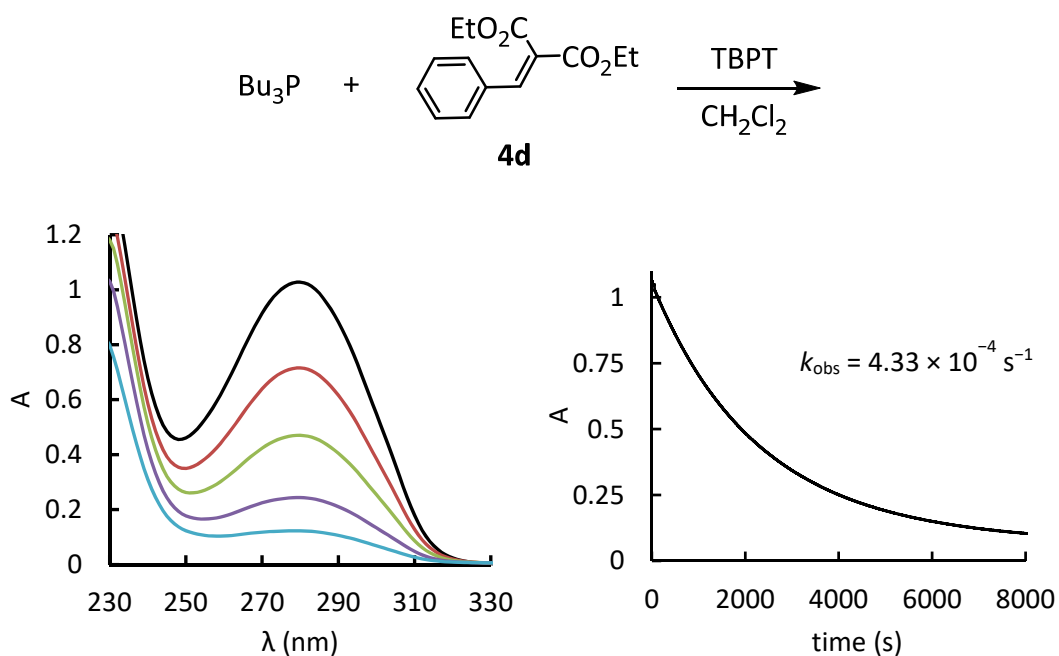
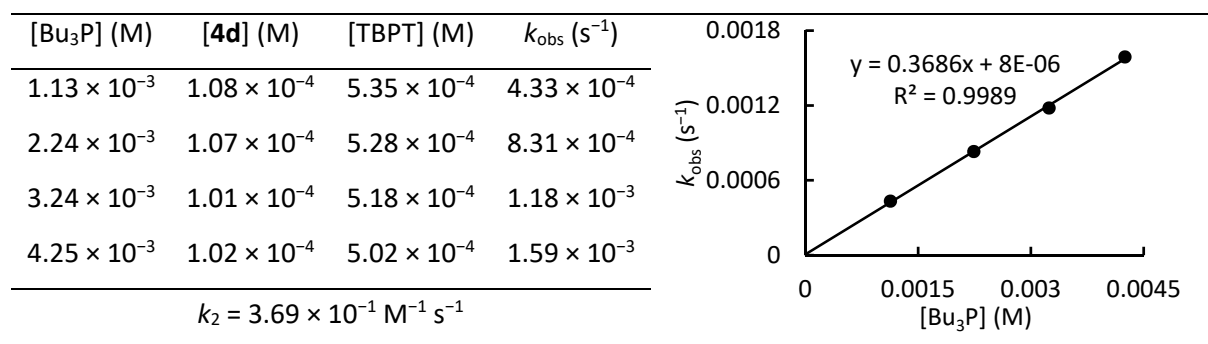


**Table S26.** Kinetics of the reactions of  $\text{Bu}_3\text{P}$  and **4d** (proton source: TBPT, conventional UV-Vis method, detection at 280 nm, in  $\text{CH}_2\text{Cl}_2$ )



### 5.3.5 Kinetics of the reaction of $\text{Bu}_3\text{P}$ with **4e**

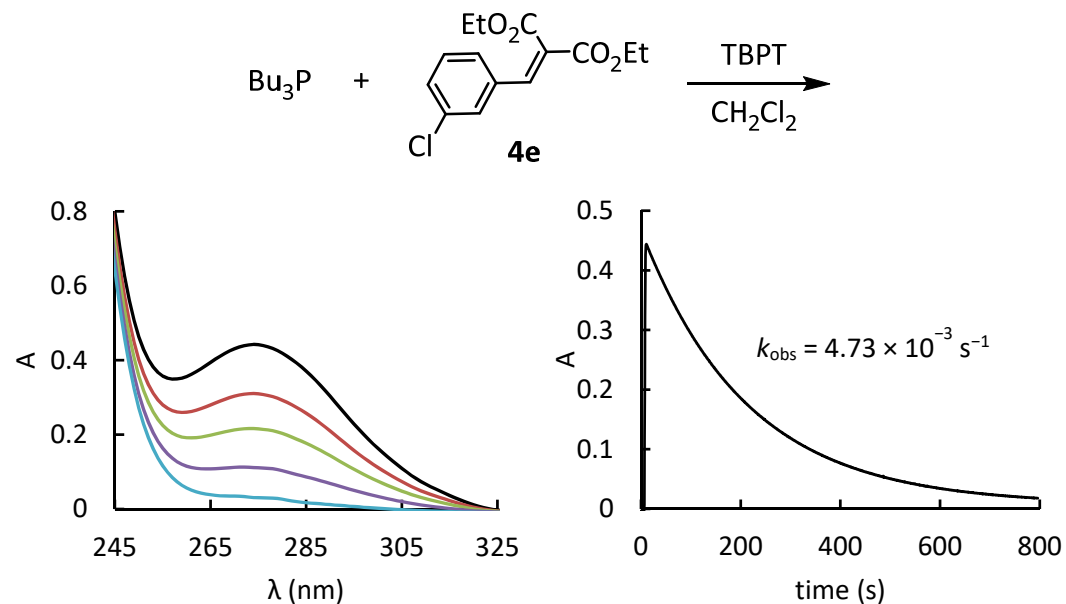
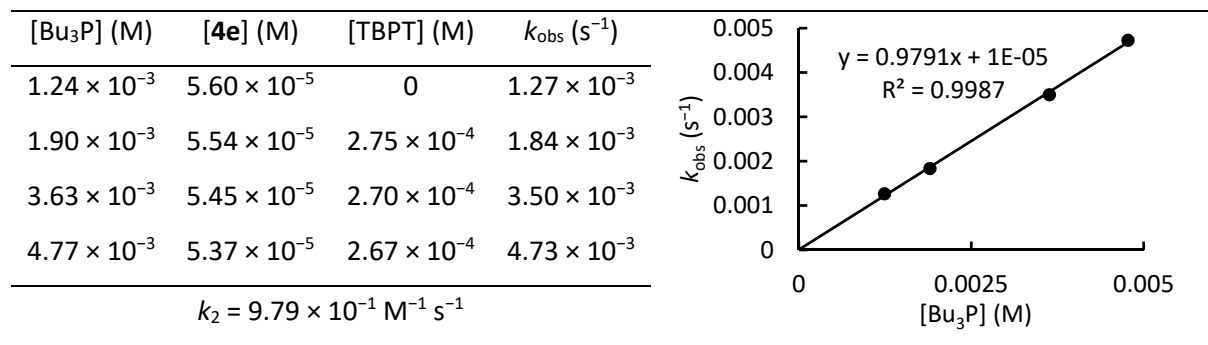


**Table S27.** Kinetics of the reactions of  $\text{Bu}_3\text{P}$  and **4e** (proton source: TBPT, conventional UV-Vis method, detection at 274 nm, in  $\text{CH}_2\text{Cl}_2$ )



### 5.3.6 Kinetics of the reaction of $\text{Bu}_3\text{P}$ with **4f**

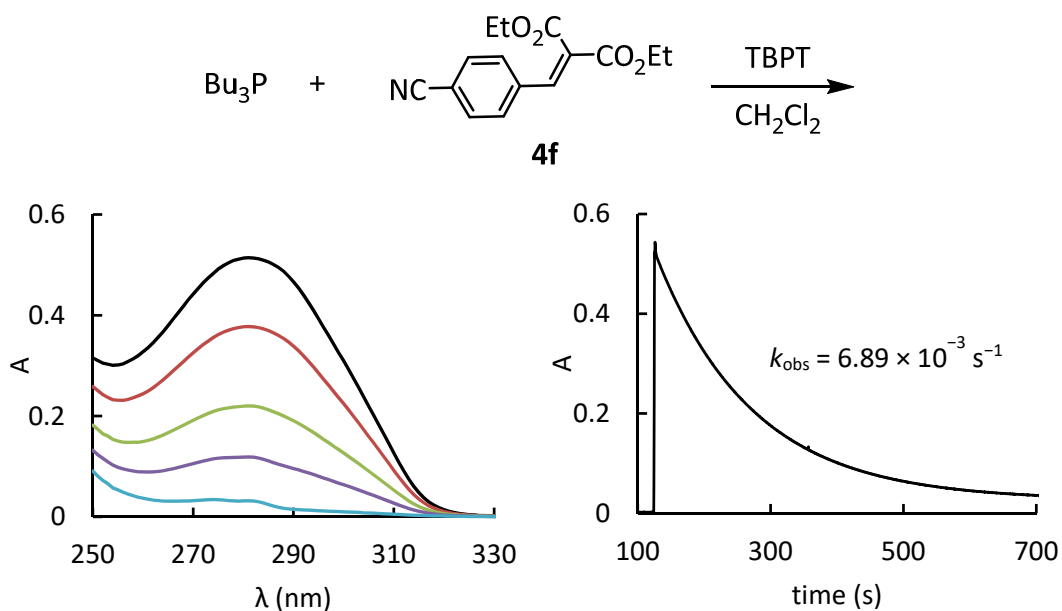
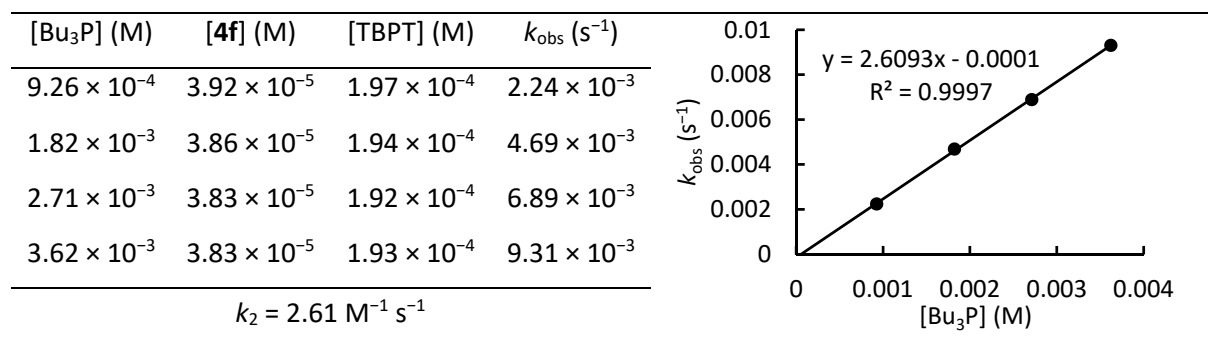


**Table S28.** Kinetics of the reactions of  $\text{Bu}_3\text{P}$  and **4f** (proton source: TBPT, conventional UV-Vis method, detection at 282 nm, in  $\text{CH}_2\text{Cl}_2$ )



### 5.3.7 Kinetics of the reaction of $\text{Bu}_3\text{P}$ with **4g**

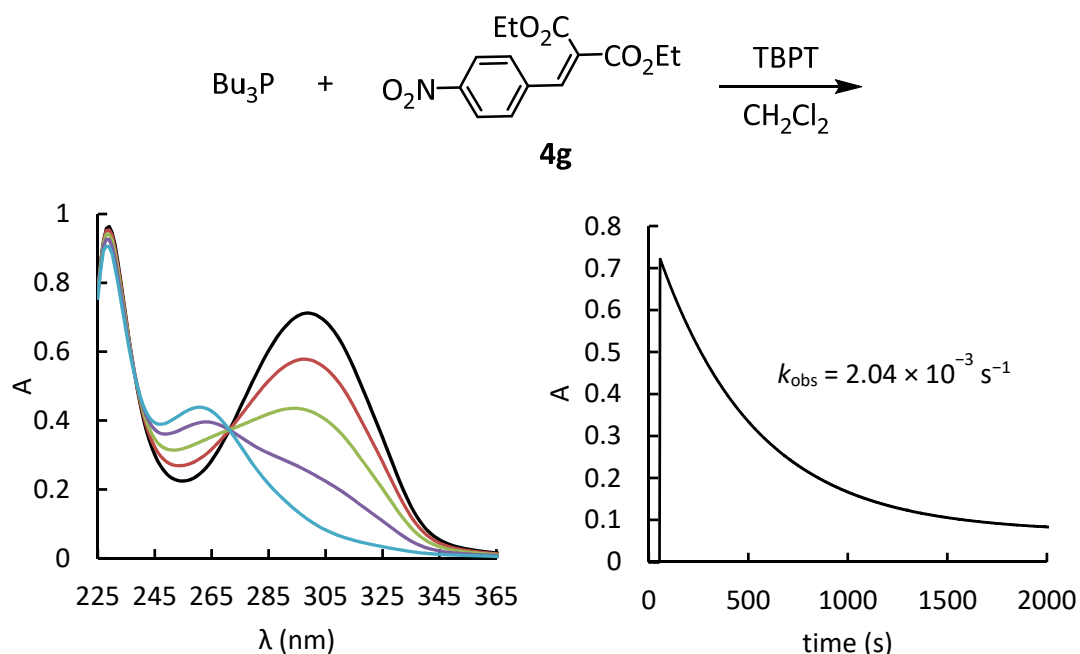


**Table S29.** Kinetics of the reactions of  $\text{Bu}_3\text{P}$  and **4g** (proton source: TBPT, conventional UV-Vis method, detection at 300 nm, in  $\text{CH}_2\text{Cl}_2$ )

$[\text{Bu}_3\text{P}] (\text{M})$	$[\text{4g}] (\text{M})$	$[\text{TBPT}] (\text{M})$	$k_{\text{obs}} (\text{s}^{-1})$	$k_2 = 3.21 \text{ M}^{-1} \text{ s}^{-1}$
$4.17 \times 10^{-4}$	$4.00 \times 10^{-5}$	$2.12 \times 10^{-4}$	$1.33 \times 10^{-3}$	
$6.29 \times 10^{-4}$	$4.01 \times 10^{-5}$	$2.13 \times 10^{-4}$	$2.04 \times 10^{-3}$	
$8.30 \times 10^{-4}$	$3.98 \times 10^{-5}$	$2.11 \times 10^{-4}$	$2.62 \times 10^{-3}$	
$1.04 \times 10^{-3}$	$3.97 \times 10^{-5}$	$2.11 \times 10^{-4}$	$3.35 \times 10^{-3}$	

A scatter plot showing the relationship between  $k_{\text{obs}}$  (s<sup>-1</sup>) on the y-axis (0 to 0.004) and  $[\text{Bu}_3\text{P}]$  (M) on the x-axis (0 to 0.0012). Four data points are plotted, showing a linear trend. The equation  $y = 3.2087x - 4E-06$  and  $R^2 = 0.9989$  are shown on the graph.

**5.3.8 Kinetics of the reaction of  $\text{Bu}_3\text{P}$  with **4h****

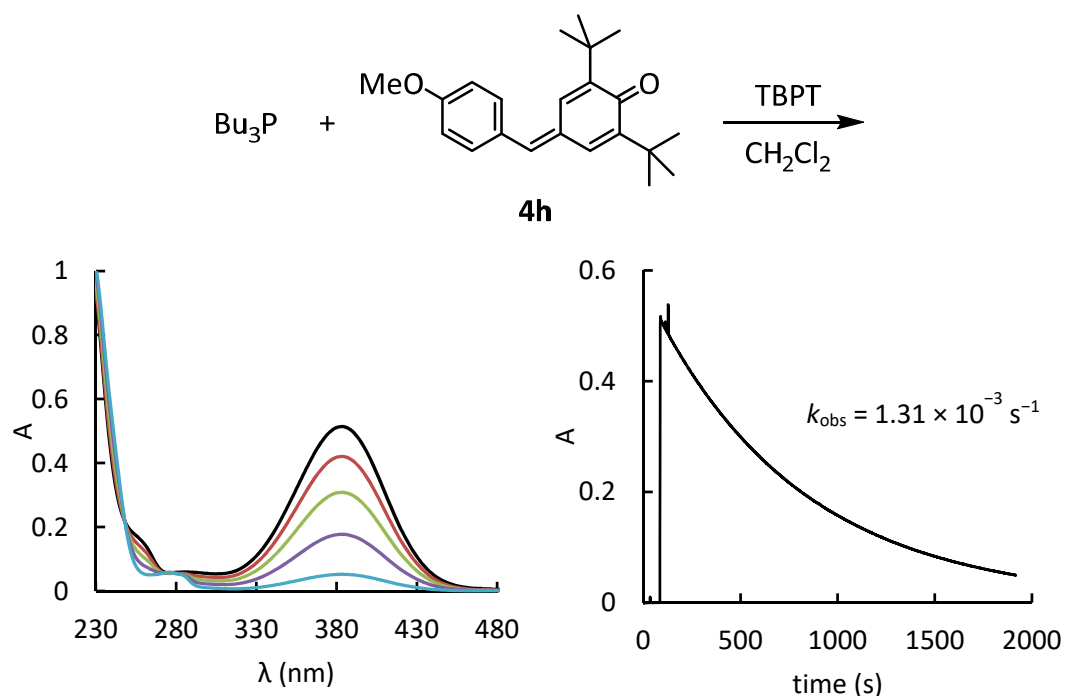
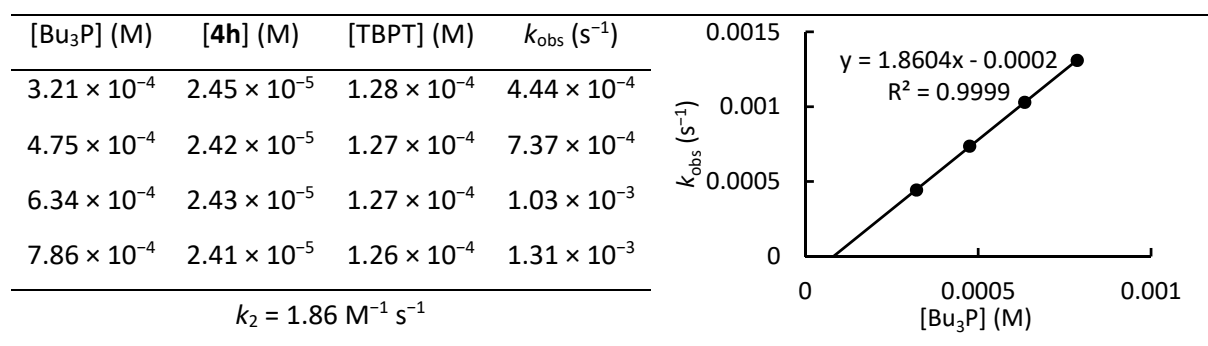


**Table S30.** Kinetics of the reactions of  $\text{Bu}_3\text{P}$  and **4h** (proton source: TBPT, conventional UV-Vis method, detection at 383 nm, in  $\text{CH}_2\text{Cl}_2$ )



### 5.3.9 Kinetics of the reaction of $\text{Bu}_3\text{P}$ with **4i**

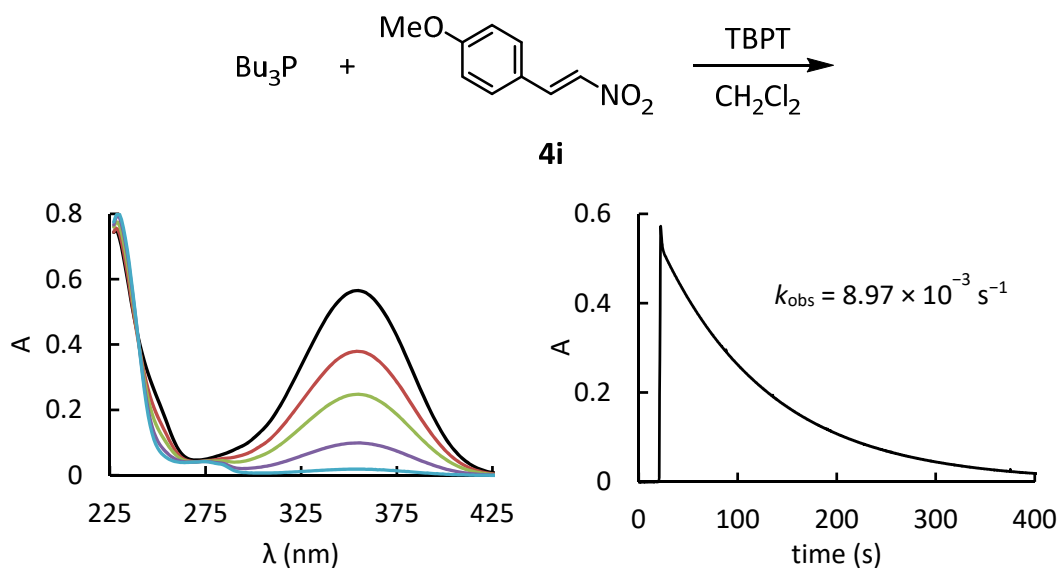
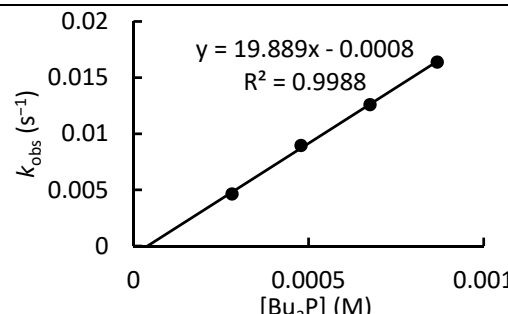


**Table S31.** Kinetics of the reactions of  $\text{Bu}_3\text{P}$  and **4i** (proton source: TBPT, conventional UV-Vis method, detection at 353 nm, in  $\text{CH}_2\text{Cl}_2$ )

$[\text{Bu}_3\text{P}] (\text{M})$	$[\text{4i}] (\text{M})$	$[\text{TBPT}] (\text{M})$	$k_{\text{obs}} (\text{s}^{-1})$	$k_2 = 1.99 \times 10^1 \text{ M}^{-1} \text{ s}^{-1}$
$2.81 \times 10^{-4}$	$2.64 \times 10^{-5}$	$1.47 \times 10^{-4}$	$4.65 \times 10^{-3}$	
$4.78 \times 10^{-4}$	$4.19 \times 10^{-5}$	$2.18 \times 10^{-4}$	$8.97 \times 10^{-3}$	
$6.75 \times 10^{-4}$	$4.18 \times 10^{-5}$	$2.17 \times 10^{-4}$	$1.26 \times 10^{-2}$	
$8.67 \times 10^{-4}$	$4.15 \times 10^{-5}$	$2.16 \times 10^{-4}$	$1.64 \times 10^{-2}$	



**5.3.10 Kinetics of the reaction of  $\text{Bu}_3\text{P}$  with **4j****

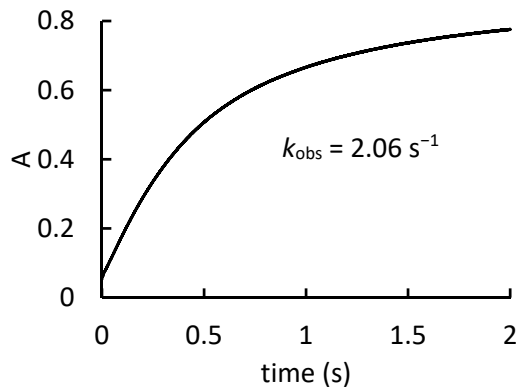
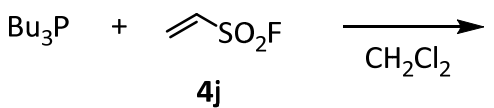


**Table S32.** Kinetics of the reactions of  $\text{Bu}_3\text{P}$  and **4j** (without added proton source, stopped-flow method, detection at 249 nm, in  $\text{CH}_2\text{Cl}_2$ )

[ $\text{Bu}_3\text{P}$ ] (M)	[ <b>4j</b> ] (M)	$k_{\text{obs}}$ ( $\text{s}^{-1}$ )
$3.21 \times 10^{-4}$	$3.11 \times 10^{-3}$	2.06
	$4.14 \times 10^{-3}$	2.88
	$5.18 \times 10^{-3}$	3.61
	$6.21 \times 10^{-3}$	4.45
	$8.28 \times 10^{-3}$	6.20
	$9.32 \times 10^{-3}$	6.99

$k_2 = 7.99 \times 10^2 \text{ M}^{-1} \cdot \text{s}^{-1}$

$y = 798.88x - 0.4602$   
 $R^2 = 0.9994$

**5.3.11 Kinetics of the reaction of  $\text{Bu}_3\text{P}$  with **4k****

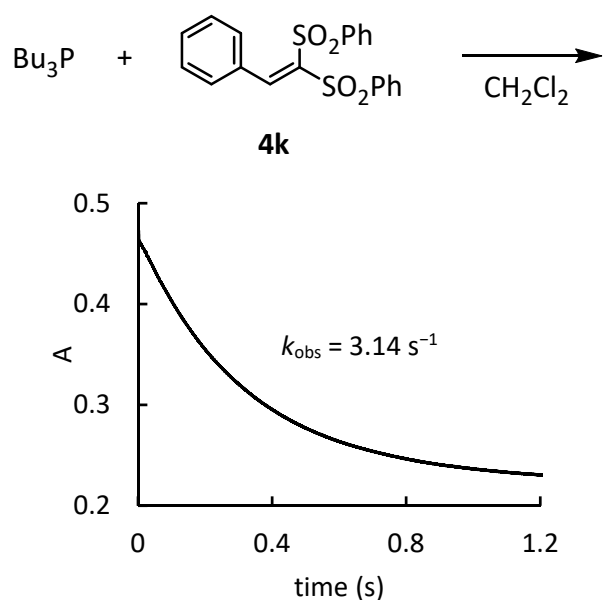
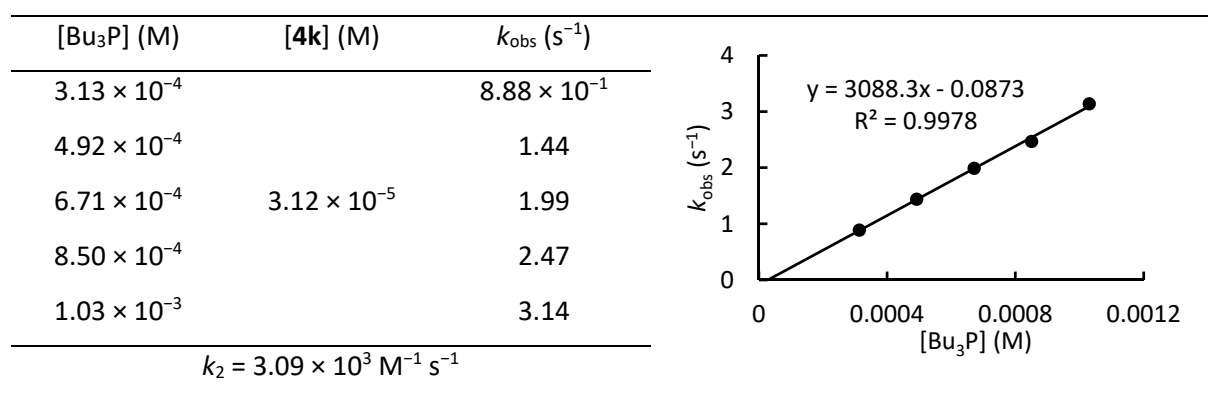


**Table S33.** Kinetics of the reactions of  $\text{Bu}_3\text{P}$  and **4k** (without added proton source, stopped-flow method, detection at 294 nm, in  $\text{CH}_2\text{Cl}_2$ )



**5.3.12 Kinetics of the reaction of  $\text{Bu}_3\text{P}$  with **4I****

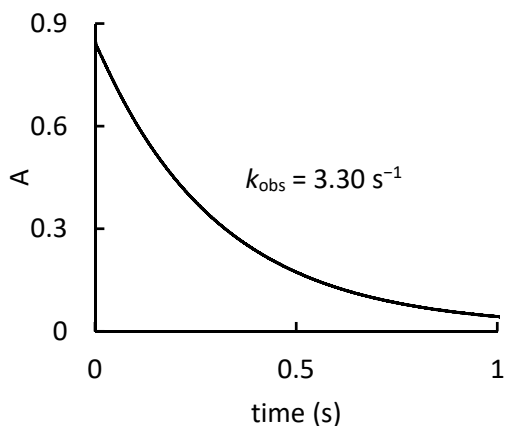
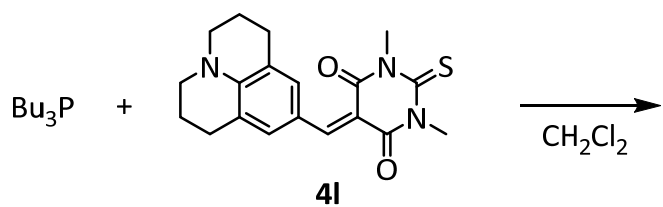


**Table S34.** Kinetics of the reactions of  $\text{Bu}_3\text{P}$  and **4I** (without added proton source, stopped-flow method, detection at 522 nm, in  $\text{CH}_2\text{Cl}_2$ )

$[\text{Bu}_3\text{P}] (\text{M})$	$[\text{4I}] (\text{M})$	$k_{\text{obs}} (\text{s}^{-1})$	
$1.34 \times 10^{-4}$		$8.08 \times 10^{-1}$	
$2.24 \times 10^{-4}$		1.42	
$3.13 \times 10^{-4}$	$6.19 \times 10^{-6}$	2.08	
$4.03 \times 10^{-4}$		2.68	
$4.92 \times 10^{-4}$		3.30	
$k_2 = 6.98 \times 10^3 \text{ M}^{-1} \text{ s}^{-1}$			

$y = 6976.4x - 0.1274$

$R^2 = 0.9998$

$k_{\text{obs}} (\text{s}^{-1})$

$[\text{Bu}_3\text{P}] (\text{M})$

**5.3.13 Kinetics of the reaction of  $\text{Bu}_3\text{P}$  with **4m****

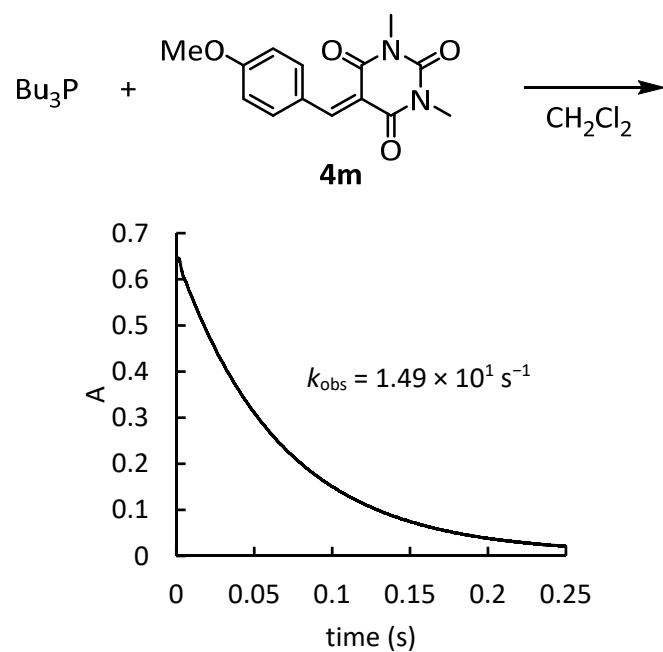
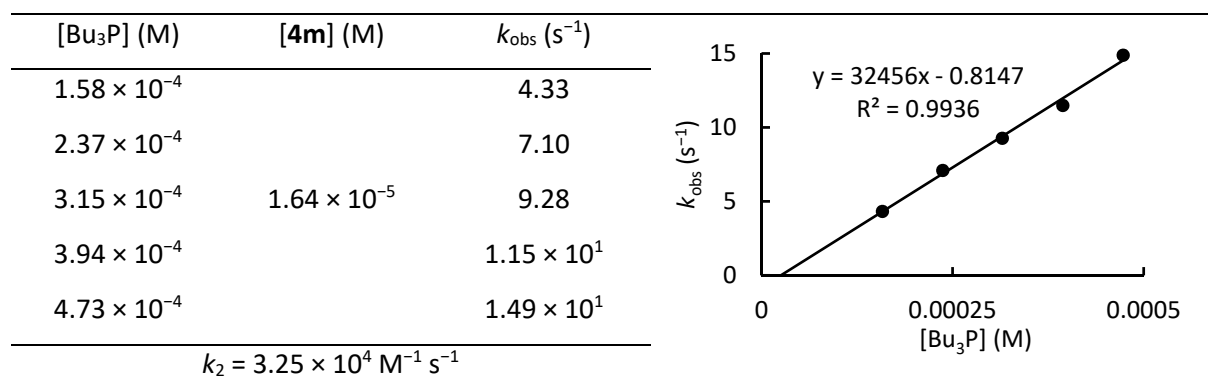


**Table S35.** Kinetics of the reactions of  $\text{Bu}_3\text{P}$  and **4m** (without added proton source, stopped-flow method, detection at 378 nm, in  $\text{CH}_2\text{Cl}_2$ )



**5.3.14 Kinetics of the reaction of  $\text{Bu}_3\text{P}$  with **4n****

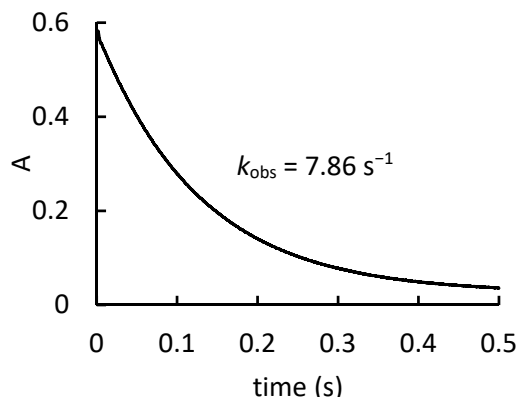
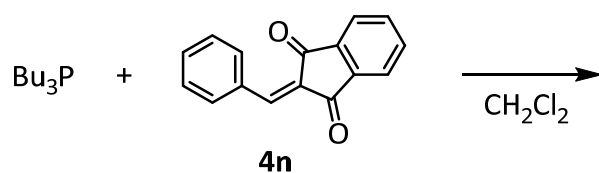


**Table S36.** Kinetics of the reactions of  $\text{Bu}_3\text{P}$  and **4n** (without added proton source, stopped-flow method, detection at 344 nm, in  $\text{CH}_2\text{Cl}_2$ )

$[\text{Bu}_3\text{P}] (\text{M})$	$[\text{4n}] (\text{M})$	$k_{\text{obs}} (\text{s}^{-1})$	$k_2 = 1.65 \times 10^4 \text{ M}^{-1} \text{ s}^{-1}$
$1.34 \times 10^{-4}$		1.94	
$2.24 \times 10^{-4}$		3.29	
$3.13 \times 10^{-4}$	$1.15 \times 10^{-5}$	4.83	
$4.03 \times 10^{-4}$		6.20	
$4.92 \times 10^{-4}$		7.86	

$y = 16479x - 0.3373$   
 $R^2 = 0.9987$ 

$k_{\text{obs}} (\text{s}^{-1})$

$[\text{Bu}_3\text{P}] (\text{M})$

**5.3.15 Kinetics of the reaction of  $\text{Bu}_3\text{P}$  with **4o****

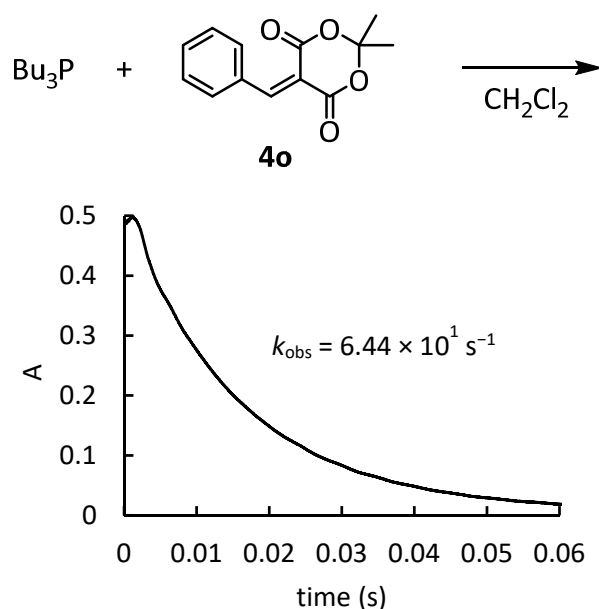
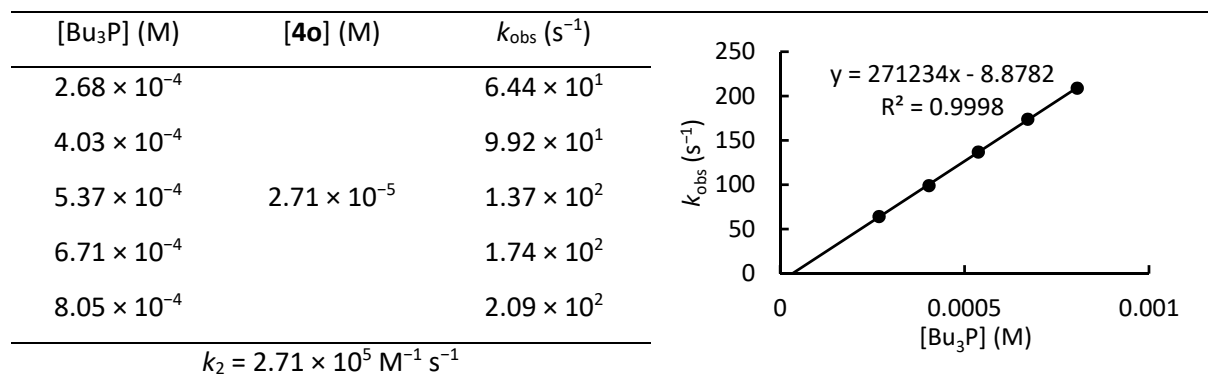
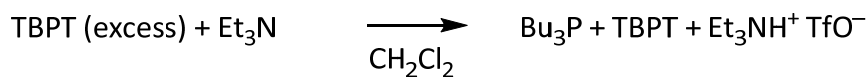


**Table S37.** Kinetics of the reactions of  $\text{Bu}_3\text{P}$  and **4o** (without added proton source, stopped-flow method, detection at 321 nm, in  $\text{CH}_2\text{Cl}_2$ )



### 5.3.16 Kinetics of the reaction of $\text{Bu}_3\text{P}$ with **4p**

first mixer: generation of a known concentration of  $\text{Bu}_3\text{P}$



second mixer: reaction of  $\text{Bu}_3\text{P}$  with **4p**

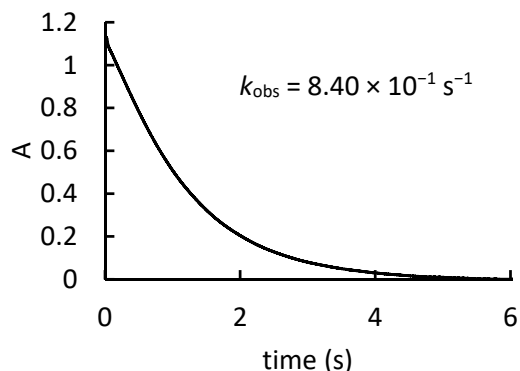
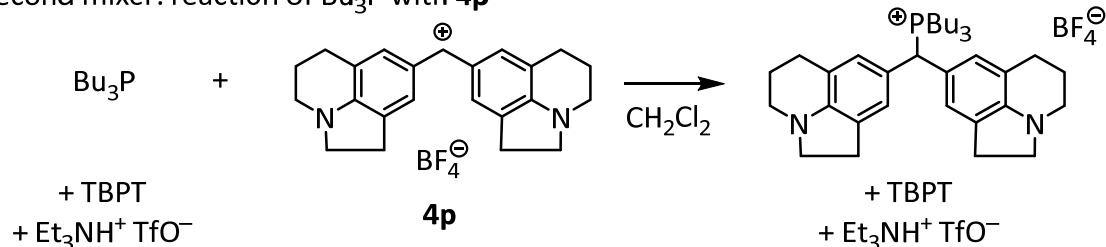
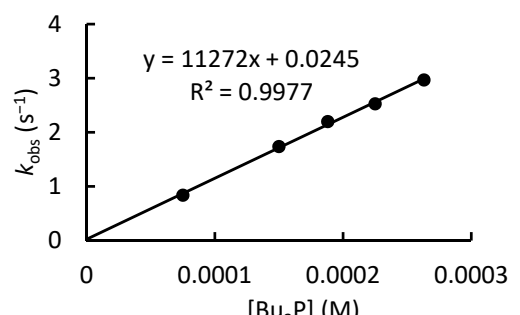


**Table S38.** Kinetics of the reactions of  $\text{Bu}_3\text{P}$  and **4p** ( $\text{Bu}_3\text{P}$  was generated by the deprotonation of TBPT with  $\text{NEt}_3$  in the first step of the sequential mixing stopped-flow method, detection at 640 nm, in  $\text{CH}_2\text{Cl}_2$ )

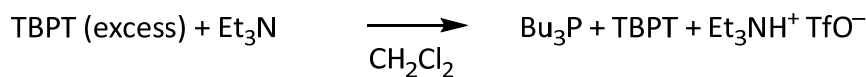
$[\text{Bu}_3\text{P}] (\text{M})$	$[\text{4p}] (\text{M})$	$k_{\text{obs}} (\text{s}^{-1})$
$7.51 \times 10^{-5}$		$8.40 \times 10^{-1}$
$1.50 \times 10^{-4}$		1.74
$1.88 \times 10^{-4}$	$7.19 \times 10^{-6}$	2.20
$2.25 \times 10^{-4}$		2.53
$2.63 \times 10^{-4}$		2.97

$k_2 = 1.13 \times 10^4 \text{ M}^{-1} \cdot \text{s}^{-1}$



### 5.3.17 Kinetics of the reaction of $\text{Bu}_3\text{P}$ with **4q**

first mixer: generation of a known concentration of  $\text{Bu}_3\text{P}$



second mixer: reaction of  $\text{Bu}_3\text{P}$  with **4q**

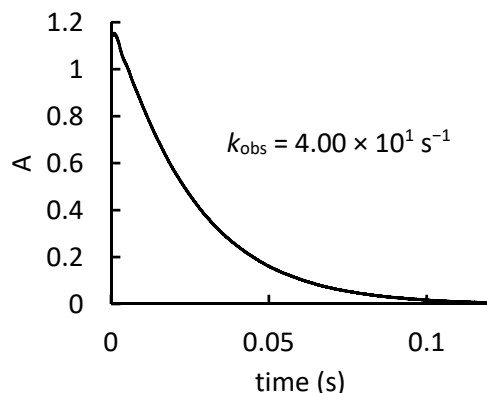
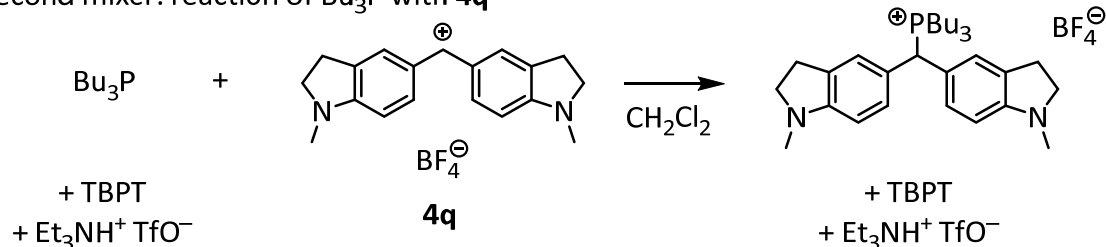


**Table S39** Kinetics of the reactions of  $\text{Bu}_3\text{P}$  and **4q** ( $\text{Bu}_3\text{P}$  was generated by the deprotonation of TBPT with  $\text{NEt}_3$  in the first step of the sequential mixing stopped-flow method, detection at 626 nm, in  $\text{CH}_2\text{Cl}_2$ )

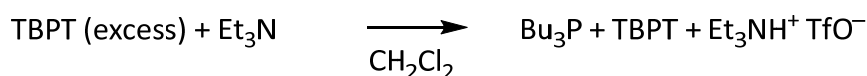
$[\text{Bu}_3\text{P}] (\text{M})$	$[\text{4q}] (\text{M})$	$k_{\text{obs}} (\text{s}^{-1})$
$1.33 \times 10^{-4}$		$1.01 \times 10^1$
$2.00 \times 10^{-4}$		$1.60 \times 10^1$
$2.67 \times 10^{-4}$	$7.35 \times 10^{-6}$	$2.20 \times 10^1$
$3.34 \times 10^{-4}$		$2.80 \times 10^1$
$4.00 \times 10^{-4}$		$3.36 \times 10^1$
$4.67 \times 10^{-4}$		$4.00 \times 10^1$

$k_2 = 8.91 \times 10^4 \text{ M}^{-1} \cdot \text{s}^{-1}$

$y = 89132x - 1.8045$   
 $R^2 = 0.9998$

### 5.3.18 Kinetics of the reaction of $\text{Bu}_3\text{P}$ with 4r

first mixer: generation of a known concentration of  $\text{Bu}_3\text{P}$



### second mixer: reaction of $\text{Bu}_3\text{P}$ with **4r**

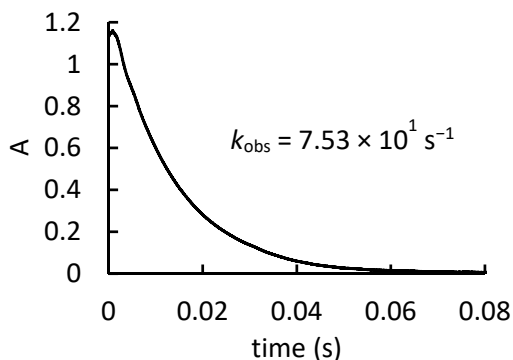
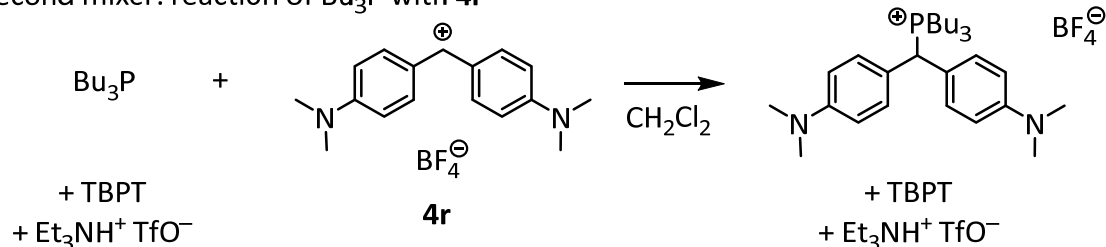


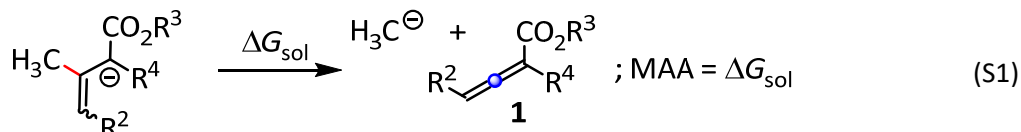
**Table S40.** Kinetics of the reactions of  $\text{Bu}_3\text{P}$  and **4r** ( $\text{Bu}_3\text{P}$  was generated by the deprotonation of TBPT with  $\text{NEt}_3$  in the first step of the sequential mixing stopped-flow method, detection at 613 nm, in  $\text{CH}_2\text{Cl}_2$ )

$[Bu_3P] \text{ (M)}$	$[4r] \text{ (M)}$	$k_{obs} \text{ (s}^{-1}\text{)}$
$6.42 \times 10^{-5}$		$7.53 \times 10^1$
$9.64 \times 10^{-5}$		$1.20 \times 10^2$
$1.28 \times 10^{-4}$		$1.56 \times 10^2$
$1.61 \times 10^{-4}$	$6.47 \times 10^{-6}$	$2.10 \times 10^2$
$1.93 \times 10^{-4}$		$2.56 \times 10^2$
$2.25 \times 10^{-4}$		$2.96 \times 10^2$

$k_2 = 1.39 \times 10^6 \text{ M}^{-1} \cdot \text{s}^{-1}$

## 6 Methyl Anion Affinities (MAA) and Phosphine Affinities (PA)

**Methyl Anion Affinities (MAA).** Using the same methodology employed successfully in earlier studies,<sup>S2</sup> methyl anion affinities (MAAs) were calculated as the free energy at 298.15 K ( $\Delta G_{\text{sol}}$ ) for the reaction shown in equation S1. [MAA = ( $\Delta G_{\text{sol}}$  of eqn S1)].

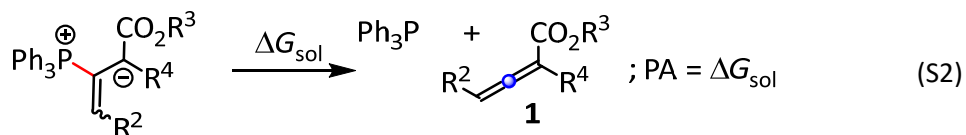


Geometry optimizations were performed at the B3LYP/6-31G(d,p) levels of theory.<sup>S19, S20</sup> Thermochemical corrections to Gibbs energies (corr.  $\Delta G$ ) and enthalpy (corr.  $\Delta H$ ) at 298.15 K were calculated using the rigid rotor/harmonic oscillator model without any scaling. Thermal corrections to Gibbs energies were alternatively evaluated using the quasi-harmonic approximation with a cutoff value of 100 cm<sup>-1</sup> (corr. qh- $\Delta G$ ) using Goodvibes.<sup>S21</sup>

Single point total electronic energies ( $\Delta E_{\text{tot}}$ ) were subsequently calculated using a combination of the B3LYP hybrid functional and the larger 6-311++G(3df,2pd) basis set.<sup>S20,S22</sup> Solvent effects on MAA values were estimated by adding single point solvation corrections ( $\Delta G_{\text{Solv}}$ ).  $\Delta G_{\text{Solv}}$  was calculated for gas phase optimized geometries using the SMD continuum solvation model.<sup>S23</sup> Thermal corrections to Gibbs energies are identical to those calculated before.<sup>S21</sup> The final free energy in solution ( $\Delta G_{\text{sol}}$ ) is then obtained as:

$$\Delta G_{\text{sol}} [\text{B3LYP/6-311++G(3df,2pd)}] = \Delta E_{\text{tot}} [\text{B3LYP/6-311++G(3df,2pd)}] + \text{corr. qh-}\Delta G [\text{B3LYP/6-31G(d,p)}] + \Delta G_{\text{Solv}} [\text{SMD(DMSO)/B3LYP/6-31G(d,p)}]$$

**Phosphine Affinities (PA)** were calculated as the free energy at 298.15 K ( $\Delta G_{\text{sol}}$ ) for reaction shown in equation S2. [PA = ( $\Delta G_{\text{sol}}$  of eqn S2)].

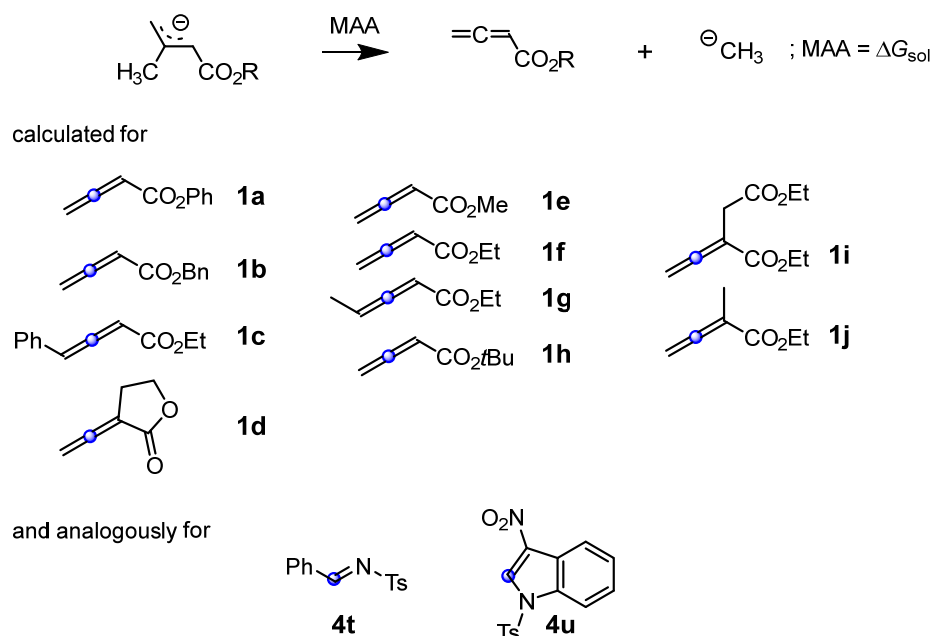


Geometry optimizations were performed with a combination of the B3LYP hybrid functional<sup>S19</sup> complemented by the D3 dispersion correction<sup>S24</sup> and the 6-31+G(d,p)<sup>S20</sup> basis set under implicit solvation that is implemented using polarizable continuum model<sup>S25</sup> (solvent=dichloromethane, radii=ua0). In the text and the tables, we refer to these settings as the PCM(DCM,ua0)/B3LYP-D3/6-31+G(d,p) level of theory. Thermochemical corrections to Gibbs energies (corr.  $\Delta G$ ) and enthalpies (corr.  $\Delta H$ ) at 298.15 K were calculated using the rigid rotor/harmonic oscillator model without any scaling. Thermal correction to Gibbs energies (corr.  $\Delta G$ ) are future treated for quasi-harmonic

approximation with cutoff value of  $100\text{ cm}^{-1}$  using Goodvibes (corr. qh- $\Delta G$ ).<sup>S21</sup> Free energies in solution have been corrected to a reference state of 1 mol/l at 298.15 K through addition of  $R\ln(24.46) = +7.925\text{ kJ mol}^{-1}$  ( $= 0.0030185$  Hartree) to the gas phase (1 atm) free energies. The value for  $R = 8.31451\text{ J K}^{-1}\text{ mol}^{-1}$ .

All calculations have been performed with Gaussian 09, Rev. D.<sup>S26</sup>

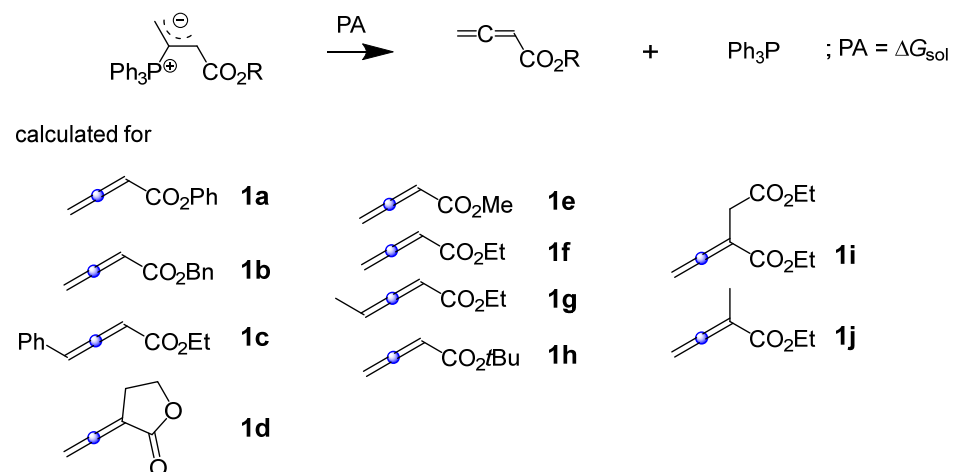
**Table S41.** Methyl anion affinities ( $\text{kJ mol}^{-1}$ , MAA) calculated at the SMD(DMSO)/B3LYP/6-311++G(3df,2pd)//B3LYP/6-31G(d,p) level of theory for electrophiles **1a-1j** and **4t-4u**.



Electrophile	Internal Reference	Based on Best Conformer				Based on Boltzmann Avg.			
		$\Delta E_{\text{tot}}$	$\Delta H_{\text{sol}}$	$\Delta G_{\text{sol}}^{\text{a}}$	$\Delta G_{\text{sol}}^{\text{b}}$	$\Delta E_{\text{tot}}$	$\Delta H_{\text{sol}}$	$\Delta G_{\text{sol}}^{\text{a}}$	$\Delta G_{\text{sol}}^{\text{b}}$
<b>1a</b>	b3	254.9	234.6	182.4	183.1	254.7	234.5	<b>182.5</b>	183.3
<b>1b</b>	b5	235.1	215.5	162.8	155.9	235.3	215.7	<b>163.1</b>	156.2
<b>1c</b>	b14	237.3	217.2	165.6	162.9	237.1	217.0	<b>165.5</b>	162.8
<b>1d</b>	d1	241.6	222.2	171.4	171.5	241.4	222.0	<b>171.2</b>	171.4
<b>1e</b>	b2	237.9	218.1	168.3	169.2	237.0	217.4	<b>167.6</b>	168.7
<b>1f</b>	b9	234.8	215.0	163.9	165.8	233.9	214.2	<b>163.4</b>	165.3
<b>1g</b>	b13	220.2	202.0	152.4	152.7	220.4	202.3	<b>152.7</b>	153.4
<b>1h</b>	b15	226.1	206.4	153.9	155.1	225.9	206.2	<b>153.9</b>	155.1
<b>1i</b>	b16	216.2	196.3	142.9	144.0	215.8	195.9	<b>142.5</b>	143.7
<b>1j</b>	b11	207.4	187.6	133.1	133.5	207.9	188.1	<b>133.6</b>	134.0
<b>4t</b>	e2	192.1	171.4	119.6	123.1	192.5	171.7	<b>120.1</b>	122.9
<b>4u</b>	e5	216.1	194.1	144.4	141.1	215.7	194.4	<b>144.6</b>	141.0

<sup>a</sup> With Truhlar's quasi-harmonic approximation based (corr. qh- $\Delta G$ ) thermal correction. <sup>b</sup> With standard (corr.  $\Delta G$ ) thermal correction.

**Table S42.** Phosphine affinities ( $\text{kJ mol}^{-1}$ , PA) calculated at the PCM(DCM,ua0)/B3LYP-D3/6-31+G(d,p) level of theory for electrophiles **1a-1j**.



Electrophile	Internal Reference	Based on Best Conformer				Based on Boltzmann Avg.			
		$\Delta E_{\text{tot}}$	$\Delta H_{\text{sol}}$	$\Delta G_{\text{sol}}^{\text{a}}$	$\Delta G_{\text{sol}}^{\text{b}}$	$\Delta E_{\text{tot}}$	$\Delta H_{\text{sol}}$	$\Delta G_{\text{sol}}^{\text{a}}$	$\Delta G_{\text{sol}}^{\text{b}}$
<b>1a</b>	b3	65.6	56.1	-13.8	-15.7	64.6	54.9	<b>-15.0</b>	-15.9
<b>1b</b>	b5	57.5	48.4	-21.4	-24.4	56.0	47.1	<b>-22.6</b>	-24.8
<b>1c</b>	b14	54.7	46.1	-23.7	-23.4	54.1	45.5	<b>-23.7</b>	-23.1
<b>1d</b>	d1	55.8	48.0	-15.8	-14.8	55.7	48.0	<b>-15.9</b>	-14.8
<b>1e</b>	b2	45.8	37.6	-26.2	-26.7	45.3	37.1	<b>-26.5</b>	-27.2
<b>1f</b>	b9	45.4	39.5	-29.4	-27.5	45.0	38.2	<b>-29.8</b>	-28.2
<b>1g</b>	b13	45.5	37.9	-29.5	-27.9	45.9	38.1	<b>-29.5</b>	-27.7
<b>1h</b>	b15	43.0	35.0	-33.1	-30.9	43.1	34.8	<b>-33.3</b>	-31.4
<b>1i</b>	b16	55.6	46.2	-26.1	-25.9	55.1	45.9	<b>-26.0</b>	-26.3
<b>1j</b>	b11	38.2	29.9	-38.8	-39.3	38.7	30.4	<b>-38.3</b>	-38.4

<sup>a</sup> With Truhlar's quasi-harmonic approximation based (corr. qh-ΔG) thermal correction. <sup>b</sup> With standard (corr. ΔG) thermal correction.

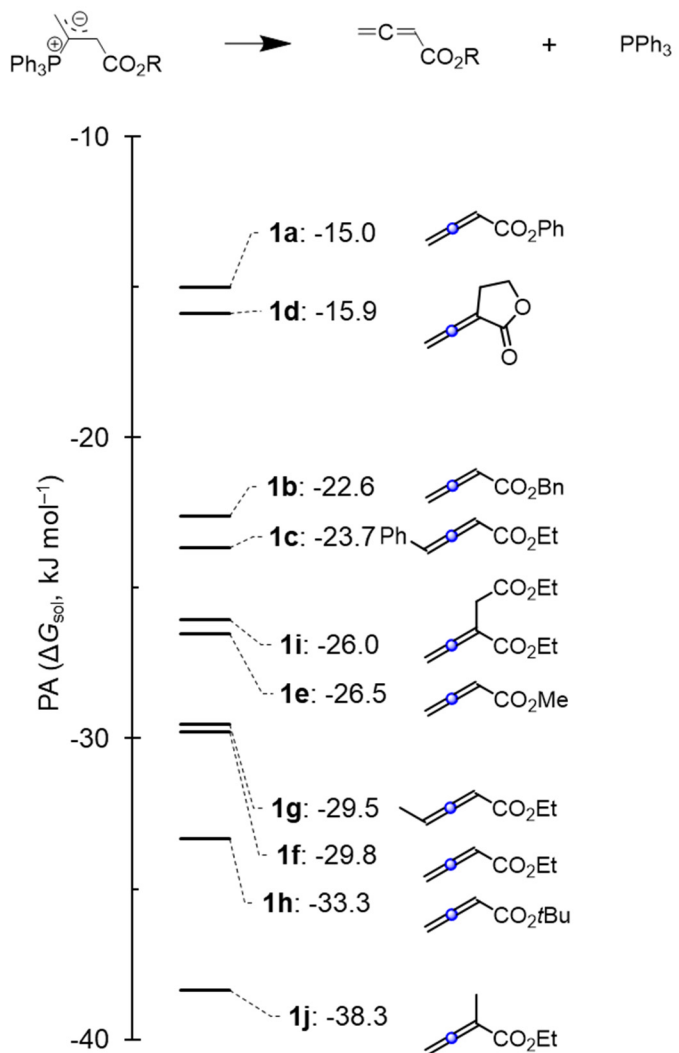


**Figure S27.** Phosphine affinities PA ( $= \Delta G_{\text{sol}}$ , kJ mol<sup>-1</sup>) calculated at the PCM(DCM,ua0)/B3LYP-D3/6-31+G(d,p) level of theory. PA values used here are Boltzmann averaged with Truhlar's quasi-harmonic approximation based (corr. qh- $\Delta G$ ) thermal corrections (from Table S42).

**Table S43.** QM properties for gas phase optimised conformers of selected allenoates (**1a-j**, a) and their corresponding methyl anion adducts (ma). <sup>a</sup> Methyl anion adducts=ma, Allenoate=a. <sup>b</sup> Truhlar quasi-harmonic treatment was used for thermal corrections. <sup>c</sup> Single point solvation corrections (in kcal mol<sup>-1</sup>) calculated at SMD(DMSO)/B3LYP/6-31G(d,p)//B3LYP/6-31G(d,p) level of theory. <sup>d</sup> Single point total electronic energies ( $\Delta E_{\text{tot}}$ ) calculated at B3LYP/6-311++G(3df,2pd)//B3LYP/6-31G(d,p). <sup>e</sup> Relative Gibbs energies (Rel.  $\Delta G_{\text{sol}}$ ) =  $\Delta E_{\text{tot}} [\text{B3LYP/6-311++G(3df,2pd)}] + \text{corr. qh-}\Delta G [\text{B3LYP/6-31G(d,p)}] + \Delta G_{\text{Solv}} [\text{SMD(DCM)}/\text{B3LYP/6-31G(d,p)}]$ .

SI	Mol.	Type <sup>a</sup>	File Name Internal Reference	B3LYP/6-31G(d,p)										$\Delta G_{\text{Solv}}^{\text{c}}$	$\Delta E_{\text{tot}}^{\text{d}}$ (hartree)	Rel. $\Delta G_{\text{sol}}^{\text{e}}$
				$\Delta E_{\text{tot}}$ (hartree)	HOMO <sub>E</sub> (hartree)	LUMO <sub>E</sub> (hartree)	Low Frequency			corr. ZPE (hartree)	corr. $\Delta H$ (hartree)	corr. $\Delta G$ (hartree)	corr. qh- $\Delta G^{\text{b}}$ (hartree)			
1	CH <sub>3</sub> <sup>-</sup>	Ref.	ch3anion	-39.7960280	0.13514	0.37353	-29	0	0	0.027840	0.031650	0.008651	0.008651	-78.86	-39.8566373	0.0
2	<b>1a</b>	a	b3_2	-536.2852306	-0.23821	-0.04796	-7	-5	-3	0.151706	0.163245	0.113531	0.115692	-6.51	-536.4625979	0.0
3		a	b3_1	-536.2850363	-0.23821	-0.04769	-4	0	0	0.151697	0.163246	0.113691	0.115854	-6.60	-536.4623199	0.8
4		a	b3_3	-536.2774258	-0.24699	-0.04823	-4	0	0	0.151426	0.163026	0.112892	0.115429	-8.43	-536.4553970	10.2
5		a	b3_4	-536.2746318	-0.23990	-0.04880	-5	0	0	0.151322	0.162888	0.113686	0.115376	-8.29	-536.4527299	17.6
6		ma	ma_b3_3	-576.2722893	0.00062	0.12682	-10	-2	0	0.189411	0.202626	0.149500	0.151944	-48.10	-576.4757030	0.0
7		ma	ma_b3_6	-576.2653644	0.00453	0.12814	-5	0	0	0.189621	0.202750	0.149888	0.152214	-49.86	-576.4696981	9.1
8		ma	ma_b3_1	-576.2669971	0.00318	0.12594	0	0	0	0.189773	0.202793	0.150231	0.152689	-48.63	-576.4708625	12.4
9	<b>1b</b>	a	b5_3	-575.6025457	-0.24944	-0.03704	-9	-6	-2	0.180668	0.193687	0.137059	0.143322	-8.11	-575.7921399	0.0
10		a	b5_2	-575.6025513	-0.24860	-0.03739	-10	-4	0	0.180669	0.193673	0.138840	0.143305	-8.02	-575.7920488	0.6
11		a	b5_5	-575.6028220	-0.24577	-0.04012	-6	0	0	0.180694	0.193671	0.138773	0.143240	-7.62	-575.7918664	2.6
12		a	b5_4	-575.6037632	-0.24727	-0.03919	-5	0	0	0.181227	0.193953	0.141116	0.143884	-7.02	-575.7921996	5.9
13		a	b5_1	-575.6035430	-0.24701	-0.03854	-4	0	0	0.181201	0.193941	0.141147	0.143915	-7.13	-575.7919823	6.1
14		a	b5_7	-575.5886826	-0.24709	-0.04689	-5	-4	0	0.180359	0.193420	0.138954	0.142766	-10.42	-575.7783665	25.0
15		a	b5_6	-575.5899441	-0.25240	-0.04233	-7	0	0	0.180759	0.193545	0.140618	0.143570	-9.68	-575.7788268	29.0
16		ma	ma_b5_10	-615.5820501	0.01134	0.10428	-4	0	0	0.218343	0.232780	0.175863	0.179478	-50.12	-615.7970296	0.0
17		ma	ma_b5_8	-615.5820983	0.01177	0.10767	-4	-2	0	0.218810	0.233115	0.177360	0.179907	-50.02	-615.7962934	3.5
18		ma	ma_b5_1	-615.5771846	0.01349	0.10423	-4	0	0	0.218647	0.232947	0.176380	0.180226	-50.69	-615.7925760	11.3
19		ma	ma_b5_5	-615.5780057	0.01334	0.10755	-12	-4	0	0.219050	0.233230	0.177707	0.180487	-50.42	-615.7924501	13.4
20	<b>1c</b>	a	b14_5	-614.9321547	-0.22790	-0.03889	-6	-2	0	0.209769	0.224125	0.166913	0.170541	-8.25	-615.1308316	0.0
21		a	b14_1	-614.9316059	-0.22776	-0.03775	-3	-3	0	0.209719	0.224084	0.167029	0.170519	-8.51	-615.1303272	0.2
22		a	b14_7	-614.9319277	-0.22791	-0.03946	-6	-1	0	0.210034	0.224252	0.167689	0.170962	-7.95	-615.1301857	4.1
23		a	b14_6	-614.9319120	-0.22804	-0.03947	-9	-4	0	0.210024	0.224248	0.167531	0.170955	-7.95	-615.1301572	4.1
24		a	b14_3	-614.9314564	-0.22803	-0.03840	0	0	0	0.210030	0.224246	0.167794	0.171011	-8.18	-615.1297173	4.5
25		ma	ma_b14_7	-654.9174389	-0.00138	0.12458	-2	0	0	0.247510	0.263444	0.203919	0.206500	-47.78	-655.1405304	0.0
26		ma	ma_b14_10	-654.9180858	-0.00262	0.12351	-8	0	0	0.247757	0.263551	0.204461	0.206998	-47.12	-655.1402590	4.8
27		ma	ma_b14_9	-654.9180551	-0.00263	0.12351	-11	-7	0	0.247713	0.263519	0.204261	0.206923	-47.12	-655.1401746	4.8

28		ma	ma_b14_1	-654.9093864	-0.00566	0.12082	-9	-5	-5	0.247561	0.263428	0.203914	0.206769	-48.59	-655.1337883	15.0
29		ma	ma_b14_8	-654.9055867	0.00004	0.13255	-5	0	0	0.246841	0.262852	0.203089	0.205853	-50.58	-655.1296561	15.1
30		ma	ma_b14_11	-654.9063862	-0.00117	0.13158	-6	-2	0	0.247172	0.262972	0.204258	0.206445	-49.90	-655.1294304	20.1
31		ma	ma_b14_3	-654.9076026	-0.00617	0.12088	-7	-3	0	0.247724	0.263436	0.204597	0.207253	-48.33	-655.1312501	24.0
32		ma	ma_b14_4	-654.9077258	-0.00581	0.12058	0	0	0	0.247859	0.263523	0.204819	0.207366	-48.36	-655.1313123	24.0
33		ma	ma_b14_2	-654.8970912	-0.00430	0.13026	-6	-4	0	0.246868	0.262776	0.203722	0.205922	-51.97	-655.1226048	28.0
34		ma	ma_b14_6	-654.8955455	-0.00445	0.12991	-6	-2	0	0.246967	0.262796	0.203792	0.206278	-51.75	-655.1204626	35.5
35		ma	ma_b14_5	-654.8953944	-0.00483	0.13016	-6	0	0	0.246988	0.262758	0.204109	0.206433	-51.69	-655.1198853	37.7
36	<b>1d</b>	a	d1_1	-382.6511448	-0.26101	-0.04077	-7	0	0	0.107421	0.115538	0.075548	0.075767	-8.08	-382.7831211	0.0
37		ma	ma_d1_2	-422.6292500	0.02045	0.20083	-7	0	0	0.144768	0.154586	0.110891	0.111172	-50.78	-422.7894073	0.0
38		ma	ma_d1_1	-422.6229489	0.02595	0.20202	-13	-8	0	0.144846	0.154486	0.111420	0.111541	-52.83	-422.7826006	10.3
39	<b>1e</b>	a	b2_1	-344.5438333	-0.26749	-0.03802	-10	-4	-3	0.099406	0.108053	0.067112	0.067542	-4.50	-344.6669600	0.0
40		a	b2_2	-344.5441270	-0.26480	-0.03898	-7	-6	0	0.099484	0.108095	0.067212	0.067493	-4.29	-344.6671856	0.2
41		a	b2_3	-344.5299781	-0.26444	-0.04472	-9	0	0	0.099201	0.107814	0.066623	0.067471	-7.45	-344.6537030	22.3
42		ma	ma_b2_2	-384.5146697	0.02715	0.20713	-4	-3	0	0.136814	0.147217	0.101911	0.102692	-50.82	-384.6660460	0.0
43		ma	ma_b2_5	-384.5094172	0.02934	0.20724	-9	0	0	0.137115	0.147391	0.102557	0.103152	-52.47	-384.6620716	4.7
44		ma	ma_b2_1	-384.5107363	0.02849	0.20501	-9	0	0	0.137156	0.147382	0.102660	0.103448	-51.18	-384.6624460	9.9
45		ma	ma_b2_4	-384.5073991	0.02222	0.20420	-15	-4	0	0.137117	0.147217	0.102685	0.103663	-51.66	-384.6600719	14.7
46	<b>1f</b>	a	b9_3	-383.8659710	-0.26273	-0.03757	-11	-8	0	0.127844	0.137752	0.093202	0.094110	-4.78	-383.9992046	0.0
47		a	b9_1	-383.8656605	-0.26502	-0.03649	-6	0	0	0.127816	0.137737	0.093307	0.094346	-4.95	-383.9989643	0.5
48		a	b9_4	-383.8657690	-0.26358	-0.03816	-9	0	0	0.128117	0.137886	0.093854	0.094594	-4.51	-383.9985832	4.0
49		a	b9_2	-383.8655085	-0.26617	-0.03722	0	0	0	0.128127	0.137895	0.093993	0.094797	-4.66	-383.9983477	4.6
50		a	b9_5	-383.8522707	-0.26221	-0.04301	-7	-6	0	0.127553	0.137534	0.092545	0.093872	-7.69	-383.9861814	21.4
51		a	b9_6	-383.8509049	-0.26215	-0.04213	0	0	0	0.127832	0.137635	0.093328	0.094436	-7.81	-383.9845082	26.8
52		a	b9_7	-383.8508840	-0.26186	-0.03990	-9	-3	0	0.127589	0.137538	0.093060	0.093823	-6.71	-383.9844083	30.0
53		ma	ma_b9_4	-423.8366995	0.02535	0.20546	-9	-7	0	0.165292	0.176929	0.128194	0.129827	-50.78	-423.9976867	0.0
54		ma	ma_b9_10	-423.8314089	0.02758	0.20556	-10	-4	-1	0.165503	0.177047	0.128606	0.130016	-52.47	-423.9935981	4.2
55		ma	ma_b9_5	-423.8378318	0.02324	0.20347	0	0	0	0.165761	0.177116	0.129617	0.130641	-49.99	-423.9976439	5.6
56		ma	ma_b9_1	-423.8326363	0.02685	0.20334	-9	-3	0	0.165542	0.177043	0.128507	0.130322	-51.18	-423.9938176	9.8
57		ma	ma_b9_12	-423.8324293	0.02570	0.20378	-1	0	0	0.165970	0.177255	0.129970	0.130907	-51.71	-423.9935107	9.9
58		ma	ma_b9_7	-423.8295742	0.02079	0.20281	-9	-3	0	0.165466	0.176945	0.128864	0.130143	-51.66	-423.9919704	12.2
59		ma	ma_b9_2	-423.8338096	0.02475	0.20153	-11	-2	0	0.165979	0.177211	0.130106	0.131136	-50.33	-423.9938747	15.3
60		ma	ma_b9_9	-423.8281844	0.01990	0.20267	0	0	0	0.165738	0.177011	0.129754	0.130660	-51.24	-423.9895380	21.7

61	<b>1g</b>	a	b13_4	-423.1873427	-0.25287	-0.03345	-4	-3	0	0.156478	0.167929	0.119438	0.120828	-5.67	-423.3308445	0.0
62		a	b13_1	-423.1871602	-0.25640	-0.03219	-17	-5	-3	0.156363	0.167878	0.119086	0.120926	-5.79	-423.3307496	0.0
63		a	b13_3	-423.1870134	-0.25725	-0.03291	-12	-5	0	0.156660	0.168020	0.119874	0.121237	-5.48	-423.3301464	3.7
64		a	b13_6	-423.1871496	-0.25341	-0.03402	-6	0	0	0.156730	0.168062	0.119961	0.121159	-5.38	-423.3302159	3.7
65		a	b13_5	-423.1871460	-0.25343	-0.03405	-4	-1	0	0.156732	0.168055	0.120109	0.121111	-5.35	-423.3302040	3.8
66		ma	ma_b13_7	-463.1553748	0.02449	0.19933	-5	0	0	0.193108	0.206447	0.153452	0.155396	-50.43	-463.3257890	0.0
67		ma	ma_b13_10	-463.1564463	0.02263	0.19758	-12	-5	0	0.193429	0.206573	0.154283	0.156093	-49.63	-463.3257528	5.3
68		ma	ma_b13_1	-463.1483542	0.01973	0.19734	-8	-7	0	0.193296	0.206479	0.154059	0.155919	-51.30	-463.3202681	12.2
69		ma	ma_b13_12	-463.1493140	0.02096	0.20103	-3	0	0	0.193545	0.206481	0.155285	0.156487	-50.58	-463.3187082	20.8
70		ma	ma_b13_11	-463.1493565	0.02086	0.20076	-3	0	0	0.193500	0.206456	0.155140	0.156480	-50.45	-463.3186099	21.6
71		ma	ma_b13_3	-463.1469913	0.01882	0.19692	-12	-6	0	0.193496	0.206486	0.154867	0.156434	-50.81	-463.3175915	22.7
72		ma	ma_b13_2	-463.1413587	0.01784	0.20123	-6	0	0	0.193266	0.206257	0.154992	0.156069	-52.30	-463.3131548	27.1
73		ma	ma_b13_6	-463.1398811	0.01748	0.19978	-12	-10	-5	0.193308	0.206235	0.154975	0.156294	-51.96	-463.3109995	34.8
74		ma	ma_b13_5	-463.1397914	0.01667	0.20089	-10	-9	0	0.193380	0.206235	0.155334	0.156578	-51.87	-463.3103814	37.5
75	<b>1h</b>	a	b15_2	-462.5035176	-0.25679	-0.03576	-11	-7	0	0.183449	0.195942	0.146320	0.147271	-4.35	-462.6559840	0.0
76		a	b15_1	-462.5032082	-0.25877	-0.03459	-5	0	0	0.183440	0.195930	0.146414	0.147320	-4.51	-462.6556887	0.2
77		ma	ma_b15_2	-502.4757427	0.01959	0.19900	-4	0	0	0.221053	0.235116	0.182030	0.183413	-48.58	-502.6539346	0.0
78		ma	ma_b15_1	-502.4715450	0.02118	0.19670	-16	-11	-7	0.221248	0.235186	0.182429	0.183988	-48.99	-502.6499318	10.3
79	<b>1i</b>	a	b16_7	-690.3824887	-0.26006	-0.03324	-5	-2	0	0.227746	0.244796	0.181394	0.185690	-9.02	-690.6189587	0.0
80		a	b16_8	-690.3815225	-0.25338	-0.03690	-3	0	0	0.227709	0.244789	0.181050	0.185853	-9.24	-690.6176437	3.0
81		a	b16_1	-690.3797924	-0.25602	-0.03523	-4	0	0	0.227742	0.244775	0.181516	0.186026	-9.44	-690.6157071	7.7
82		a	b16_6	-690.3799728	-0.26211	-0.03252	-1	0	0	0.228018	0.244898	0.182252	0.186213	-9.21	-690.6157431	9.0
83		a	b16_4	-690.3800104	-0.26240	-0.03213	-5	-2	0	0.227943	0.244846	0.182044	0.186146	-9.14	-690.6155928	9.5
84		a	b16_5	-690.3802253	-0.26199	-0.03195	-7	-5	0	0.227846	0.244811	0.181346	0.186110	-8.99	-690.6157012	9.8
85		a	b16_11	-690.3811994	-0.25466	-0.03777	-7	-2	0	0.228212	0.245023	0.182648	0.186599	-8.59	-690.6161774	11.5
86		a	b16_9	-690.3793030	-0.25668	-0.03622	-6	0	0	0.228164	0.244998	0.182180	0.186629	-8.89	-690.6143398	15.1
87		a	b16_2	-690.3790237	-0.25629	-0.03659	-5	-5	0	0.228317	0.245050	0.183188	0.186741	-8.83	-690.6140158	16.5
88		ma	ma_b16_12	-730.3576450	0.00917	0.15527	-10	-4	0	0.265518	0.284032	0.217542	0.222268	-49.36	-730.6193365	0.0
89		ma	ma_b16_2	-730.3563036	0.00966	0.15889	-12	-1	0	0.265731	0.284115	0.218284	0.222577	-49.45	-730.6180759	3.7
90		ma	ma_b16_8	-730.3546796	0.01030	0.15834	-4	-1	0	0.265706	0.284072	0.218485	0.222514	-50.66	-730.6160808	3.8
91		ma	ma_b16_10	-730.3585729	0.00738	0.15486	-8	-4	0	0.265925	0.284216	0.218627	0.223042	-48.48	-730.6191722	6.1
92		ma	ma_b16_6	-730.3563530	0.00904	0.15758	-8	0	0	0.266085	0.284318	0.219031	0.223089	-49.04	-730.6170496	9.5
93		ma	ma_b16_15	-730.3582709	0.00735	0.15287	-5	0	0	0.266226	0.284363	0.219483	0.223304	-48.39	-730.6182591	9.6

94		ma	ma_b16_11	-730.3586622	0.00677	0.15379	-6	0	0	0.266205	0.284373	0.219179	0.223426	-48.18	-730.6183127	10.7
95		ma	ma_b16_5	-730.3569348	0.00799	0.15615	-10	0	0	0.266462	0.284484	0.219961	0.223736	-48.50	-730.6170611	13.4
96		ma	ma_b16_7	-730.3569361	0.00793	0.15619	-4	0	0	0.266506	0.284485	0.220282	0.223829	-48.50	-730.6170333	13.7
97		ma	ma_b16_1	-730.3540099	0.00601	0.17316	-7	-5	0	0.265602	0.283957	0.218615	0.222618	-48.83	-730.6149116	14.8
98		ma	ma_b16_4	-730.3542372	0.00501	0.16945	0	0	0	0.266279	0.284263	0.220511	0.223685	-48.10	-730.6136965	23.8
99	<b>1j</b>	a	b11_3	-423.1875852	-0.25754	-0.03100	-9	0	0	0.155912	0.167440	0.119000	0.120363	-4.44	-423.3304022	0.0
100		a	b11_4	-423.1873664	-0.25819	-0.03162	-7	0	0	0.156203	0.167570	0.119892	0.120853	-4.21	-423.3297139	4.1
101		a	b11_1	-423.1856083	-0.25816	-0.02967	-5	0	0	0.155999	0.167442	0.119483	0.120720	-4.93	-423.3281430	4.8
102		a	b11_2	-423.1854317	-0.25856	-0.03039	-10	0	0	0.156242	0.167560	0.119931	0.121129	-4.59	-423.3275275	8.9
103		ma	ma_b11_10	-463.1505478	0.02436	0.20083	-11	-5	0	0.193874	0.206647	0.155819	0.157310	-49.39	-463.3200794	0.0
104		ma	ma_b11_5	-463.1516378	0.02241	0.19912	-17	0	0	0.194261	0.206806	0.156872	0.158107	-48.57	-463.3200936	5.5
105		ma	ma_b11_1	-463.1450568	0.02922	0.20247	0	0	0	0.193714	0.206541	0.155665	0.156862	-50.65	-463.3142054	9.0
106		ma	ma_b11_3	-463.1460068	0.02746	0.20078	-13	0	0	0.194031	0.206670	0.156356	0.157673	-49.84	-463.3140734	14.8
107	<b>4t</b>	a	e2_1	-1144.6604725	-0.25325	-0.07526	-4	-3	0	0.241158	0.258291	0.194102	0.199002	-12.79	-1144.9686985	0.0
108		a	e2_2	-1144.6547663	-0.25776	-0.07343	-31	-11	-5	0.240884	0.257228	0.195835	0.199360	-14.71	-1144.9650800	2.4
109		ma	ma_e2_2	-1184.6230863	-0.05639	0.10814	-7	-4	0	0.278568	0.297370	0.229421	0.235239	-53.72	-1184.9589197	0.0
110		ma	ma_e2_1	-1184.6229082	-0.05364	0.10930	-4	0	0	0.278565	0.297331	0.229693	0.235282	-53.62	-1184.9591214	0.0
111		ma	ma_e2_4	-1184.6223730	-0.05529	0.10927	-12	-4	-1	0.278505	0.297352	0.228913	0.235296	-53.73	-1184.9588237	0.4
112		ma	ma_e2_8	-1184.6163866	-0.05721	0.10918	-5	0	0	0.278739	0.297480	0.230630	0.235526	-54.26	-1184.9513732	18.3
113		ma	ma_e2_10	-1184.6149012	-0.05507	0.11151	-8	0	0	0.278770	0.297557	0.229575	0.235759	-54.63	-1184.9497771	21.6
114		ma	ma_e2_12	-1184.6164873	-0.03978	0.10929	-3	0	0	0.278797	0.297517	0.230615	0.235375	-53.37	-1184.9499128	25.5
115		ma	ma_e2_11	-1184.6159449	-0.03960	0.10976	-7	0	0	0.278693	0.297479	0.229779	0.235273	-53.49	-1184.9495971	25.5
116	<b>4u</b>	a	e5_1	-1387.2683067	-0.23897	-0.08281	-5	-3	0	0.250831	0.270489	0.200762	0.206356	-13.05	-1387.6662036	0.0
117		a	e5_3	-1387.2683063	-0.23897	-0.08282	-9	-5	0	0.250782	0.269546	0.202878	0.207054	-13.05	-1387.6662033	1.8
118		ma	ma_e5_2	-1427.2481016	-0.02865	0.06069	-9	0	0	0.288280	0.309565	0.237986	0.242296	-49.76	-1427.6723115	0.0
119		ma	ma_e5_1	-1427.2458821	-0.03243	0.06313	-4	0	0	0.288307	0.309691	0.237576	0.242198	-49.17	-1427.6698618	8.6
120		ma	ma_e5_3	-1427.2410800	-0.02518	0.05234	0	0	0	0.288067	0.309486	0.236984	0.241913	-51.61	-1427.6648273	10.9
121		ma	ma_e5_4	-1427.2418801	-0.02634	0.05595	-11	-4	-1	0.288287	0.309685	0.237139	0.242283	-50.34	-1427.6658762	14.4

**Table S44.** QM properties for gas phase optimized conformers of selected allenoates (**1a-j**, a) and their corresponding PPh<sub>3</sub> adducts (pa). <sup>a</sup> PPh<sub>3</sub> adducts=pa, Allenoate=a. <sup>b</sup> Truhlar quasi-harmonic treatment was used for thermal corrections. <sup>c</sup> Relative Gibbs energies (Rel.  $\Delta G_{\text{sol}}$ ) =  $\Delta E_{\text{tot}} + \text{corr. qh-}\Delta G$  calculated at PCM(DCM,ua0)/B3LYP-D3/6-31+G(d,p) level of theory.

SI	Mol.	Type <sup>a</sup>	File Name Internal Reference	PCM(DCM,ua0)/B3LYP-D3/6-31+G(d,p)									Rel. $\Delta G_{\text{sol}}^{\text{c}}$	
				$\Delta E_{\text{tot}}$ (hartree)	HOMO <sub>E</sub> (hartree)	LUMO <sub>E</sub> (hartree)	Low Frequency			corr. ZPE (hartree)	corr. $\Delta H$ (hartree)	corr. $\Delta G$ (hartree)	corr. qh- $\Delta G^{\text{b}}$ (hartree)	
1	PPh3	Ref.	p1_3	-1036.3867840	-0.22445	-0.03450	0	0	0	0.272896	0.289760	0.226637	0.231592	0.0
2	<b>1a</b>	a	b3_2	-536.3288171	-0.25968	-0.06174	-16	-6	0	0.150655	0.162288	0.111760	0.114650	0.0
3		a	b3_1	-536.3285250	-0.25914	-0.06290	-16	-5	0	0.150628	0.162259	0.112103	0.114697	0.9
4		a	b3_3	-536.3240374	-0.26048	-0.06779	-13	0	0	0.150539	0.162147	0.111890	0.114551	12.3
5		a	b3_4	-536.3224907	-0.25503	-0.06410	-11	0	0	0.150490	0.162045	0.112790	0.114695	16.7
6		pa	pa_b3_200	-1572.7375669	-0.17432	-0.05627	-3	0	0	0.428062	0.455675	0.369964	0.376470	0.0
7		pa	pa_b3_8	-1572.7358786	-0.17675	-0.05364	-10	-6	0	0.427586	0.455418	0.367655	0.375833	2.8
8		pa	pa_b3_7	-1572.7349136	-0.17545	-0.05307	-7	-4	0	0.427545	0.455409	0.367212	0.375774	5.1
9		pa	pa_b3_13	-1572.7349749	-0.17681	-0.06118	-12	0	0	0.427655	0.455639	0.366778	0.375988	5.5
10		pa	pa_b3_12	-1572.7336307	-0.17508	-0.06149	-7	0	0	0.427521	0.455531	0.366376	0.375470	7.7
11		pa	pa_b3_4	-1572.7332041	-0.17651	-0.05374	-5	0	0	0.427587	0.455427	0.367411	0.375719	9.5
12		pa	pa_b3_10	-1572.7252180	-0.17813	-0.05821	-12	-11	0	0.427035	0.455034	0.366263	0.375054	28.7
13	<b>1b</b>	a	b5_5	-575.6519010	-0.26129	-0.05682	-13	-3	0	0.179916	0.192871	0.138806	0.142401	0.0
14		a	b5_2	-575.6517700	-0.26159	-0.05731	-2	0	0	0.179927	0.192852	0.139278	0.142512	0.6
15		a	b5_4	-575.6518587	-0.26032	-0.05669	-11	0	0	0.180240	0.193029	0.139677	0.142899	1.4
16		a	b5_1	-575.6517246	-0.26033	-0.05705	-8	0	0	0.180196	0.192997	0.139633	0.142926	1.8
17		a	b5_6	-575.6427432	-0.26010	-0.06457	-25	-10	0	0.179808	0.192659	0.139093	0.142646	24.7
18		a	b5_7	-575.6419924	-0.26341	-0.06465	-9	0	0	0.179760	0.192752	0.138870	0.142249	25.6
19		pa	pa_b5_154	-1612.0575812	-0.16728	-0.05621	-8	-4	0	0.457165	0.486125	0.397330	0.404066	0.0
20		pa	pa_b5_111	-1612.0569534	-0.16994	-0.05473	-8	0	0	0.457070	0.485981	0.397164	0.404144	1.9
21		pa	pa_b5_1	-1612.0569154	-0.16686	-0.05776	-1	0	0	0.457239	0.486185	0.397345	0.404146	2.0
22		pa	pa_b5_143	-1612.0568299	-0.16777	-0.05419	-10	-1	0	0.456981	0.485988	0.396192	0.404175	2.3
23		pa	pa_b5_158	-1612.0565335	-0.17006	-0.05107	-12	-4	0	0.457059	0.485922	0.396696	0.404298	3.4
24		pa	pa_b5_151	-1612.0563183	-0.16874	-0.05074	-8	0	0	0.456940	0.485788	0.397188	0.404086	3.4
25		pa	pa_b5_4	-1612.0560393	-0.16833	-0.05416	0	0	0	0.456871	0.485890	0.396201	0.403978	3.8
26		pa	pa_b5_116	-1612.0562405	-0.16959	-0.05120	-9	-4	0	0.457095	0.486088	0.395302	0.404250	4.0

27		pa	pa_b5_115	-1612.0535517	-0.16812	-0.05142	-10	-8	0	0.456517	0.485837	0.393104	0.403109	8.1
28		pa	pa_b5_137	-1612.0522463	-0.17345	-0.05091	-13	-7	0	0.457170	0.486032	0.396413	0.404395	14.9
29		pa	pa_b5_120	-1612.0519109	-0.17256	-0.05072	-14	-7	0	0.457133	0.486094	0.395643	0.404327	15.6
30		pa	pa_b5_110	-1612.0508626	-0.17316	-0.05713	-9	-8	-4	0.456254	0.485411	0.395397	0.403291	15.6
31		pa	pa_b5_123	-1612.0513717	-0.17344	-0.05105	-10	-7	0	0.456919	0.485893	0.395239	0.404181	16.6
32		pa	pa_b5_126	-1612.0496272	-0.17473	-0.05098	-8	-3	0	0.456779	0.485984	0.393971	0.403381	19.1
33		pa	pa_b5_139	-1612.0420121	-0.17689	-0.05687	-5	0	0	0.456165	0.485425	0.393798	0.402946	37.9
34	<b>1c</b>	a	b14_5	-614.9829014	-0.23902	-0.05716	-10	-5	0	0.208749	0.223123	0.165864	0.169482	0.0
35		a	b14_1	-614.9824898	-0.24002	-0.05729	-8	-3	0	0.208724	0.223101	0.165987	0.169493	1.1
36		a	b14_6	-614.9823329	-0.23904	-0.05730	-8	-4	0	0.208958	0.223215	0.166442	0.169872	2.5
37		a	b14_7	-614.9822752	-0.23899	-0.05732	-11	0	0	0.208969	0.223220	0.166592	0.169870	2.7
38		a	b14_2	-614.9820129	-0.24002	-0.05752	0	0	0	0.209016	0.223237	0.166785	0.169927	3.5
39		a	b14_3	-614.9819694	-0.23996	-0.05746	-10	0	0	0.208962	0.223208	0.166709	0.169914	3.6
40		pa	pa_b14_18	-1651.3874877	-0.16535	-0.05439	-4	-2	0	0.485521	0.516139	0.422650	0.430930	0.0
41		pa	pa_b14_9	-1651.3867843	-0.16530	-0.05391	-4	0	0	0.485264	0.516118	0.421514	0.430338	0.3
42		pa	pa_b14_201	-1651.3870125	-0.16549	-0.05750	-7	-6	0	0.485710	0.516244	0.423728	0.430972	1.4
43		pa	pa_b14_19	-1651.3865537	-0.16554	-0.05359	-6	0	0	0.485501	0.516223	0.421521	0.431013	2.7
44		pa	pa_b14_16	-1651.3853467	-0.16588	-0.05321	-10	-5	0	0.485258	0.516187	0.420814	0.430454	4.4
45		pa	pa_b14_200	-1651.3856223	-0.16496	-0.05702	-4	0	0	0.485565	0.516195	0.422846	0.430889	4.8
46		pa	pa_b14_27	-1651.3855217	-0.16627	-0.05291	-7	0	0	0.485487	0.516217	0.421629	0.430955	5.2
47		pa	pa_b14_23	-1651.3854150	-0.16624	-0.05328	-2	0	0	0.485517	0.516207	0.422304	0.430931	5.4
48		pa	pa_b14_1	-1651.3829721	-0.17108	-0.05438	-6	-4	0	0.485572	0.516285	0.422106	0.430753	11.4
49		pa	pa_b14_6	-1651.3820645	-0.17010	-0.05464	-8	-1	0	0.485646	0.516247	0.422601	0.431098	14.7
50		pa	pa_b14_14	-1651.3820110	-0.17045	-0.05422	-7	0	0	0.485639	0.516244	0.422356	0.431127	14.9
51		pa	pa_b14_2	-1651.3817294	-0.17171	-0.05348	-5	0	0	0.485704	0.516436	0.422187	0.430967	15.2
52		pa	pa_b14_12	-1651.3807027	-0.17086	-0.05338	-11	-6	-3	0.485625	0.516305	0.422052	0.431052	18.1
53		pa	pa_b14_11	-1651.3804385	-0.17093	-0.05329	-5	-1	0	0.485717	0.516394	0.422159	0.431079	18.9
54		pa	pa_b14_26	-1651.3745597	-0.17199	-0.05831	-10	-5	0	0.485083	0.515859	0.421060	0.430477	32.8
55	<b>1d</b>	a	d1_1	-382.6858145	-0.28036	-0.05999	-9	0	0	0.106955	0.115068	0.075123	0.075314	0.0
56		pa	pa_d1_2	-1419.0908257	-0.16798	-0.05371	-11	-7	0	0.383226	0.407779	0.328629	0.334185	0.0
57		pa	pa_d1_1	-1419.0862075	-0.16577	-0.06328	0	0	0	0.383937	0.408208	0.330132	0.335220	14.8
58	<b>1e</b>	a	b2_2	-344.5732599	-0.28378	-0.05735	-14	-13	0	0.098890	0.107487	0.066683	0.066966	0.0
59		a	b2_1	-344.5732682	-0.28896	-0.05762	-15	-10	0	0.098854	0.107463	0.066699	0.067114	0.4

60		a	b2_3	-344.5635137	-0.29020	-0.06556	-19	0	0	0.098791	0.107371	0.066234	0.067165	26.1
61		pa	pa_b2_11	-1380.9744888	-0.16735	-0.05123	-12	0	0	0.375521	0.400361	0.320956	0.326005	0.0
62		pa	pa_b2_12	-1380.9744271	-0.16734	-0.05125	-12	0	0	0.375517	0.400360	0.320922	0.326004	0.2
63		pa	pa_b2_1	-1380.9729478	-0.16783	-0.05496	0	0	0	0.375525	0.400352	0.321199	0.326065	4.2
64		pa	pa_b2_14	-1380.9709872	-0.17429	-0.05084	-12	-9	0	0.375809	0.400495	0.321093	0.326696	11.0
65		pa	pa_b2_3	-1380.9661837	-0.17190	-0.05780	-7	0	0	0.375111	0.399872	0.321144	0.325904	21.5
66		pa	pa_b2_110	-1380.9621797	-0.17595	-0.05630	-9	0	0	0.375316	0.400073	0.320616	0.326151	32.7
67		pa	pa_b2_114	-1380.9528496	-0.17734	-0.06030	-14	-7	0	0.374785	0.399705	0.319833	0.325441	55.3
68	<b>1f</b>	a	b9_3	-383.8985206	-0.28214	-0.05598	-27	-12	0	0.127113	0.137031	0.092515	0.093335	0.0
69		a	b9_1	-383.8984764	-0.28720	-0.05639	0	0	0	0.127174	0.137044	0.092935	0.093726	1.1
70		a	b9_4	-383.8979756	-0.28224	-0.05621	-15	0	0	0.127320	0.137118	0.093027	0.093752	2.5
71		a	b9_2	-383.8979223	-0.28719	-0.05650	0	0	0	0.127365	0.137142	0.093265	0.094016	3.4
72		a	b9_5	-383.8891899	-0.28815	-0.06370	-18	-14	-9	0.126983	0.136937	0.092055	0.093394	24.7
73		a	b9_6	-383.8882269	-0.28848	-0.06271	-25	-15	0	0.127139	0.136969	0.092198	0.093817	28.3
74		a	b9_7	-383.8875722	-0.28277	-0.05826	-7	-4	0	0.127035	0.136943	0.092658	0.093319	28.7
75		pa	pa_b9_16	-1420.2992854	-0.16693	-0.05107	-4	0	0	0.403745	0.429947	0.346620	0.353120	0.0
76		pa	pa_b9_111	-1420.2993378	-0.16789	-0.05530	-8	-5	0	0.404159	0.430108	0.348789	0.353662	1.3
77		pa	pa_b9_17	-1420.2992889	-0.16739	-0.05080	-5	0	0	0.404126	0.430060	0.348126	0.353853	1.9
78		a	ts_p1a_9_ircr_o	-1420.2995844	-0.16720	-0.05063	-24	-10	0	0.403906	0.429053	0.349559	0.354261	2.2
79		pa	pa_b9_118	-1420.2985171	-0.16600	-0.05501	-8	0	0	0.404147	0.430094	0.348550	0.353710	3.6
80		pa	pa_b9_121	-1420.2981638	-0.16628	-0.05477	-3	0	0	0.404032	0.430029	0.348103	0.353690	4.4
81		pa	pa_b9_1	-1420.2958438	-0.17354	-0.05062	-5	0	0	0.404021	0.430068	0.347454	0.353414	9.8
82		pa	pa_b9_2	-1420.2946083	-0.17287	-0.05050	0	0	0	0.404174	0.430127	0.347576	0.353841	14.2
83		pa	pa_b9_113	-1420.2922301	-0.17183	-0.05794	-12	-9	0	0.403647	0.429615	0.348162	0.353373	19.2
84		pa	pa_b9_119	-1420.2905995	-0.17101	-0.05741	0	0	0	0.403484	0.429527	0.347666	0.353021	22.5
85		pa	pa_b9_120	-1420.2886045	-0.17031	-0.05833	-13	-8	0	0.403538	0.429574	0.347730	0.353147	28.1
86	<b>1g</b>	a	b13_4	-423.2228539	-0.26924	-0.05380	-14	-8	0	0.155661	0.167111	0.118716	0.119958	0.0
87		a	b13_1	-423.2227431	-0.27355	-0.05407	-20	-9	-5	0.155563	0.167064	0.118472	0.120075	0.6
88		a	b13_5	-423.2222889	-0.26927	-0.05405	-6	0	0	0.155840	0.167194	0.119166	0.120172	2.0
89		a	b13_6	-423.2222677	-0.26926	-0.05401	-13	-1	0	0.155843	0.167201	0.119083	0.120217	2.2
90		a	b13_2	-423.2222370	-0.27360	-0.05432	-8	0	0	0.155801	0.167175	0.119048	0.120326	2.6
91		pa	pa_b13_7	-1459.6237884	-0.16372	-0.05015	-7	-3	0	0.431924	0.459735	0.373004	0.379960	0.0
92		pa	pa_b13_19	-1459.6239639	-0.16391	-0.04975	-11	0	0	0.432143	0.459791	0.373387	0.380440	0.8

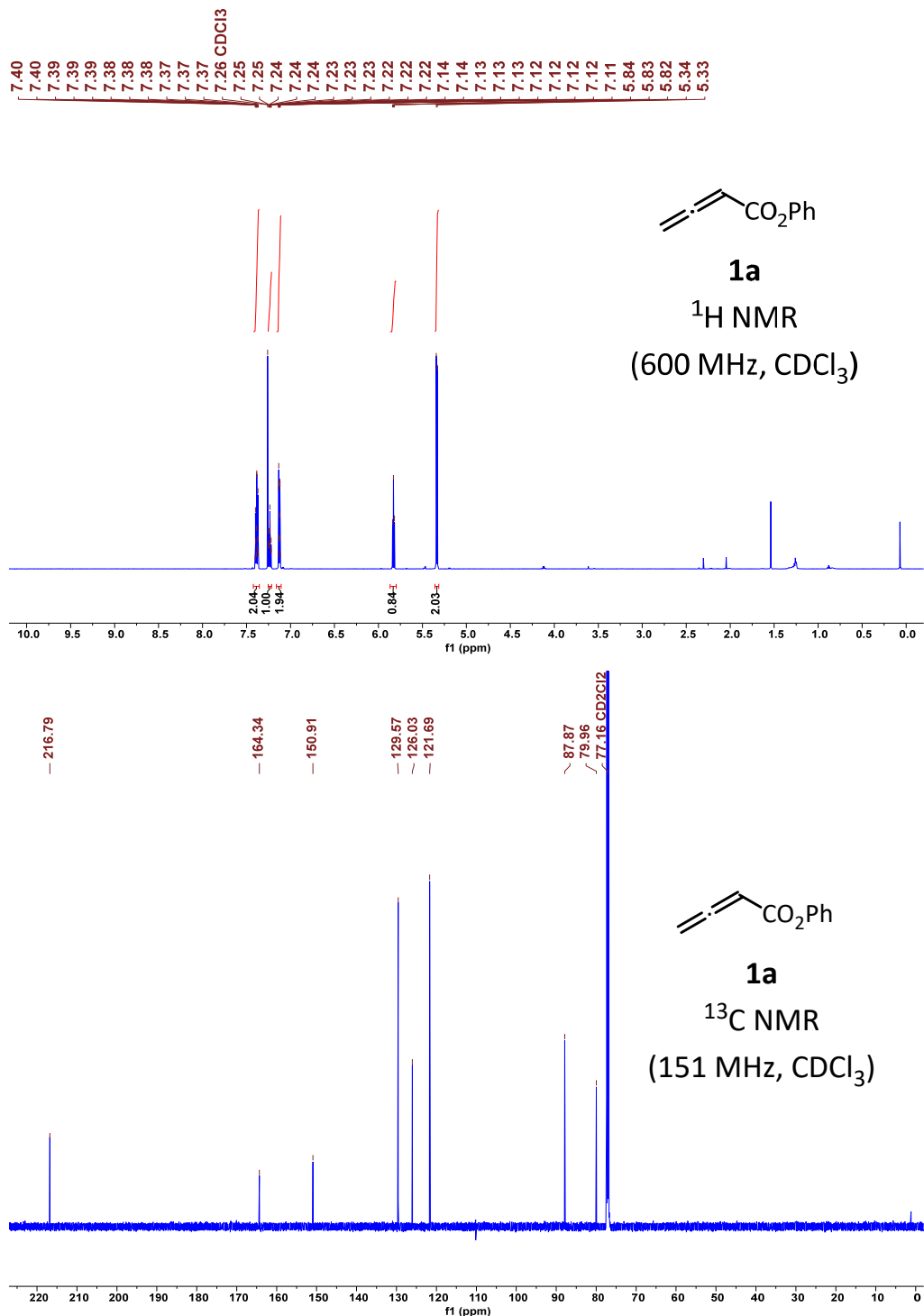
93		pa	pa_b13_12	-1459.6236044	-0.16411	-0.04984	-9	0	0	0.432172	0.459782	0.374016	0.380479	1.8
94		pa	pa_b13_200	-1459.6239297	-0.16469	-0.05422	0	0	0	0.432673	0.460033	0.376040	0.381043	2.5
95		pa	pa_b13_1	-1459.6205267	-0.17042	-0.04975	-12	0	0	0.432058	0.459795	0.373248	0.380015	8.7
96		pa	pa_b13_8	-1459.6191079	-0.16959	-0.04962	-4	0	0	0.432421	0.459972	0.374297	0.380620	14.0
97		pa	pa_b13_3	-1459.6191575	-0.16950	-0.04967	0	0	0	0.432415	0.459930	0.374398	0.380706	14.1
98		pa	pa_b13_4	-1459.6190305	-0.16972	-0.04981	-5	0	0	0.432462	0.460011	0.374156	0.380680	14.4
99		pa	pa_b13_17	-1459.6153200	-0.16520	-0.05486	0	0	0	0.431217	0.459151	0.372474	0.378624	18.7
100		pa	pa_b13_11	-1459.6127515	-0.17207	-0.05511	-12	-10	0	0.431263	0.459278	0.371319	0.378806	25.9
101		pa	pa_b13_16	-1459.6112788	-0.17123	-0.05507	-6	0	0	0.431518	0.459353	0.372543	0.379212	30.9
102	<b>1h</b>	a	b15_2	-462.5446932	-0.27554	-0.05305	-15	-8	0	0.182821	0.195267	0.145646	0.146670	0.0
103		a	b15_1	-462.5444808	-0.28005	-0.05339	-7	-6	0	0.182788	0.195241	0.145749	0.146671	0.6
104		pa	pa_b15_3	-1498.9448304	-0.16467	-0.04962	-10	-1	0	0.459444	0.488059	0.401006	0.407223	0.0
105		pa	pa_b15_2	-1498.9447072	-0.16497	-0.04938	-11	-6	0	0.459383	0.488049	0.400294	0.407220	0.3
106		pa	pa_b15_4	-1498.9448089	-0.16368	-0.06036	-19	-5	0	0.460405	0.488689	0.402704	0.408565	3.6
107		pa	pa_b15_5	-1498.9353007	-0.16802	-0.05728	-15	-6	0	0.459343	0.487885	0.401452	0.407152	24.8
108	<b>1i</b>	a	b16_7	-690.4414700	-0.28046	-0.05476	-21	-4	0	0.226676	0.243714	0.180279	0.184563	0.0
109		a	b16_8	-690.4413506	-0.27411	-0.05531	-11	-6	0	0.226694	0.243701	0.180820	0.184769	0.9
110		a	b16_1	-690.4409317	-0.27512	-0.05479	-7	0	0	0.226738	0.243699	0.181232	0.184971	2.5
111		a	b16_4	-690.4409664	-0.28074	-0.05460	-16	-12	0	0.227145	0.243915	0.182206	0.185404	3.5
112		a	b16_11	-690.4407141	-0.27440	-0.05510	-13	-10	0	0.227180	0.243934	0.181965	0.185631	4.8
113		a	b16_5	-690.4401999	-0.28057	-0.05464	-7	0	0	0.226964	0.243825	0.181340	0.185247	5.1
114		a	b16_6	-690.4399280	-0.28085	-0.05480	-3	0	0	0.226883	0.243782	0.180956	0.185076	5.4
115		a	b16_9	-690.4401894	-0.27561	-0.05532	-10	0	0	0.227203	0.243925	0.182280	0.185673	6.3
116		a	b16_2	-690.4400728	-0.27491	-0.05597	-11	0	0	0.227436	0.244060	0.182918	0.185961	7.3
117		pa	pa_b16_4	-1726.8462372	-0.17011	-0.05478	-8	-5	0	0.504159	0.537043	0.438567	0.447113	0.0
118		pa	pa_b16_18	-1726.8464033	-0.17052	-0.05005	-14	-10	-7	0.504131	0.537039	0.438355	0.447399	0.3
119		pa	pa_b16_2	-1726.8459853	-0.17023	-0.04889	-4	0	0	0.504043	0.536944	0.438399	0.447093	0.6
120		pa	pa_b16_21	-1726.8458553	-0.16917	-0.05498	-4	0	0	0.504111	0.536993	0.439144	0.447195	1.2
121		pa	pa_b16_16	-1726.8460370	-0.17043	-0.04940	-9	-4	0	0.504242	0.537077	0.438980	0.447406	1.3
122		pa	pa_b16_8	-1726.8445277	-0.17031	-0.04979	0	0	0	0.503534	0.536779	0.436061	0.446274	2.3
123		pa	pa_b16_3	-1726.8455869	-0.17002	-0.05475	-11	-10	-6	0.504208	0.537014	0.438890	0.447387	2.4
124		pa	pa_b16_12	-1726.8450198	-0.16921	-0.05372	-8	0	0	0.503877	0.536911	0.437576	0.446847	2.5
125		pa	pa_b16_1	-1726.8454387	-0.16999	-0.04885	-7	0	0	0.504186	0.537009	0.438298	0.447415	2.9

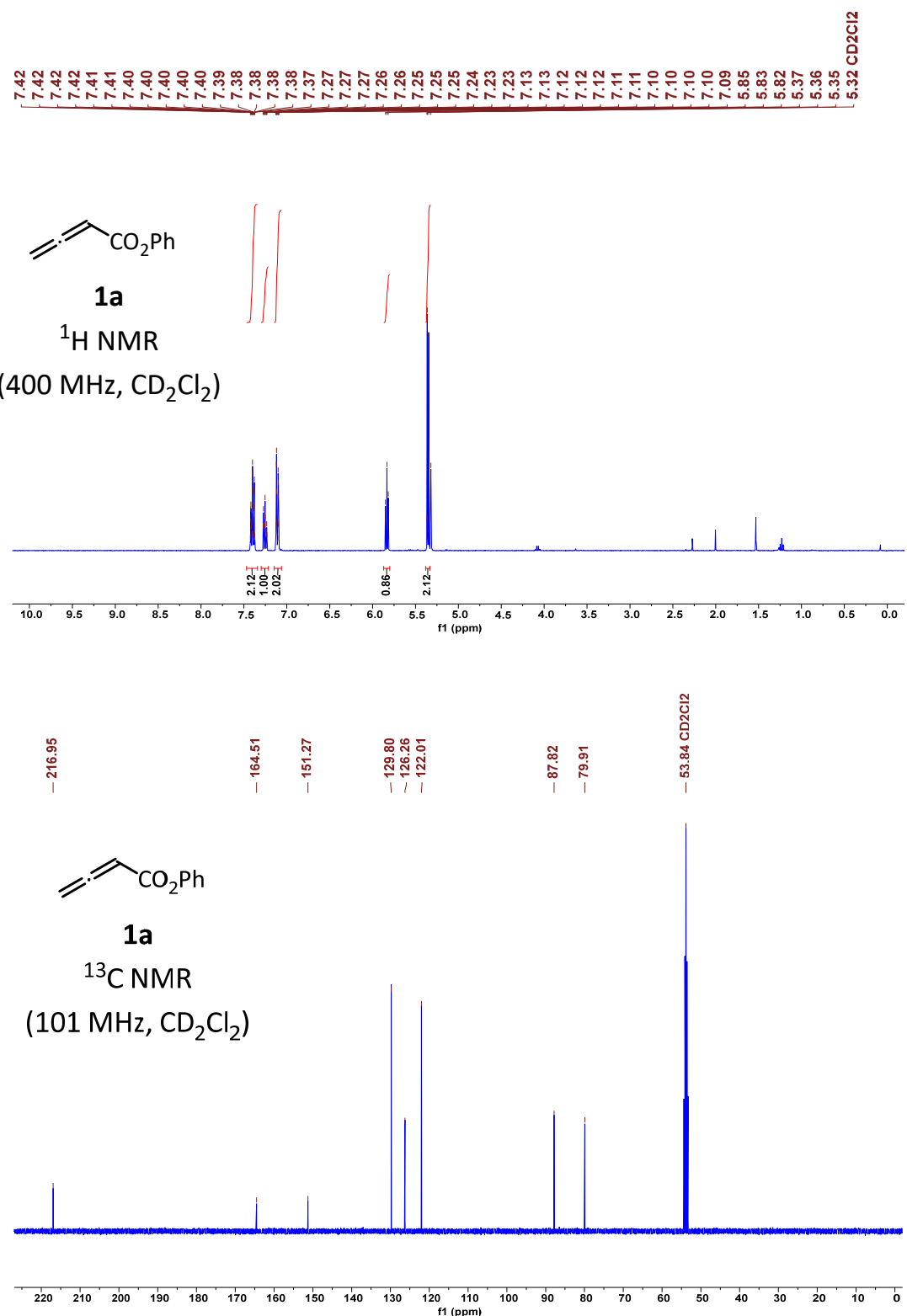
126		pa	pa_b16_24	-1726.8451486	-0.17065	-0.04941	-10	0	0	0.504136	0.537058	0.438007	0.447407	3.6
127		pa	pa_b16_26	-1726.8450996	-0.16916	-0.05516	-7	-6	0	0.504281	0.537111	0.439218	0.447487	4.0
128		pa	pa_b16_23	-1726.8446667	-0.17062	-0.04954	-5	0	0	0.504015	0.536974	0.437448	0.447064	4.0
129		pa	pa_b16_22	-1726.8446602	-0.17057	-0.04968	-4	0	0	0.504097	0.537039	0.437376	0.447288	4.6
130		pa	pa_b16_9	-1726.8443666	-0.16927	-0.05379	-11	-7	0	0.503998	0.536970	0.437845	0.447070	4.8
131		pa	pa_b16_29	-1726.8444587	-0.16884	-0.05414	-9	0	0	0.504248	0.537062	0.439189	0.447306	5.2
132		pa	pa_b16_20	-1726.8434891	-0.16878	-0.05400	-9	-1	0	0.504057	0.536920	0.438566	0.447068	7.1
133		pa	pa_b16_17	-1726.8438750	-0.17059	-0.05013	-13	-7	0	0.504398	0.537204	0.438768	0.447752	7.9
134		pa	pa_b16_13	-1726.8414265	-0.16973	-0.05796	-11	-9	-6	0.503889	0.536835	0.439742	0.446858	12.0
135		pa	pa_b16_6	-1726.8404896	-0.16891	-0.05633	-10	0	0	0.504187	0.536914	0.440495	0.447314	15.6
136		pa	pa_b16_19	-1726.8396092	-0.17005	-0.05789	-15	-10	0	0.503824	0.536824	0.438635	0.446867	16.8
137		pa	pa_b16_27	-1726.8370619	-0.16996	-0.05801	-7	-1	0	0.503256	0.536387	0.436611	0.446106	21.4
138		pa	pa_b16_11	-1726.8382404	-0.16808	-0.05614	-10	0	0	0.504251	0.537020	0.440231	0.447516	22.1
139		pa	pa_b16_15	-1726.8378338	-0.16893	-0.05650	-10	0	0	0.504161	0.537087	0.438162	0.447330	22.6
140		pa	pa_b16_14	-1726.8373065	-0.16839	-0.05853	0	0	0	0.503855	0.536779	0.439045	0.446875	22.8
141		pa	pa_b16_28	-1726.8363574	-0.17042	-0.05958	-9	0	0	0.503289	0.536555	0.437189	0.445927	22.8
142		pa	pa_b16_30	-1726.8345277	-0.16989	-0.05928	-11	0	0	0.503245	0.536494	0.437481	0.445834	27.4
143		pa	pa_b16_31	-1726.8268128	-0.16796	-0.06388	-9	0	0	0.503776	0.536738	0.439906	0.446533	49.5
144	<b>1j</b>	a	b11_3	-423.2218997	-0.27338	-0.05034	-16	-7	0	0.155220	0.166692	0.118658	0.119738	0.0
145		a	b11_4	-423.2213195	-0.27351	-0.05061	-7	0	0	0.155369	0.166747	0.119095	0.120026	2.3
146		a	b11_1	-423.2207766	-0.27265	-0.05024	-15	-4	0	0.155258	0.166697	0.118842	0.119935	3.5
147		a	b11_2	-423.2201887	-0.27272	-0.05056	-11	0	0	0.155462	0.166777	0.119224	0.120362	6.1
148		pa	pa_b11_201	-1459.6199522	-0.16288	-0.04800	0	0	0	0.432141	0.459626	0.374543	0.380378	0.0
149		pa	pa_b11_16	-1459.6202236	-0.16312	-0.04763	-2	0	0	0.432278	0.459618	0.375021	0.380863	0.6
150		pa	pa_b11_202	-1459.6202235	-0.16312	-0.04763	-2	0	0	0.432278	0.459618	0.375025	0.380863	0.6
151		pa	pa_b11_200	-1459.6198476	-0.16352	-0.04752	-9	-1	0	0.432236	0.459618	0.374471	0.380858	1.5
152		pa	pa_b11_2	-1459.6189621	-0.16184	-0.05329	-6	0	0	0.432577	0.459789	0.376246	0.381111	4.5
153		pa	pa_b11_6	-1459.6185601	-0.16203	-0.05307	-7	0	0	0.432386	0.459703	0.375436	0.380886	5.0
154		pa	pa_b11_4	-1459.6121839	-0.16255	-0.05693	-4	0	0	0.431934	0.459314	0.375734	0.380233	20.0
155		pa	pa_b11_5	-1459.6103835	-0.16163	-0.05622	-11	-1	0	0.431201	0.458953	0.372987	0.379256	22.2

## 7 Copies of NMR Spectra

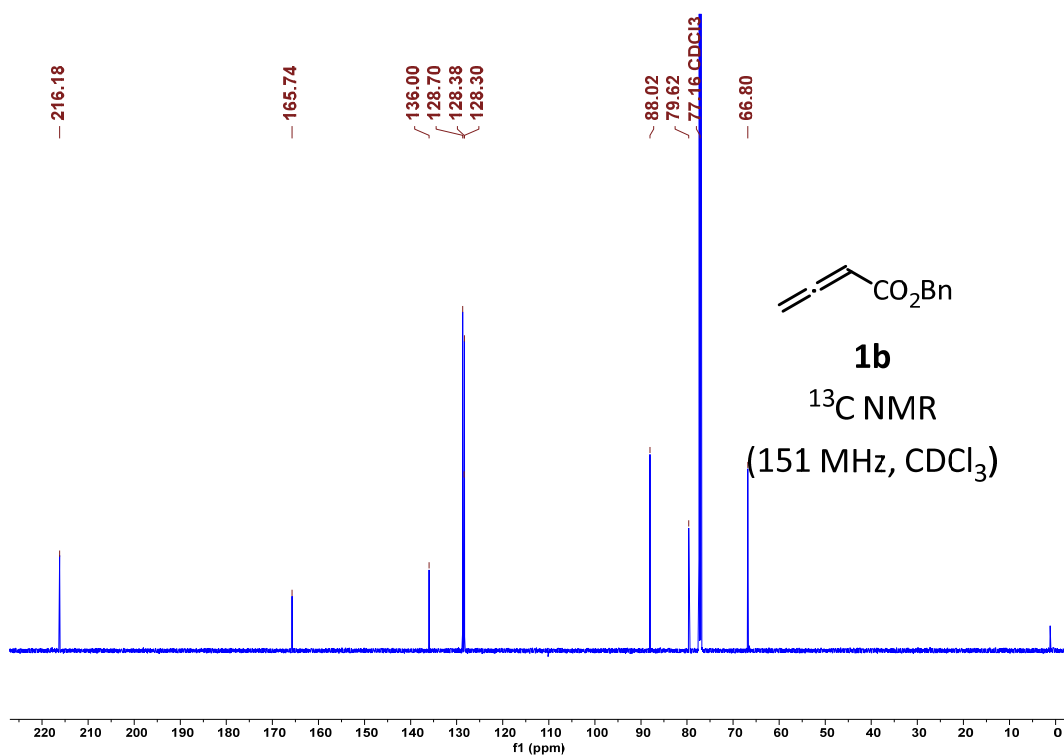
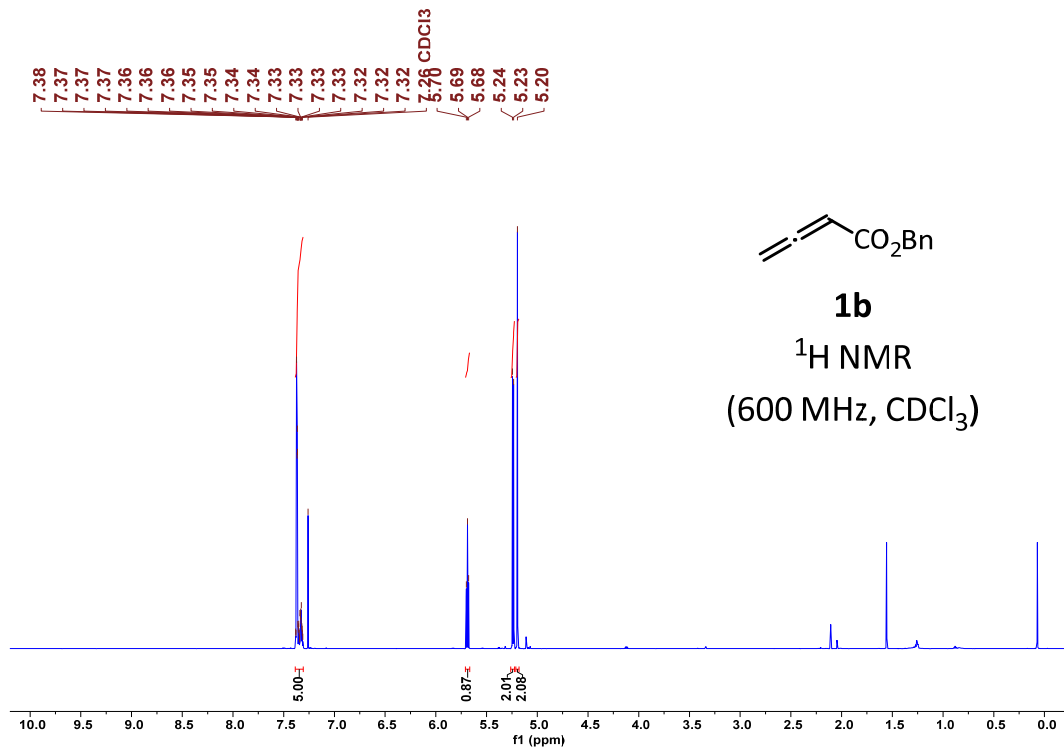
### 7.1 NMR spectra of alkyl allenoates 1

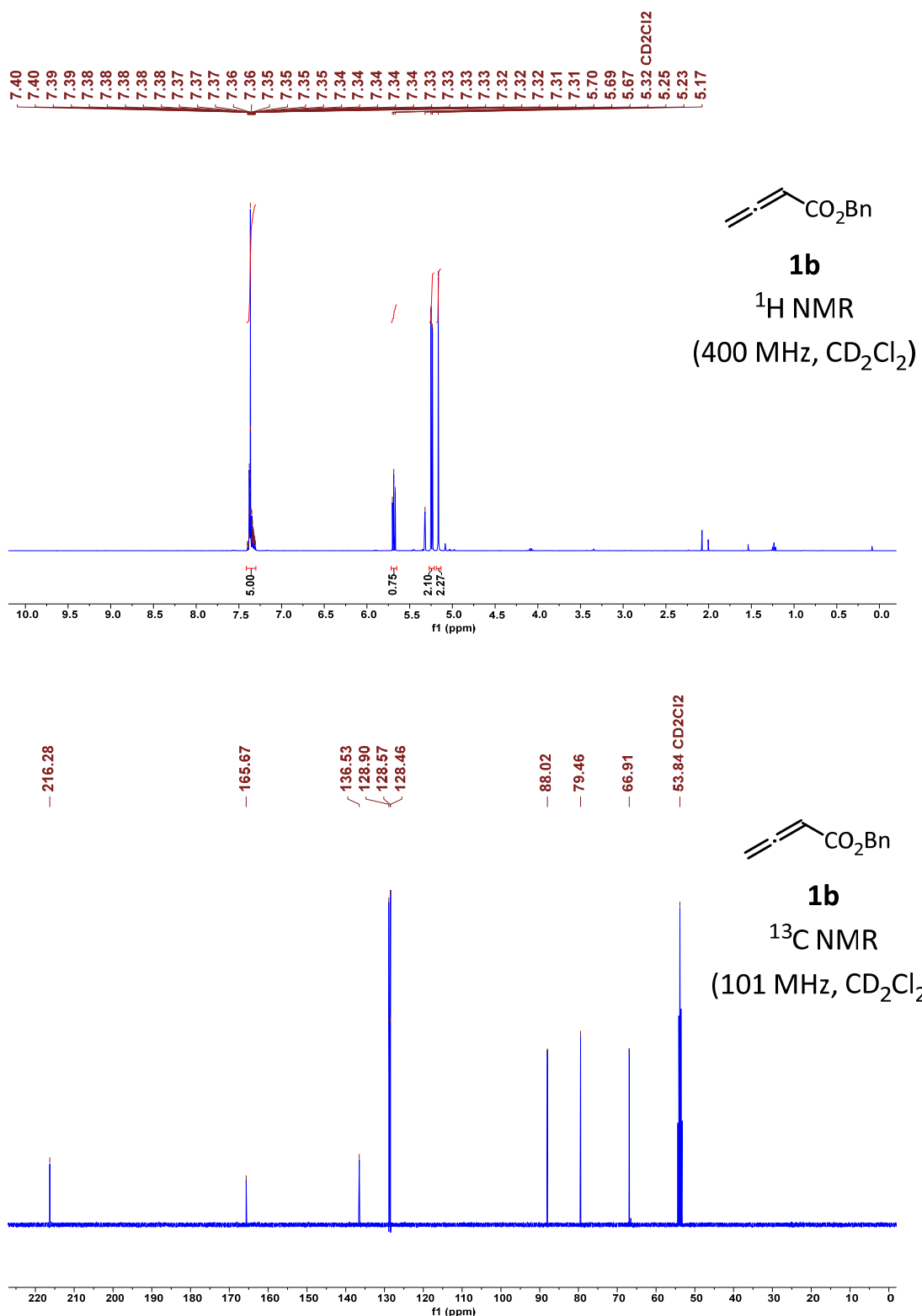
#### 7.1.1 Phenyl buta-2,3-dienoate (1a)



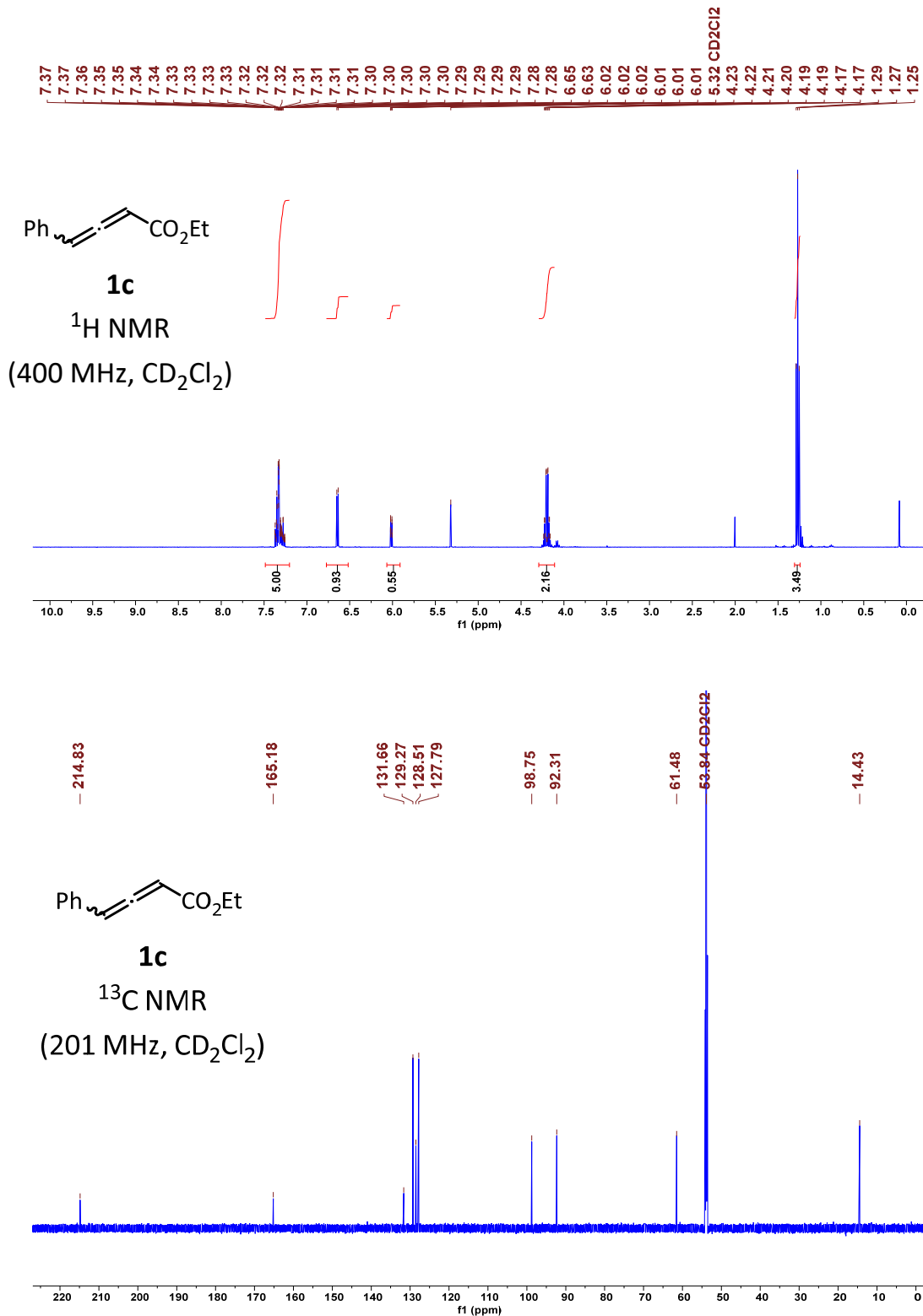


### 7.1.2 Benzyl buta-2,3-dienoate (1b)

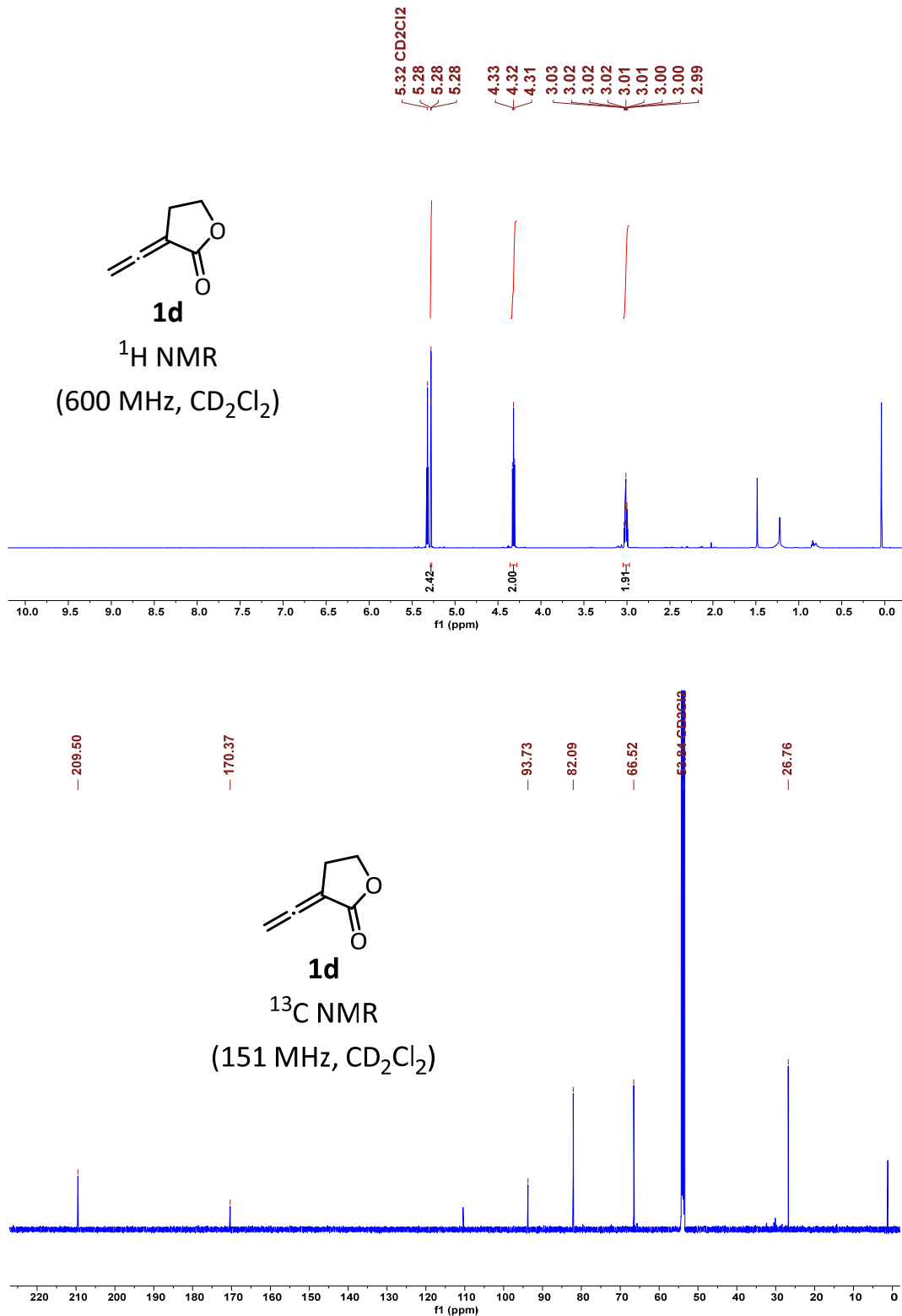




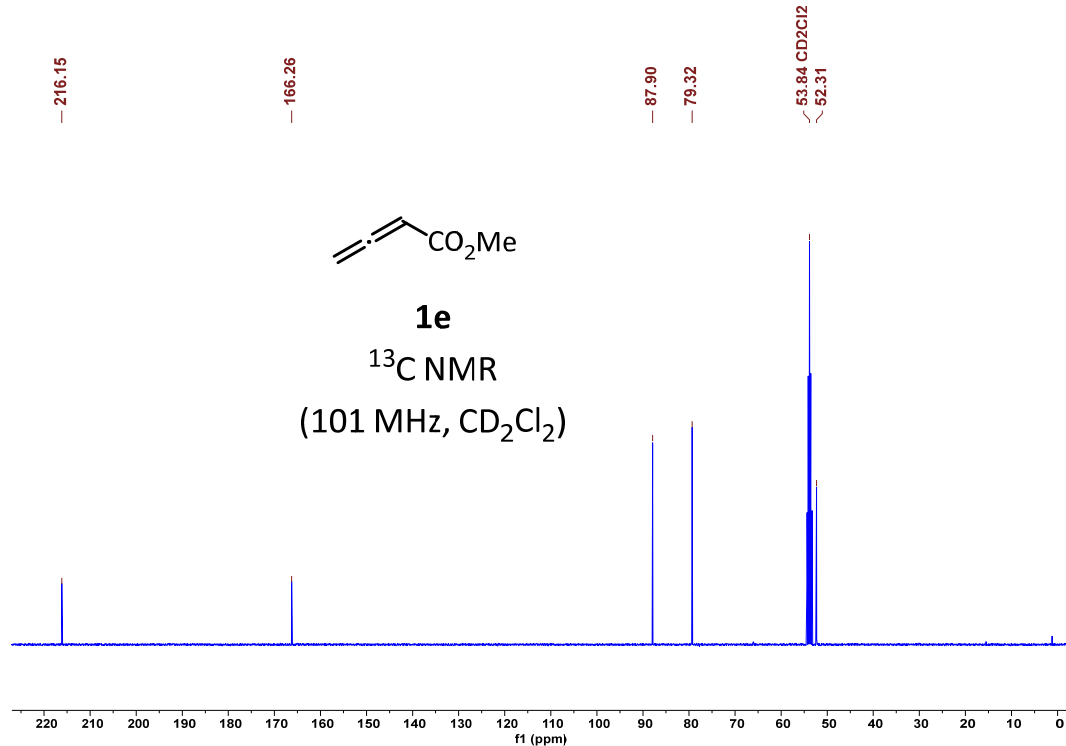
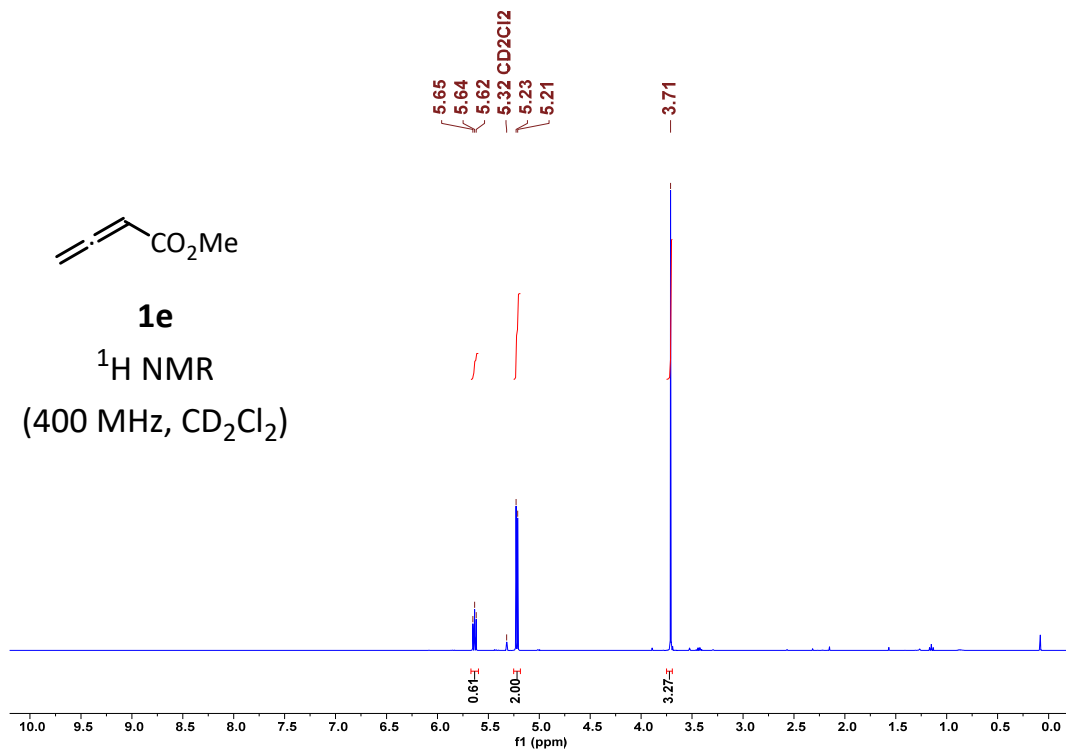
**7.1.3 Ethyl 4-phenylbuta-2,3-dienoate (1c)**



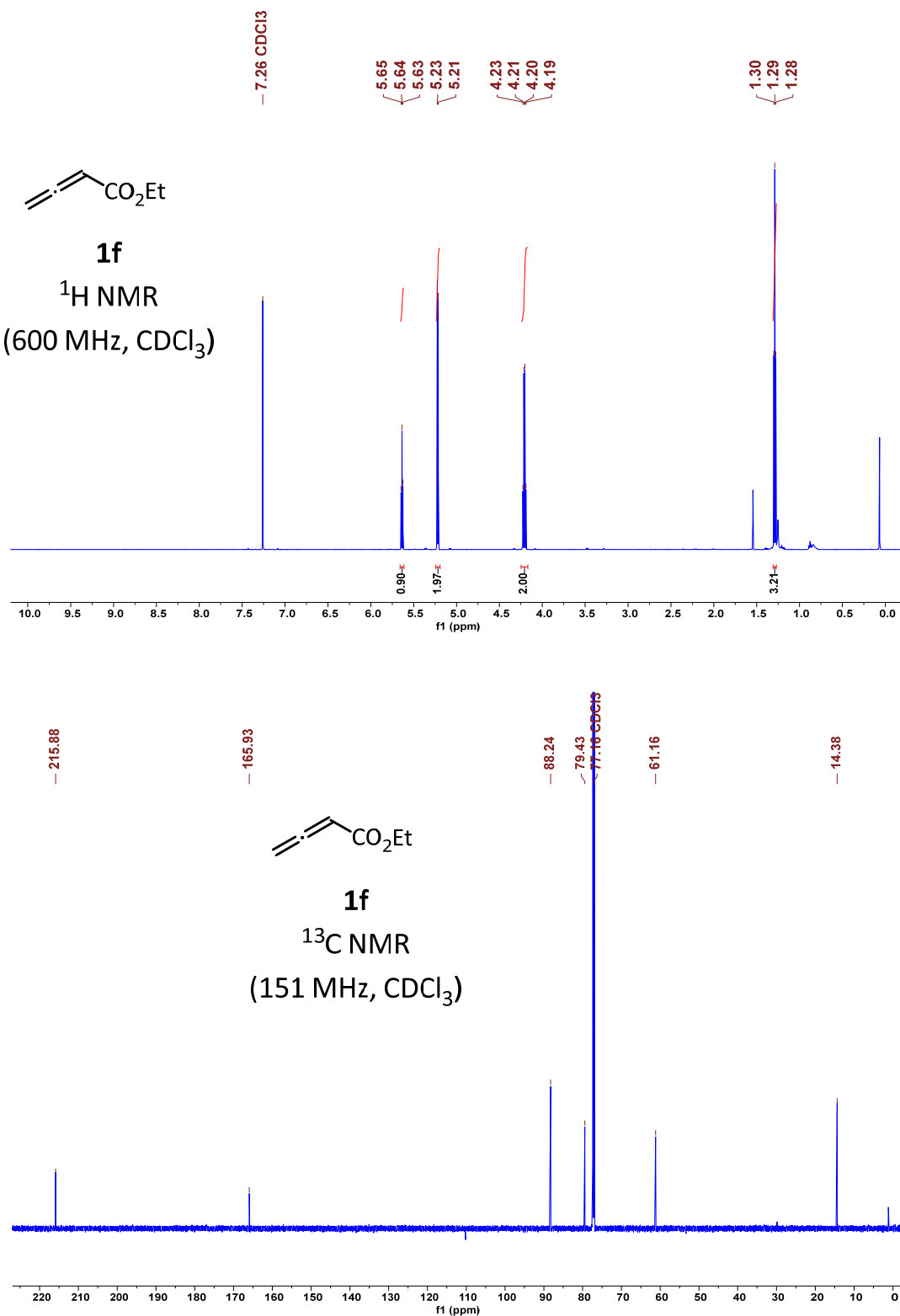
**7.1.4 3-Vinylidenedihydrofuran-2(3H)-one (1d)**

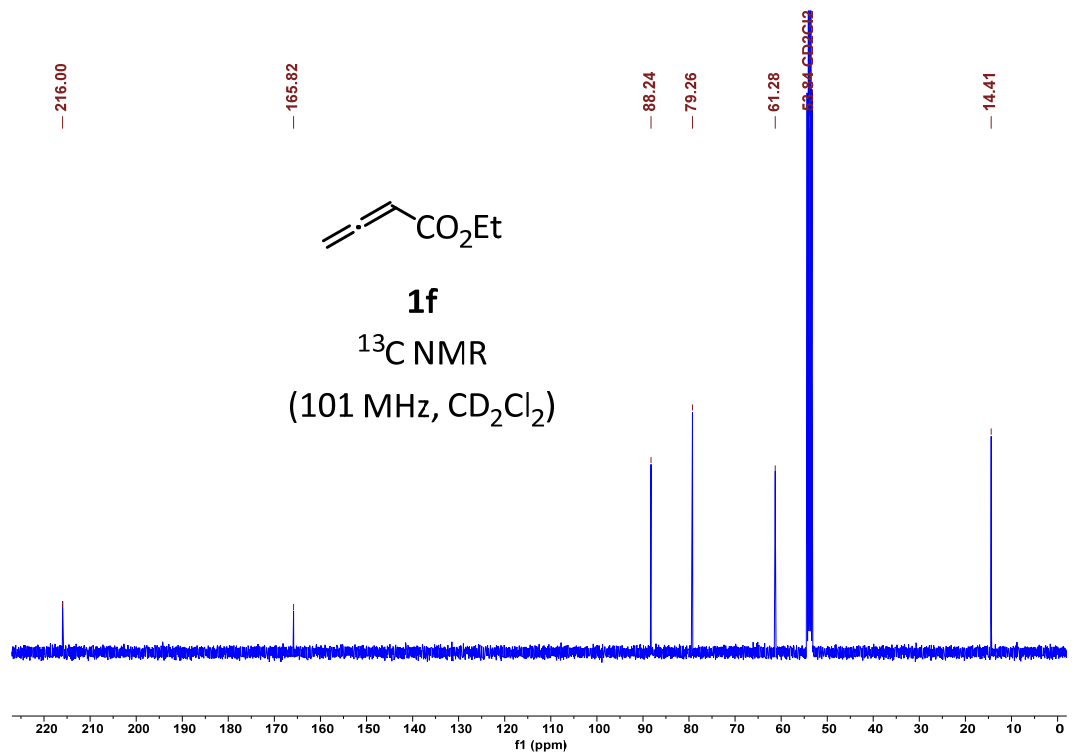
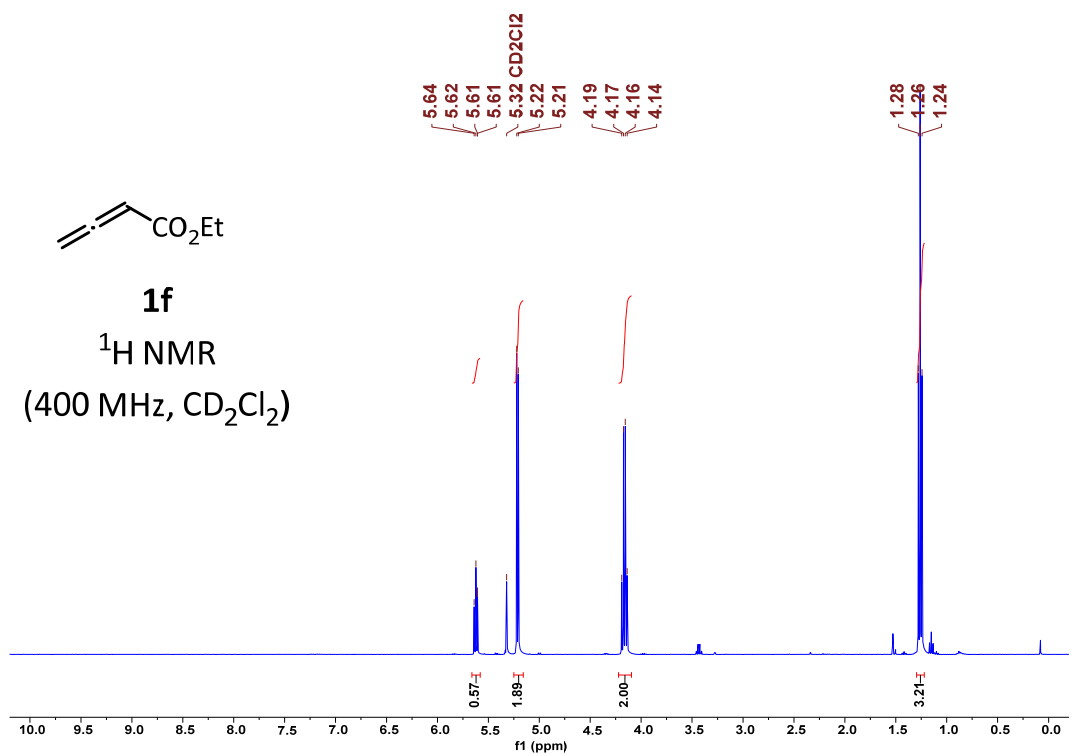


### 7.1.5 Methyl buta-2,3-dienoate (1e)

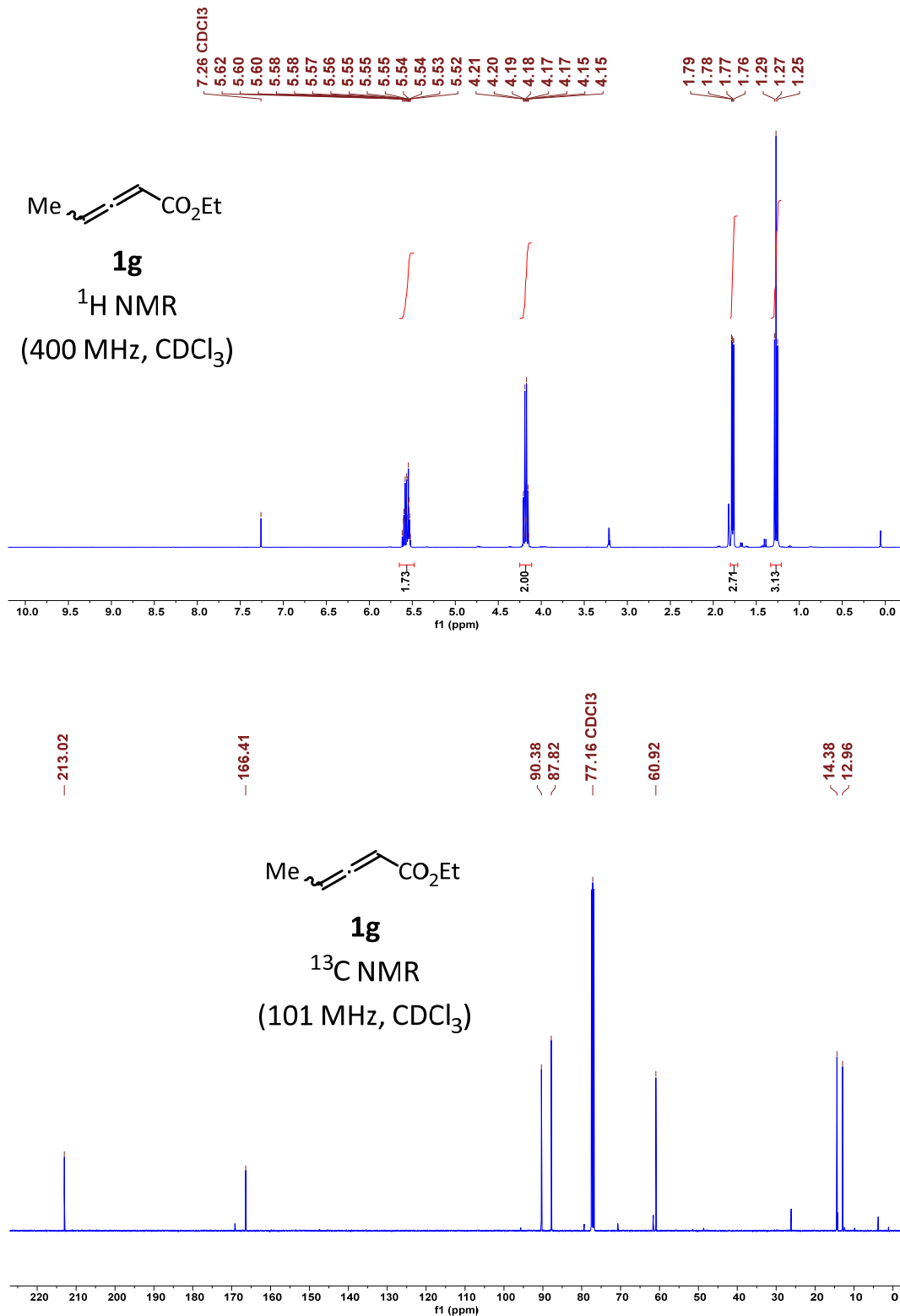


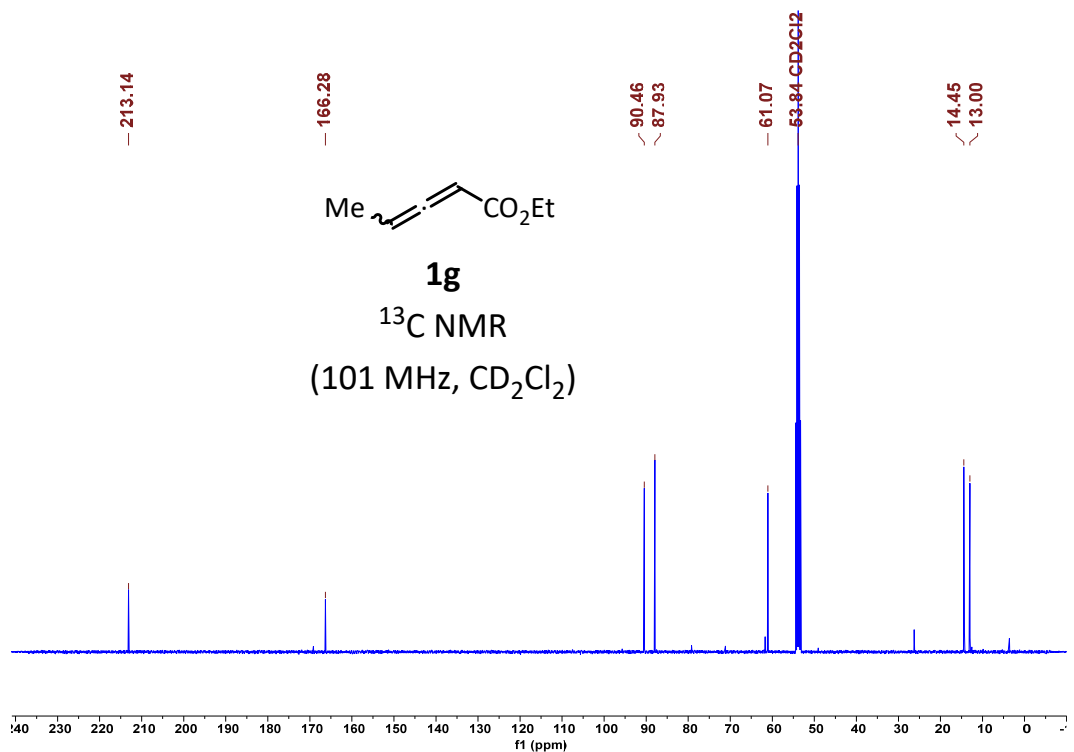
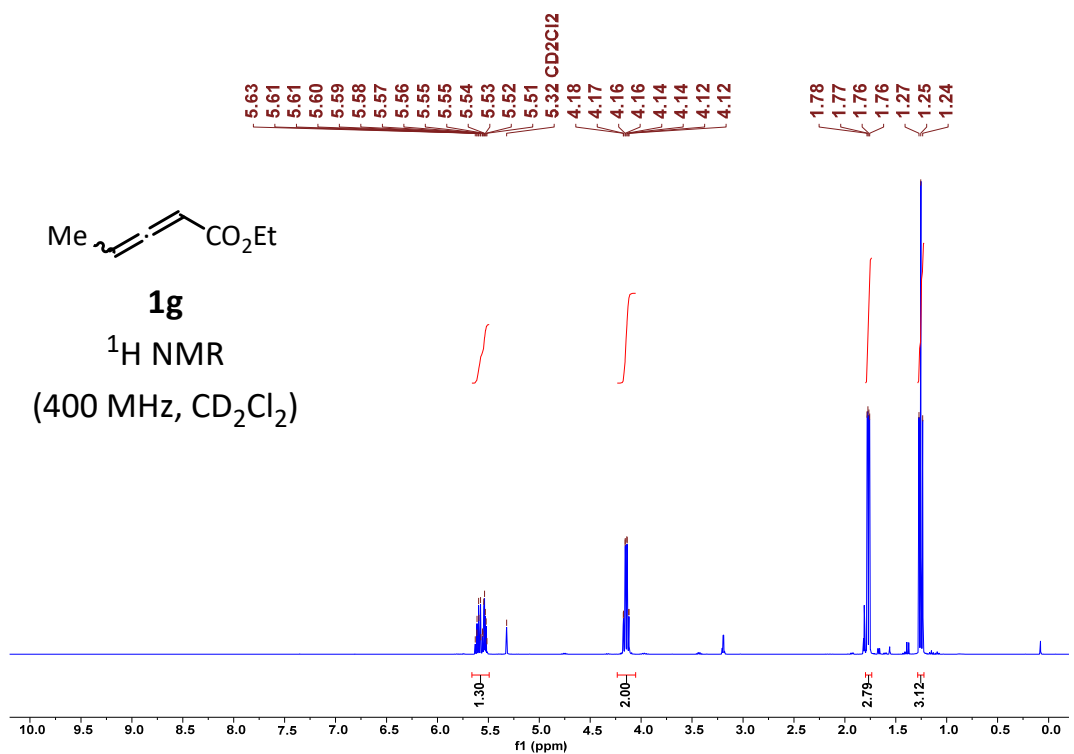
**7.1.6 Ethyl buta-2,3-dienoate (1f)**



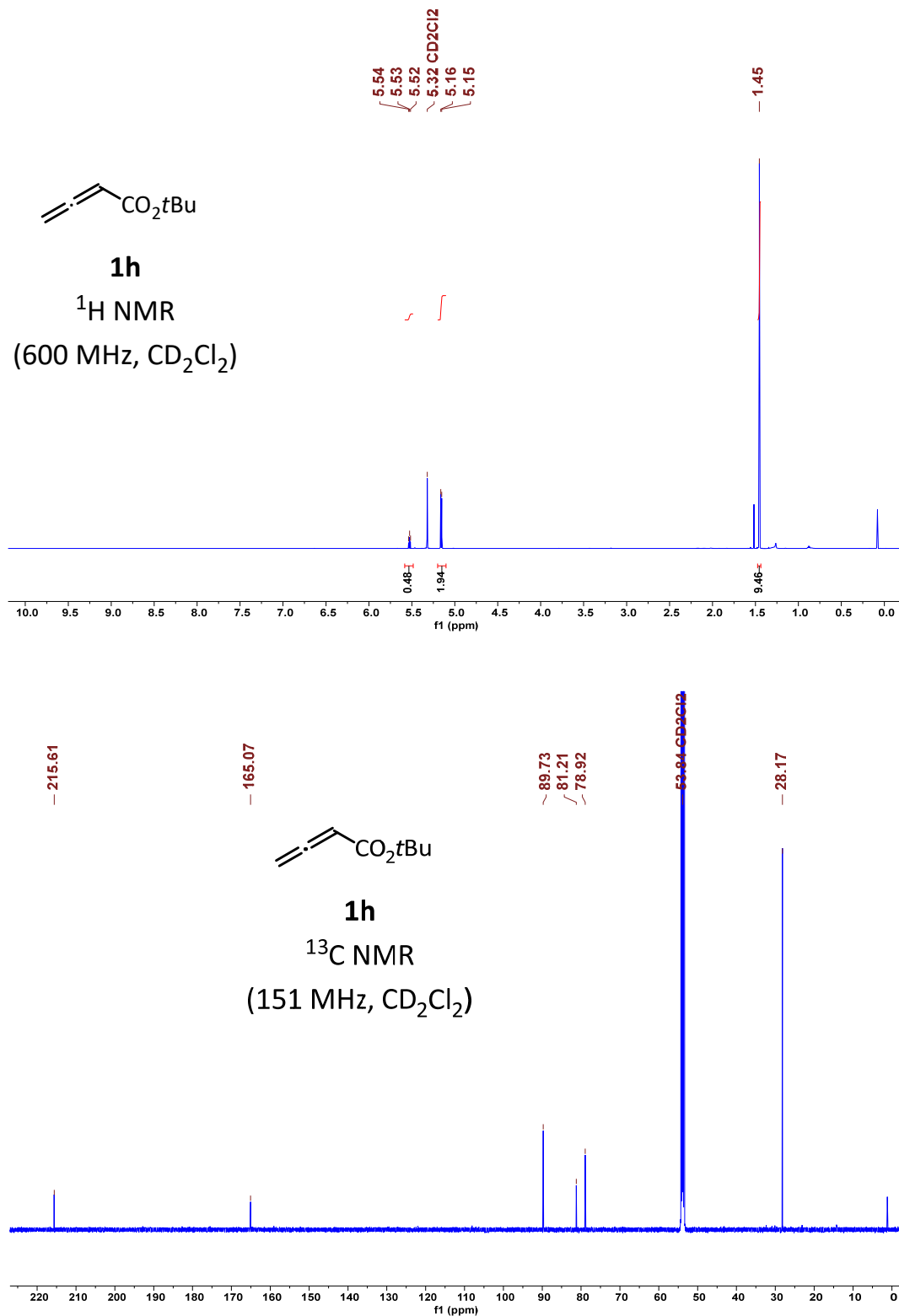


**7.1.7 Ethyl penta-2,3-dienoate (1g)**

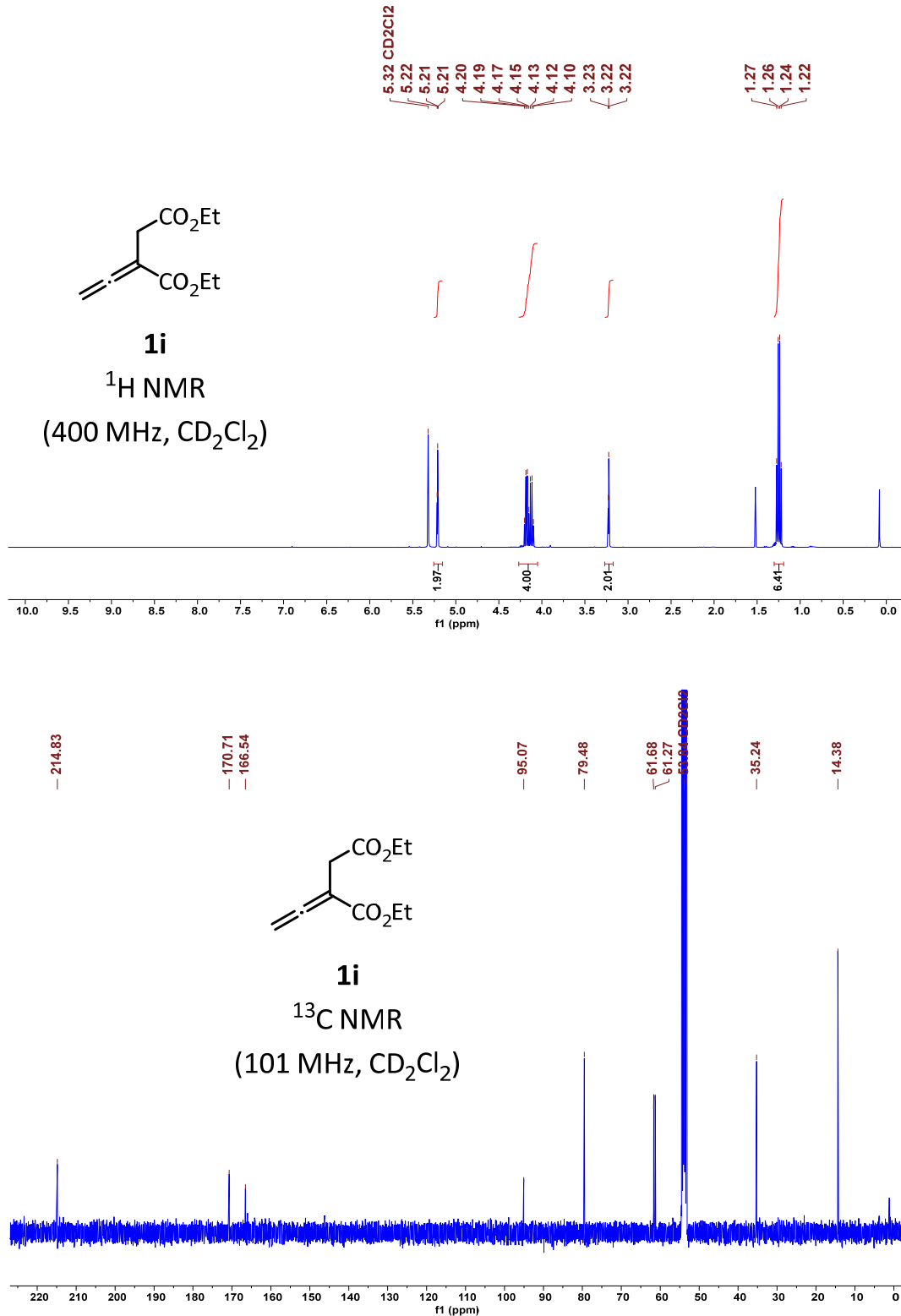




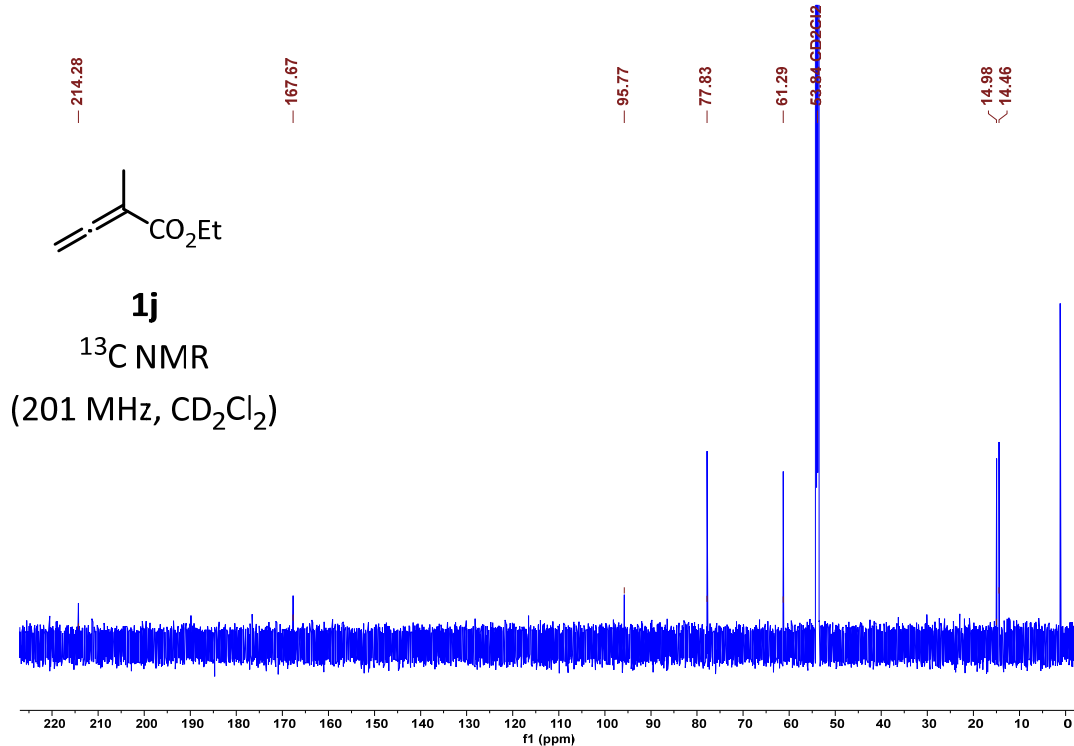
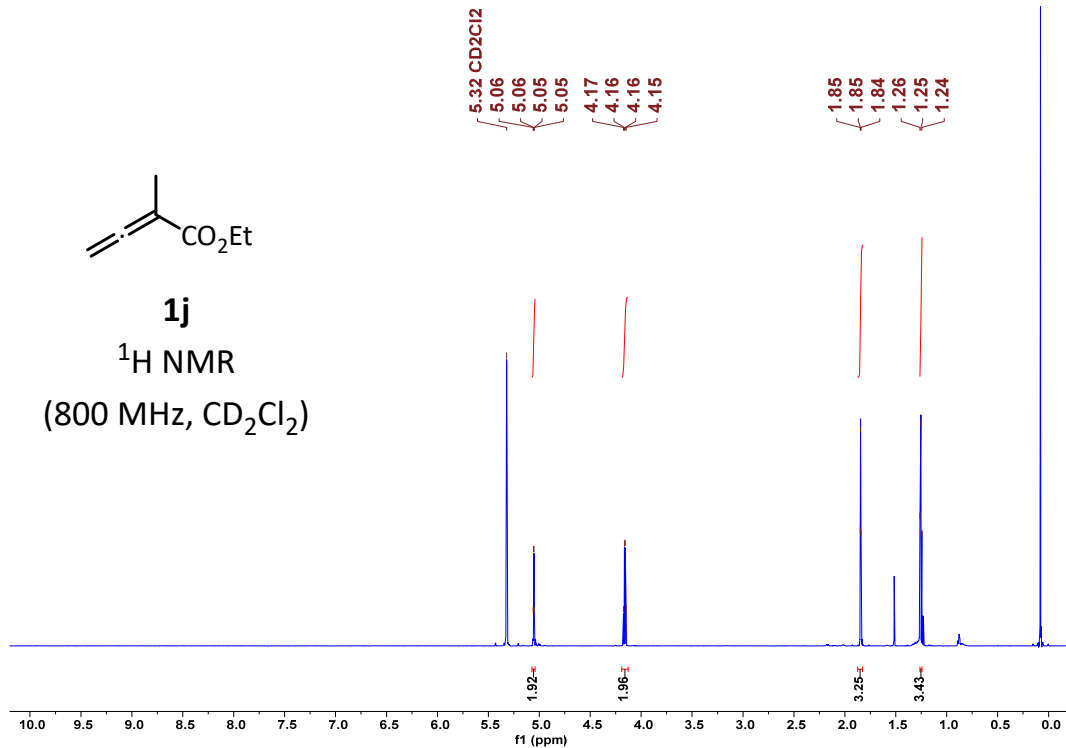
**7.1.8 *tert*-Butyl buta-2,3-dienoate (1h)**



**7.1.9 Diethyl 2-vinylidenesuccinate (1i)**

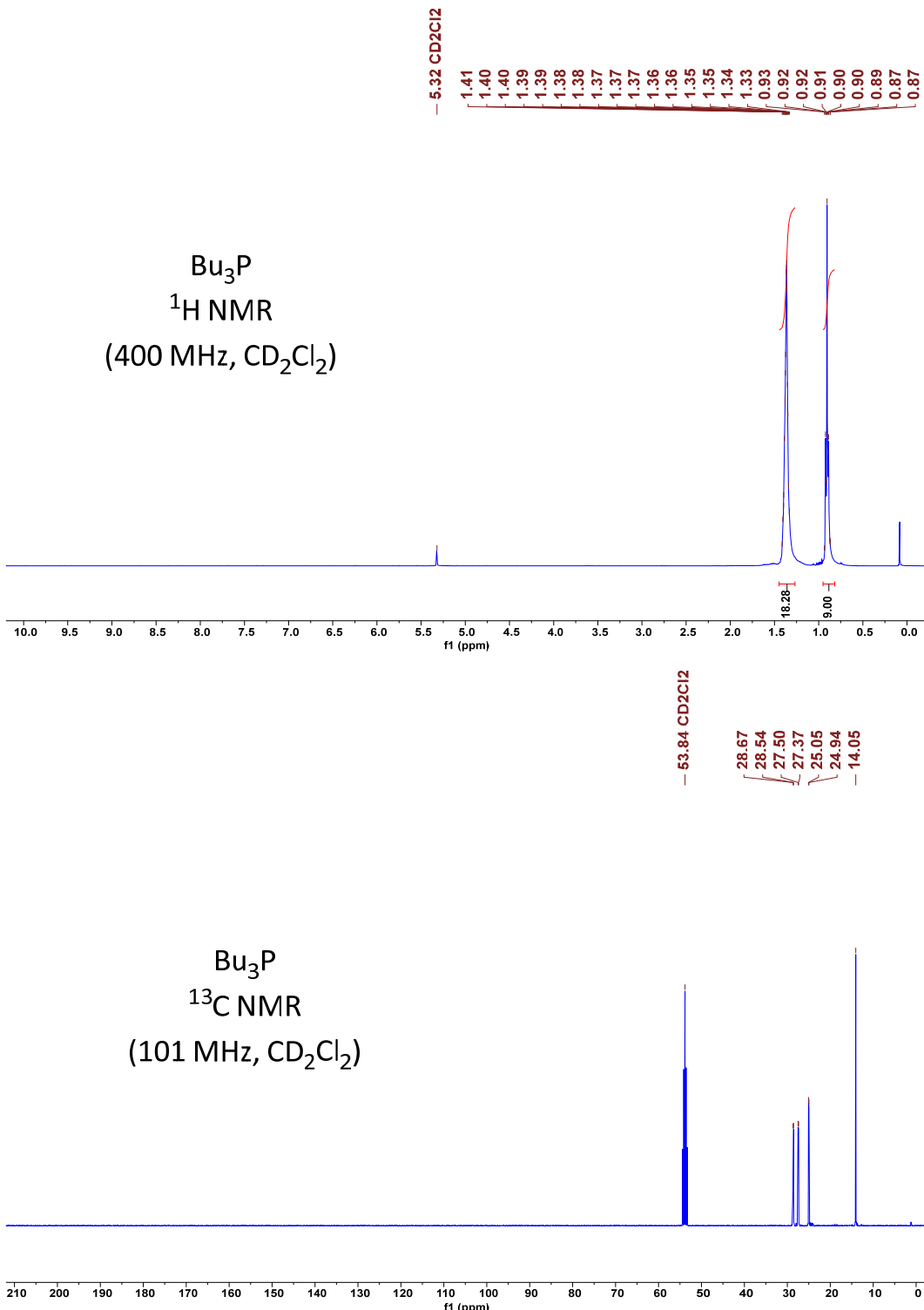


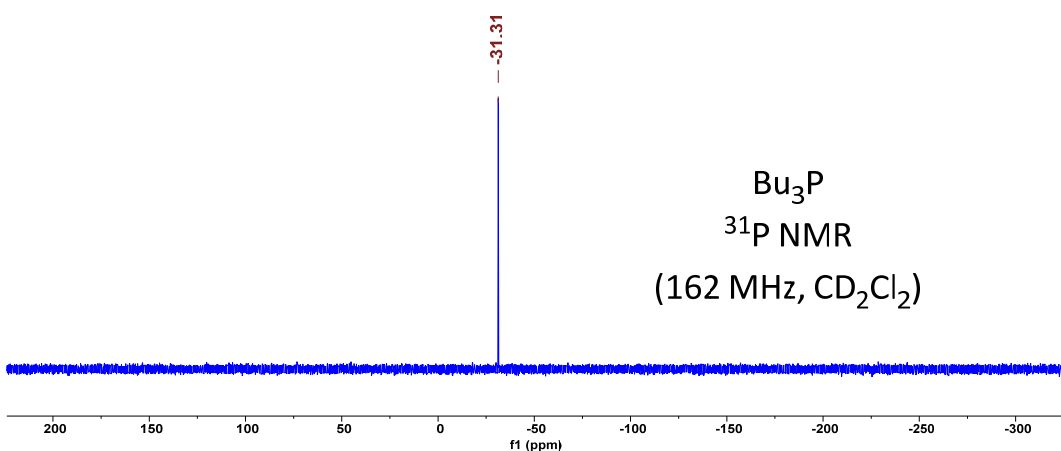
**7.1.10 Ethyl 2-methylbuta-2,3-dienoate (1j)**



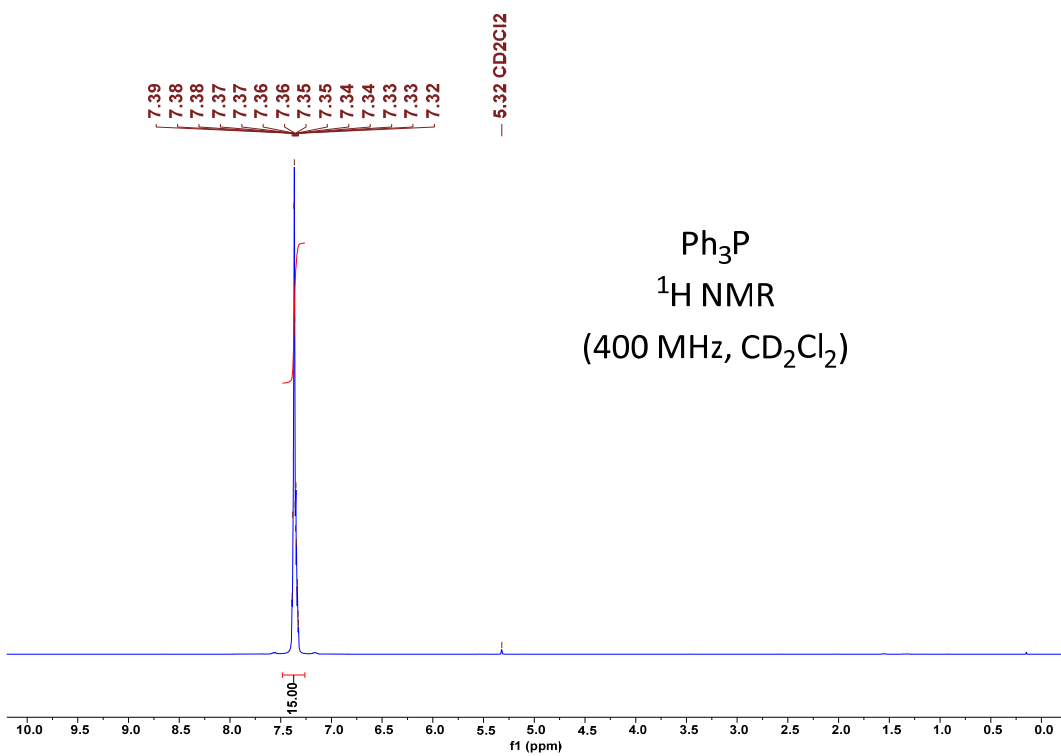
## 7.2 NMR spectra of phosphines

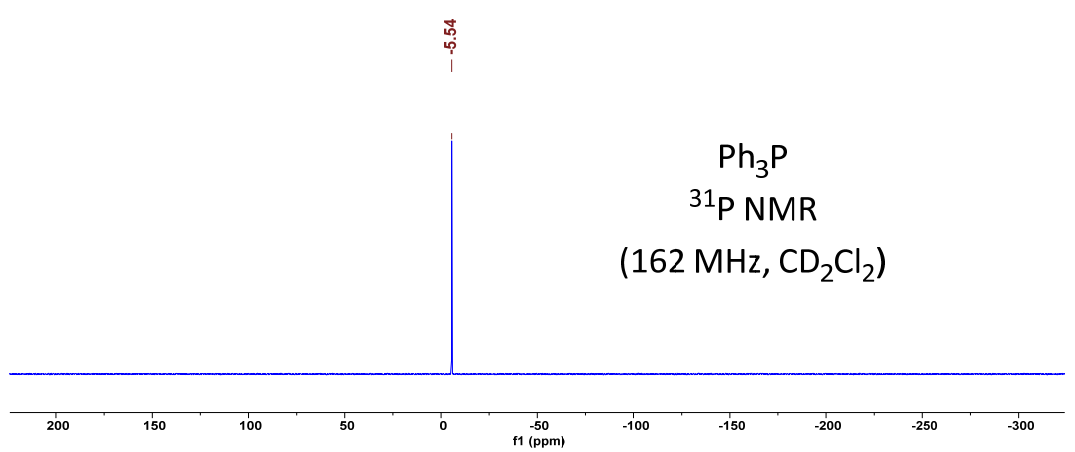
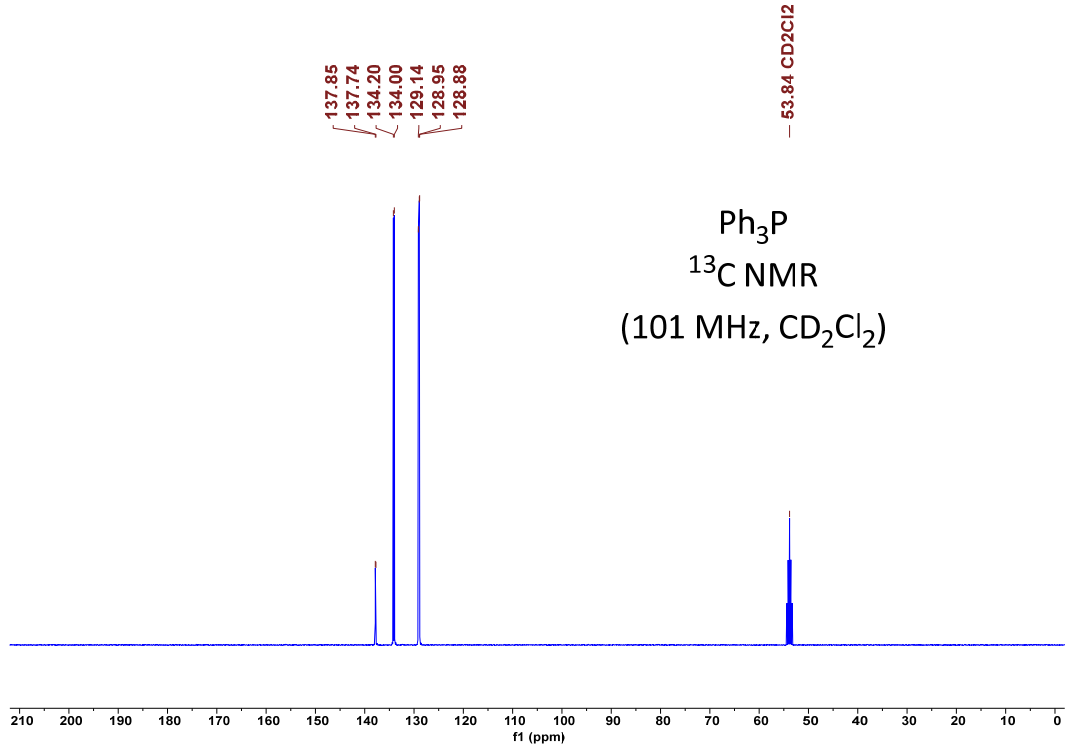
### 7.2.1 Tributylphosphine ( $\text{Bu}_3\text{P}$ )





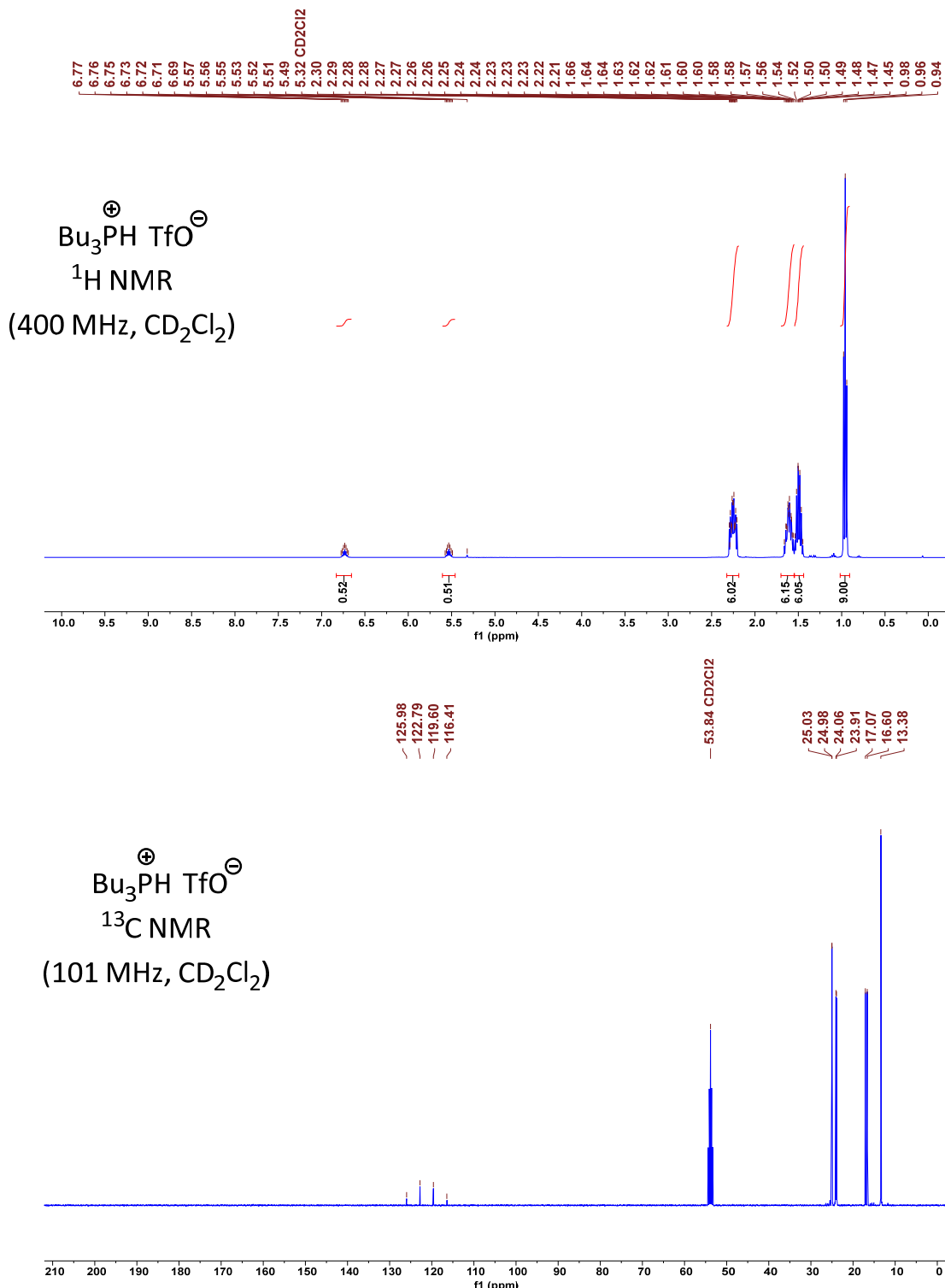
### 7.2.2 Triphenylphosphine ( $\text{Ph}_3\text{P}$ )

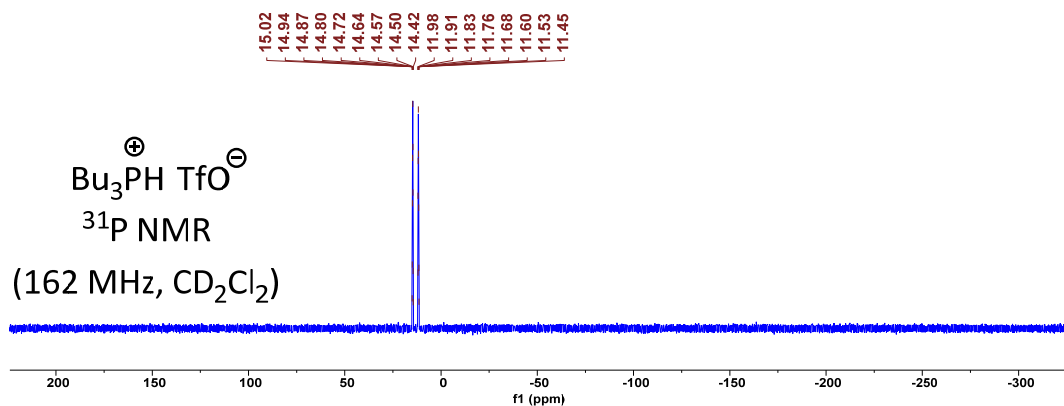




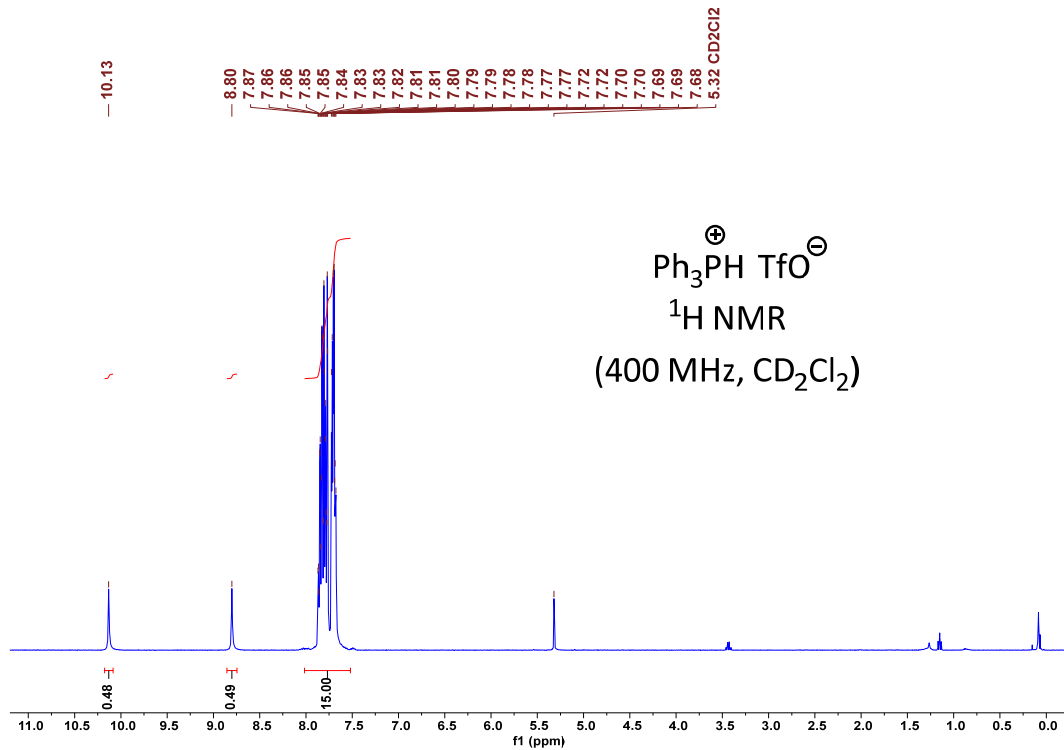
## 7.3 NMR spectra of phosphonium triflates and 2,4,6-collidinium triflate

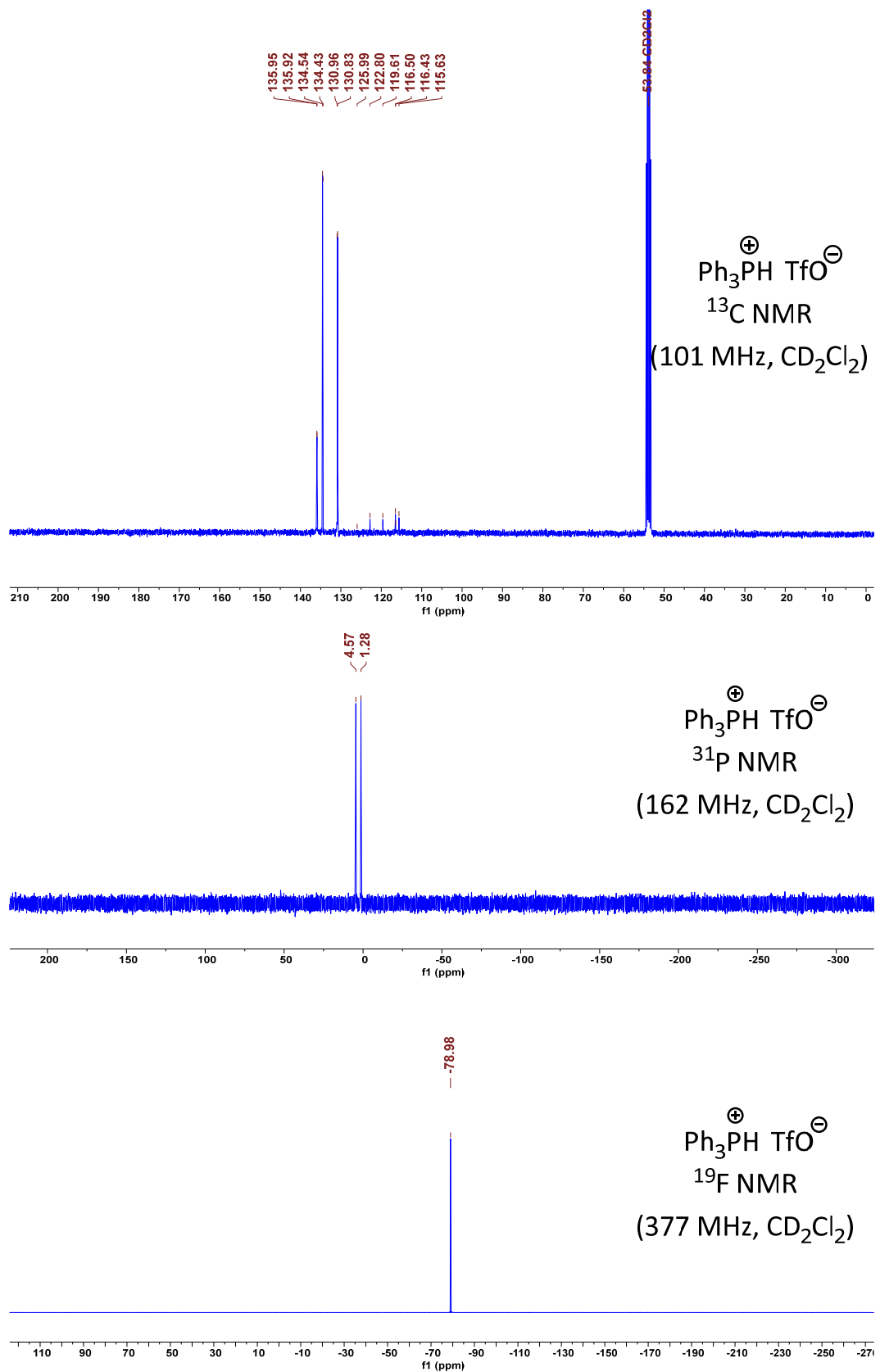
### 7.3.1 Tributylphosphonium triflate (TBPT)



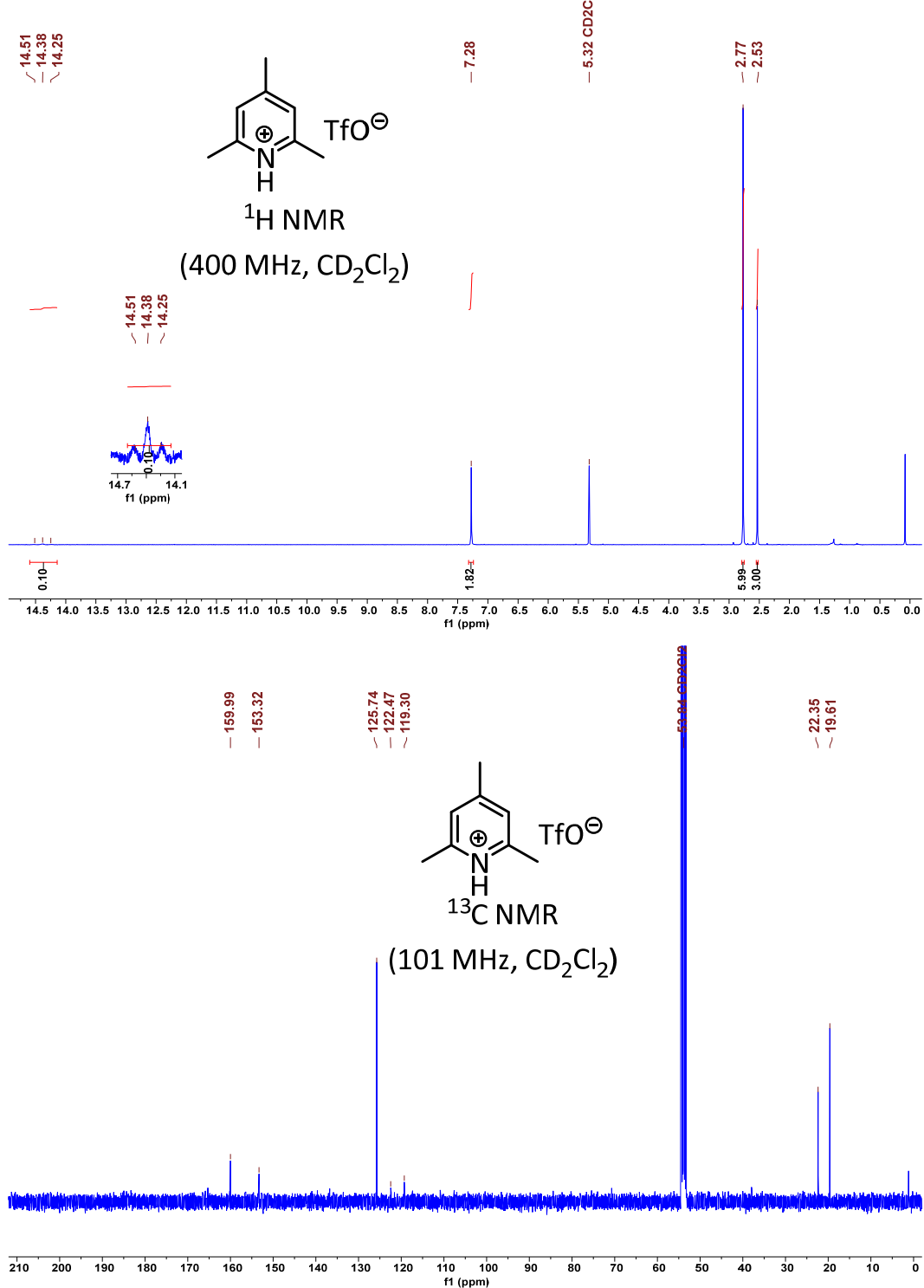


### 7.3.2 Triphenylphosphonium triflate (TPPT)



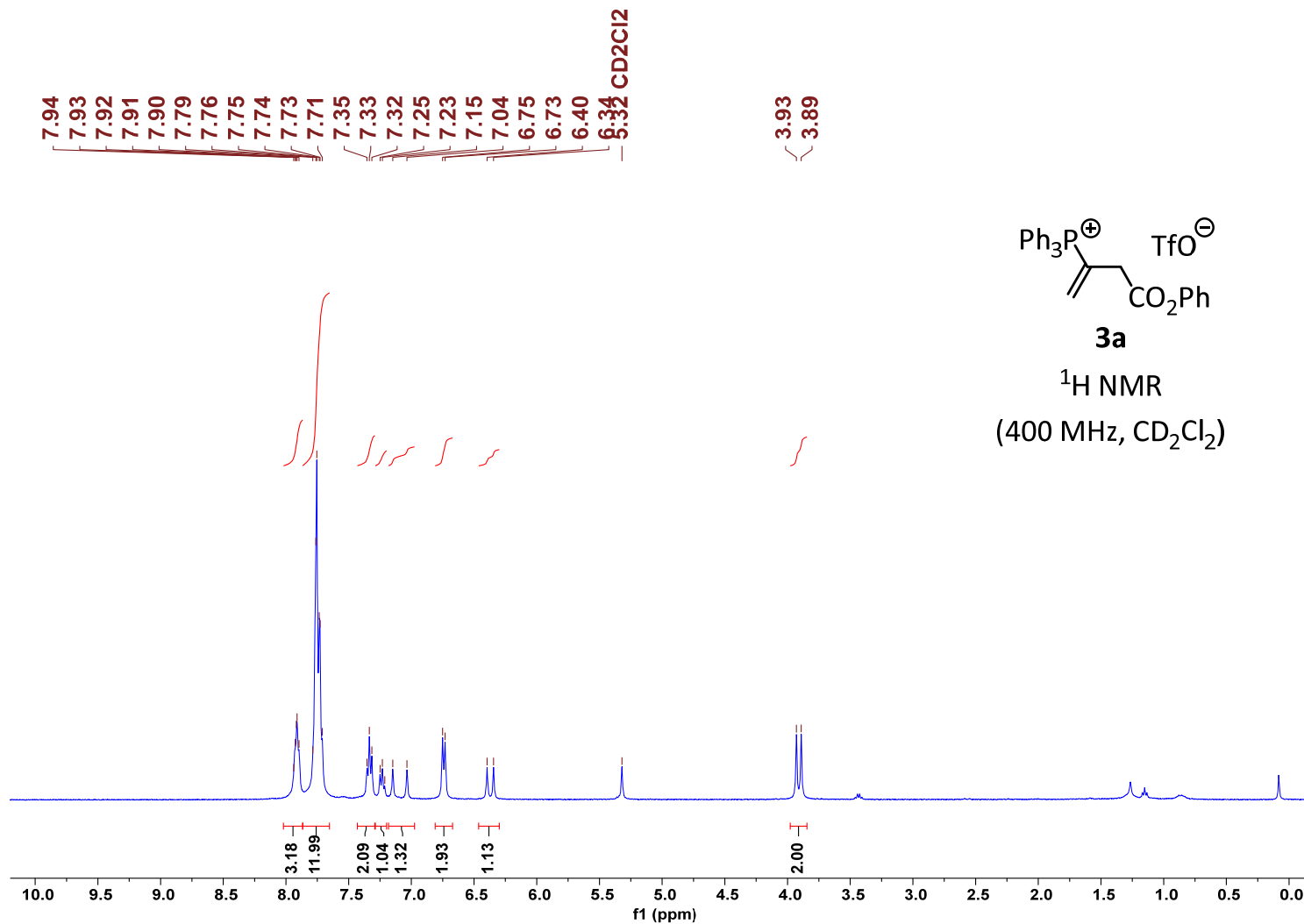


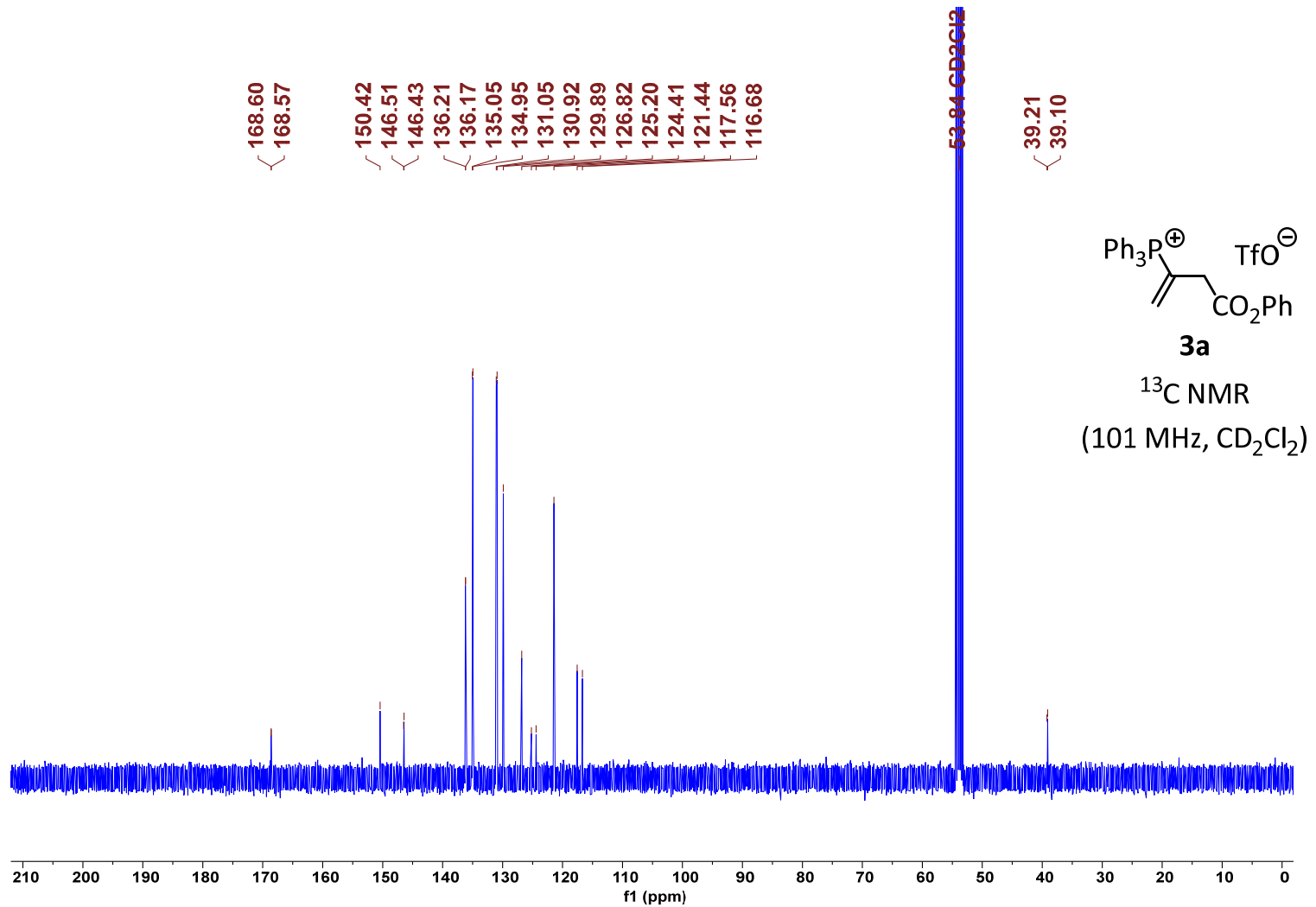
### 7.3.3 2,4,6-Collidinium triflate (CT)

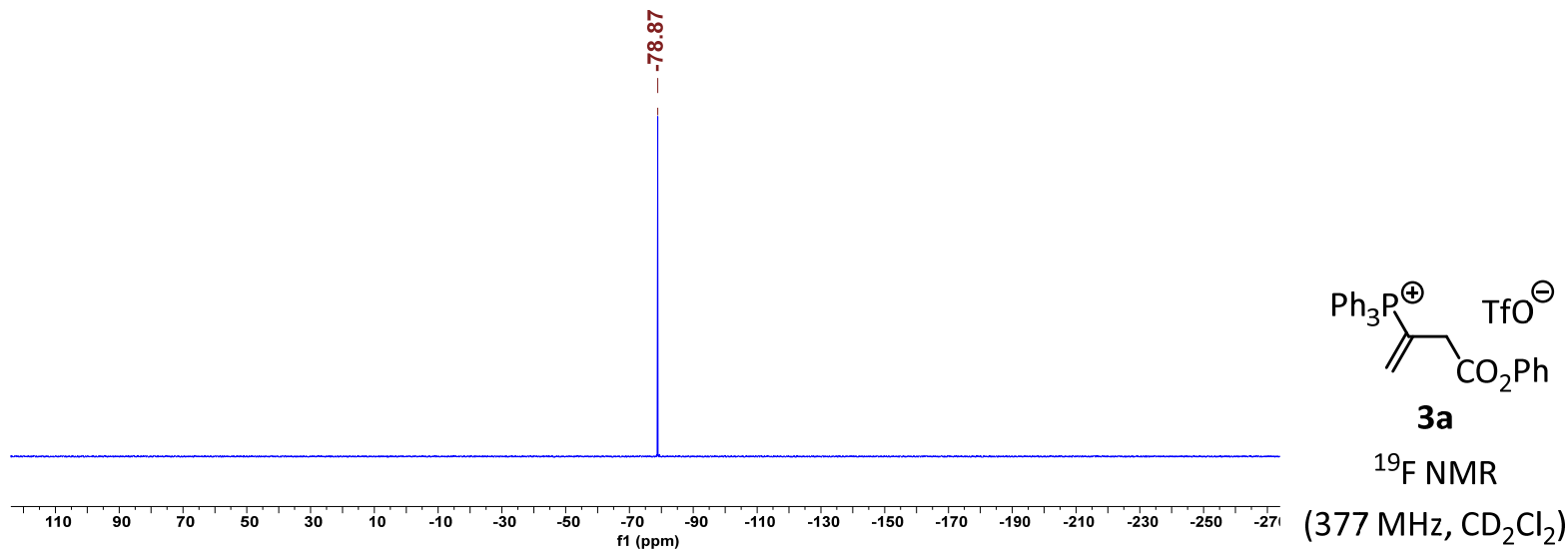
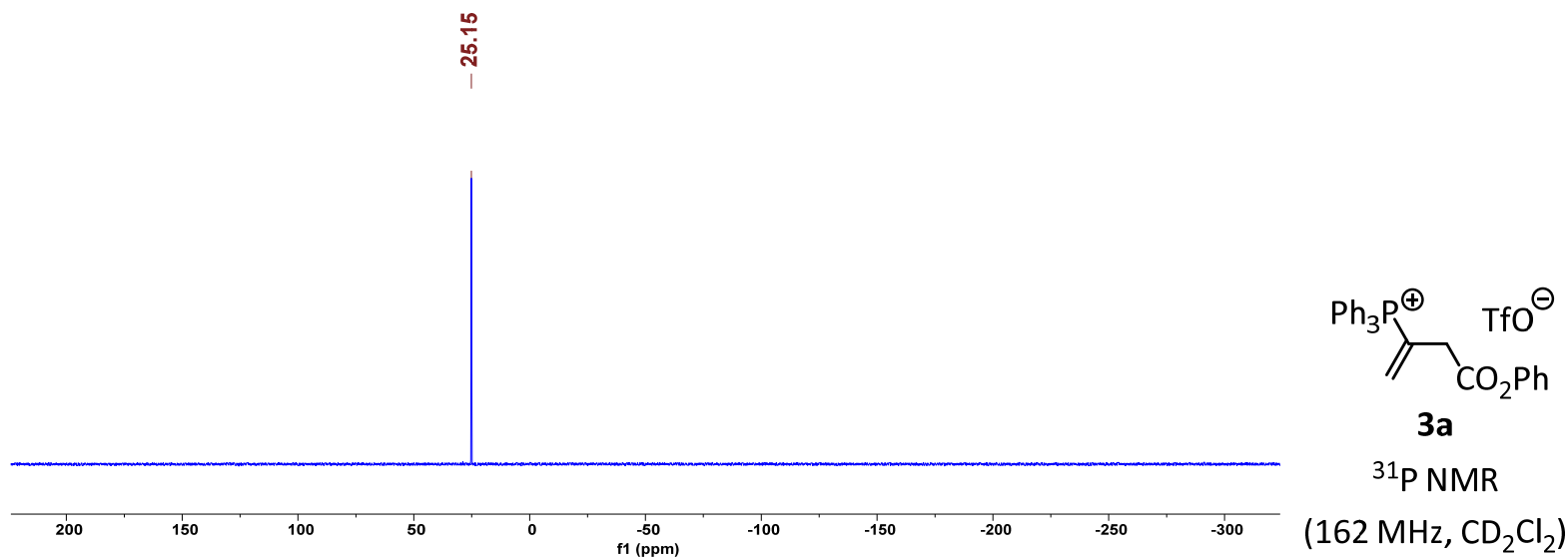


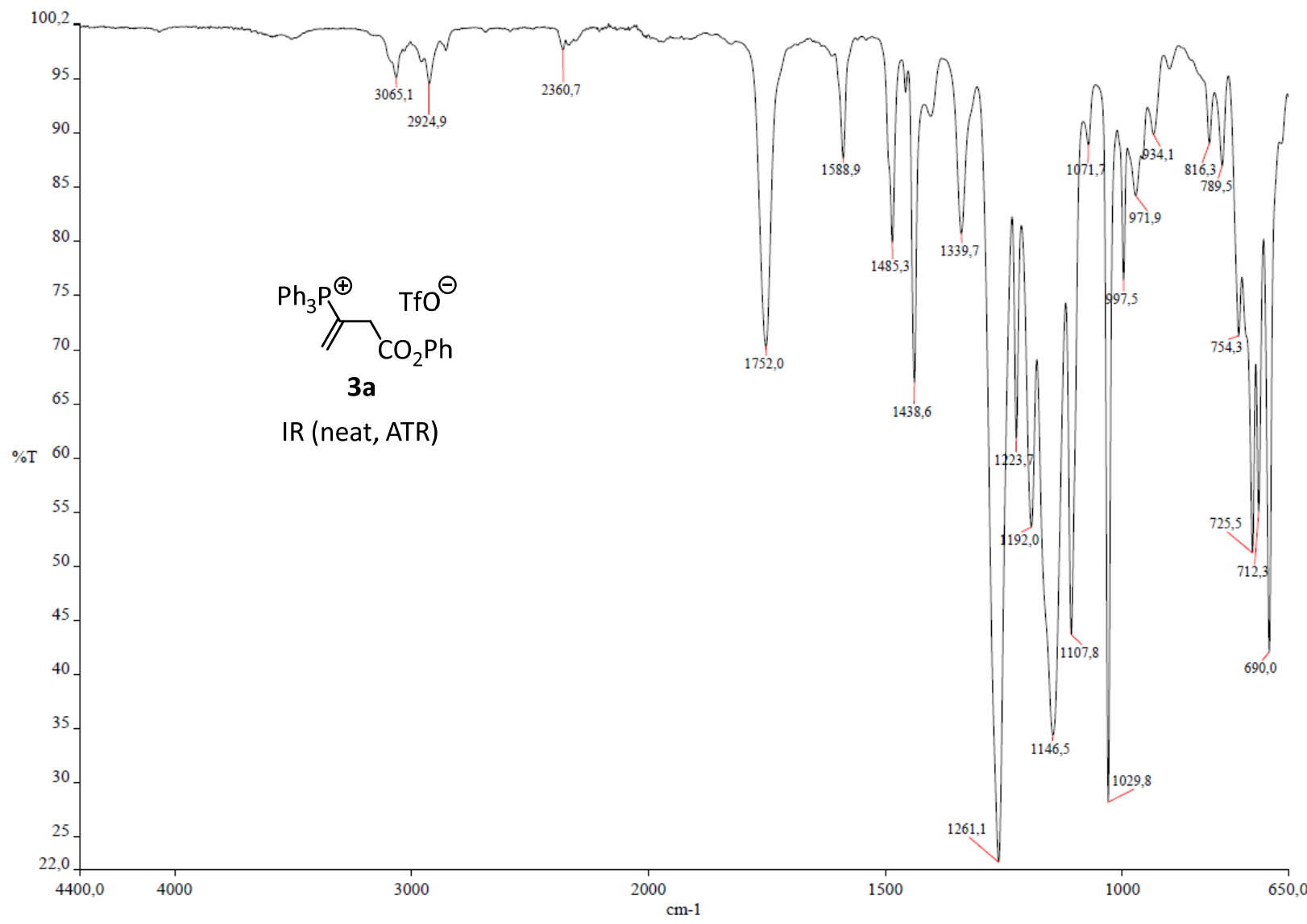
## 7.4 NMR and IR spectra of the product studies

### 7.4.1 (4-Oxo-4-phenoxybut-1-en-2-yl)triphenylphosphonium triflate (**3a**) from TPPT and phenyl buta-2,3-dienoate (**1a**)

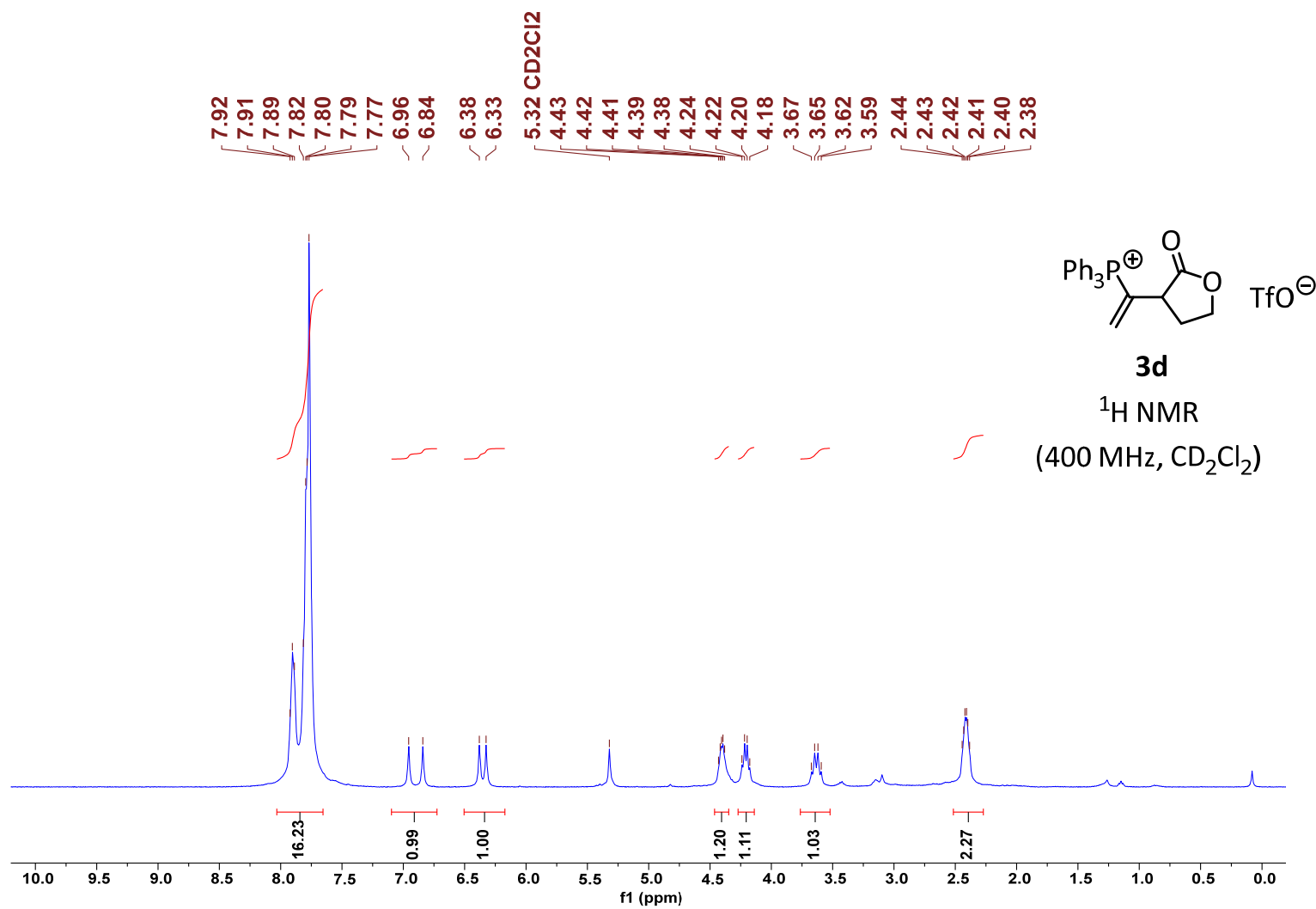


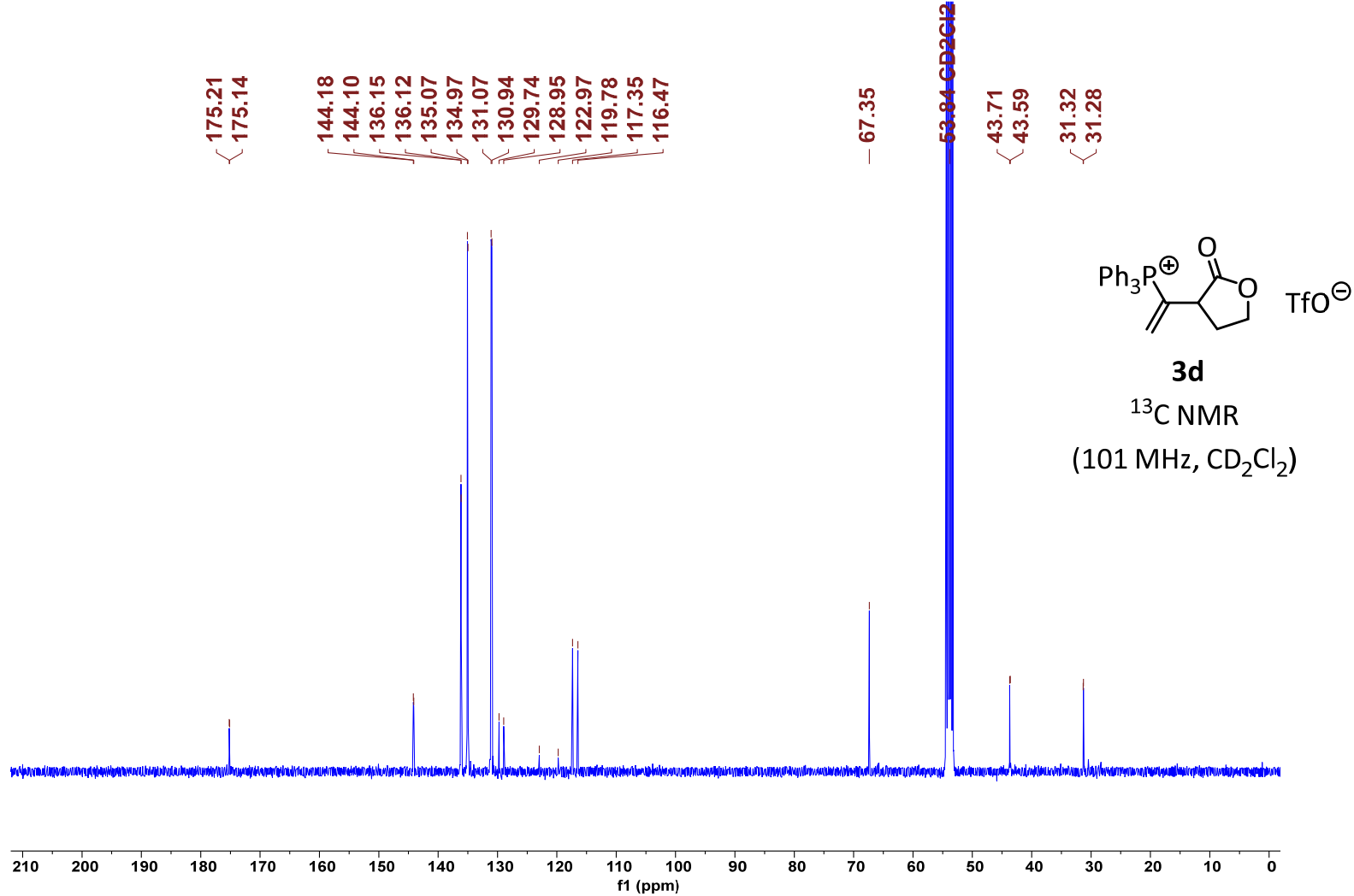


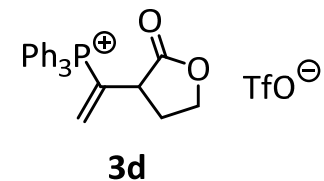
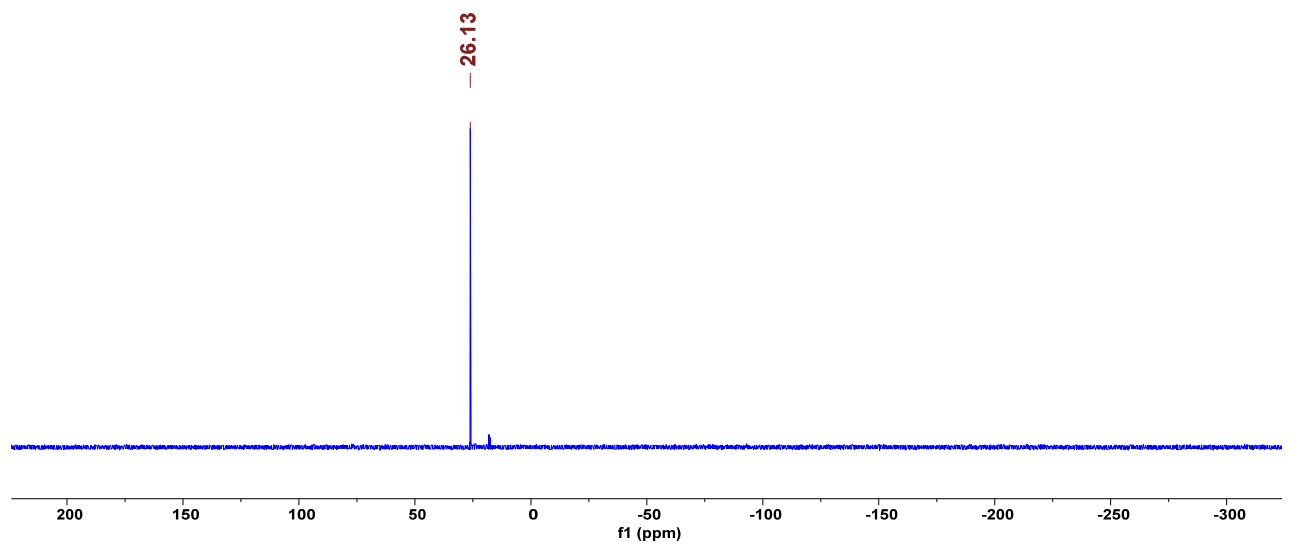




7.4.2 (1-(2-Oxotetrahydrofuran-3-yl)vinyl)triphenylphosphonium triflate (**3d**) from TPPT and 3-vinylidenedihydrofuran-2(3H)-one (**1d**)

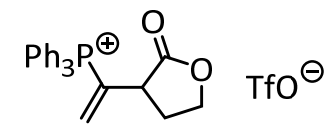
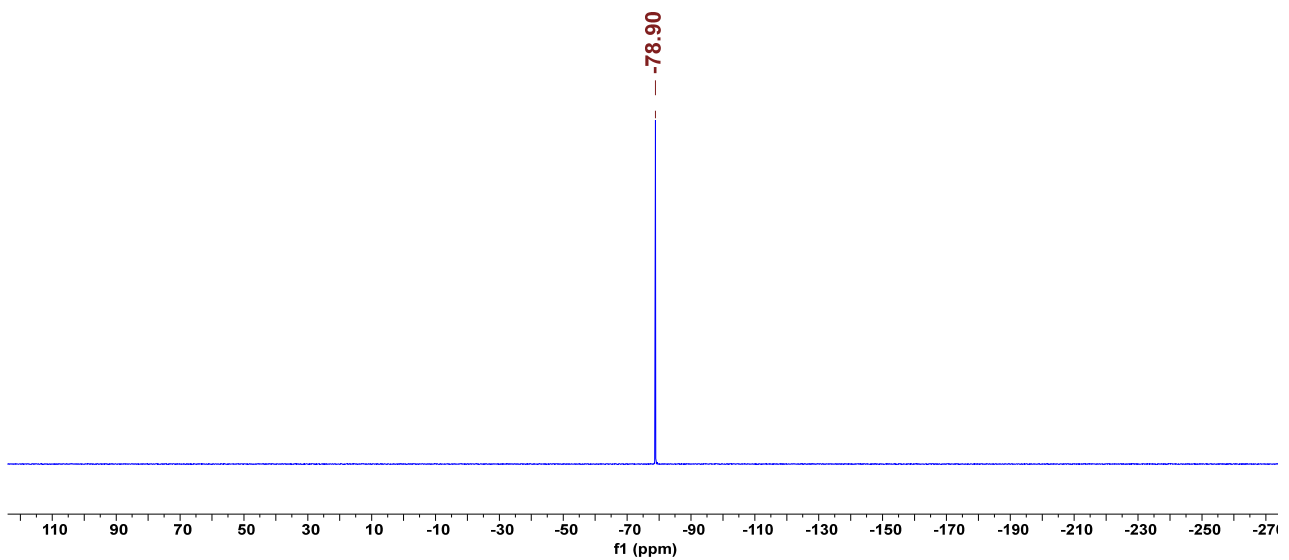






$^{31}\text{P}$  NMR

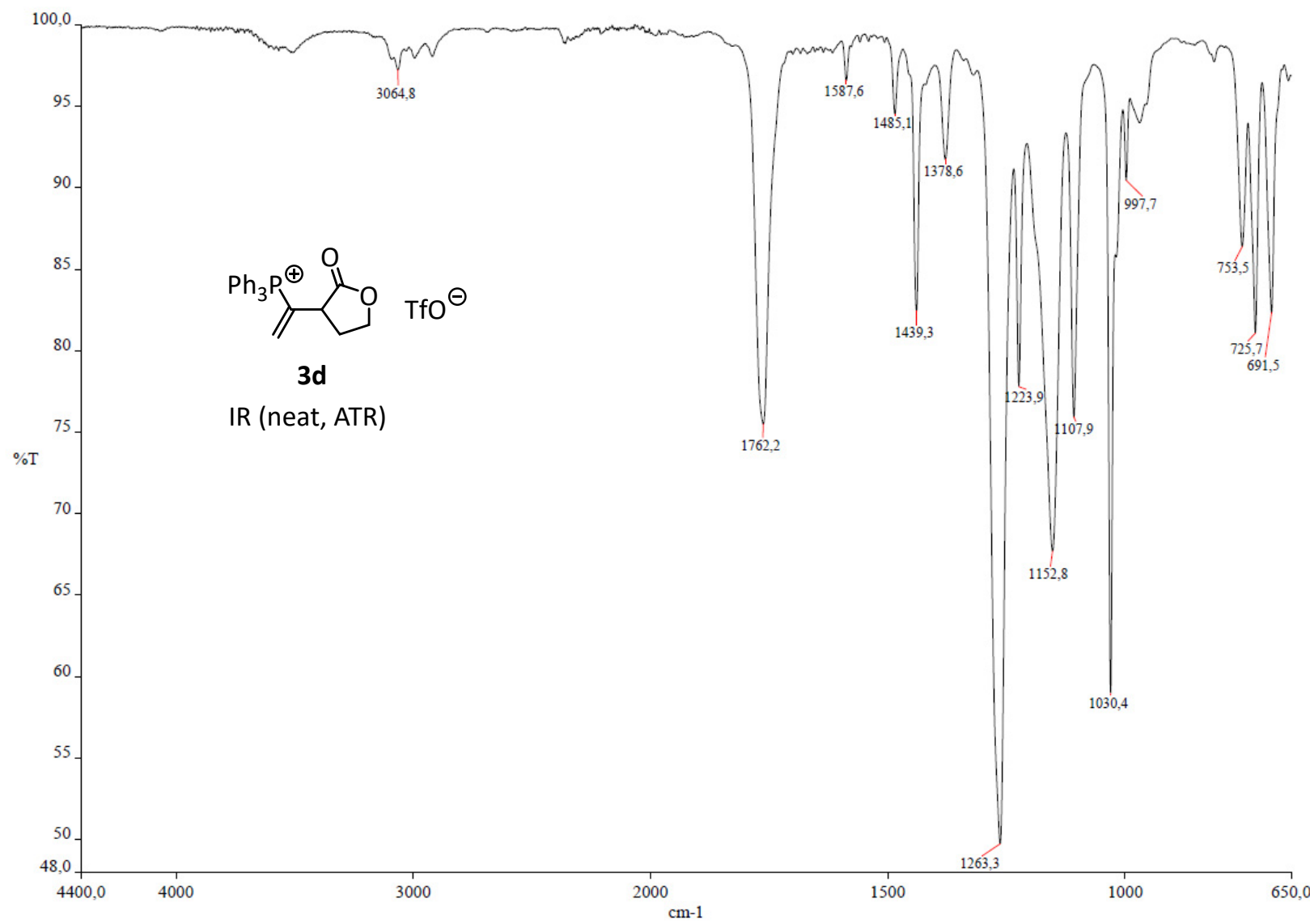
( $162\text{ MHz}, \text{CD}_2\text{Cl}_2$ )



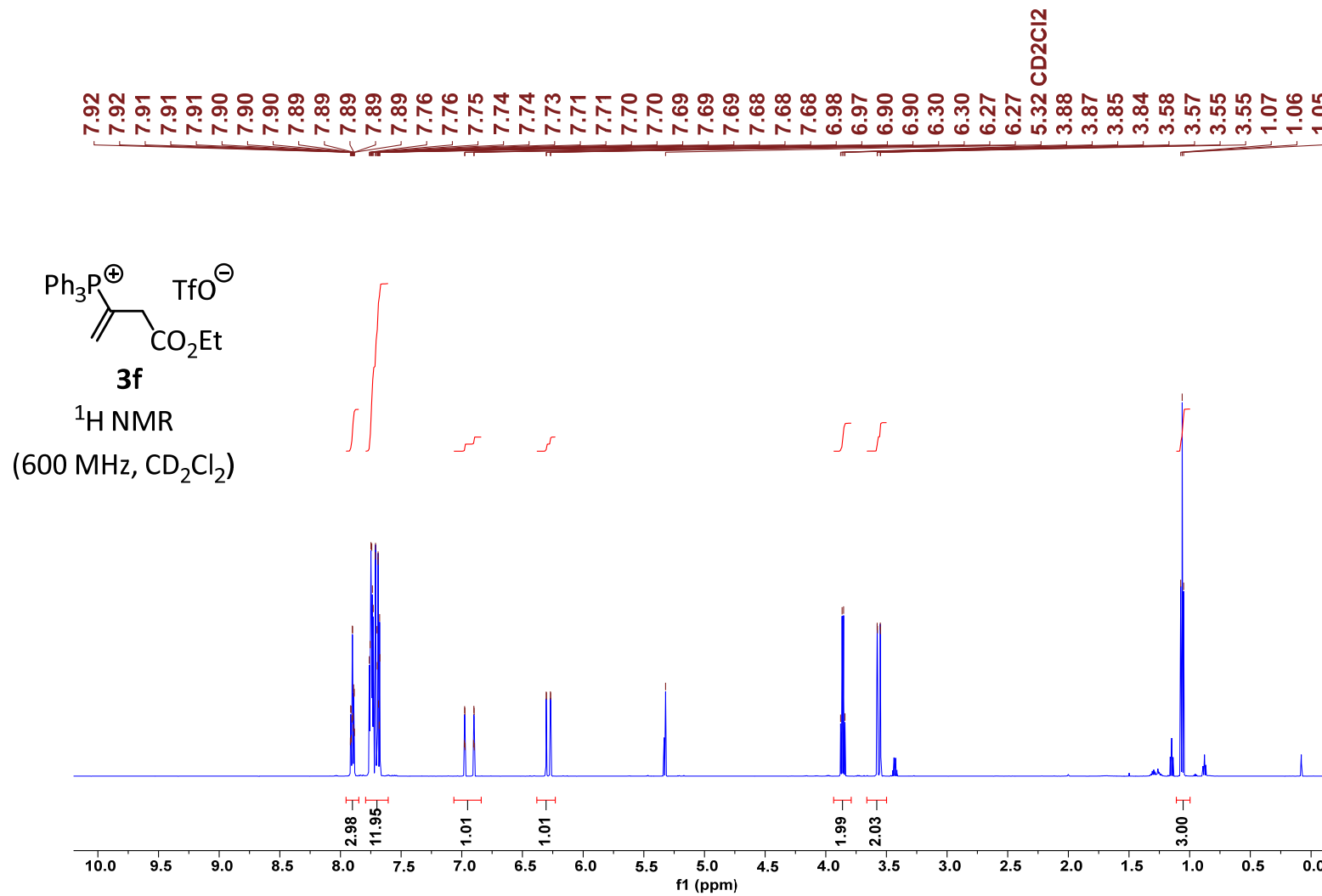
**3d**

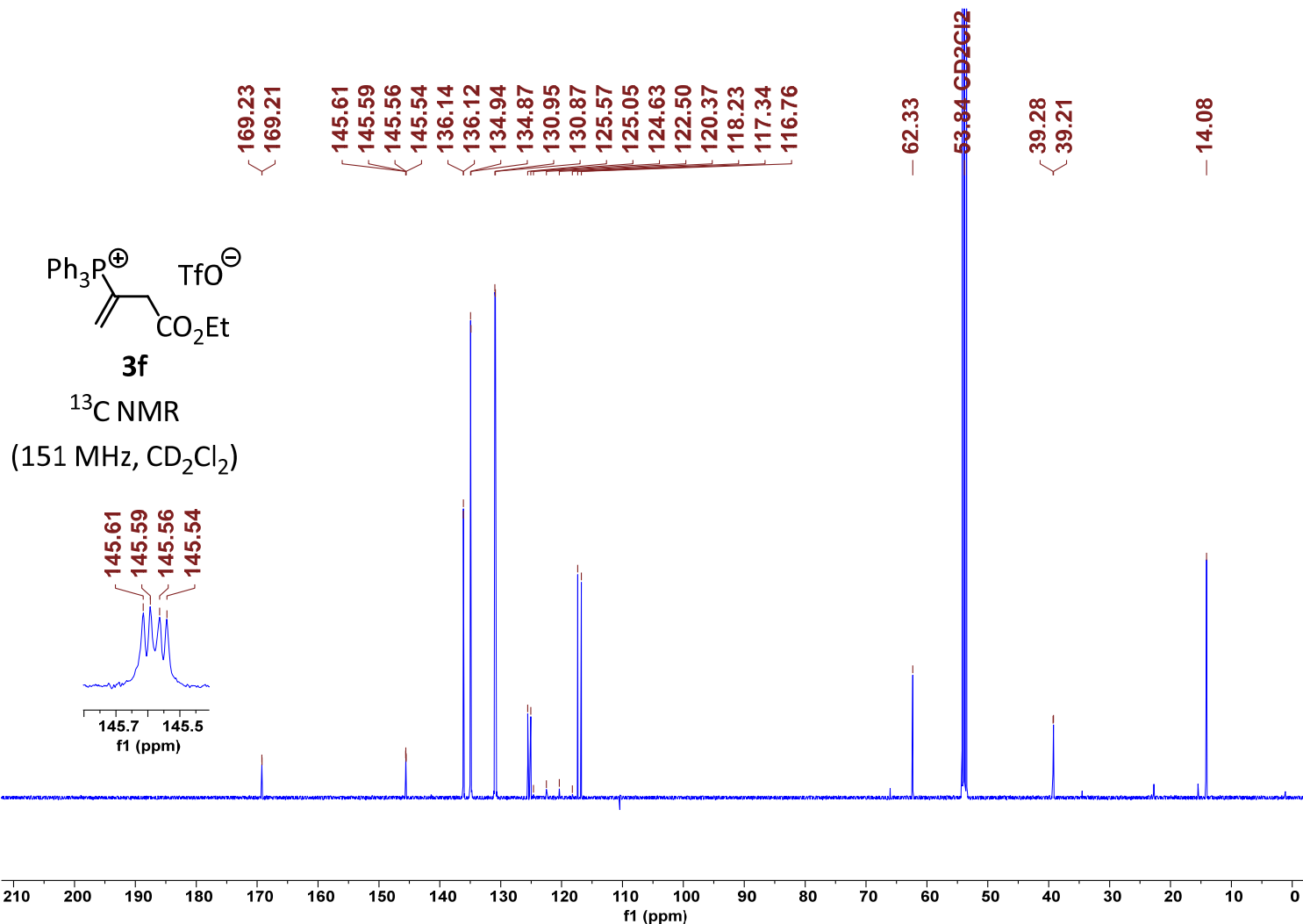
$^{19}\text{F}$  NMR

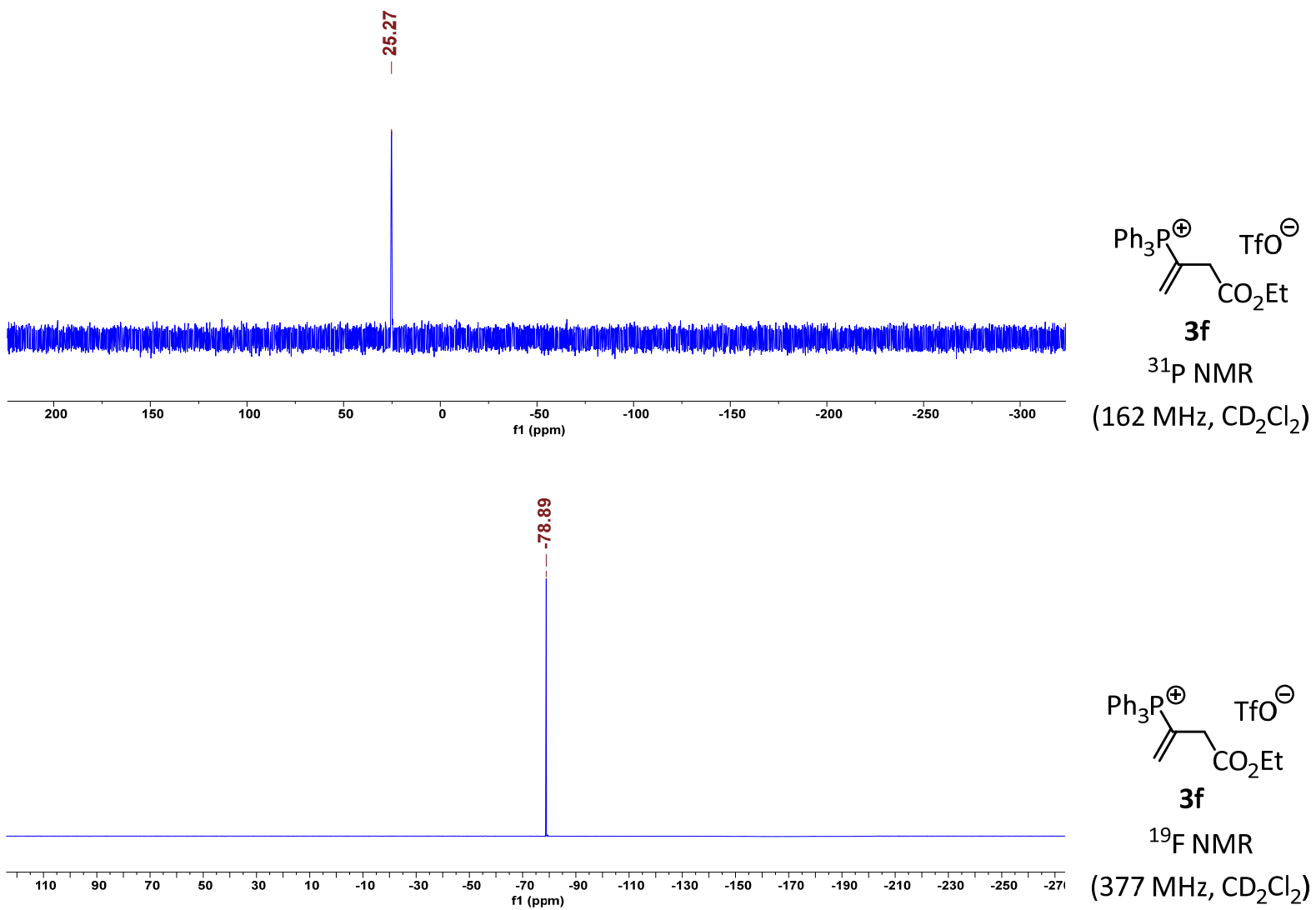
( $377\text{ MHz}, \text{CD}_2\text{Cl}_2$ )

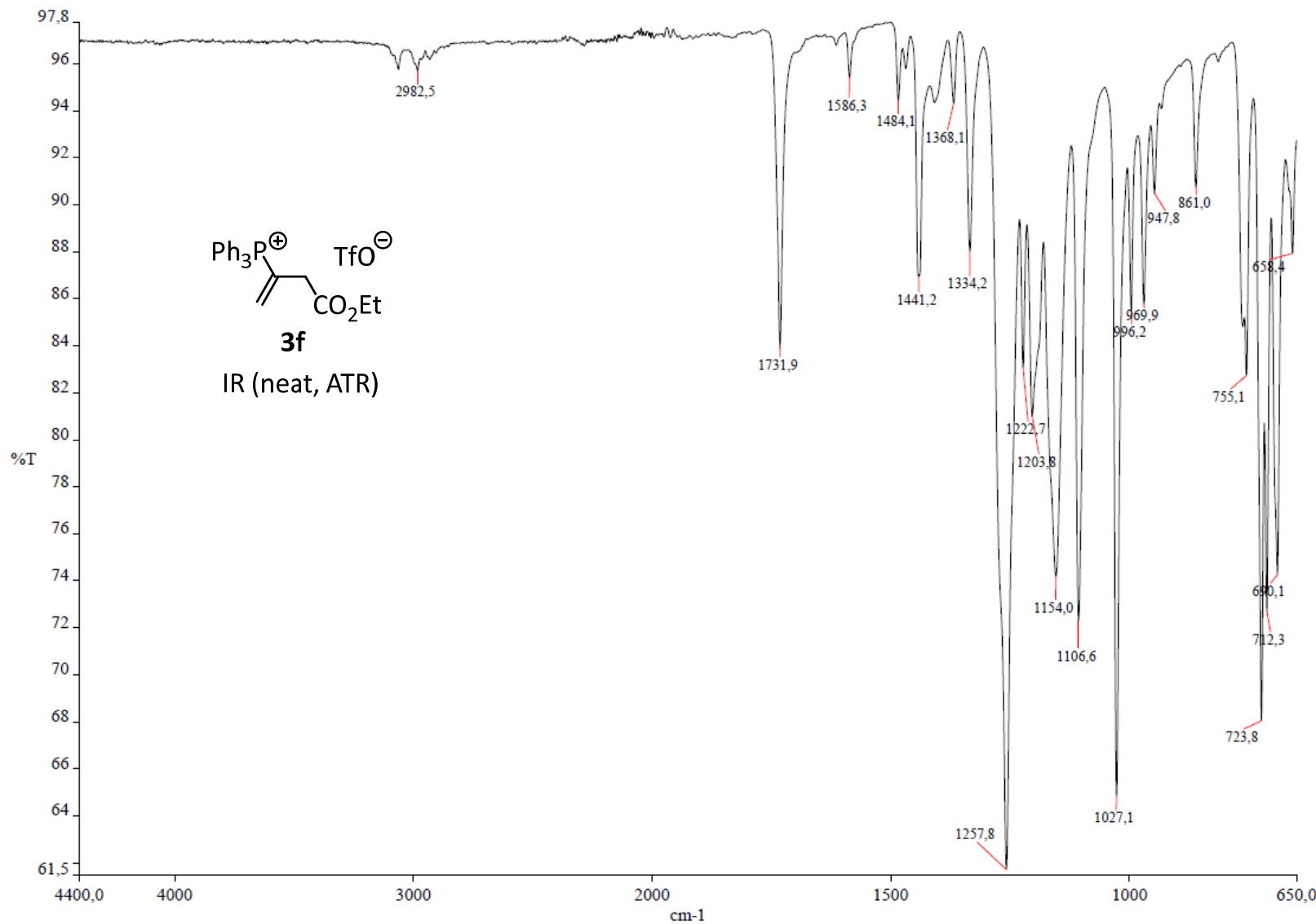


**7.4.3 (4-Ethoxy-4-oxobut-1-en-2-yl)triphenylphosphonium triflate (**3f**) from TPPT and ethyl buta-2,3-dienoate (**1f**)**

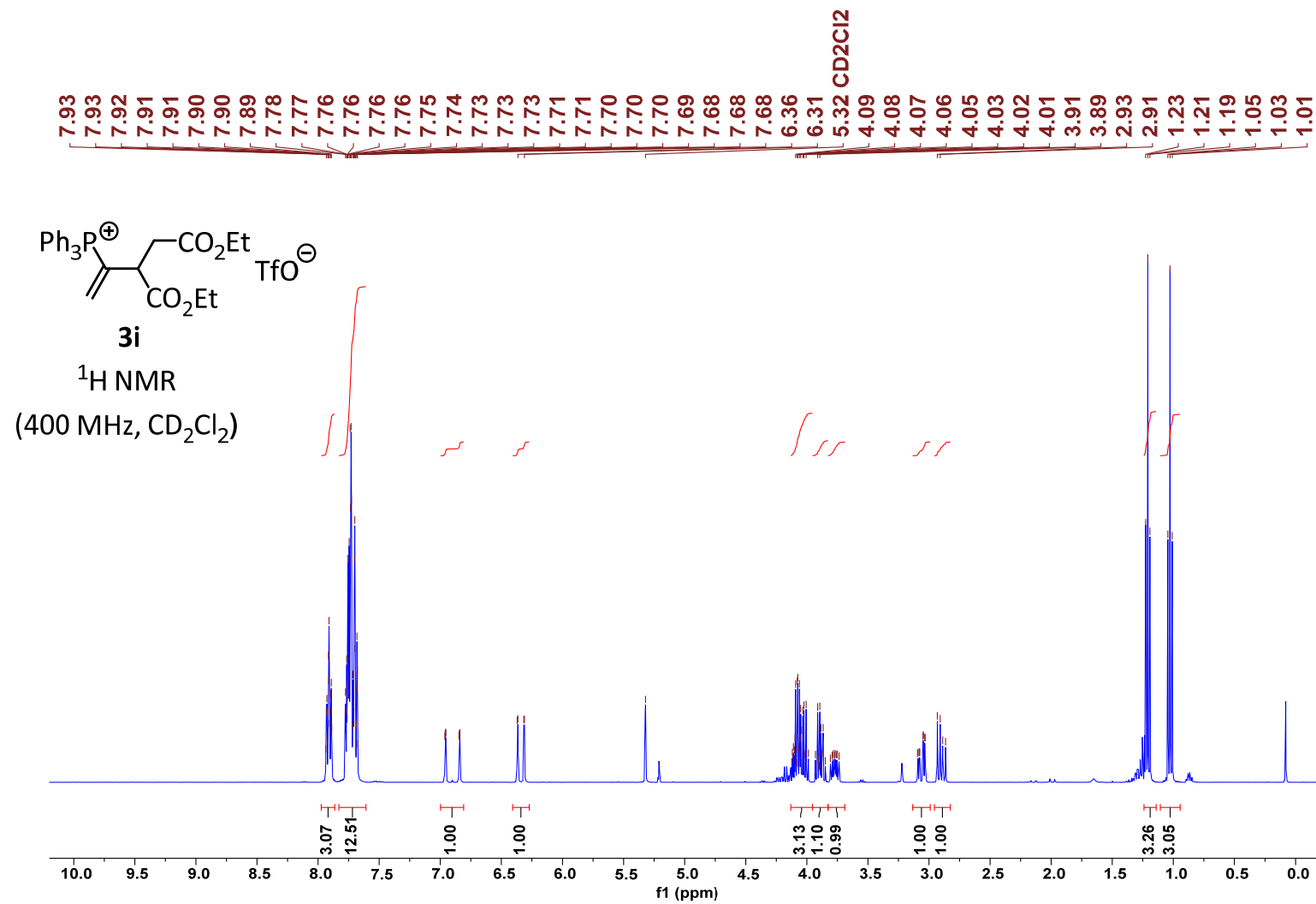


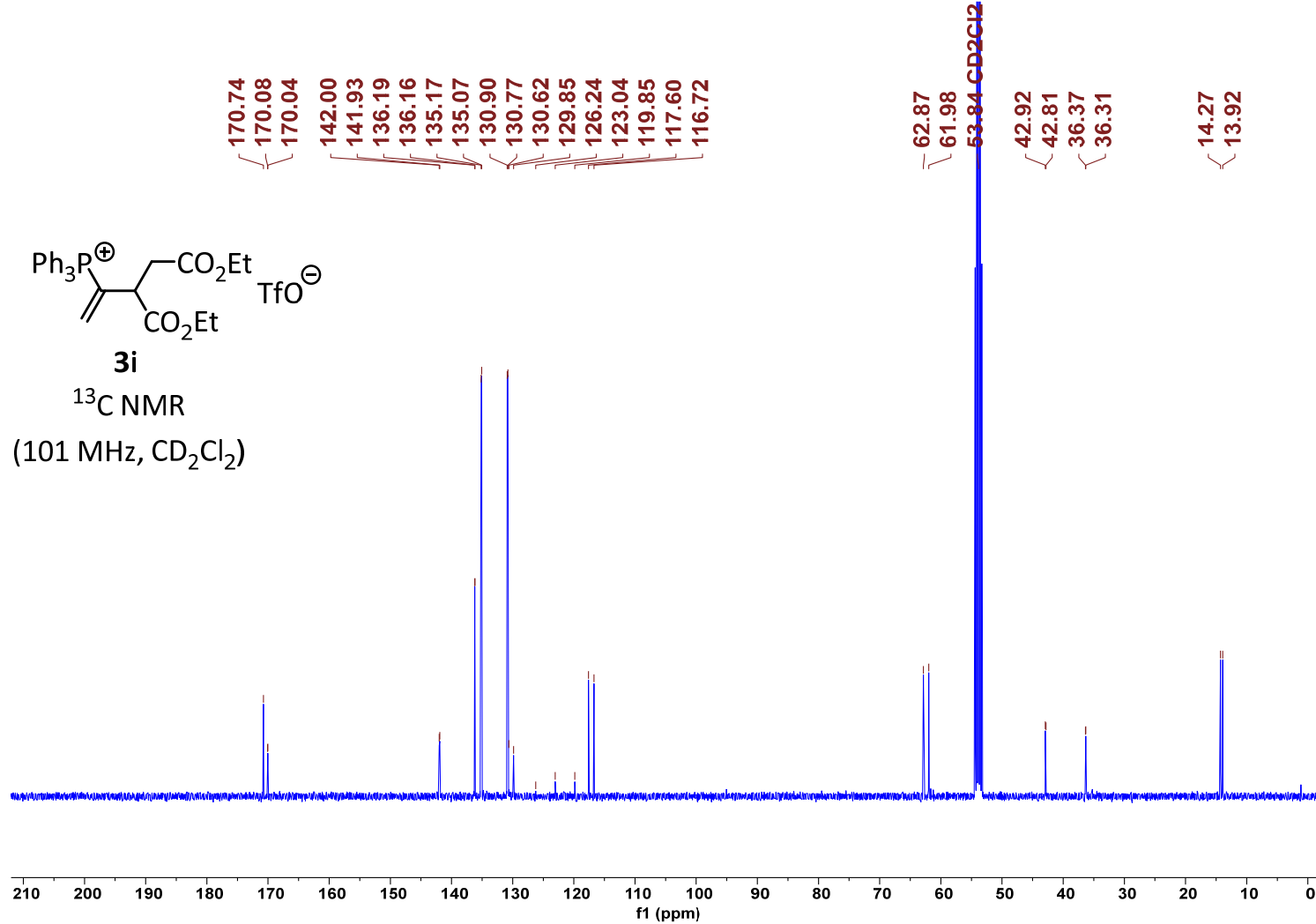


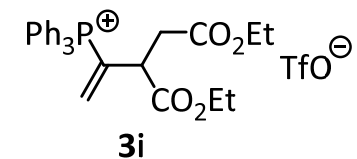
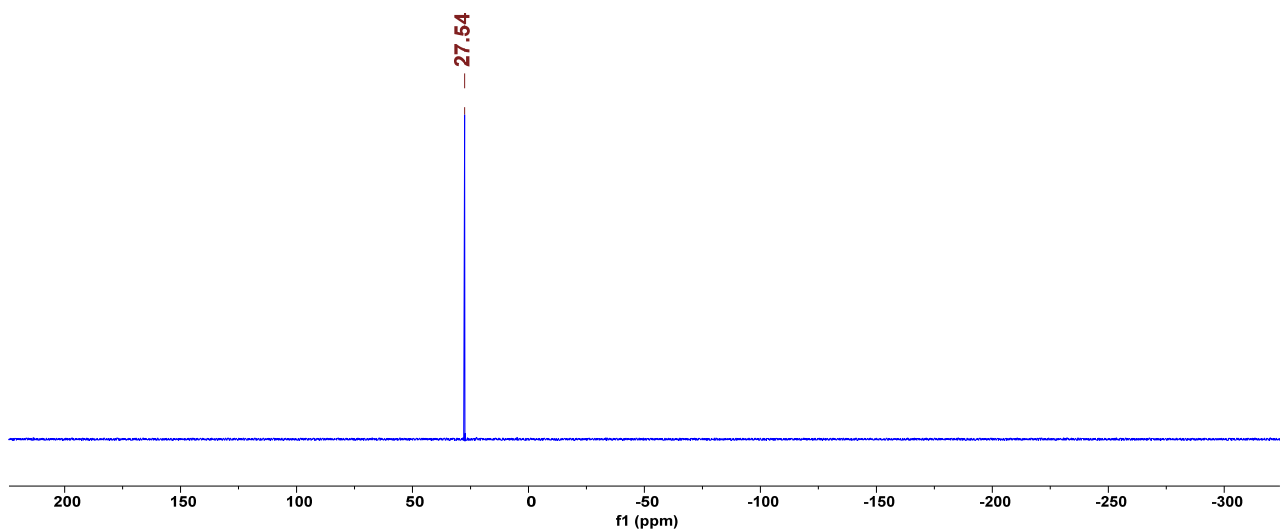




7.4.4 (5-Ethoxy-3-(ethoxycarbonyl)-5-oxopent-1-en-2-yl)triphenylphosphonium triflate (**3i**) from TPPT and diethyl 2-vinylidenesuccinate (**1i**)

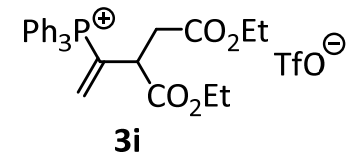
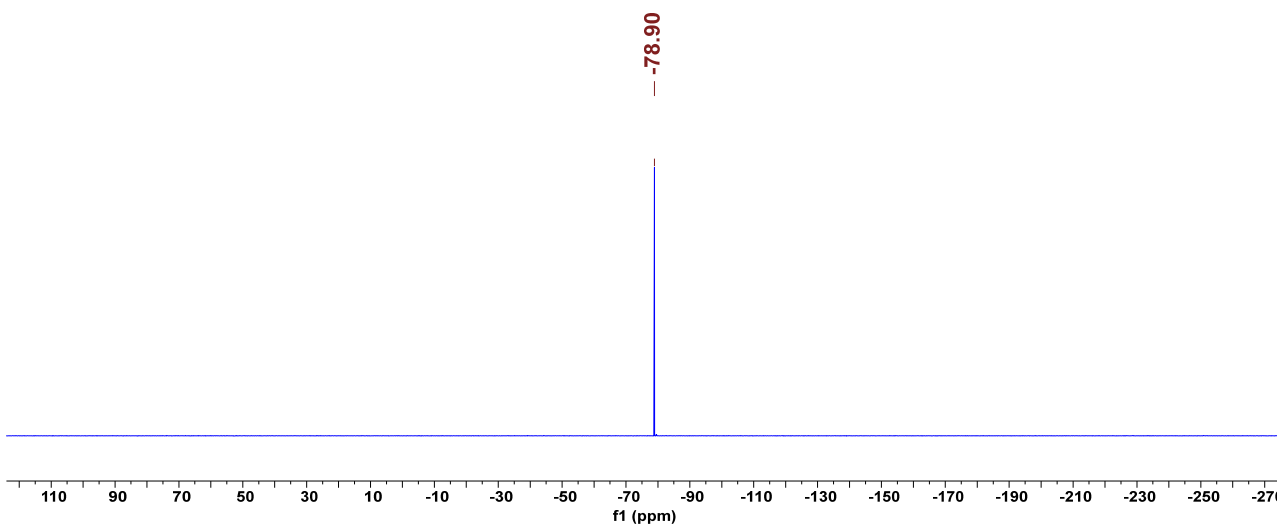






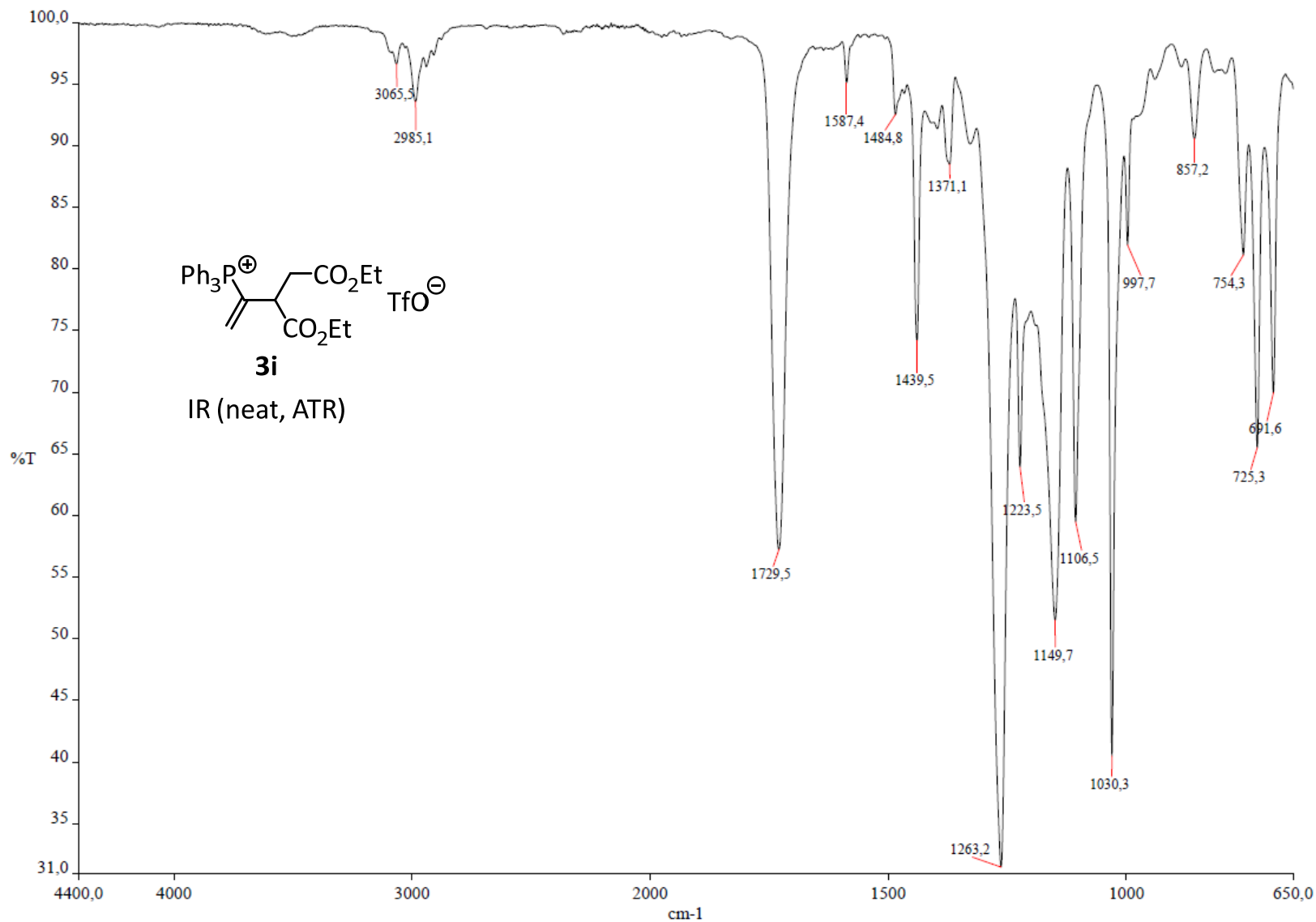
$^{31}\text{P}$  NMR

(162 MHz,  $\text{CD}_2\text{Cl}_2$ )



$^{19}\text{F}$  NMR

(377 MHz,  $\text{CD}_2\text{Cl}_2$ )



## 8 References

---

- (S1) For a freely accessible database of  $E$ ,  $N$ , and  $s_N$  parameters, see: <https://www.cup.lmu.de/oc/mayr/DBintro.html>.
- (S2) D. S. Allgäuer, H. Jangra, H. Asahara, Z. Li, Q. Chen, H. Zipse, A. R. Ofial and H. Mayr, *J. Am. Chem. Soc.*, 2017, **139**, 13318-13329.
- (S3) G. R. Fulmer, A. J. M. Miller, N. H. Sherden, H. E. Gottlieb, A. Nudelman, B. M. Stoltz, J. E. Bercaw and K. I. Goldberg, *Organometallics*, 2010, **29**, 2176-2179.
- (S4) B. J. Cowen, L. B. Saunders and S. J. Miller, *J. Am. Chem. Soc.*, 2009, **131**, 6105-6107.
- (S5) G. Himbert, D. Fink and K. Diehl, *Chem. Ber.*, 1988, **121**, 431-441.
- (S6) L. M. Conner, Y. Xu and K. M. Brown, *J. Am. Chem. Soc.*, 2015, **137**, 3482-3485.
- (S7) Y. Gao, J. Zhang, W. Shan, W. Fei, J. Yao and W. Yao, *Org. Lett.*, 2021, **23**, 6377-6381.
- (S8) T. Liu, C. He, F. Wang, X. Shen, Y. Li, M. Lang, G. Li, C. Huang and F. Cheng, *Synthesis*, 2021, **53**, 518-526.
- (S9) H. Panchal, C. Clarke, C. Bell, S. N. Karad, W. Lewis and H. W. Lam, *Chem. Commun.*, 2018, **54**, 12389-12392.
- (S10) R. W. Lang and H. J. Hansen, *Org. Synth.*, 1984, **6**, 202.
- (S11) E. Lee, J. Bang, J. Kwon and C.-M. Yu, *J. Org. Chem.*, 2015, **80**, 10359-10363.
- (S12) a) H. Clavier, K. Le Jeune, R. De Innocenzo, A. Tenaglia and G. Buono, *Org. Lett.*, 2011, **13**, 308-311. b) D. Mal and S. Jana, *J. Org. Chem.*, 2016, **81**, 11857-11865.
- (S13) W. Chen, J. C. L. Walker and M. Oestreich, *J. Am. Chem. Soc.*, 2019, **141**, 1135-1140.
- (S14) H. Guo, Q. Xu and O. Kwon, *J. Am. Chem. Soc.*, 2009, **131**, 6318-6319.
- (S15) Y.-R. Chen, G. M. Reddy, S.-H. Hong, Y.-Z. Wang, J.-K. Yu and W. Lin, *Angew. Chem. Int. Ed.*, 2017, **56**, 5106-5110.
- (S16) a) L. L. Tolstikova, A. V. Bel'skikh and B. A. Shainyan, *Russ. J. Gen. Chem.*, 2011, **81**, 474-480., b) V. V. Levin and A. D. Dilman, *Chem. Commun.*, 2021, **57**, 749-752.
- (S17) C. Mao, Z. Wang, Z. Wang, P. Ji and J.-P. Cheng, *J. Am. Chem. Soc.*, 2016, **138**, 5523-5526.
- (S18) A  $^{31}\text{P}$  NMR chemical shift of +25.5 ppm for **3f** with a phenyltetrazole counteranion was reported in: D. Virieux, A. F. Guillouzic and H.-J. Cristau, *Tetrahedron*, 2006, **62**, 3710-3720.
- (S19) (a) A. D. Becke, *J. Chem. Phys.* 1993, **98**, 5648-5652. (b) C. Lee, W. Yang and R. G. Parr, *Phys. Rev. B*, 1988, **37**, 785-789.

- 
- (S20) (a) R. Ditchfield, W. J. Hehre and J. A. Pople, *J. Chem. Phys.*, 1971, **54**, 724-728. (b) R. Krishnan, J. S. Binkley, R. Seeger and J. A. Pople, *J. Chem. Phys.*, 1980, **72**, 650-654.
- (S21) G. Luchini, J. V. Alegre-Requena, I. Funes-Ardoiz and R. S. Paton. *GoodVibes*: automated thermochemistry for heterogeneous computational chemistry data [version 1; peer review: 2 approved with reservations]. *F1000Research* 2020, **9**: 291 (<https://doi.org/10.12688/f1000research.22758.1>).
- (S22) T. Clark, J. Chandrasekhar, G. W. Spitznagel and P. v. R. Schleyer, *J. Comput. Chem.*, 1983, **4**, 294-301.
- (S23) A. V. Marenich, C. J. Cramer and D. G. Truhlar, *J. Phys. Chem. B*, 2009, **113**, 6378-6396.
- (S24) (a) S. Grimme, J. Antony, S. Ehrlich and H. Krieg, *J. Chem. Phys.*, 2010, **132**, 154104. (b) S. Grimme, S. Ehrlich and L. Goerigk, *J. Comput. Chem.*, 2011, **32**, 1456-1465.
- (S25) (a) E. Cancès, B. Mennucci and J. Tomasi, *J. Chem. Phys.*, 1997, **107**, 3032-3041. (b) J. Tomasi, B. Mennucci and R. Cammi, *Chem. Rev.*, 2005, **105**, 2999-3094.
- (S26) M. J. Frisch, G. W. Trucks, H. B. Schlegel, G. E. Scuseria, M. A. Robb, J. R. Cheeseman, G. Scalmani, V. Barone, B. Mennucci, G. A. Petersson, H. Nakatsuji, M. Caricato, X. Li, H. P. Hratchian, A. F. Izmaylov, J. Bloino, G. Zheng, J. L. Sonnenberg, M. Hada, M. Ehara, K. Toyota, R. Fukuda, J. Hasegawa, M. Ishida, T. Nakajima, Y. Honda, O. Kitao, H. Nakai, T. Vreven, J. A. Montgomery, Jr., J. E. Peralta, F. Ogliaro, M. Bearpark, J. J. Heyd, E. Brothers, K. N. Kudin, V. N. Staroverov, T. Keith, R. Kobayashi, J. Normand, K. Raghavachari, A. Rendell, J. C. Burant, S. S. Iyengar, J. Tomasi, M. Cossi, N. Rega, J. M. Millam, M. Klene, J. E. Knox, J. B. Cross, V. Bakken, C. Adamo, J. Jaramillo, R. Gomperts, R. E. Stratmann, O. Yazyev, A. J. Austin, R. Cammi, C. Pomelli, J. W. Ochterski, R. L. Martin, K. Morokuma, V. G. Zakrzewski, G. A. Voth, P. Salvador, J. J. Dannenberg, S. Dapprich, A. D. Daniels, O. Farkas, J. B. Foresman, J. V. Ortiz, J. Cioslowski, and D. J. Fox, *Gaussian 09 Revision D.01*, Gaussian, Inc., Wallingford CT, **2013**.